TRANSACTIONS OF THE AMERICAN • SOCIETY • FOR METALS

JUNE, 1936

Volume XXIV Number 2

The TRANSACTIONS *of the*
AMERICAN SOCIETY FOR METALS

Published quarterly and Copyrighted, 1936, by the AMERICAN SOCIETY FOR METALS
7016 Euclid Avenue, Cleveland, Ohio

SUBSCRIPTIONS: (members) $2.50 per year
(non-members) $5.00 per year, $2.00 per copy
Foreign (non-members) $6.50 per year, $2.50 per copy

Entered as second class matter, November 9, 1931, at the Post Office at Cleveland, Ohio, under the Act of March 3, 1879

RAY T. BAYLESS, *Editor*

Vol. XXIV June, 1936 No. 2

The object of the Society shall be to promote the arts and sciences connected with either the manufacture or treatment of metals, or both.

Table of Contents

Printed in U. S. A.

ON NAMING THE AGGREGATE CONSTITUENTS IN STEEL

By J. R. Vilella, G. E. Guellich and E. C. Bain

Abstract

Some twenty photomicrographs are employed to illustrate and classify, from the structural standpoint, the modes of transformation of austenite and the tempering of martensite in carbon steel. These structural types are considered genetically and a simple basis of nomenclature is set forth.

The authors propose that the word "pearlite" be applied to all the lamellar (ferrite and carbide layer) structures formed directly by nodular growth from nuclei in the austenite at comparatively high sub-critical temperatures, and that the word "sorbite" be applied to tempered martensite structures. If the word "troostite" is to be maintained it should preferably be applied in such a way as to introduce no ambiguities or confusion; at the present a suitable category for troostite is not apparent though some possibilities not wholly logical are mentioned. The word "spheroidite" is suggested to designate the more coarsely spheroidized carbide structures.

IN MARCH, 1934, Clayton[1] clearly voices the mild, though persistent, dissatisfaction which most of the students of steel metallography have felt with respect to the names of the aggregate constituents of steel, particularly *sorbite* and *troostite*. In the meantime Lucas[2] has contributed discussion to this subject and more recently Koselev and Poboril[3] of the Skoda Works in Pilzen have outlined their criticism of the current nomenclature. With similar intention the present writers are inclined to add what they may to the trend toward "stock-taking" with respect to these metallographic names.

[1]Charles Y. Clayton, "What Does Sorbite Look Like?", Metal Progress, Vol. 25, 1934, No. 3, p. 43.

[2]F. F. Lucas, "Troostite; Its Structure," Metal Progress, February, 1935, p. 24. See also "Structure and Nature of Troostite," Bell System Technical Journal, 1930, p. 101.

[3]V. Koselev and F. Poboril, "Troostite, Sorbite, Pearlite," Metal Progress, March, 1935, p. 56.

A paper presented before the Seventeenth Annual Convention of the Society held in Chicago, September 30 to October 4, 1935. Of the authors, J. R. Vilella and G. E. Guellich are associated with the Research Laboratory, U. S. Steel Corp., Kearny, N. J.; and E. C. Bain is assistant to vice president in charge of research, U. S. Steel Corp., New York City. Manuscript received June 6, 1935.

The early workers in steel microscopy have very properly been honored by having these steel structures named after them in the manner of the mineralogists, and it is as desirable today as it was at the time of the assignment of these names to accord the pioneers this honor and to have their names before us. To H. C. Sorby particularly is due respect and admiration. But the definitions of the 1912 Congress[4] are not wholly satisfying nor adequate today because we not only recognize important differences among certain structures to which the same name has been applied but also because increased knowledge reveals inconsistencies within the definitions themselves. Teachers, particularly, may find occasion to be grateful for any limited readjustment of these names and definitions so that they may be more acceptable to the scientific mind. This paper suggests a few simple changes in definition of Pearlite, Troostite, and Sorbite which, it is thought, would resolve most of the inconsistencies with a minimum of reconstruction.

Scientists have usually found themselves extensively engaged in the naming of things; it has generally been expedient for them to apply names to new substances, new properties, new behaviors, new effects, and new conditions, as soon as they are discovered, even before very much is really known about them. The value of this prompt naming of things lies in the resulting convenient interchange of information, one observer with another, which is greatly facilitated by the verbal economy of a name. After a short interval, this new name requires a rigid definition, for persons who gladly employ the new term will wish to know to just how great a departure from the original observation the name is still applicable. Very often the name finds well-marked natural limits, which then fix the definition by tacit agreement or convention. In other cases, wherein the nature of the original observation is less comprehensively recognized and described, confusion sooner or later arises. Such confusion may become so great as to force the abandonment of the word altogether. The dropping of a word from scientific usage generally indicates that the appellation connotes such an incorrect or vague concept that no acceptable category at all can be found for it, for there appears

[4] A report of Committee 53, on the nomenclature of the microscopic substances and structures of steel and cast iron, Sixth Congress of the International Association for Testing Materials, New York, September 1912, may be found in Appendix II, "The Metallography of Iron and Steel" by Albert Sauveur (McGraw-Hill), and in "Microscopic Analysis of Metals," Osmond and Stead, p. 287. (C. Griffin and Co., Ltd.). The excellent work of this Committee may well be accounted for by the outstanding authorities named in its membership: Prof. H. M. Howe, Chairman; Prof. Albert Sauveur, Secretary; Prof. W. Campbell; Prof. Carl Benedicks; Prof. F. Wüst; Prof. A. Stansfield; Dr. J. E. Stead; Prof. L. Guillet; Prof. E. Heyn; and Dr. Walter Rosenhain.

to be a strong philological tendency toward permanence in language; at least words efface themselves slowly.

By way of example, a competent chemist might have considerable difficulty, if he set himself the task today, in defining "phlogiston" or "dephlogisticated" in modern chemical language, however clearly the sense of the word may have expressed the views of the early chemists who first employed it; the concept to which the word applies is simply no longer tenable and the word is therefore obsolete. On the other hand, the word "anneal," because its original sense was never at too great variance with growing knowledge was able to survive, although at one time it must have meant burn-on, char, or blacken rather than to soften or equilibrate by means of heating. The persistence of the word "temper" through its diverse successive meanings indicates how preferable it is to the technical mind to admit a degree of flexibility to a word so that it may be allowed a lively retention in the language. Again, the expression "chemical affinity" is probably at the moment obsolescent because the tacit assumption in its use, i.e., of a simple correlation between a fundamental first cause for chemical action and a superficial appearance of activity (which has more to do with mere rate of reaction), is no longer acceptable to the enquiring scientist. The simple concept has been replaced by a more applicable, though more complex, concept and there is really no suitable category for the older expression.

The study of the physical chemistry of solid steel—in short, the heat treatment of steel—has been facilitated by coining a number of words to designate single constituents and conglomerates. It would be equivalent to holding a low opinion, indeed, of the advance in the science of steel treating to expect that the names assigned to the several aggregates in steel are now as aptly applied as they were at the close of the nineteenth century. Indeed, it is rather to be expected that the application of improved research tools in a comparatively new field might result in the revision of a large number of word definitions.

In any event, the phases and finely-dispersed aggregates in steel have been named and these names served very well so long as everyone agreed that the definitions were compatible with the mode of formation and occurrence as described. If there is incompatibility, then a minimum revision, sufficient to restore consistency, should be made.

The names of the principal steel constituents are as follows:

1. Cementite
2. Austenite
3. Ferrite
4. Martensite
5. Ledeburite
6. Osmondite
7. Pearlite
8. Troostite
9. Sorbite

Of these names for the structural states in steel, the first six are now unquestionably so defined as to be acceptable to essentially all metallurgists; so far as these words are concerned there appears to be no serious diversity of opinion as to just what is meant. The following definitions are believed to give the sense of those generally in use and to avoid controversial points:

Cementite: The principal carbide compound of iron, and limited amounts of other elements substituting for iron, having the characteristic orthorhombic crystal form of Fe_3C. Other carbides of different crystallinity carrying moderately large proportions of other elements are generally termed "special carbides."

Austenite: The iron solid solutions with the gamma form of iron acting as solid solvent. Atomic arrangement, face-centered cubic.

Ferrite: The iron solid solutions with the alpha or delta form of iron acting as solid solvent. Atomic arrangement, body-centered cubic.

Martensite: The product of the low temperature transformation of austenite; structurally, the iron appears to be ferrite, not in polyhedral grains, however, but highly stressed and highly strained, and usually greatly supersaturated with respect to carbon; whatever units of martensite exist which could possibly be classed as grains are probably plates; in all probability extremely fine carbide particles are usually dispersed therein within a short time; the higher carbon martensite is often tetragonal with indefinite ratio up to about 1.06. It is often, but not necessarily, associated with some retained austenite.

Ledeburite: The carbide-austenite eutectic, in which, however, the austenite is already further transformed to ferrite and carbide except as the word is used to denote the aggregate at the eutectic temperature. Ledeburite is not found normally in steels other than such high alloys as high speed steel.

Osmondite: There is nothing vague about the meaning of "osmondite," if one will accept as a definition "that

aggregate of carbide particles in ferrite resulting from the reheating of martensite, which shows the maximum dissolution rate in dilute sulphuric acid." Osmond himself gives directions for preparing it: "Hardened carbon steel of about one per cent carbon when reheated (tempered) to 350-400 degrees Cent. (662-752 degrees Fahr.) passes through the stage of troostite to that of osmondite, and on higher heating to that of sorbite." Osmond warns that it is a term not likely to be familiar to general readers. Whatever disposition one makes of the names sorbite and troostite, the osmondite is still accurately, however irrelevantly, defined by specifying its behavior in dilute acid.

One might mention also the word

Hardenite: This term is now so little used that it seems almost to be obsolescent and need not be considered in detail here. It appears to have meant "either austenite or martensite of eutectoid composition," but clearly there are no particular properties associated alone with this composition except those having to do purely with the eutectoid behavior, not inherently involved in quenching.

There remain, then, two, and possibly three terms which are in daily use but upon which there seems to be no close agreement as to precise meaning: sorbite and troostite—and, contingently, the third, pearlite, which must be defined in a manner compatible with these two. The purpose of this discussion is two-fold; first, to point out how the increase of knowledge concerning the structures to which these names were applied has rendered the definitions inadequate for acceptably accurate descriptive literature, and second, to propose certain slight changes in definition which would make possible a unanimity of meaning and a more orderly system of nomenclature. The present authors have no desire to formulate definitions nor to exert any energy in the direction of having their own suggestions accepted by other metallurgists; they believe, however, that ultimate good would result from some changes, and hope that the suggestions made here will assist eventually in finding the minimum change which will result in clarity and unanimity. Their attitude is best set forth by repeating the dialogue quotation used by Howe[5] in his famous chapter on Classification and Nomenclature:

[5] "The Metallography of Steel and Cast Iron," H. M. Howe (McGraw-Hill), p. 36.

Socrates: "But why should we dispute about names when we have realities of such importance to consider?"

Glaucon: "Why indeed, when any name will do which expresses the thought of the mind with clearness?"—Plato: The Republic.

At present the chief shortcomings in definition have to do with (1) over-lapping domains of two words, (2) inherently different structures covered by one word which incorrectly implies a close similarity, and (3) certain implications which are not in accord with observation. Faced even with these serious defects in a nomenclature, one would still be ill-advised to contemplate anything approaching an upsetting of the present scheme; almost any amount of compromise would have a greater potential benefit for the situation. Let us first consider the names and their significance. Of the name pearlite there is little need for any extensive re-consideration, but its limitations can profitably be broadened.

Pearlite

When Sorby's[6] patient and skillful hand-polishing and simultaneous etching of a microscopic specimen had served to reveal to him the alternate layers of ferrite and carbide, the reason for the pearly iridescent appearance of the annealed steel surface was at once explained. With Sorby's assent Howe named the aggregate (Sorby's *pearly constituent*) "pearlite,"—originally "pearlyte." The name would not have been applied to any but a lamellar structure for only by the tendency of these layers in relief to act as a grating in decomposing light was the pearly appearance produced. This circumstance would appear to be ample reason for excluding any but the lamellar structures from the category of pearlite, and conversely, consistency urges that all lamellar structures be termed pearlite, since they possess the requirements for pearly appearance. Fortunately, this conforms reasonably well with general usage. A complication arises with respect to "spheroidized pearlite" but even this designation can have no ambiguity if care is taken always to specify "spheroidized" except when the structure is really lamellar, and to remember that *spheroidized* pearlite is not pearlite, but any structure which has been spheroidized. This subject is discussed further.

[6]See particularly "On the Application of Very High Powers to the Study of the Microscopical Structures of Steel," H. C. Sorby, *Journal*, Iron and Steel Institute (Great Britain) 1886, p. 140.

If now, these lamellae of pearlite were always clearly observed by *any* metallographer with *any* microscope and with *any* polishing and etching technique, no ambiguity could have arisen, but unfortunately this is not true. The lamellae are not always equally spaced; on the contrary, for any certain steel, the mean spacing of the carbide plates is a function of the precise temperature at which the austenite transformed to pearlite. The more rapidly the austenite is cooled, the greater will be the undercooling prior to transformation and, in turn, the thinner, and more numerous, the pearlitic (ferrite and carbide) lamellae. This is illustrated in the series of photomicrographs, Figs. 1, 2, 3, 4, 5 and 6. Obviously, in the finer pearlites the separate lamellae are well resolved only in those parts of the specimen in which the lamellae make a small angle with the polished surface, and then only by a good modern microscope. In this case (for example, Fig. 5) the *traces* of the finest resolved lamellae are probably not more than 0.00013 millimeter apart and there is no possible reason for inferring that other parts of this specimen are very differently constituted. The structure is considered to be lamellar and pearlitic. But Sorby's microscope, to judge by his later images (more remarkable for the nineties than any now shown in 1935!) would render only as a smooth surface any cementite ridges closer than about 0.0004 millimeter. There must have been then a considerable group of fine pearlites which the early authorities, being unable to identify as lamellar, were unwilling to include as such, and to which, quite properly, they applied another name. Consistency, however, would seem to indicate the extension of the scope of pearlite to include not only the coarse, but, as well, the finer lamellar structures unresolvable to the early observers, because of their inferior equipment and technique. A situation of this sort is inevitable in any lively science and cannot be construed as indicative of anything but progress, and carries no possible disparagement of early work; the only reprehensible attitude would be a failure to recognize the need for a revision of concepts and names.

The question may be raised as to whether pearlite might not include merely a certain coarse range of lamellar structures. The answer to this question would appear to depend upon the tenacity with which it is maintained that pearlite is *essentially* lamellar. If so, then the range of structures so to be named is wide. The usual means of depressing the temperature of actual transformation and hence of reducing the spacing of the pearlite lamellae is that of cooling a steel

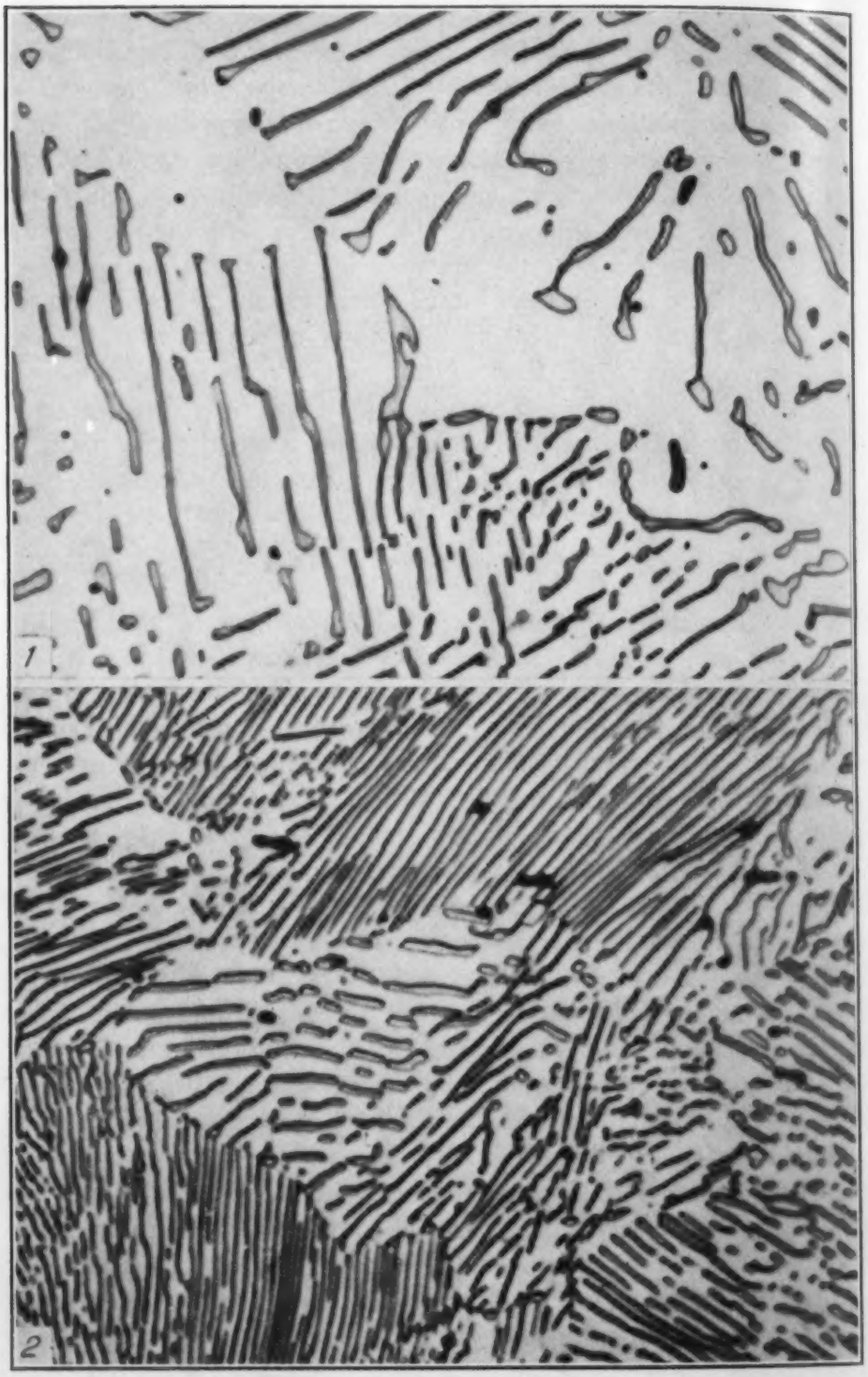

Fig. 1—Pearlite Formed in a 0.78 Per Cent Carbon Steel at 1325 Degrees Fahr. (720 Degrees Cent.). Hardness 7 Rockwell C. × 3000.
Fig. 2—Pearlite Formed in a 0.78 Per Cent Carbon Steel at 1300 Degrees Fahr. (705 Degrees Cent.). Hardness 15 Rockwell C. × 3000.

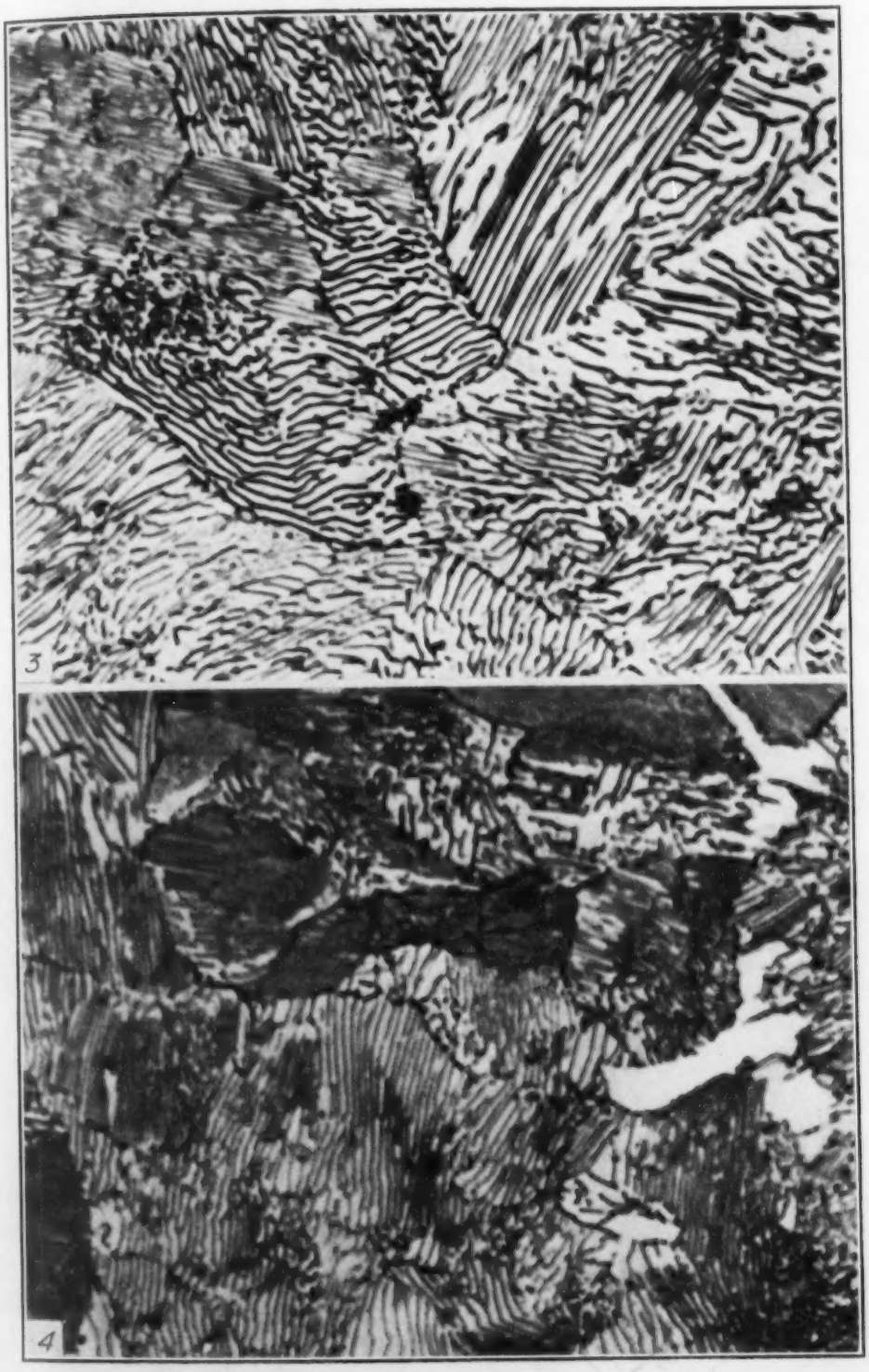

Fig. 3—Pearlite Formed in a 0.78 Per Cent Carbon Steel at 1250 Degrees Fahr. (675 Degrees Cent.). Hardness 22 Rockwell C. × 3000.

Fig. 4—Pearlite Formed in a 0.78 Per Cent Carbon Steel at 1200 Degrees Fahr. (650 Degrees Cent.). Hardness 28 Rockwell C. × 3000.

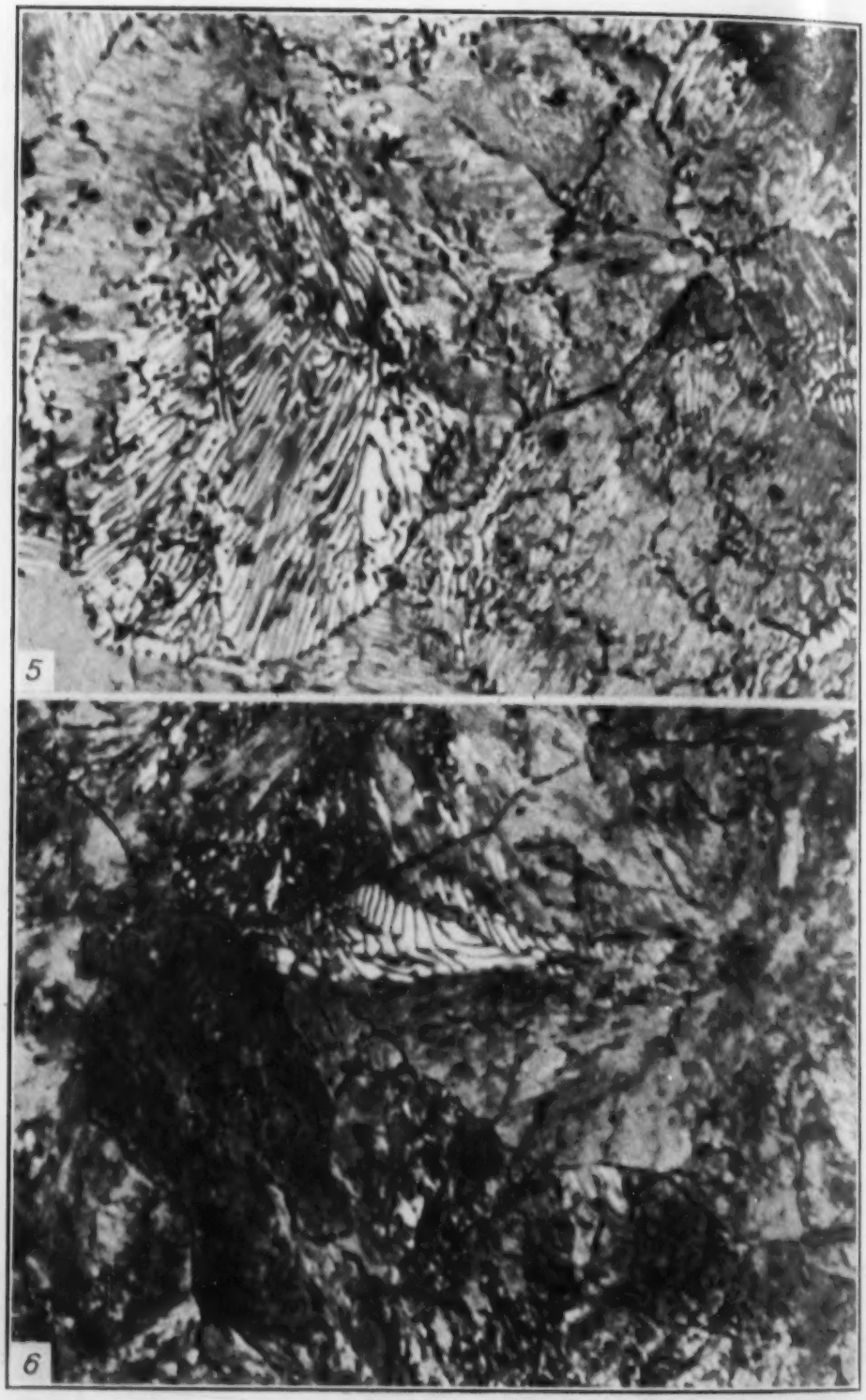

Fig. 5—Fine Pearlite Formed in a 0.78 Per Cent Carbon Steel at 1100 Degrees Fahr. (595 Degrees Cent.). Hardness 33 Rockwell C. × 3000.
Fig. 6—Fine Pearlite Formed in a 0.78 Per Cent Carbon Steel at 1000 Degrees Fahr. (540 Degrees Cent.). Hardness 36 Rockwell C. × 3000.

more and more rapidly. Finally, when the so-called critical cooling rate is just reached (provided the coolant is at some low temperature —below about 100 degrees Cent.) the austenite transforms, at least in part, to characteristic martensite. At these rates of cooling near the critical the martensite will be in broken areas mixed with a product which transformed at some 500 degrees Cent. (930 degrees Fahr.). Such material certainly represents the normal limit of fineness of carbide lamellae, and the microscope still shows that there are lamellae present. The photomicrograph of Fig. 7 confirms this, and the product of transformation at the minimum A′ temperature therefore fulfills the requirements for pearlite. Lucas[2] has likewise found this material to be lamellar, and we will wish to use his photomicrographs as references later on. In the authors' laboratory and in the publications therefrom the words "fine pearlite" have been used exclusively to designate this material.

In the strictest sense, pearlite is always nodular, in that it forms by the gradual encroachment upon the remaining austenite grain of several nodules spreading from a number of nuclei located usually in the grain boundary. A grain of austenite may transform by going over to lamellar ferrite and carbide upon a dozen different fronts. As soon as the pearlite is formed, its lamellae remain quite definitely unchanged for hours, or days, even when the temperature of the transformation is maintained; the coarseness of the lamellae is established, once and for all, by the temperature of the transforming austenite for any particular composition and grain-size. Coarse lamellar pearlite never forms from nodules of fine lamellae. The pearlite mechanism is well shown in Figs. 8 to 12, which may be regarded as a brief moving picture of the growth of pearlite nodules. If now the temperature of actual transformation is somewhat lower, the nodular aspect is more pronounced, merely because the single "colonies" are more rosette-like in contour.

This in turn is due to the fact that at elevated temperatures the pearlite often forms in only one of the two (or three) grains sharing the nucleus in the grain boundary, and very irregularly, whereas the finer pearlite (lower temperature of transformation) usually grows out rather uniformly in all directions into both grains. In really following the transformation, austenite to pearlite, the special significance of "nodular" is nearly lost and no longer appears very important. By this time it will have become apparent that the nodular fine pearlite of this discussion is one of the constituents heretofore

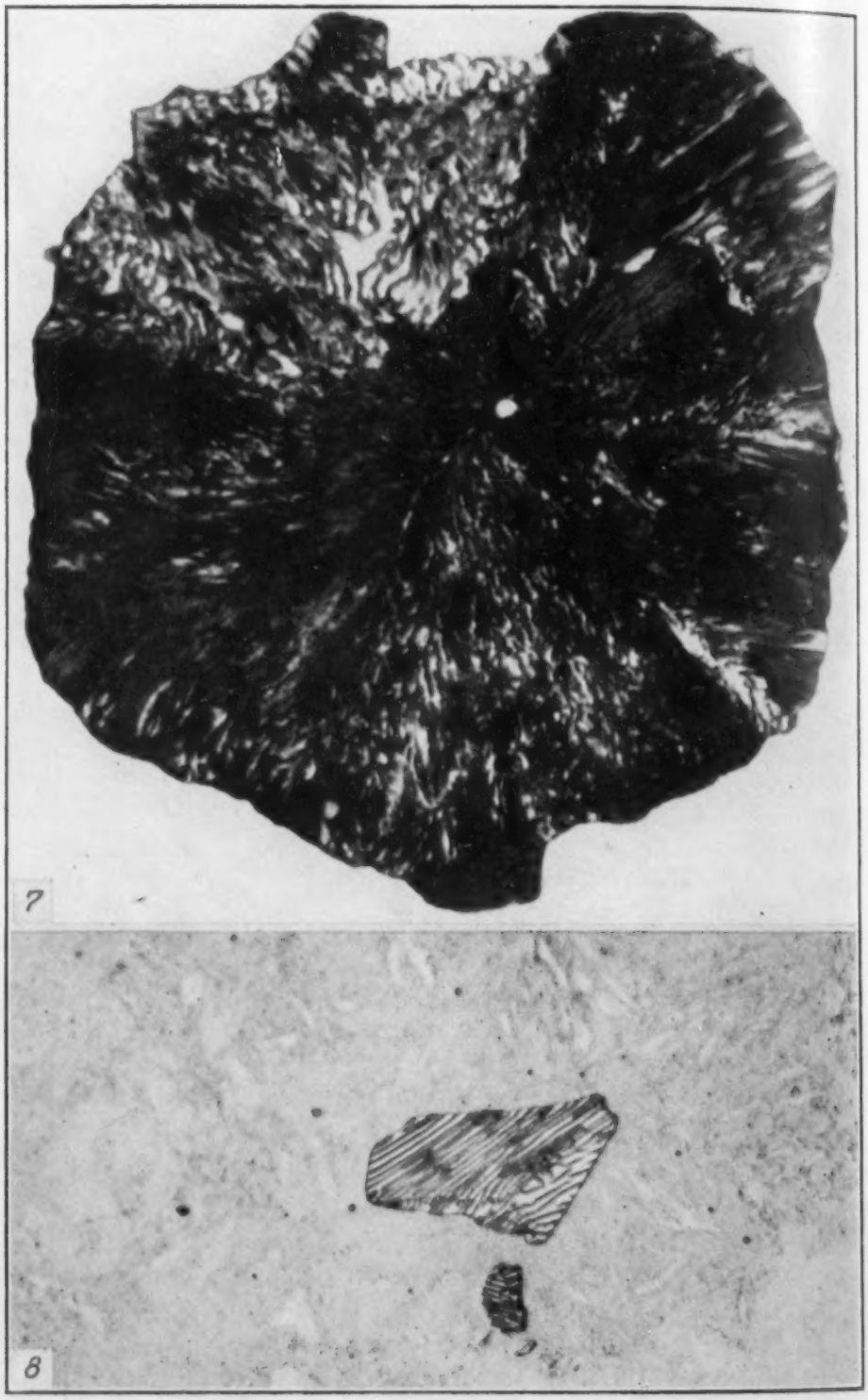

Fig. 7—Nodular Fine Pearlite (Troostite) Associated with Martensite in a Quenched 0.85 Per Cent Carbon Steel. Note Lamellar Structure. × 2500.

Fig. 8—First Traces of Pearlite Formation After 320 Seconds at 1300 Degrees Fahr. (705 Degrees Cent.) in an 0.85 Per Cent Carbon Steel. × 1000.

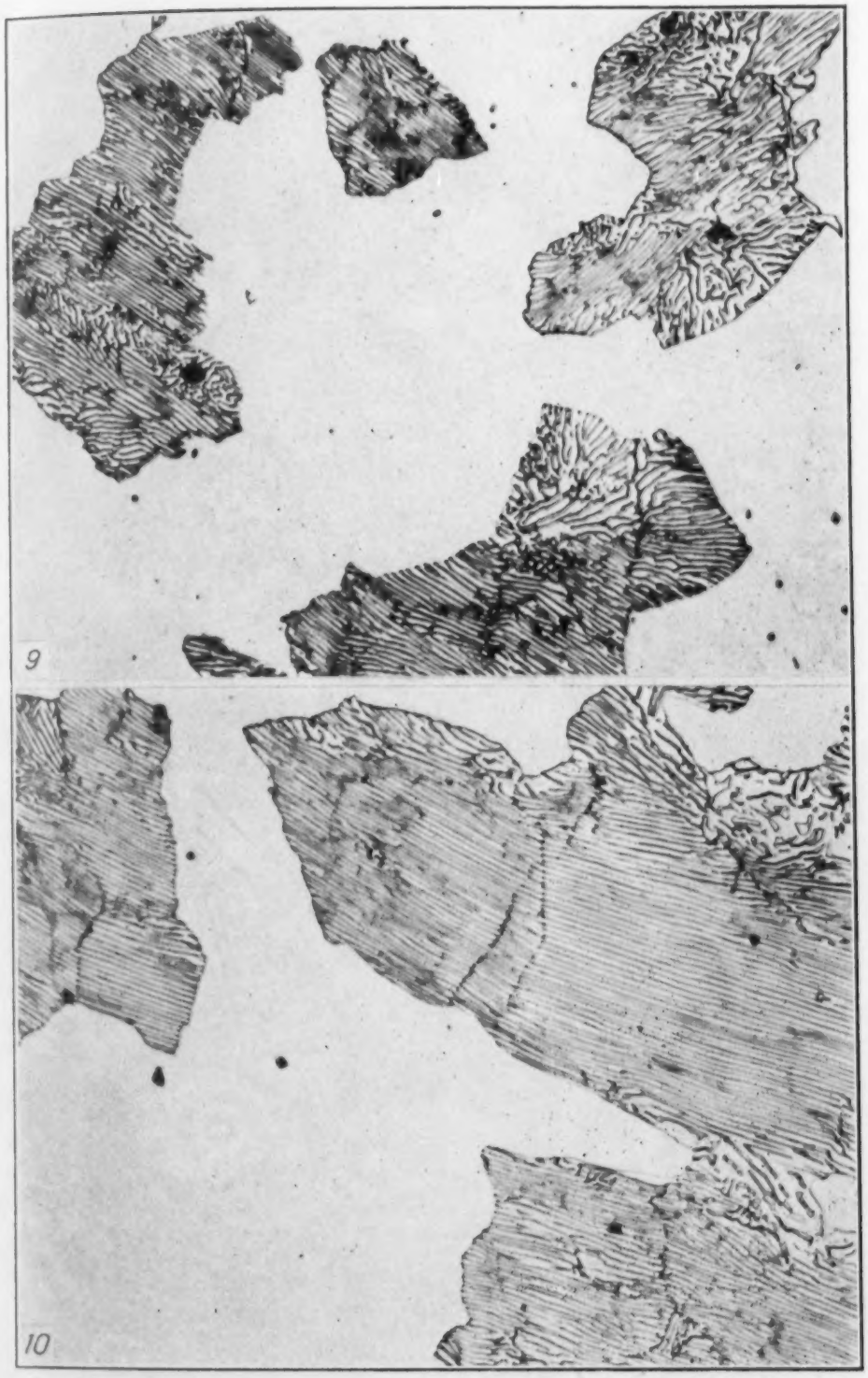

Fig. 9—Pearlite Formation in Steel of Fig. 8 Advanced to 25 Per Cent (75 Per Cent Austenite) After 1150 Seconds. × 1000.

Fig. 10—Pearlite Formation as in Figs. 8 and 9 Advanced to 50 Per Cent (50 Per Cent Austenite) After 1320 Seconds. × 1000.

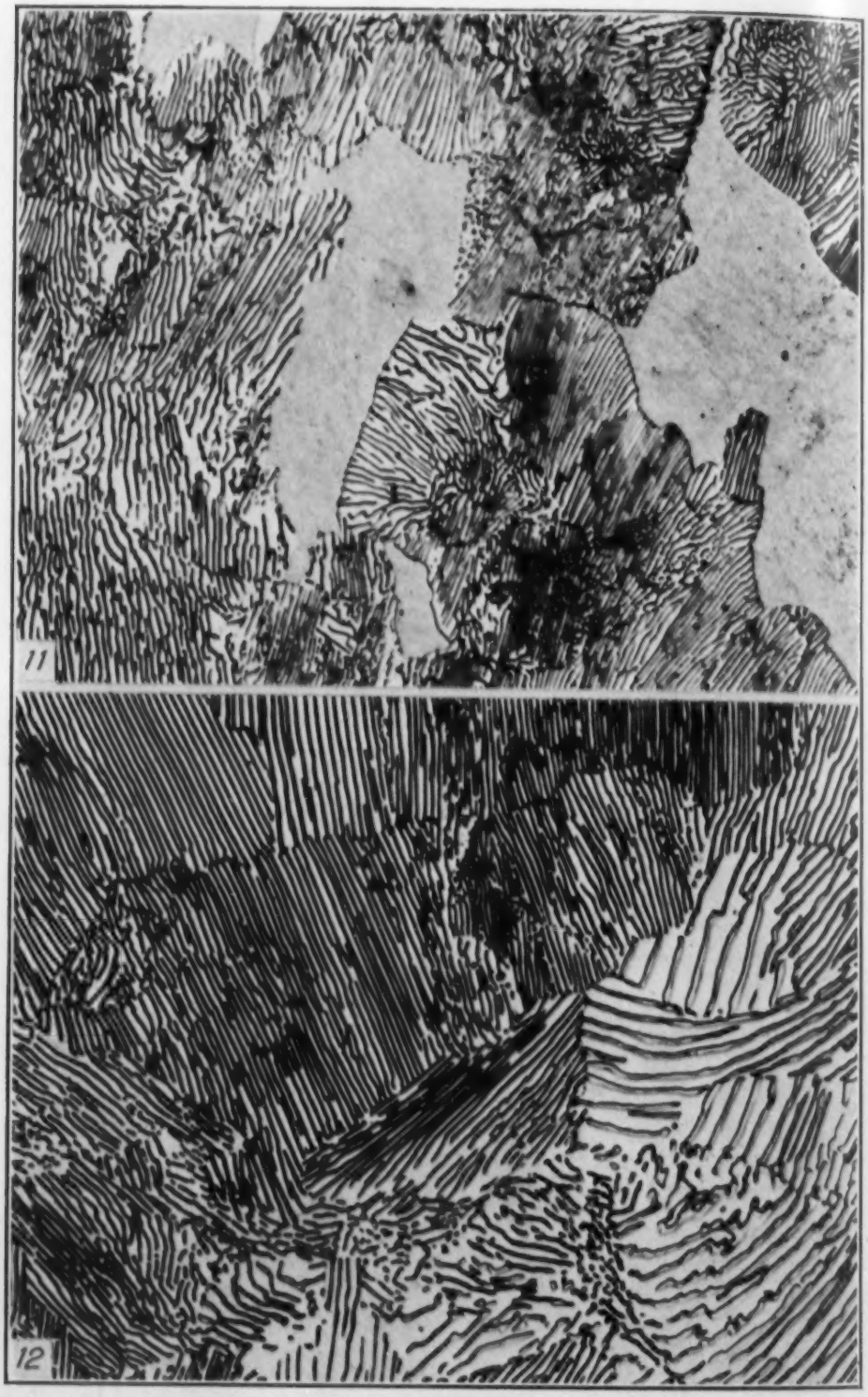

Fig. 11—Pearlite Formation as in Figs. 8, 9 and 10 Advanced to 75 Per Cent (25 Per Cent Austenite) After 1450 Seconds. × 1000.

Fig. 12—Pearlite Formation Completed in Steel of Figs. 8, 9, 10 and 11 After 4000 Seconds. × 1000.

designated as nodular troostite. One can scarcely believe that a word other than pearlite would have been applied to any of the continuous series of lamellar structures had the microscopic equipment and technique of today been available.

It would seem indisputable that the characteristics of a material which are involved in the definition of its name, should, so far as possible, reside in and be inseparable from the thing itself. Thus, the definition of pearlite should not depend upon the progress of optics, if it can be prevented, and by suitable choice of words this contingency may be anticipated and avoided. The following is suggested as a definition of pearlite:

Pearlite is the *lamellar* aggregate of ferrite and carbide resulting from the direct transformation of austenite at temperatures—usually above about 500 degrees Cent. (930 degrees Fahr.) for carbon steels—at which the diffusivity of carbon is sufficient to permit the simultaneous formation of ferrite and carbide rather than an acicular structure, however transient, of ferrite supersaturated with respect to carbon.

The extension of the designation pearlite to include all lamellar dispersions of carbide in ferrite makes almost no change in its definition but serves to remove therefrom certain vague limitations which result in different designations being applied to the same sample depending upon the resolving power of the microscope in the hands of the investigator. For example, a one-inch bar of eutectoid carbon tool steel, if oil-quenched, would be pronounced troostitic or sorbitic by one microscopist and as pearlitic by another who employed a higher magnification with lenses of good resolving power. According to the above definition the absence of traces of acicular markings and, instead, the indications of nodular growth would be reason enough to pronounce the structure fine-pearlite, for the dispersion of its primary constituents is most certainly lamellar.

Spheroidization

In heterogeneous systems the reduction of interface area results in a slight but definite evolution of heat and represents a trend toward a state of lower energy and greater stability. This necessitates a mild but often observably effective driving force toward particle growth, which reduces surface area. Thus a sludge of extremely fine particles of the solute material in a saturated liquid solution is gradually converted to coarse crystals, or a single large suspended crystal may

grow in the supernatant liquid at the expense of this fine aggregate. Similarly, all the various aggregates of ferrite and carbide in steel, as well as martensite, will, if sufficient mobility is provided (through increased temperature) to permit diffusion, tend to form a coarse dispersion of roughly spheroidal particles in ferrite. This action may *possibly* proceed at finite, although practically immeasurably slow, rates at even low temperatures but it appears more probable that the "internal friction" is too great to allow any coalescence unless the temperature exceeds a critical value for any certain state of dispersion. In any event, at temperatures near A′, the carbide in carbon steels forms rough spheroids which may be resolved by a microscope at as low a magnification as × 100; such a spheroidized structure is shown in Fig. 13. A *coarse* lamellar structure will show no tendency to spheroidize, even in a thousand hours, at a temperature which, employed for tempering martensite, produces only a *fine* spheroidal structure, for such a spheroidization would imply an *increase* in interface area. Indeed, very coarse lamellar pearlite coalesces to spheroids very slowly at any temperature.

This matter is introduced here as a background for a consideration of the naming of the coarser spheroidized structure produced commercially in the interest of maximum softness, particularly after a homogenizing treatment which leaves the metal somewhat hard, (e.g. fine-pearlite).

The sound logic involved in the application of the word pearlite to pearly, i.e., lamellar, structures, at once urges the exclusion of any spheroidized structure from this category. Such spheroidized structures might well have been named "Spheroidite," but one hesitates to think of adding yet another name to a list already too long. Perhaps "spheroidized cementite," or "spheroidized pearlite" will suffice although the name "spheroidite" might be very useful as a designation for the coarse structure brought about in the interest of softness.

The question of the two remaining commonly employed terms is a difficult one, and one, also, upon which there is less likelihood of finding agreement. Before making any suggestions it is perhaps desirable to consider briefly what fundamental characteristics of the products of austenite transformation there are which might serve for classification purposes and hence for logical identification.

Modes of Transformation

It now appears that there are two, and only two, *easily* distin-

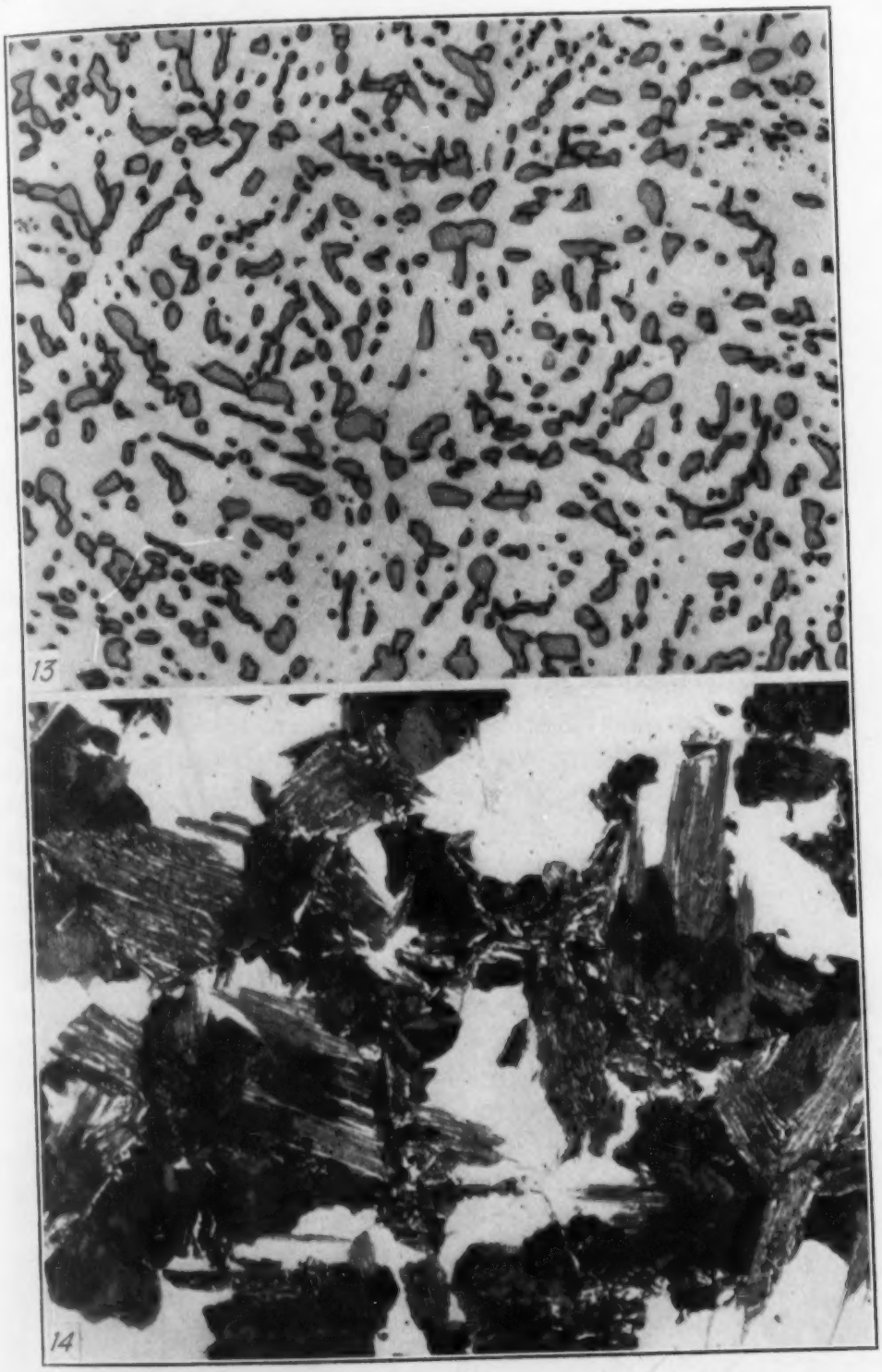

Fig. 13—Spheroidized Carbide in a 0.94 Per Cent Carbon Steel. First Quenched and Maintained 24 Hours at 1200 Degrees Fahr. (650 Degrees Cent.). × 2000. Compare Fig. 17.

Fig. 14—Simultaneous Formation of Both Lamellar (i.e. Nodular) and Acicular Products of Austenite Transformation at 1000 Degrees Fahr. (540 Degrees Cent.). × 1000.

guishable mechanisms for the transformation of austenite, and that they relate, for any particular steel, to the actual temperature of the particular portion of austenite undergoing transformation.

1. The Pearlite Reaction. Simultaneous formation of ferrite and carbide layers, directly from austenite, (after the proeutectoid reaction is locally complete) by a steady encroachment of roughly parallel plates (lamellae) upon the receding austenite boundary. The products are similar, differing only in spacing and regularity; they may be called pearlite without confusion.

2. The Acicular Reaction. The successive, abrupt formation of flat plates of supersaturated ferrite along certain crystallographic planes of the austenite grains; this supersaturated ferrite begins at once to reject carbide *particles,* (not lamellae), at a rate depending upon temperature. In effect, this is the *acicular mode* of transformation, even though the temperature be such as to limit the actual life of the quasi-martensite to millionths of a second.

In carbon steels[7] the decomposition of the austenite proceeds according to the pearlite reaction (1) at temperatures down to about 540 degrees Cent. (1000 degrees Fahr.) and at all temperatures below about this point according to the acicular reaction (2). Indeed, there is a narrow range of temperature at which both reactions proceed at so nearly the same statistical rate that both products may be seen in the same specimen as in Fig. 14. In this figure the background represents pure austenite out of which the transformation products were formed, but, as photographed, it is, of course, martensite produced by the quenching employed to interrupt the concurrent low temperature lamellar, and high temperature acicular, reactions.

When, by virtue of rapid quenching and the resultant extreme undercooling, the acicular reaction occurs below some 150 degrees Cent. (300 degrees Fahr.) the product, if immediately further cooled, is generally the hard, highly supersaturated, strained ferrite, i.e., martensite, in which, probably, the carbide particle precipitation has not occurred to any considerable extent. This material, freshly quenched martensite, which does not darken rapidly during ordinary etching for microscopic examination, is illustrated in Fig. 15.[8] A

[7]In mentioning a temperature for the change in mode of transformation from lamellar to acicular it is important to specify the kind of steel. Chromium steels, for example, transform by the acicular mode at much higher temperature than that given for carbon steels and high manganese steels transform to lamellar pearlite at considerably lower temperatures.

[8]The photomicrograph of martensite employed here is believed to be more representative of this constituent as normally encountered than the more picturesque structures often

reheating brings about a shower of carbide particles and the products are *now* known (along with the finer lamellar structures, i.e., fine pearlite) as troostite or sorbite depending upon the degree of coalescence by reheating. The structures resulting from such reheating are illustrated in Figs. 16, 17 and 18. All attempts to produce a lamellar distribution of ferrite and carbide by tempering martensite have failed and this should serve to indicate conclusively that pearlite is a direct transformation product of austenite even if the direct study of pearlite formation in the microscope, Figs. 8 to 12, were ignored.

The microscopic appearance of the softer (non-martensitic) acicular products formed directly from austenite, as would be expected, resembles somewhat that of the tempered martensite, although this resemblance is less marked at higher magnifications. An experienced metallographist is generally able to distinguish between the two acicular forms rather easily, as in Figs. 18 and 19. Mechanically the former is superior to the latter presumably due to the smaller disruptive stresses set up during transformation, and due perhaps also to a somewhat different carbide distribution. In any event the right-line markings in any of these structures provide a means of recognizing their original acicular mode of formation. It should not, however, be assumed that there is no dissimilarity between the non-martensitic structures of low temperature and of high temperature direct acicular transformation; the characteristic difference is illustrated in Figs. 21 and 22. The plates formed at the higher temperatures, e.g., 500 degrees Cent. (930 degrees Fahr.) are thicker than those formed at lower temperatures near the pure martensite zone, indeed the acicular products formed at the very highest possible temperatures, at which the nodular pearlite reaction may also occur, are quite distinctive. (See also Fig. 14). Nearly the whole of a grain may transform as a single block in which all portions have the same gross or superficial orientation, whatever the atomic arrangement in the phases may be. This modification of the acicular type of product is in itself particularly interesting and warrants special study. Traces of it are occasionally found along with the nodular fine pearlite in the transition zone of critical cooling rate in surface-hardened, quenched steel.

used in detailed studies of this constituent, for which purpose it is customary to examine the product derived from considerably coarsened austenite. This policy of presenting photomicrographs of the most commonly observed varieties of structures has been adhered to throughout all the illustrations of this paper.

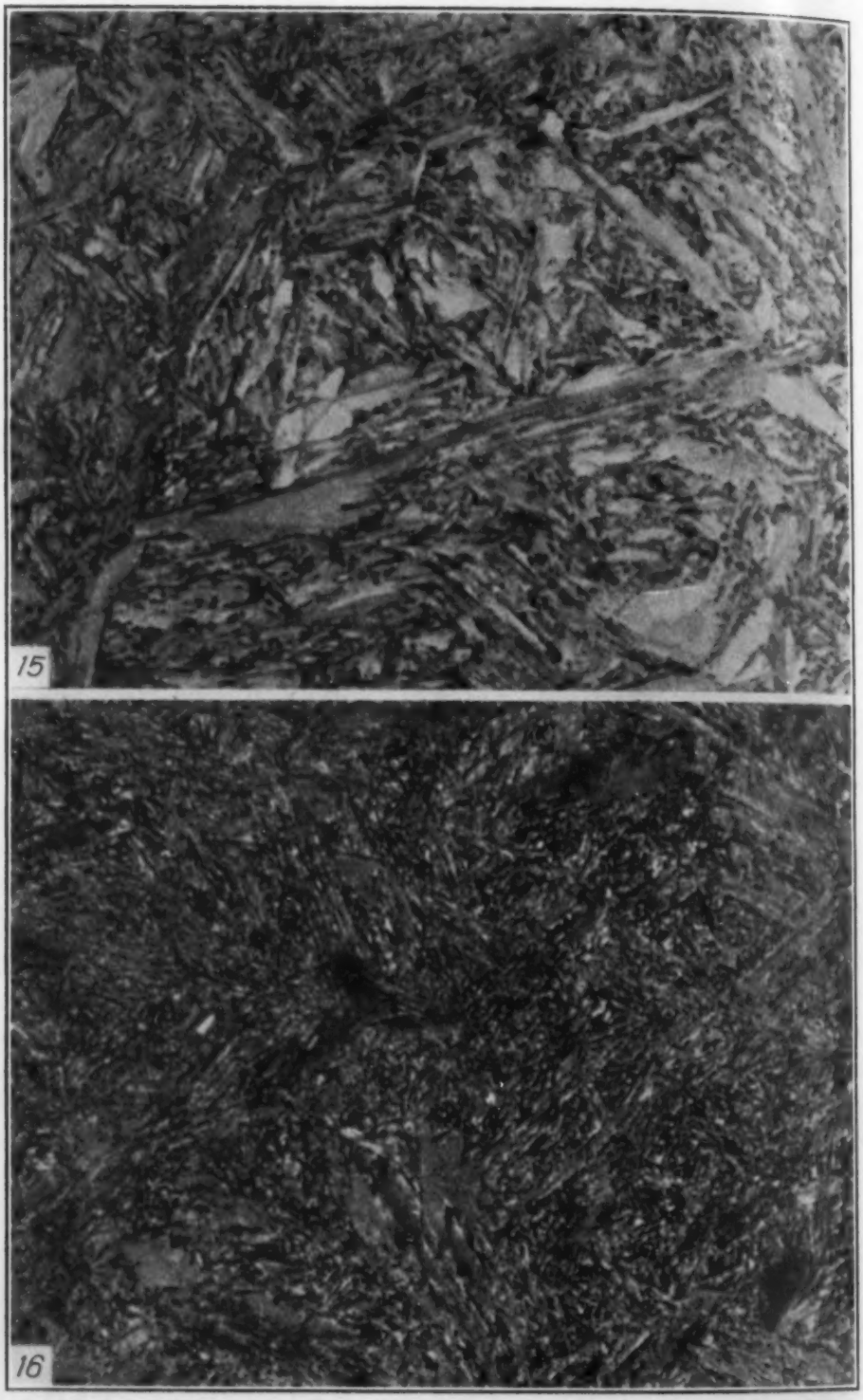

Fig. 15—Typical Martensite in Eutectoid Steel, 0.85 Per Cent Carbon. × 2000.
Fig. 16—Tempered Martensite Prepared from Material of Fig. 15 by Heating for 2 Hours at 445 Degrees Fahr. (230 Degrees Cent.). × 2000.

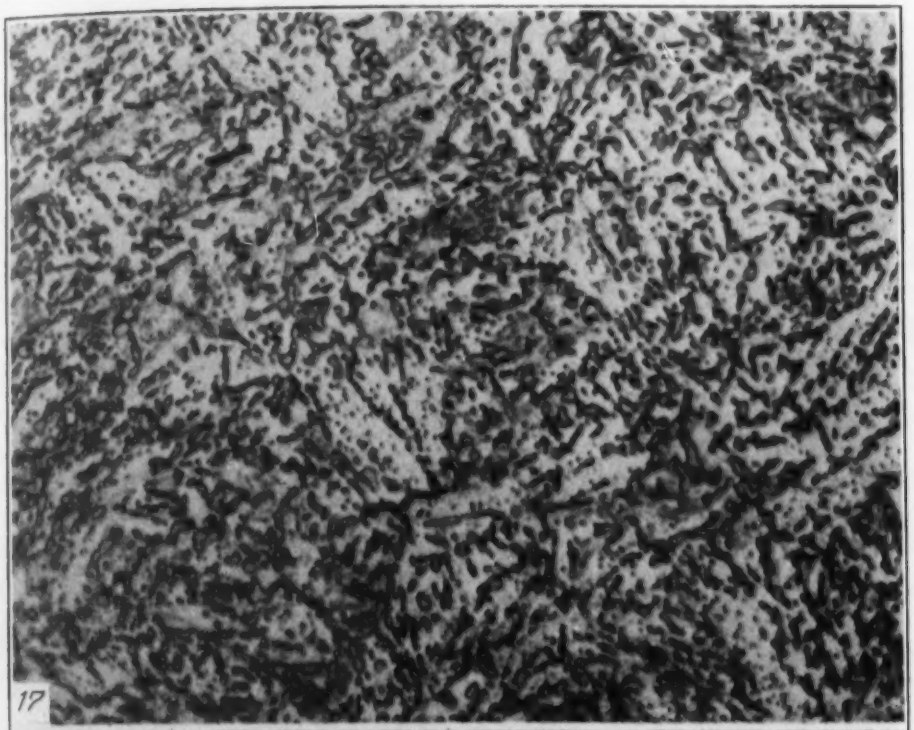

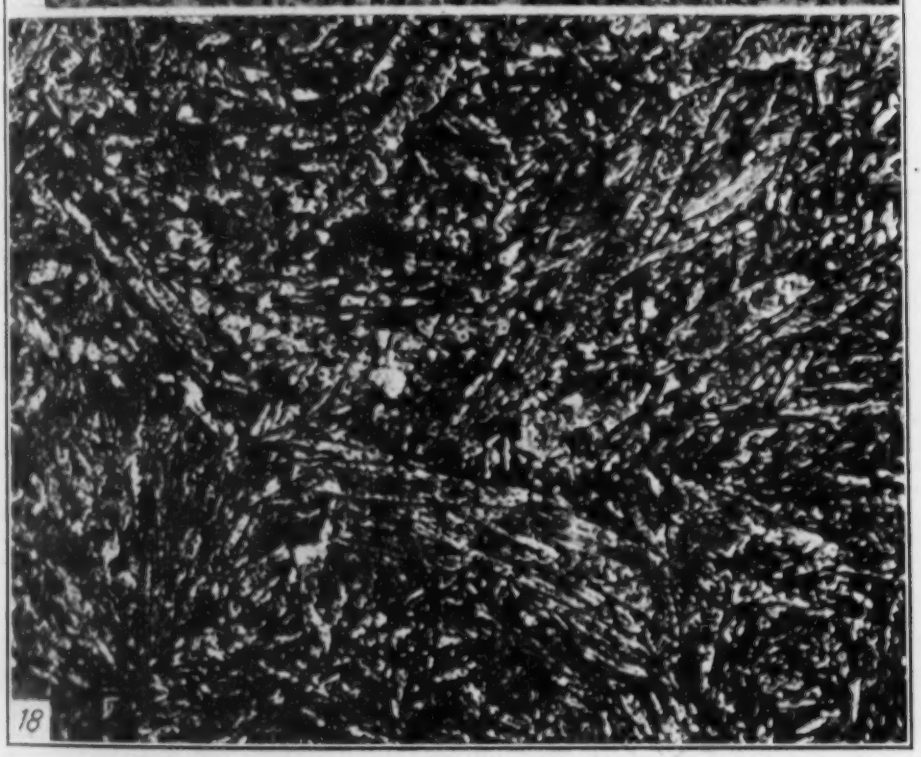

Fig. 17—Tempered Martensite Prepared from Material of Fig. 15 by Heating for 5 Minutes at 1200 Degrees Fahr. (650 Degrees Cent.). × 2000. (Sorbite).

Fig. 18—Tempered Martensite Prepared from Material of Fig. 15 by Heating for 2 Hours at 840 Degrees Fahr. (450 Degrees Cent.) to Develop Exactly a Hardness of 41 Rockwell C. × 2000. Compare Figs. 19 and 20.

On the basis of the two-fold classification, the name pearlite more than ever would appear to suffice for the lamellar structures. The particular acicular structure formed at low temperatures—in the vicinity of 150 degrees Cent. (300 degrees Fahr.) or lower—in which any carbide precipitation is in so fine a colloidal state as to be largely speculative, has been named martensite and no reasonable ground exists for even a carping criticism of this designation. By way of summary, the softer acicular structures are formed in one of two ways:

1. By tempering martensite.
2. By direct austenitic transformation at temperatures usually between about 500 degrees Cent. (930 degrees Fahr.) and 150 degrees Cent. (300 degrees Fahr.).

The latter is as yet only rarely carried out commercially and the product may at some later time require a name. At the moment the tempered martensites are spoken of as either troostite or sorbite, the less markedly softened structures being called troostite and the more thoroughly softened martensite being termed sorbite.

Troostite

The 1912 Congress evolved a consistent definition for an aggregate of this name, troostite:

"In the transformation of austenite, the stage following martensite and preceding sorbite (and osmondite if this stage is recognized)." This is a definition which, if the term persists, may well be preserved, but unfortunately for the present student, equipped with a good modern microscope, the Congress, too generously provided two methods of developing the structure, one of which is incompatible with the definition. To quote:

"It (troostite) arises either on reheating hardened (i.e., martensite) steel to slightly below 400 degrees Cent., or on cooling through the transformation range at an intermediate rate, e.g., in small pieces of steel quenched in oil, ... or in the middle of larger pieces quenched in water from above the transformation range." It is further stated that it is habitually associated with martensite which identifies the product of the second method of formation with the dark-etching nodules illustrated in Fig. 7 which we see as fine pearlite.

Considering now the first method prescribed for the formation of troostite, one finds that the structure is very different as illustrated

in Fig. 18, which reveals a particle precipitation structure with sufficient right-line markings to prove its acicular origin. It would appear necessary to exclude this lamellar structure of nodular origin which formed by the direct pearlite reaction at A′ from the category of troostite and to consider only its application to tempered martensite —in which case, one may employ the 1912 definition except perhaps for the first five words which might be replaced with "In the gradual tempering of the freshly hardened steel."

In this connection, it appears that Arnold realized the lamellar nature of all the direct higher temperature transformation products of austenite, i.e., the products of the A′ transformation for he counselled the use of "troostitic pearlite" for the finest and hardest direct products and "sorbitic pearlite" for the coarser and somewhat softer structures. Curiously enough, his proposals were rejected because "This is contrary to general usage, which restricts pearlite to microscopically resoluble masses." But the very structures under discussion are today resoluble, or resolvable and by the same good reasoning should be called pearlite.

Sorbite

Much of what has been written about troostite is applicable to sorbite. The 1912 definition designates:

"In the transformation of austenite, that stage following troostite, and osmondite if the stage is recognized, and preceding pearlite."

This definition is thoroughly consistent in itself if one write "spheroidized pearlite" in place of pearlite. This might well have been done in the 1912 definition because pearlite was recognized as lamellar even then ("The iron-carbon eutectoid, consisting of alternate masses of ferrite and cementite"), and simple experiment shows that no reheating of troostite or sorbite can ever develop coarser lamellar structures, but instead merely causes spheroidization.

The discussion of the preparation of this aggregate, like that of troostite, however, provides means of making two dissimilar structures instead of a single type of aggregate. The one, made directly, by a sub-critical cooling rate, is, as would be expected merely the fine pearlite of Lucas' photographs while the other is an acicular product in which the carbide particles are somewhat coarsened. (Compare Fig. 4 with Fig. 17, and Fig. 18 with Fig. 20.) It would again appear logical not to include under sorbite the pearlite struc-

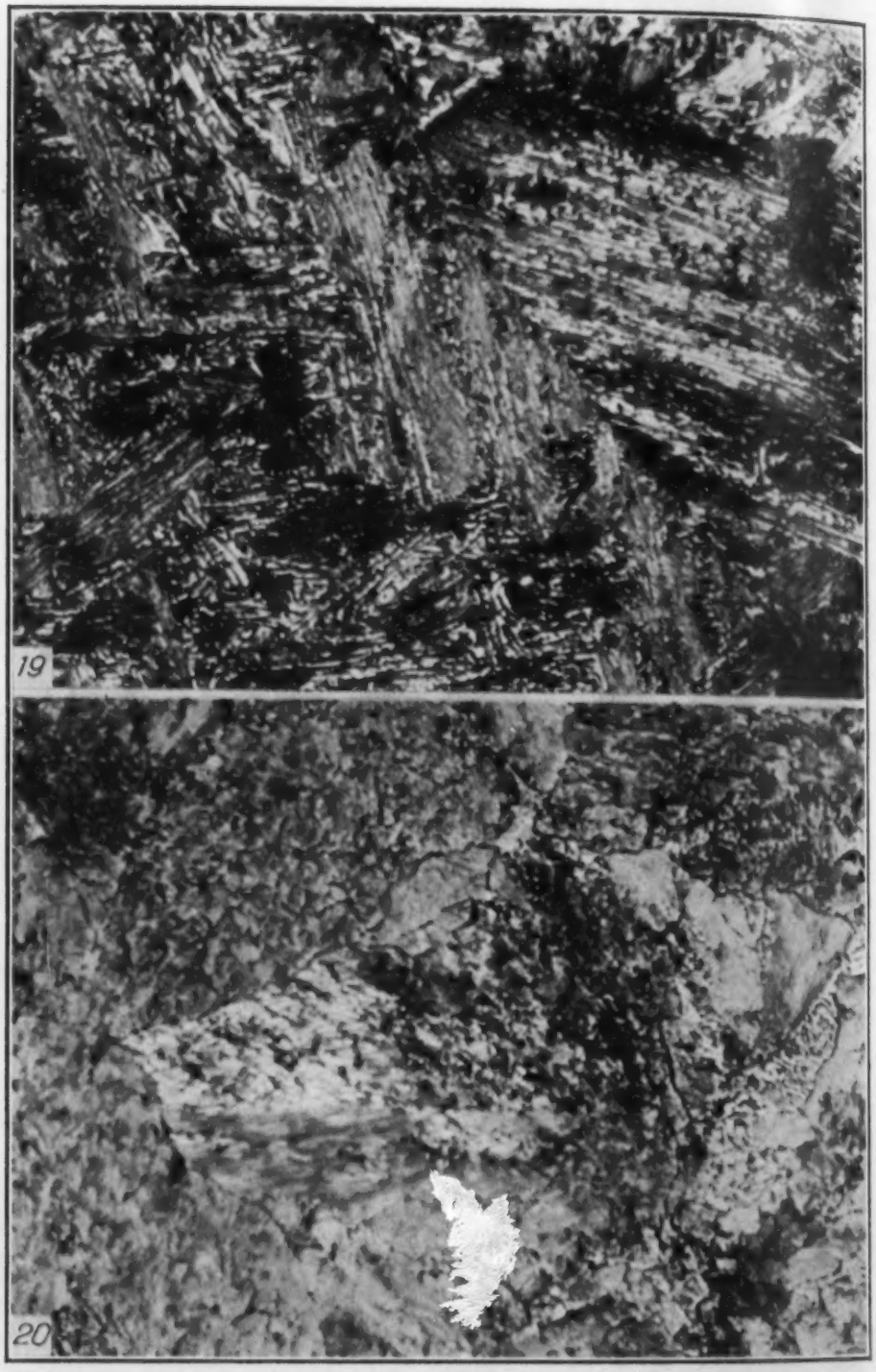

Fig. 19—Acicular Product of Direct Austenite Transformation at 850 Degrees Fahr. (455 Degrees Cent.). With Hardness of Exactly 41 Rockwell C. × 2000. Compare Figs. 18 and 20.

Fig. 20—Fine Pearlite Formed in Same Steel as in Figs. 18 and 19 at 1100 Degrees Fahr. (595 Degrees Cent.) With Hardness of Exactly 41 Rockwell C. × 2000. Compare Figs. 18 and 19.

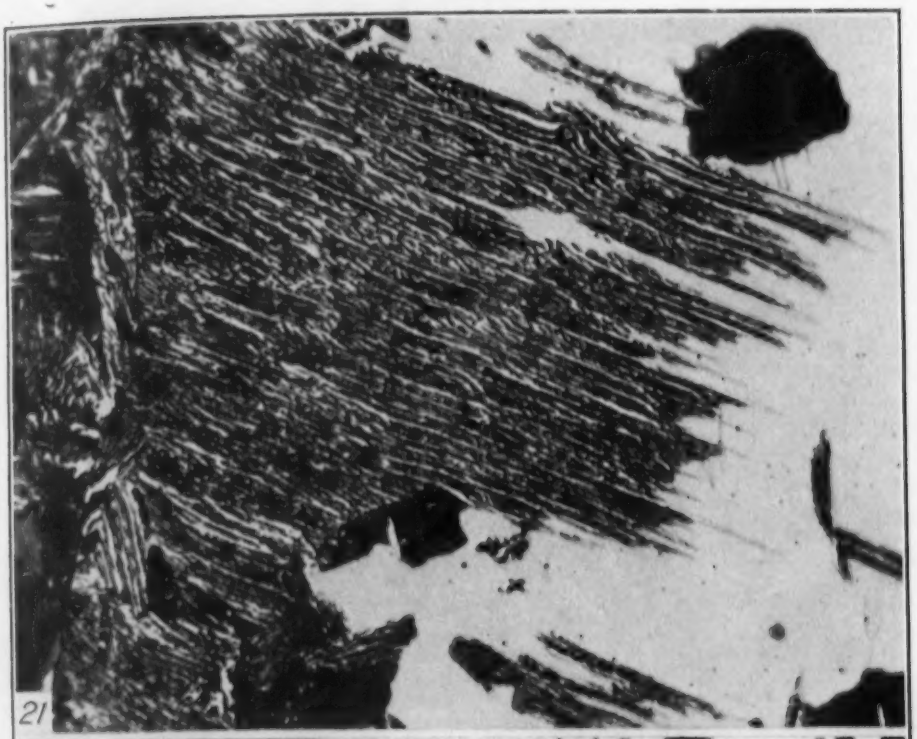

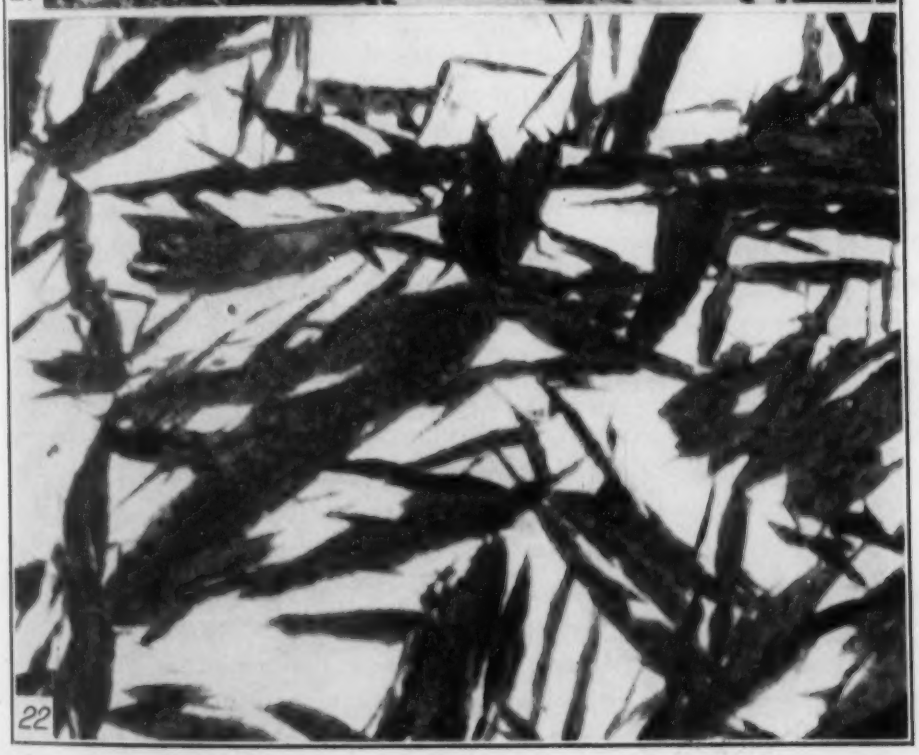

Fig. 21—Acicular Structure Characteristic of Transformation Near the Upper Temperature Limit for this Mode of Transformation. × 1500. Incompleted Reaction in Eutectoid Steel at 1000 Degrees Fahr. (540 Degrees Cent.).

Fig. 22—Acicular Structure Characteristic of Transformation Near the Martensite Temperature Range. × 2500. Incompleted Reaction in Eutectoid Steel at 550 Degrees Fahr. (290 Degrees Cent.).

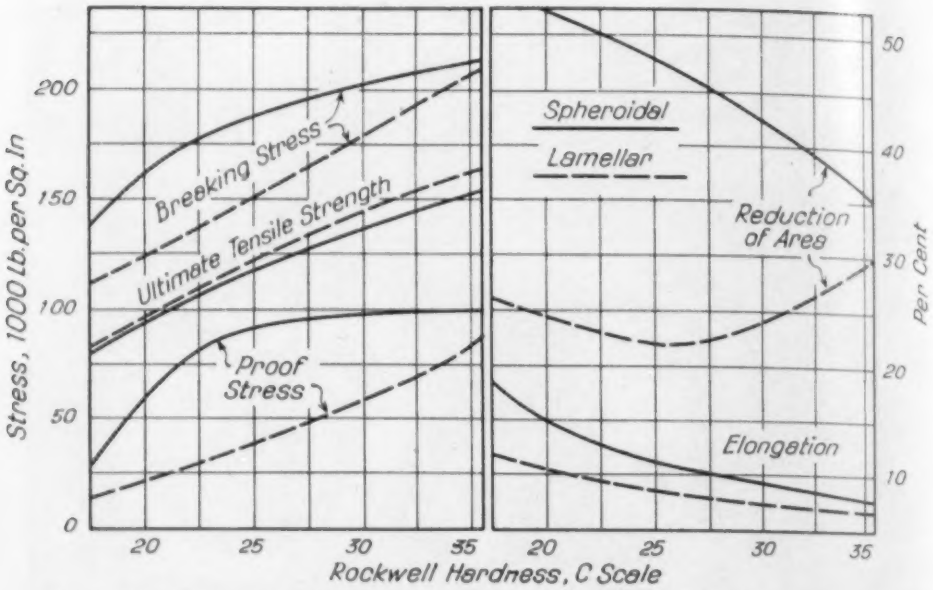

Fig. 23—A Comparison of the Tensile Properties (Ultimate Tensile Strength, Proof Stress and Breaking Stress Computed on the Reduced Section) of Spheroidal Structures (Tempered Martensite) and Pearlitic Structures in the Same Steel at Various Hardnesses.

Fig. 24—A Comparison of the Tensile Properties (Reduction of Area and Elongation) of Spheroidal Structures (Tempered Martensite) and Pearlitic Structures in the Same Steel at Various Hardnesses.

ture which, in fact, is not even extremely fine and instead to confine the definition to the tempered martensite.

If there is reluctance to attach significance to a distinction between structures of substantially the same hardness which is based only on the difference between a lamellar dispersion and a particle dispersion, an inquiry into the resulting physical properties may be convincing. Two series of structures have been prepared from a single 0.84 per cent carbon steel, the one lamellar, the other tempered martensite, in short, by the two alternate methods outlined by the 1912 Congress for the preparation of sorbite. Each series covers a fair range of hardness. The mechanical properties, as reflected in the tensile test, are plotted against the common Rockwell C Hardness in Figs. 23 and 24 for easy comparison of the two types of dispersion at comparable hardness. It will be seen that, regardless of hardness, no similar assortment of tensile properties can be found for the two structures; the difference in properties is at a maximum in the characteristic hardness range of so-called sorbite. The photomicrographs of Figs. 18, 19 and 20 show respectively structures of precisely the same hardness in specimens of the same bar of steel produced (18) by tempering martensite, (19) by direct transforma-

tion to the softer acicular constituent and (20) by formation of fine pearlite.

Suggestions for Sorbite and Troostite

The observations set forth above persuade the writers that neither of these words need include the lamellar structures, which Clayton sets apart by the designation "primary." If it were not for the tacit assumption that there was something discontinuous in the lamellar series and that these aggregates were not pearlitic, the names "primary sorbite" and "primary troostite" would be very acceptable, and in our opinion happily chosen, but that assumption is encouraged by the use of the two names.

The tempered martensite series from the slightly reheated aggregates to the coarser, softer products of high reheating temperature is also completely continuous and the application of different words tends to obscure this continuity, which is perhaps the most important feature of precipitation phenomena in metals. Whether or not different stages of coalescence are better distinguished by different names is largely a matter of individual taste. Those who incline to such names may point to such series as dust, sand, gravel, stones, etc., and there is no fitting rejoinder in refutation which may be made by the others who find the fact of continuity the more striking circumstance.

At any rate, the assignment of the word troostite to the dispersions finer and harder than those of sorbite is almost universal. Furthermore, as seemingly with all precipitation alloys there is a degree of fineness or dispersion which is most rapidly attacked in a corrosive medium, such as the etching reagents for metallographic preparation, and this condition of maximum attack may, as well as not, constitute the boundary zone between two of the designations, if it is felt that such designations are necessary or helpful. Unfortunately the mean size of the particles represented by this maximum rate of dissolution is not known, nor have we at present any means of determining it. At best, such a criterion of name is somewhat irrelevant.

If one of these names were to be gradually dropped from current usage it would probably be troostite, since it would appear Sorby was somewhat more actively engaged in furthering the metallography of steel than was Troost. Certainly metallurgists could do nicely with but one name for tempered martensite and the word

"sorbitize" would be synonymous with "temper" or the less precise "draw."

At any rate, one may justifiably summarize these suggestions and ascertain how seriously, if at all, the changes would affect the usage of the words in question. The following schematic representations are consistent with the observations and the reasoning therefrom:

For carbon steel:

Austenite—below A_1 and above about 550 degrees Cent. (1000 degrees Fahr.) → Pearlite.

Austenite—below about 150 degrees Cent. (300 degrees Fahr.) → Martensite.

Austenite—between about 150 and 550 degrees Cent. (300 and 1000 degrees Fahr.) → un-named, dark etching, acicular aggregate somewhat similar to tempered martensite; hardness and coalescence dependent upon transformation temperature.

Martensite—reheated to about 150 to 400 degrees Cent. (300 to 750 degrees Fahr.) → Troostite.

Martensite or troostite—reheated to about 400 to 700 degrees Cent. (750 to 1290 degrees Fahr.) → Sorbite.

Martensite or troostite or sorbite—reheated to about 700 degrees Cent. (1290 degrees Fahr.) but below A_1 → spheroidized cementite in ferrite ("spheroidite").

Fine pearlite—at temperatures above its own formation temperature, e.g., 600 degrees Cent. (1100 degrees Fahr.) but below A_1 → spheroidized cementite in ferrite, i.e., "spheroidite," or perhaps coarse sorbite.

The dropping of the word troostite would clearly cause no great hardship and at the same time its use permits the possibility of ambiguity unless it be definitely assigned to some arbitrarily limited range of a continuous series, at least a highly artificial means of preserving its use.

In conclusion the authors suggest that (1) pearlite apply to all lamellar structures in steel formed by direct nodular transformation and that (2) sorbite apply only to tempered martensite.

If troostite is to be retained, it might apply either (1) to the slightly tempered martensite or even, though less satisfactorily, (2) to the particularly fine lamellar pearlite associated with martensite in the not quite fully hardened zones of quenched steel, but certainly not to both.

DISCUSSION

Written Discussion: By B. L. McCarthy and R. F. Cameron, Wickwire Spencer Steel Co., Buffalo, N. Y.

The authors are to be complimented on the manner in which they have presented their views, and the evidence offered to substantiate them. The differences that exist between the structures produced directly from austenite and those resulting from the tempering of martensite are apparent to most metallographers and the suggested changes in our present nomenclature are, in our opinion, quite justifiable.

The need of better terminology is particularly obvious in the manufacture of high carbon steel wire. For many years the desired structure of the patented rod or wire has been termed sorbite or sorbito-pearlite. However, by the use of more modern polishing and etching technique and employing the modern microscope, these structures are resolved into lamellar pearlite in varying degrees of fineness.

Recent studies to determine the most desirable structure from which to draw high carbon steel wire have shown:

1. That fine pearlite, because of the more even distribution of cementite and ferrite and its relative ductility, is the most suitable.
2. That coarse pearlite, because of the resistance to plastic deformation resulting from the thick cementite plates, is not desirable.
3. That structures resulting from the tempering of martensite at temperatures below 1000 degrees Fahr. are too hard for plastic deformation.
4. That the coalesced cementite and free ferrite of the structures resulting from the tempering of martensite above 1000 degrees Fahr. does not produce high quality wire because of the uneven distribution of these constituents.

This marked difference between the cold working properties of the pearlite produced in the patenting treatment and the structures resulting from the tempering of martensite may be used as evidence of the dissimilarity of the two structures commonly termed troostite or sorbite.

As a means of evaluating patented structures in our laboratory we classify the structure of pearlite as follows:

Coarse	Resolved at 1000 diameters of magnification.
Medium	Unresolved at 1000 diameters of magnification. Resolved at 2000 diameters of magnification.
Fine	Unresolved at 2000 diameters of magnification.

While we agree with the authors that the transformation of austenite produces either martensite or pearlite, or both, depending on the position of the Ar_1, we feel that the use of the terms "coarse," "medium" and "fine" would more clearly indicate the temperatures of transformation that result from annealing and normalizing.

In our opinion the use of the terms troostite and sorbite or just sorbite as suggested, should apply only to structures produced by tempering martensite.

Written Discussion: By S. L. Hoyt, director of research, A. O. Smith Corporation, Milwaukee.

With the paper of Messrs. Vilella, Guellich, and Bain in hand, I decided to review the subject matter briefly before reading it and knowing only its

general purport. The names by which we call familiar things are of importance to us, far beyond having merely a convenient term to specify what one has in mind. Accomplishing that useful purpose would be sufficient justification for the usage but I believe the importance of names reaches further. It is in their power for good or evil that names acquire their deepest significance. How clarifying is Langmuir's "space charge"; how obscuring is the forgotten scientist's "suspended animation." One teaches while the other stultifies; let us be sure of what we are doing here.

A little reflection soon convinced me that there is no need for considering the advisability of renaming or redefining the constituents of steel; recent investigations had shown only too clearly that existing nomenclature was faulty and inadequate. Having taken that step I passed at once to more important matters. Broadly how should the constituents be differentiated and what names should be given preference with least disturbance to our present concepts? Rather easily the subject seemed to resolve itself about as follows: Those constituents (old style) which form from austenite on cooling to produce lamellar aggregates of ferrite and cementite are generically and genetically the same and should be given the same name. Those constituents (still old style) which form from martensite on heating should likewise be given the same name. Obviously some of the present names would have to be dropped and it was equally clear that pearlite would not be one of them, nor would austenite or martensite. At this stage, things rested between retaining sorbite or troostite and inasmuch as "sorbite," the name, not only depicted the most important constituent of many steels but also honored the father of our science, I crossed the Rubicon.

At about this time I read the paper itself. Then it became clear that I had simply been following the teachings of the authors and associates over the past few years. Their studies in steel structures have so clearly described the transformations and the reaction products that it seemed futile to try to add to their discussion. It did not seem to be such a vital matter, my crossing the Rubicon.

The authors have accomplished a worthy purpose in a scholarly manner. So clear is their presentation that teachers and students of the metallography of steel will, I am willing to say, necessarily use its teachings as their text and adopt the nomenclature proposed therein. Indeed, to be correct, we shall have to think as they do of these matters and to think easily, we had best use the terms that they have found to be correct and appropriate.

To what they write I have but few suggestions to make. The dark etching, acicular aggregate which forms from austenite at black heat is left nameless. Unless I am in error, this structure was first produced and observed in the authors' laboratory and it should be their privilege and honor to name it. I regret that they did not do so for this discussion. The structure which has been called "granular pearlite" is the only one we are asked to call by a new name, "spheroidite." In view of the several geneses of this structure the authors are on sound ground when they select a name which refers to appearance rather than to origin. This name seems to me to be well chosen.

By means of this paper and others relating to the terminology of aggregates in steel a movement has been started which should be carried to a logical con-

clusion. Here a word of caution seems to be appropriate for workers in other lands have the same interest in nomenclature as we here at this meeting. To build permanently and satisfactorily we would be well advised to secure the co-operation of metallographists in all countries.

Written Discussion: By Howard Scott, Westinghouse Electric and Manufacturing Co., East Pittsburgh, Pa.

The question of terminology is a perplexing one that must be met eventually. Mr. Vilella and collaborators have proposed a solution which, however, lacks somewhat the explicitness necessary to improve our present situation. Our chief problem is to draw sharp lines of demarcation between the several overlapping constituents, namely: ferrite and martensite, martensite and troostite, troostite and sorbite, sorbite and spheroidized pearlite. The microscope alone appears incompetent to provide the final criterion in all cases. Certain physical properties and their changes on tempering, however, reveal end points of the reactions involved and in conjunction with the microscope their use should lead to sharp demarcations between constituents.

Another thing greatly needed in this connection is a generic term for the product of slow cooling embracing what is now called fine pearlite, lamellar pearlite and spheroidized pearlite. In practice it is necessary to distinguish more frequently between the products of slow and fast cooling relative to the critical cooling rate than to make the finer distinctions between the sub-members of each class. This need is a very practical one because of the usual great difference in physical properties of the members. Also it simplifies the presentation of ferrous metallography to students, a matter of importance in our educational activities.

The generic term to use for the products of slow cooling it seems to me is "pearlite." Its classical derivation is interesting but not of controlling importance in determining its usage. Use of pearlite in this sense avoids the need for a new term and is close to present practice. For finer distinctions we have modifying adjectives such as fine, lamellar and spheroidized. The situation is quite different with regard to the products of fast cooling, the members of the sub-classes being produced by the tempering of martensite so that martensite serves very well as a generic term.

Summarizing these comments, the present looseness of the terminology of ferrous metallography can be overcome by sharply distinguishing the significant microconstituents one from the other with the microscope fortified by appropriate physical tests. Also this nomenclature can be simplified to great advantage by adoption of a generic term for the products of slow cooling.

Written Discussion: By Colonel N. T. Belaiew, Paris, France.

Mr. Bain and his collaborators are to be congratulated on the excellent paper they have presented on the naming of the constituents of steel; on the very interesting review of the present position of the question and on their suggestions, as to the reconsidering of the whole problem of our nomenclature. Some of their suggestions, accompanied as they are by most excellent photomicrographs appeal even to one who has taken part in the New York Congress of 1912, and, subsequently, in the work of the Committee on Nomenclature, under the chairmanship of the late and ever lamented Professor Henry Marion Howe.

The authors propose in the first instance that the word "pearlite" should apply to all lamellar structures such as are designed now by the terms of "lamellar pearlite" and "nodular" troostite, considering that pearlite is a lamellar aggregate resulting from a direct transformation of austenite at temperatures usually above about 500 degrees Cent. (refer to page 239). In the course of their paper the authors, and Mr. Bain in his previous papers, have recourse to subdivisional terms like "fine," "medium" and "coarse" pearlite. Thus, all these as well as nodular troostite are to be covered by one appellation.

All the above mentioned terms are usually used in a quantitative and not in a qualitative sense. It seems to us that if they were defined qualitatively a good deal of confusion would be avoided, and, moreover, some ground might be found to judge whether there is, or there is not a demarcation line between the microscopical constituents known up to now as pearlite and troostite, and as such having become familiar to the practical microscopical engineer.

In 1922, in a paper to the Iron and Steel Institute on the "Inner Structure of the Pearlite Grain" we have introduced the notion of "Delta Zero," as the spacing between the carbide lamellae in pearlite. A suggestion was put forward that this factor is a constant in a given volume of pearlite, and therefore can be considered as a characteristic of both pearlite as a microscopical constituent and, also, of the heat treatment of steel. These views have been subsequently developed in a series of papers, where various aspects of the question were treated and the methods of computing the Δ_0 given. To check these views special researches were carried out in England, France, Poland and Czechoslovakia, and especially in the United States, by O. V. Greene.

Examining pearlitic structures produced by usual velocities of cooling, we found that the spacing Δ_0 was pretty constant, being a function of the temperature of transformation Ar_1 and of the velocity of transformation. In specimens cooled in air the limits were between 270—280 $\mu\mu$ (milli-microns) and from 300 to 360 for those cooled in sand; these last named figures are the most usual and those met with in the daily laboratory practice. Mr. O. V. Greene examined rails of eutectoid composition and found Δ_0 from 266 to 376$\mu\mu$. Their respective Brinell Hardness numbers were from 302 to 215, giving a formula: $H \times \Delta_0 = 79.59$, where H is the hardness and Δ_0 — the spacing (the interlamellar distance).

In his Campbell Lecture Mr. Bain has described pearlitic structures of 210, 265 and 315 Brinell; these would correspond to Δ_0 of 379, 300 and 253$\mu\mu$. As Mr. Bain calls the first "coarse" and the last "medium," we can say, that, "microscopically," his coarse pearlite is just a little above the medium limits for sand cooling, and his medium pearlite will be one characterized by spacings from 253 to 300$\mu\mu$. As these figures correspond well with those of Greene and those we have examined for a considerable period of time, we may put forward the suggestion, that instead of qualitative designations like coarse and fine, pearlites be classified according to their interlamellar distances Δ_0. As stated in our papers, these spacings can be perfectly computed from photomicrographs at a magnification of 1000 to 2000, provided the N. A. of the lens is sufficient, i.e., of the usual value of 1.32. Such lenses are now included in the equipment of most of the research and even work-laboratories. That the method does not present any difficulties is best shown by the above mentioned work of

O. V. Greene, which was accomplished at a works laboratory, as a part of routine examination.

From the material at hand, our impression is to include in the class of "medium" pearlites those with spacings around 300 to 350 $\triangle_0$, i.e., to go a little higher than in the samples of Mr. Bain. As to the "fine" pearlite, he mentions structures with 45 Rockwell C, and, in another place, with a Brinell hardness of 340; this last figure would correspond to a spacing of 234 and is a little below the value of 250$\mu\mu$. Examining structures with such spacings we have noticed, and that observation was also confirmed by Mr. Greene, that lamellar pearlite becomes irregular and the mechanical properties begin to show a sudden change.

In a paper presented in 1925 to the Royal Society on the Inner Crystalline Structure of Ferrite and Cementite we have shown that the microscopic analysis of ferrite reveals the existence of small isolated "cubes," with an edge of about 250$\mu\mu$. Similar cubes were observed in martensite by Lucas. In this and in following papers to the Iron and Steel Institute (1931; on Nodular Troostite) and in the *Revue de Metallurgie* (1935; on the Genesis of Pearlite) the nature of this "secondary" structure was examined and related to that of the spacings ($\triangle_0$) in pearlite. It seems, that for all spacings exceeding that of the edge of the "little cubes" (250$\mu\mu$), the designation PEARLITE can safely be applied, as composition and mechanical properties vary but slightly and are function of the $\triangle_0$. As soon as we step outside the mentioned limits, properties begin to change rather abruptly, and we arrive at a product with a set of different mechanical properties, notwithstanding the fact, that under microscopical examination it remains a lamellar structure.

In our paper on "Nodular Troostite" (1932, *Journal*, Iron and Steel Institute, No. II, f. 1931, pp. 195-214), examining various structures of this type and, among them, a beautiful photomicrograph sent us by F. F. Lucas, we arrived at the conclusion that the spacing in Nodular Troostite is about 100$\mu\mu$. Thus troostitic structures not only prove to be lamellar, like pearlite, but also, like pearlite, can be defined quantitatively. The hardness of troosite, in the vicinity of 450 Brinell is considerably higher than that of pearlite, which latter varies from about 200 to 300. On the other hand, the hardness of troostite is considerably lower than it would be if it complied with Greene's formula. This fact, as well as its formation at the critical point Ar′ put troostite in a class by itself and explains the popularity of its name in work practice.

In the same paper we have mentioned that lamellar structures intermediate in hardness and in spacings correspond to sorbites. These are more closely associated with pearlites, than troostite, but a clear demarcation line between pearlite and sorbite is supplied by the fact, that sorbitic structures do not comply, in common with troostite, with Greene's formula, this latter being applicable only to true pearlites.

Thus, pearlite, sorbite and troostite have in common their origin, at velocities of cooling not exceeding the critical one; and, resulting from this, a lamellar structure of a various degree of fineness. Nevertheless, all three possess distinct and different characteristics. Pearlite is a eutectoid of a mean carbon content of 0.9 per cent carbon; its temperature of occurrence is the eutectoid temperature Ar_1; its spacing under usual conditions of cooling is 300 to 350$\mu\mu$; its hardness varies between 200 to 300 Brinell, in accordance

with Greene's rule. Troostite is a lamellar structure of a varying carbon content, of a spacing of about 100$\mu\mu$ and with a hardness of about 450; it is formed at the Ar' point (Portevin and Garvin). Sorbite is a lamellar structure intermediate in spacing and hardness between pearlite and troostite, but possessing a set of properties which made heat treatments resulting in its appearance widely used in work-practice and make the retention of its name desirable.

Prof. C. Y. Clayton, in his letter to METAL PROGRESS (1934, No. 3, p. 43) on Sorbite suggests for these constituents the designation "primary." Mr. Bain (p. 251) also considers them as being happily chosen, "if it were not," adds he, "for the tacit assumption that there was something discontinuous in the lamellar series." The purpose of my papers and of that communication is to show that there is some ground to admit such discontinuity. Then, the objection for the retention of the names would be overcome. Thus, it seems to us that Prof. Clayton's suggestion could be adopted, and the three constituents put into one "Lamellar" group, under the designation of primary pearlite, sorbite and troostite.

It seems, however, to us, that a way can be found to avoid the use of two names, and to continue to call the "cooling" constituents, pearlite, sorbite and troostite. This could be done by an extension of the name "Osmondite" to "temper" troostite and sorbite. Such extension had been discussed at the time of the introduction of the term of Osmondite by Heyn, but had to be dropped in view of Osmond's reluctance to see the name of his teacher Troost superceded by his own. It seems to us that Osmond's wishes would be complied with by the retention of the designation TROOSTITE, for the nodular troostite, and, in spirit, his intentions would be respected. On the other hand, the difficulties mentioned by the present authors and by those who previously took part in the discussions in METAL PROGRESS would also be met with. The lamellar series, arising at cooling, will form a series by themselves, and those, resulting from the decomposition of martensite would bear the name of the founder of the modern metallographic methods, Floris Osmond.

The authors also object to the use of the name GLOBULAR PEARLITE, their objection being that once globular pearlite ceases to be an iridescent component, and *eo ipso* to be pearlite. We do not think that the objection is so serious as to necessitate the departure from a well established name in practice. The main characteristic of pearlite is its being a eutectoid, i. e., a mechanical aggregate of ferrite and cementite of a medium eutectoid carbon content; its lamellar structure on cooling is a very important, but secondary property, as the number of eutectics and eutectoids of lamellar composition is very small indeed. Therefore, we would suggest the retention of that name also.

To sum up, we should welcome the materialization of the authors' suggestions for the better definition and classification of the constituents at cooling and on tempering, but should like to see this end achieved with a minimum departure from the views of the fathers of the present day nomenclature Osmond and Howe, and also, from the present day practice, which in the main is following them. This could be arrived at, by continuing the use of the names pearlite, sorbite and troostite—in the "cooling" (lamellar) series, and by the extension of the designation OSMONDITE to cover the temper structures.

Oral Discussion

HOWARD SCOTT[1]: Figs. 23 and 24 are a very material contribution to our knowledge of mechanical properties of hardened steel. Presumably the steel tested is a plain carbon steel. A statement of its carbon content would be useful. Apparently it is too low in ductility for a carbon steel which suggests that perhaps the advantages to be gained by alloys may be associated, at least, in part, with this spheroidal condition.

O. V. GREENE[2]: It is to be regretted that the authors do not refer to the work of Col. N. T. Belaiew in the discussion on pearlite. Col. Belaiew's work, as reported in texts and to the British Iron and Steel Institute, helps to clarify the qualitative terminology used for describing pearlite. In his work, the fineness or coarseness of the true pearlite grain, i.e., the distance between the lamellae on a normal plane, is reported in microns. This method affords a quantitative measurement for lamellar pearlite. The nature of troostite and sorbite as recorded by the authors here has also been described by Belaiew.

LOUIS ZIFFRIN[3]: Mr. Vilella mentions the name ledeburite. This constituent, I believe, should be confined to the cast iron series, as it is the eutectic containing 4.3 per cent carbon at 1130 degrees Cent.

Pearlite and its decomposition products as given by Arnold show:

1st stage. Sorbitic pearlite with emulsified Fe_3C with a strength of 140,000 pounds per square inch maximum and 10 per cent elongation.

2nd stage. Normal pearlite with some segregated Fe_3C, having a tensile strength of 110,000 pounds per square inch and elongation of 15 per cent.

3rd stage. Laminated pearlite with completely segregated Fe_3C (normal pearlite), having a tensile strength of 70,000 pounds per square inch maximum, with 5 per cent elongation in 2 inches.

4th stage. Laminated pearlite passing into massive Fe_3C and ferrite, having a tensile strength of 60,000 pounds per square inch.

Here we see pearlite passing from a stage showing structural fineness, or the 1st stage, to a structure showing a decided deterioration of quality, or the 4th stage, where the structural components break up into larger and larger masses of Fe_3C and ferrite.

Pearlite, aside from being recognized by its pearly appearance, is of a definite eutectoid ratio containing 87.25 per cent ferrite and 12.75 per cent cementite. Sorbitic steels do not necessarily on heating distribute their cementite into pearlitic patches of a definite eutectoid ratio plus free ferrite or free cementite depending on whether the steel is hypoeutectoid or hypereutectoid. Instead, the cementite is distributed more uniformly among all the ferrite present.

On naming the aggregate constituents as suggested by Messrs. Vilella, Guellich and Bain, much importance should be placed upon the different stages of pearlite and the corresponding changes in its mechanical properties.

The authors should be commended for what we hope may be a start toward a probable revision in naming the aggregate constituents in steel, and it is hoped that more work will be done on this subject.

---

[1]Westinghouse Research Laboratories, E. Pittsburgh, Pa.

[2]The Carpenter Steel Company, Reading, Pa.

[3]Metallurgist, Testing and Research Laboratories, Deere & Company, Moline, Ill.

Authors' Closure

It is always a satisfying circumstance to find that one's views, arrived at after years of thought and criticism, are concurred in by others; when the confirmation is offered by Dr. Hoyt it is an enhanced satisfaction. We note with especial interest the suggestion that due consideration be given the views of metallographists in other countries. This remark is timely since already new names have been employed for some of the structures in Germany. We venture to guess that there will exist everywhere the same conservatism and reluctance toward a change of names, particularly on the part of those authorities on the subject whose greatest familarity is with the steels which develop only constituents about which no inconsistency is encountered.

The clear and concise remarks of Messrs. McCarthy and Cameron will illustrate the point that for some fields of steel metallography, the present scheme of naming constituents is utterly unsatisfactory. They propose a suitable modification to remove all ambiguity in respect to their particular field of interest, and we would concur entirely with it in its broadest implications. The fact that the manufacturers of steel wire products have faced the problem and found its solution should lend weight to the case against the present ambiguous system of nomenclature.

We find ourselves in sympathy with the views of Howard Scott, who would welcome a sharper distinction between constituents having different names. No one surely can disagree very seriously with his concept of pearlite, if only the word "spheroidized" is not carelessly omitted when it should be employed. (The physical properties are quite different for lamellar and spheroidized structures even of the same hardness). Our thought is that when the distinction between constituents becomes too difficult to find, then the diagnosis is definite, i.e., too many names. Again we propose dropping one of the names applied to tempered martensite.

It is a great pleasure to have a communicated discussion from Colonel Belaiew, who has for many years been an outstanding authority on the structure pearlite. His careful studies of inter-lamellar spacing has been of great importance in understanding this constituent, and O. V. Greene has employed his methods to good purpose in this country. For a quantitative classification of pearlite, nothing could serve better than the inter-lamellar spacing and we would heartily concur with Colonel Belaiew's proposals. We debated whether or not to include a discussion of the Δ_0 concept, and only the thought of conserving space led us into what now is shown to be a serious omission.

We are, however, unable to recognize a really important and fundamental discontinuity in the lamellar structures which should warrant a special name, or special names for the finer ones. To be sure, the fine lamellar structures are less regular than the coarser ones, but this is a progressive change and it has long been known that Ar′ is not a temperature relating to equilibrium, but merely a function of cooling rate.

It is no criticism of the work of O. V. Greene, which the authors hold in high esteem and to which they have frequently referred, to say that there is no reason *a priori* why a certain linear relation should exist between lamellar spacing and physical properties. Only measurement alone can establish

the relationship for any steel, and it is purely fortuitous that over a wide range of spacings a simple mathematical relationship expresses well enough the numbers actually found by measurement of spacing and properties. A departure from the approximate rule is more or less to be expected.

If one regard the variation of the composition of pearlite for any particular steel one will find that it widens as the cooling rate increases and as the actual temperature of formation falls and as the lamellar spacing decreases. If at some particular point in these series the name is suddenly changed to sorbite, the limits of composition will still be the same. All these features are quite *gradually* changed as the temperature of formation decreases. This was particularly evident in the work which was in part published by Davenport and Bain, A.I.M.E. Technical Paper No. 348, "Transformation of Austenite at Constant Subcritical Temperatures." Nevertheless, a very attractive possibility for a unanimity of opinion on names lies in the suggestion of Clayton that the word "Primary" set off the lamellar series from the tempered martensites, as pointed out by Colonel Belaiew. It would be fitting to hear the name of Osmond, as well as others of the pioneers, more frequently spoken in referring to the constituents, if only too great change is not thereby involved.

As Mr. Ziffrin points out, ledeburite is not exactly pertinent to the present discussion since it is a cast iron constituent and occurs in steels so rarely,—mainly in certain high carbon, high chromium die steels, and in high speed steel. We are not quite certain as to the inference to be drawn from the reference to Arnold. Certainly it is not accurate to consider any individual specimen of sorbitic pearlite as passing to a more coarsely laminated pearlite. At any temperature (short of the re-establishment of austenite) the only change which a "sorbitic-pearlite" can undergo, is spheroidization. Any one may easily satisfy himself on this point by heating such a finely lamellar pearlite, as we believe is meant, and observing the changes. A coarse lamellar structure is always so formed directly from austenite,—never to our knowledge from anything else. In this connection it is strange that the investigators who taught that lamellar pearlite formed from martensite through the series martensite-troostite-sorbite-pearlite did not try heating martensite to the appropriate temperature, and then report just what really resulted. The interest in, and the appraisal of, the problem, as expressed by Mr. Ziffrin, is appreciated and lends weight to the trend toward a better system of nomenclature.

With reference to the data on Figs. 23 and 24, it should be mentioned that these specimens employed were sub-standard, ¼ inch diameter by 2 inch gage length, and that the composition of the steel was as follows:

Carbon 0.84 per cent, manganese 0.23 per cent, silicon 0.205 per cent, sulphur 0.011 per cent, phosphorus 0.020 per cent, chromium 0.11 per cent.

In conclusion, we would like to re-state our main contention with respect to the lamellar series in the language employed by Dr. Hoyt, "Those constituents which form from austenite on cooling, to produce aggregates of ferrite and cementite, are genetically and genitically the same, and should be given the same name." The same reasoning applied likewise to the constituents formed from martensite upon heating completes a logical path toward simplicity in names.

ENDURANCE OF CASE HARDENED GEARS

By O. W. McMullan

Abstract

This paper describes the results of dynamometer breakdown tests of rear axle drive gears and pinions. Tests on oil hardened and several case hardened steels are given. Comparison of results are made with physical properties obtained on laboratory test specimens. The conditions of service make it necessary for the pinion to resist softening due to high operating temperatures at tooth contacts under conditions of partial lubrication while the gear is better cooled and lubricated and requires a strong steel with good wear resistance at lower temperatures. Wear was found to be excessive on medium carbon, oil hardened steel. S.A.E. 4615 directly quenched gave good results in pinions, and double treated Krupp and S.A.E. 4820 in gears gave the best results among those steels tested.

Properties Derived from Laboratory Tests

A PAPER presented by the writer at the last convention of the Society[1] contained data on the physical properties of several analyses of case hardened steel of different grain sizes, case depths and heat treatments. The conclusions arrived at were that, with the exception of fine-grained S.A.E. 4615, steels case hardened by direct quenching decreased in load-carrying capacity with increase of case depth. The decrease in strength was more noticeable with higher alloy contents. When cooled in compound and single treated, this tendency was reversed with the lower alloy contents and lessened with the higher. The strength of all double treated samples increased with increase of case depth. Highest load-carrying capacities were obtained with the higher alloy steels such as S.A.E. 2512, 4820 and Krupp and the uncased oil hardening steels were comparable in value to those steels both for load-carrying and shock resistance.

[1]O. W. McMullan, "Physical Properties of Case Hardened Steels," Transactions, American Society for Metals, Vol. 23, June 1935, p. 319.

A paper presented before the Seventeenth Annual Convention of the Society, held in Chicago, September 30 to October 4, 1935. The author, O. W. McMullan, is a member of the Society and is metallurgist with the International Nickel Co., Bayonne, New Jersey. Manuscript received May 1, 1935.

The results obtained from those laboratory experiments, taken by themselves, would point to the conclusion that for many steels and treatments shallow cases would give a better combination of physical properties than deep cases, and if double treated the higher alloy case hardened steels and the oil hardened steels would give the best service. There are, however, other factors which enter into the life of case hardened parts in practical applications which show such a conclusion would be wrong for certain types of service.

Description of Dynamometer Tests

To approach closely service conditions, dynamometer tests were made on a number of steels with various heat treatments. They were made into automotive rear axle spiral bevel drive gears and pinions and tested to destruction with inspection at regular intervals. The tooth load applied was equal to 60 per cent above full motor torque at low speed of the truck motor for which the gears were designed. This was 6400 foot-pounds which gave a calculated stress of 52,500 pounds per square inch in tension at the root of the tooth. The lubricant used was in quantity equal to that of a similar rear axle for production and contained an E.P. addition. Housings were water cooled to keep the maximum oil temperature around 200 degrees Fahr. Surface temperatures at tooth contacts were unknown but became sufficiently high in many cases to discolor the steel. The pinion speed was 350 revolutions per minute and the gear ratio 6⅗ to 1. Table I shows the average of three sets on each of the steels and treatments listed.

Types of Failures

Three typical sets were photographed to illustrate types of failure. Figs. 1 and 2 are of a pinion and ring gear made from S.A.E. 4340 not case hardened. The parts were heated in a furnace at 1525 degrees Fahr. (830 degrees Cent.) quenched in oil and drawn at 400 degrees Fahr. (205 degrees Cent.). The average life of 67,300 cycles obtained was reasonably good before final failure but it will be noticed that considerable wear occurred. Wear to the extent shown would destroy accuracy of bearing contact, increase backlash, and cause gears to be noisy. Heating up in operation at the point of tooth contact probably did not enter into the failure since the

Table I

Endurance Records

Ring Gear Steel and Treatment	Pinion Steel and Treatment	Number of Cycles	Remarks
S.A.E. 4340 Not cased. 1525° F. Oil. 400° F. Draw.	Same.	67,300	Failure by teeth breaking out of gears. Both pinions and gears show much wear.
S.A.E. 4340 Carburized. 1525° F. Oil. 400° F. Draw.	S.A.E. 4340 Pot quench. 400° F. Draw.	35,700	Gears failed by teeth breaking out without much wear. Pinions show some wear and pitting of root at heel of teeth.
S.A.E. 4340 Carburized. 1525° F. Oil. 600° F. Draw.	Same. Pot quench. 600° F. Draw.	37,600	Many teeth broken out of the gears. Teeth show some wear. Pinions pitted at root of heel.
S.A.E. 4340 Carburized. 1525° F. Oil. 800° F. Draw.	Same. Pot quench. 800° F. Draw.	52,700	Many teeth broken out of the gears. Not much wear. Pinions badly pitted and scuffed.
S.A.E. 4340 Not cased. 1525° F. Oil. 400° F. Draw.	S.A.E. 4615 Pot quench.	81,000	One or more teeth broken out of gears. Not much wear on either gears or pinions.
Krupp Cool in pot. 1550° F. Oil. 1400° F. Oil. 300° F. Draw.	Krupp Pot quench. 1400° F. Oil. 300° F. Draw.	43,700	One to three teeth out of gears. Pinions badly scuffed and pitted.
Krupp Cool in pot. 1550° F. Oil. 1400° F. Oil. 300° F. Draw.	S.A.E. 4615 Pot quench.	108,500	Two teeth out of the gears but they do not show much wear. Pinions not worn much but show some pitting at root.
S.A.E. 4820 Cool in pot. 1550° F. Oil. 1400° F. Oil. 350° F. Draw.	S.A.E. 2315 Pot quench.	65,300	Teeth worn and four broken out of one gear; others not broken but show some wear. Pinions pitted at root of heel. Final failure on two of the three tests was in the differential and the average number of cycles probably should be higher.
S.A.E. 4820 Cool in pot. 1550° F. Oil. 1400° F. Oil. 350° F. Draw.	S.A.E. 4615 Pot quench.	136,000	One to three teeth broken out of gears. Gears show some wear. Pinion teeth pitted at the root of the heel.
S.A.E. 4615 Cool in pot. 1525° F. Oil. 350° F. Draw.	S.A.E. 4615 Pot quench.	50,600	One tooth out of gears; other teeth cracked. Not much wear. Pinions show some wear and pitting.

Note—Except where mentioned all the above pinions were not drawn on the teeth except due to heat creeping up from the stems when the latter were drawn at 1250 degrees Fahr. in lead.

hardness would be little affected. None of the parts were file hard after treatment.

Figs. 3 and 4 are taken from a double treated Krupp pinion and ring gear. After treatment these parts had a scleroscope hardness of 90-95 and the expected martensitic structure in the case with some excess carbide present. The heat treatment produced enough decarburization to form a skin which could be filed. The

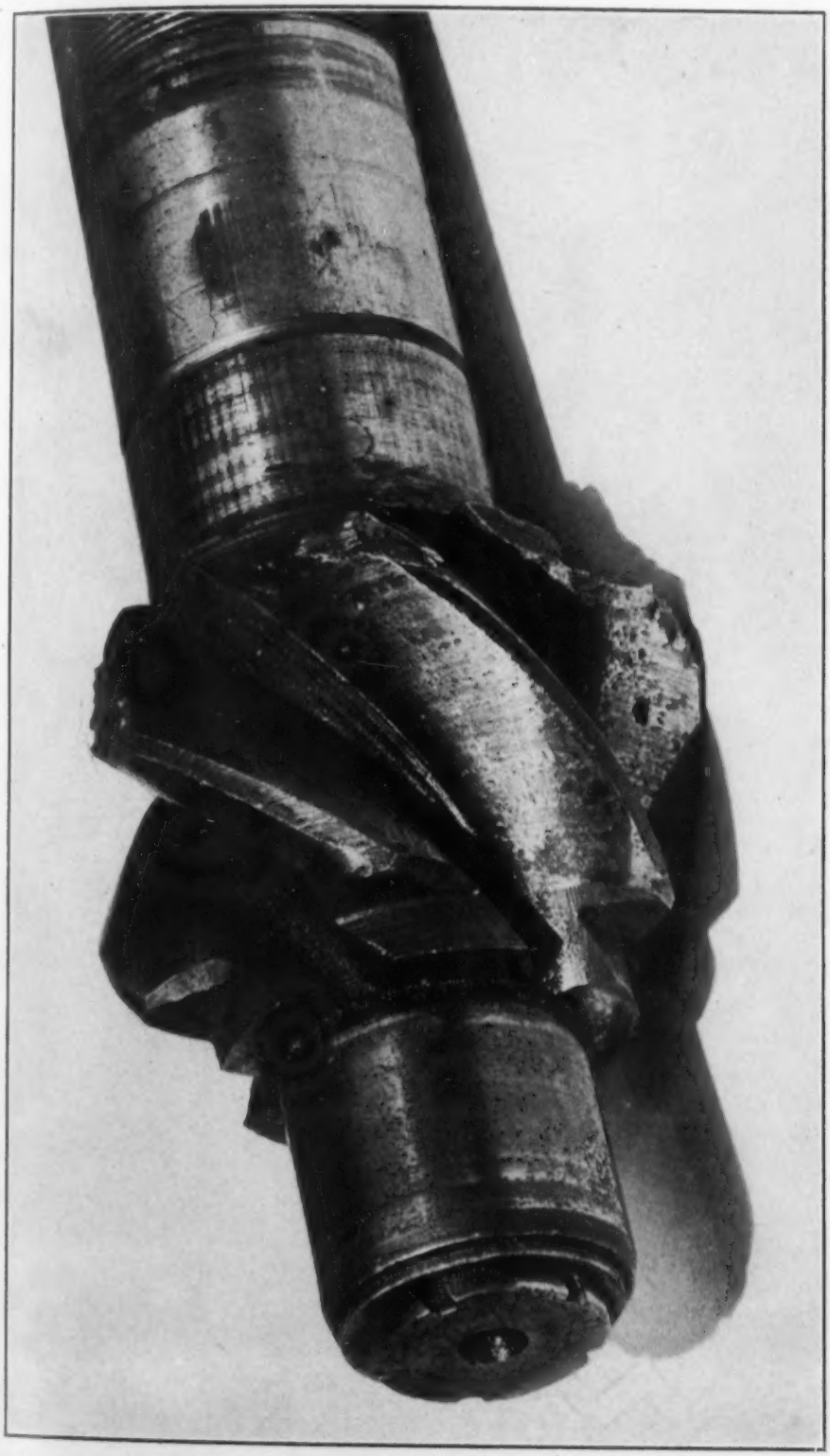

Fig. 1—Rear Axle Pinion Made from S.A.E. 4340 Steel. Not Cased. Quenched from 1525 Degrees Fahr. (830 Degrees Cent.) Into Oil and Drawn at 400 Degrees Fahr. (205 Degrees Cent.).

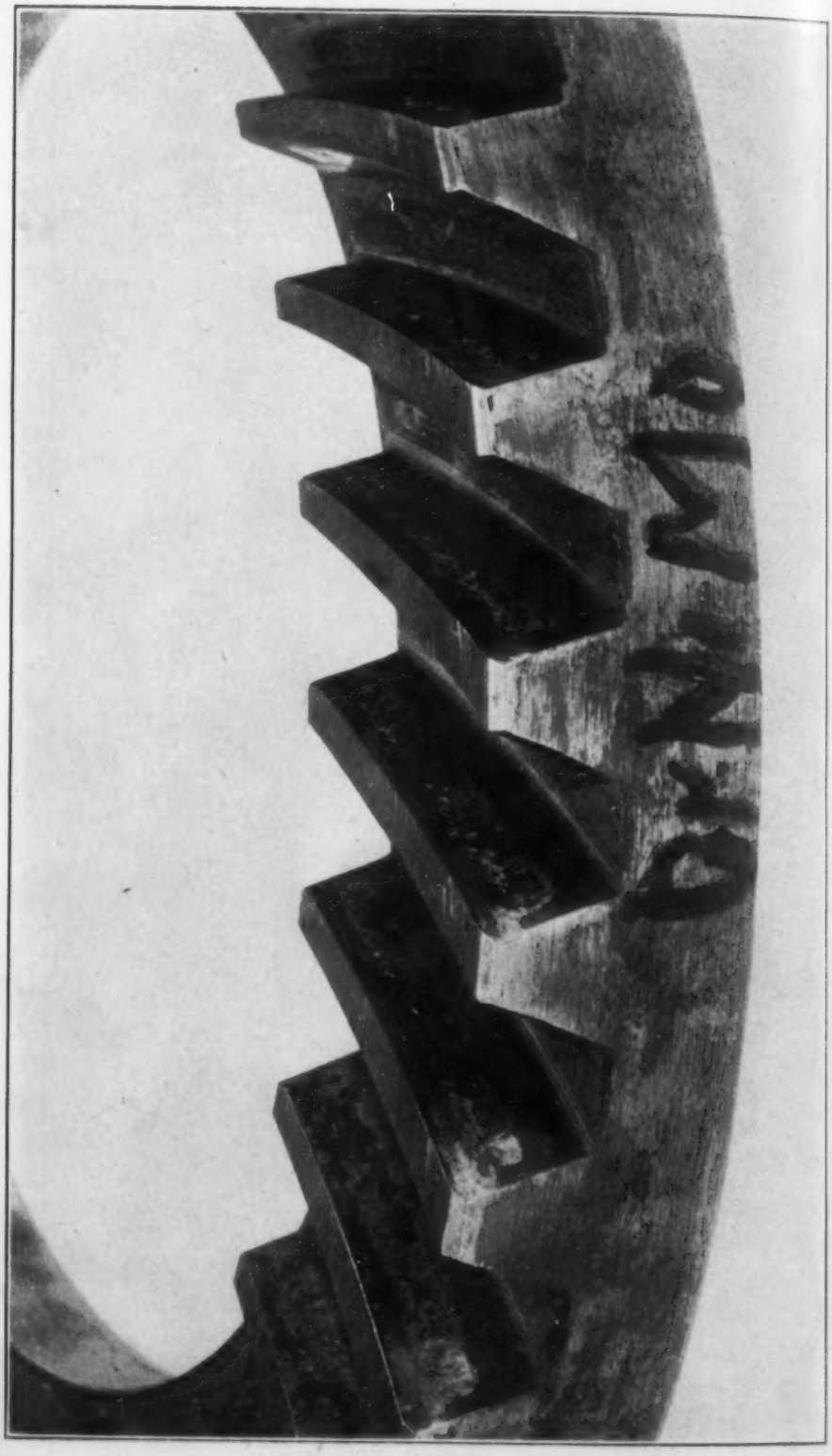

Fig. 2—Rear Axle Ring Gear of Same Steel and Treatment as Pinion of Fig. 1 and Run with that Pinion. Average Life of Three Sets was 67,300 Pinion Revolutions.

Fig. 2—Rear Axle Ring Gear of Same Steel and Treatment as Pinion of Fig. 1 and Run with that Pinion. Average Life of Three Sets was 67,300 Pinion Revolutions.

Fig. 3—Rear Axle Pinion Made of Krupp Steel. Carburized and Cooled in Pot. Reheated to 1525 Degrees Fahr. (830 Degrees Cent.) and Oil-quenched. Reheated to 1400 Degrees Fahr. (760 Degrees Cent.) and Oil-quenched.

Fig. 4—Rear Axle Ring Gear Made of Krupp Steel. Carburized and Cooled in Pot. Reheated to 1525 Degrees Fahr. (830 Degrees Cent.) Oil-quenched; Reheated to 1400 Degrees Fahr. (760 Degrees Cent.); Oil-quenched; Drawn at 300 Degrees Fahr. (150 Degrees Cent.). When Run With the Pinion of Fig. 3, the Average Life of Three Sets was 43,700 Pinion Revolutions.

average life of 43,700 cycles obtained was low. Failure was due to the pinion becoming badly pitted and worn. As a result of this wear the tooth contact changed toward the top of the gear teeth thus increasing the stress at the root of the teeth and finally resulting in cracking and breaking out of gear teeth. During operation the ring gear rotates through the oil and consequently is kept cool but the pinion operates under partial lubrication. Under heavy loads, surface temperatures become high enough to discolor and temper the case so that it becomes soft. The structure of the double treated Krupp pinion was susceptible to considerable softening under these conditions and early failure occurred.

Figs. 5 and 6 are of an S.A.E. 4615 pot-quenched pinion run with a double treated Krupp gear of identical treatment to that in Fig. 4. The average life of three sets was 108,500 cycles. Failure in these sets was due to fatigue and breaking out of ring gear teeth. Neither the pinion nor the gear showed much wear. The partially austenitic structure in the case of the direct quenched S.A.E. 4615 pinion was more resistant to the tempering action arising from sliding tooth contact under pressure in operation. The ring gear rather than the pinion teeth broke out in fatigue since the latter were designed with a heavier section.

Other failures listed in the table can be described as coming mostly within one or more of the above three types of failure. When S.A.E. 4340 was case hardened and drawn at 400 degrees Fahr. (205 degrees Cent.), the teeth of the gears were brittle and early failure occurred by teeth breaking out before showing much wear. Drawing at 600 degrees Fahr. (315 degrees Cent.) did not improve the condition much. Drawing at 800 degrees Fahr. (425 degrees Cent.) increased the life considerably but the pinions were soft enough to wear and scuff badly. The combination of a heat treated gear of S.A.E. 4340 and a pot-quenched pinion of 4615 gave a good life of 81,000 cycles since the gear had the necessary tooth strength and the pinion remained practically file hard at the operating temperature.

When S.A.E. 4615 was used in both the gears and pinions the life was fair but under the high tooth loads used, failure occurred from cracking and breaking out of ring gear teeth. Heating in operation apparently does not influence the life of the gear, the tooth strength only being the deciding factor as long as the pinion stands up. The life of the 4615 gears was not as great as those made from the stronger higher alloy steels. The combination of S.A.E. 4820

Fig. 4—Rear Axle Ring Gear Made of Krupp Steel. Carburized and Cooled in Pot. Reheated to 1525 Degrees Fahr. (830 Degrees Cent.), Oil-quenched; Reheated to 1400 Degrees Fahr. (760 Degrees Cent.) Oil-quenched. Drawn at 300 Degrees Fahr. (150 Degrees Cent.). When Run With the Pinion of Fig. 3, the Average Life of Three Sets was 43,700 Pinion Revolutions.

Fig. 5—Rear Axle Pinion Made of S.A.E. 4615 Steel. Carburized and Quenched Directly from the Pot into Oil.

Fig. 5—Rear Axle Pinion Made of S.A.E. 4615 Steel. Carburized and Quenched Directly from the Pot into Oil.

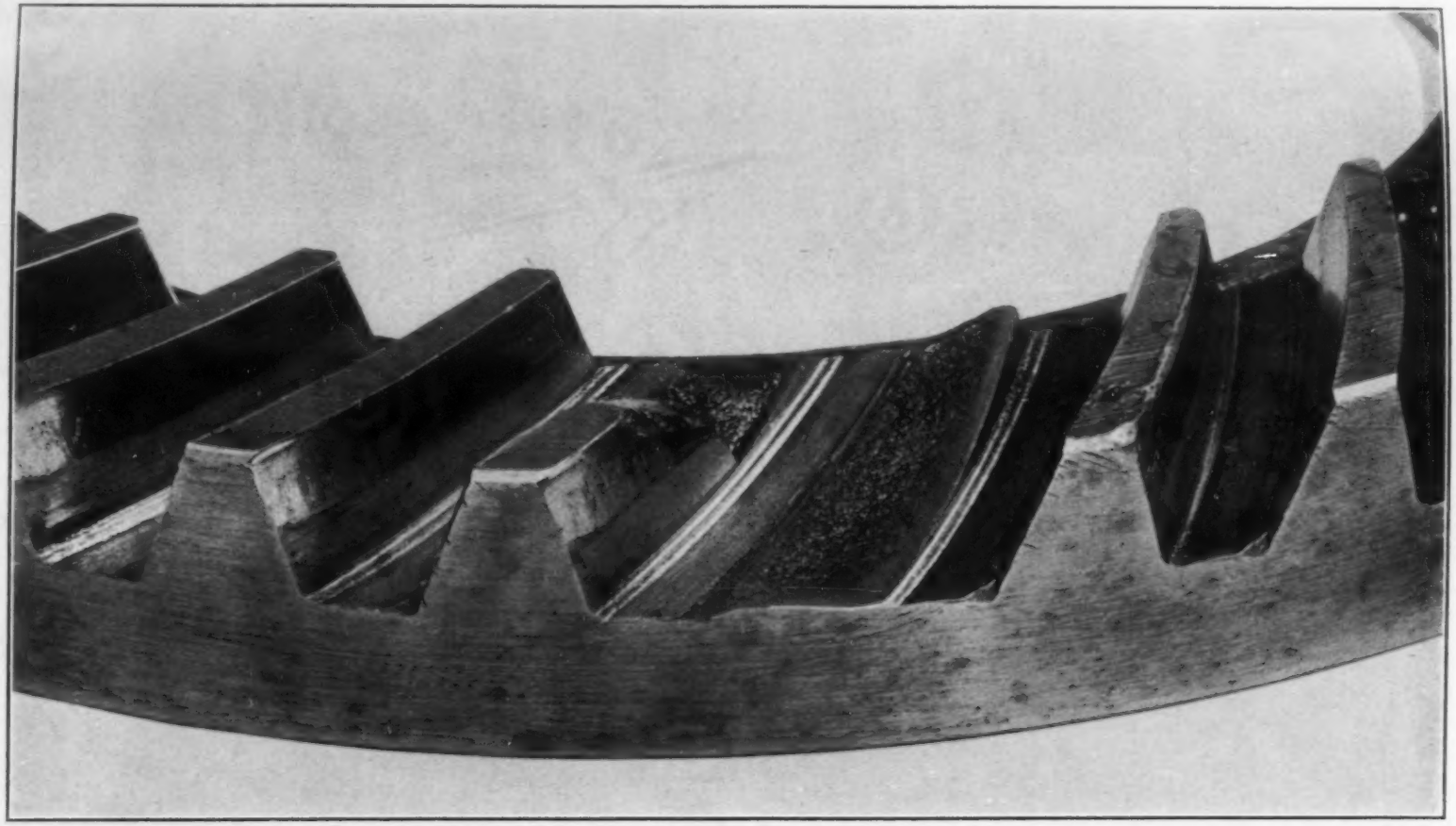

Fig. 6—Rear Axle Ring Gear Made of Same Steel and Treatment as Gear of Fig. 4. When Run With Pinion of Fig. 5, the Average Life of Three Sets was 108,500 Pinion Revolutions.

double treated gears and pot-quenched 2315 pinions was fairly good but failure occurred in the pinions since the structure was not as resistant to operating temperatures as 4615. Gears made from double treated S.A.E. 4820 and pot-quenched 4615 pinions gave the best results, the average life being 136,000 cycles. The laboratory load carrying tests showed the double treated 4820 to have the highest strength. This combination therefore gave the desired high strength in the gear teeth and the resistance to tempering and softening of the pinion.

Other factors outside of the gears and pinions, such as carrier and housing deflection, undoubtedly had an influence on the results but these outside factors would tend to be balanced in the average of a number of tests. Case depth is another important factor in the life of case hardened gears. However, when deeper than a certain minimum it appears to have but little influence when maintained within rather wide limits. The minimum for the parts tested appeared to be around 0.040 inch of well hardened case.

Conclusion

The dynamometer breakdown tests of rear axle ring gear and pinion sets were made in conjunction with laboratory tests described in a previous paper by the author. It was found that some of the higher alloy gear steels when carburized and double treated had the highest load carrying capacities. Those results have been confirmed in the endurance tests, but it also was found that other factors than strength and hardness as treated may greatly influence the life. The operation of a ring gear and pinion is such that the gear is constantly running in oil and hence is well lubricated and cooled. The pinion is not so well lubricated and cooled and its greater number of contacts produce momentary high surface temperatures which cause tempering and softening thus increasing wear, changing of bearing contacts, and lessening fatigue resistance.

Uncased oil-hardened steels such as S.A.E. 4340 have good tooth strength for the gear but do not have the wear resistance necessary for long pinion life. Double treated Krupp steel has excellent strength but is softened at low temperatures and life is short due to pinion failure. Pot-quenched 4615 apparently has sufficient austenite in the case to maintain file hardness at high operating temperatures and proved to be much better for pinions than stronger steels such

as Krupp. The combination of pinions of pot-quenched 4615 and gears of Krupp or 4820 double treated gave long life because of the necessary resistance to softening and wear and of strength where each was needed. The parts were so designed that the pinions of the weaker steel had sufficient strength when softening of the case did not occur.

It is possible that better results might have been obtained with some of the steels had different treatments been given them to make them more suitable for pinion service. The results indicate that to obtain maximum life, steels must be selected and heat treated according to the service they must perform when highly stressed.

DISCUSSION

Written Discussion: By C. F. Smart, metallurgist, Pontiac Motor Co., Pontiac, Mich.

It has been instructive, indeed, to study this excellent paper. Our own test results on differential ring gears and pinions agree, in general, with those of the author. We find a definite practical difference shown by life tests of gears made from the various steels and heat treating methods generally used for these parts. A careful comparison of heat treating practices for carburized gears has indicated clearly that direct pot quenching of both ring gears and pinions gave considerable improvement over cooling in the carburizing pots, followed by reheating and quenching. Softness of tooth surfaces, whether the result of decarburization through slow cooling in the carburizing pots or by tempering after hardening, decreased gear life. Accordingly, in our practice, direct pot quenching with no subsequent tempering operation was adopted for both ring gears and pinions with highly gratifying results.

We agree with the author that the case depth for maximum life must not fall below approximately 0.040 inch. Tests run for determining the effect of case depth showed beyond doubt that tooth failures occurred earlier with a thin case. The reason for this has been ably pointed out by Almen and Boegehold in their paper, "Rear Axle Gears, Factors Which Influence Their Life," recently presented before the American Society for Testing Materials.

Every example of differential ring gear or pinion tooth failure which has ever come to our attention indicated clearly by the nature of the fracture that failure was by fatigue, never by impact. Assuming proper tooth contact in the original gear setting, and assuming adequate rigidity of the supporting members, then the relative gear life for a given design and intensity of loading is dependent upon (1) the inherent strength of the gear tooth, both case and core; and (2) the resistance to change of tooth contact by wear, scoring or pitting. Proper tooth contact is vital to good gear life, and undoubtedly many tooth failures, noisy gears and scored gears have been due to laxness in this regard. For these reasons, those elements of gear steels and gear practice which affect machining, distortion in heat treatment, case depth and hardness, and core structure and strength, must all be given due consideration. We have dif-

fered from the author's practice in regard to preferred grain-size of the gear steel, our preference being for a medium grain rather than a fine-grained steel. This is because the fine-grained steels require considerably higher annealing temperature to produce a structure satisfactory for machining, and because we feel that the medium grained steels respond better in carburizing and hardening treatments.

It is our belief, based on carefully conducted comparative tests, that there is considerable difference in the life of gears made from some of the commonly used alloy carburizing steels. The following tabulation is offered in evidence of this statement:

		Hours 4-Square Life		
Steel	No. of Tests	Minimum	Maximum	Average
3115-A	6	215.5	1134*	574.4
2315-A	12	66.58	812.5	341.98
4615-A	9	50.5	283.5	168.53

*No failures on this set.

These tests were run on 4-Square equipment, under closely observed set-up for proper tooth contact, on gear sets of the same design, run with identical conditions of loading, lubrication, etc. Material conditions—All were 4 to 6 McQuaid-Ehn grain-size, five point carbon ranges, carburized and pot quenched, 0.040 to 0.050 case depth, file hard tooth surfaces, and Rockwell (33) C minimum core hardness in center of tooth.

Axle shaft speed 436.6 revolutions per minute. Propeller shaft speed 1940.6 revolutions per minute. Load—219.3 foot-pounds torque in propeller shaft. Direction of load changed each 2 hours. Direction of rotation reversed each half hour. Cycles covered by test—Ring gear 1,322,898 to 29,706,264; Pinions—5,880,018 to 132,038,424.

The hardened case of the 3115 steel appears to offer greater resistance to wear and pitting than either of the other steels tested, and the improvement in fatigue life is believed to be due to this factor. It is probable that running tests at maximum torque loads for fewer cycles fail to bring out this factor as well as lesser loads more nearly representative of average service.

Mr. McMullan's data on S.A.E. 4340 steel not carburized is interesting. While we have no data on ring gears and pinions made from steels of this type, we are reminded of work done a number of years ago on 0.50 per cent carbon, chromium steel gears for transmissions. Heat treating practice on these was to harden by oil quenching from 1500 to 1525 degrees Fahr. followed by tempering at 425 degrees Fahr. Comparative tests in transmissions absorbing full torque through second speed gears showed that gears which were hardened from a cyanide bath, with about 0.005 inch penetration of cyanide case, ran at least ten times longer before pitting of tooth surfaces occurred than in the case of open furnace hardened gears. Such results again emphasize the importance of the surface layer in gear tooth life.

I take this opportunity to assure the author of our appreciation of this and other work which he has presented.

Written Discussion: By E. F. Davis, metallurgist, Warner Gear Co., Muncie, Indiana.

The writer wishes to compliment Mr. McMullan on this excellent treatise and considers it a very valuable contribution to gear metallurgy.

In endurance runs of gears, failure generally ensues from fatigue cracks

which usually originate at the base of the teeth. Generally a deep etch will reveal most of the teeth have fatigue cracks of varying depths but which have not progressed as far as those which have actually failed.

Wear almost invariably occurs first. Unless the metal is actually defective the tooth surfaces show considerable erosion near the pitch line before any teeth break. Fatiguing always seems to follow the destruction of the true involute pathway of the rolling gears and the life on the dynamometer run is in proportion to the maintenance of correct tooth form. Mechanical errors likewise affect the endurance of a dynamometer run.

Assuming the mechanical errors are at a minimum and nearly true rolling action is maintained then the only factor is the preservation of surfaces hard enough to maintain the true involute. The excellent service of direct cyanided gears when steels are used having cores testing over 400 Brinell and therefore brittle indicates the importance of presenting the hardest possible surface on the gear teeth.

The operation of carburizing is the synthetic production of a tool steel case of varying carbon content ranging from 1.35 per cent carbon down to approximately 0.50 per cent carbon, being highest of course on the outer layers and gradient. In this carburized case are liable to be outer layers extremely brittle with a tendency to spall or crack and with different physical properties and response to heat treatment through the carburized area. The extreme outer layers of certain alloy steels carburized and hardened are liable to contain considerable austenite. The writer has observed ring gears which scored very quickly due to an austenitic skin.

Another phenomenon which sometimes occurs when gears are carburized deeply is the exhaustion of the carburizing gases and an unbalanced C, CO and CO_2 reaction toward the end of the operation whereby the carburizing gases react with the carbon deposited in the steel and this decarburized surface ultimately reduces the wearing qualities. This could likewise occur when light case work is carburized if the carburizer were weak or the sealing of the box improperly done, but the hazards are always greater when the carburizing time is prolonged. Slightly decarburized surfaces develop fatigue cracks very quickly under overload.

We are concerned solely with the preservation of outer surface for long endurance runs. Since tooth wear develops before fatigue failure we should carefully investigate the area close to the surface as the most important cause of Mr. McMullan's results.

Written Discussion: By O. J. Horger, 2034 Dorr Street, Ann Arbor, Michigan.

The author shows in Table I how the life of the various steel and heat treated gears compare at one particular load. If the test load used represented service conditions, then the merit of the gears may be rated in order of their life. Since it becomes impractical to select any one test load as representing service conditions, Table I in itself may become very misleading. The accompanying curves illustrate this point.

The author is testing on the slope of the S-N curves for gears A,B,C, and D as shown at load giving stress S. It is apparent that while gear B has longer life than gear A at the same stress S, that at some other stress this con-

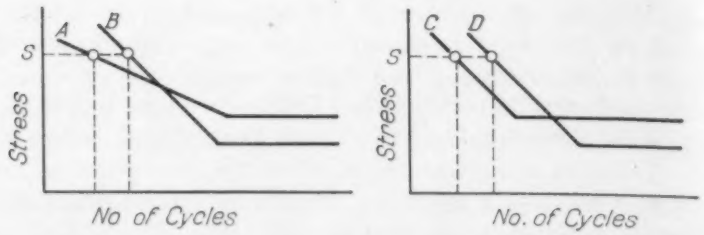

dition is reversed. A similar condition is exhibited by gears C and D.

It would also appear from the paper that test conditions of deflection of gear and mounting parts as well as lubrication give failure conditions not simulating service conditions. The single variable of oil viscosity at tooth contact under service conditions is an important factor in contact stress problems and associated with satisfactory gear operation.

Therefore it would appear as though the author should make tests at least at several different loads in order to justify the making of conclusions.

Written Discussion: By A. L. Boegehold, metallurgist, General Motors Corp., Detroit.

In the author's conclusion it is stated that the results of laboratory tests, showing load-carrying capacities on some of the higher alloy gear steels carburized and double treated were confirmed in rear axle endurance tests. It would appear, for reasons which will be given, that any correlation that was observed between the laboratory results obtained with flexural tests and results of rear axle tests were purely accidental. In paper by J. O. Almen and the writer on rear axle gears, presented before the American Society for Testing Materials in June 1935, it was rather conclusively demonstrated that a high strength obtained in a flexural test does not indicate that a similar result will be obtained in a rear axle test.

There are several factors operating in a rear axle test, not presented in a laboratory test, which prevent an ordinary flexural test from being an indication of durability of material in rear axle gears. Under the conditions of the author's tests apparently one of the most important was the operating temperature which was sufficient to cause softening of the steel. The second factor is the influence of stress concentration caused by the notch effect at the bottom of the tooth. Another factor which is very important in determining the durability of rear axle gears but which was not mentioned by the author is the change in tooth contact caused by distortion of the gears in the heat treating process. Depending upon the nature of the contact between the gear teeth, the actual stress existing at the bottom of the tooth may be increased considerably. It should be clearly understood also that only a small change of stress intensity will cause a considerable change in fatigue life so that all the difference in life from the minimum to the maximum, cited in the table by the author, could easily be accounted for by variation in stress intensity.

It is well known that a steel like S.A.E. 4340 is a decidedly deep hardening steel, therefore would tend to distort a great deal more in hardening than a gear made from low carbon steel and carburized. It is believed that the early failure of gears made of S.A.E. 4340, case hardened, was due to a large extent to the increase of stress concurrent with distortion and poor tooth contact.

A parallel result was experienced and described in the above paper in connection with S.A.E. 2330 steel, case hardened. This steel showed the highest strength in a plain flexural test and the highest fatigue endurance limit in a plain rotating beam fatigue test but showed a relatively short life when tested as a rear axle drive pinion. In these tests the torque imposed was somewhat lower than in the tests described by Mr. McMullan, therefore, the problem of softening due to a high operating temperature was not present.

Summing up, it might be appropriate to repeat a word of caution to those selecting materials for gears that a plain flexural test is very unlikely to indicate what may be expected from that material in a rear axle gear and also that one of the most important considerations in selecting a gear steel is that it shall permit heat treating with a minimum distortion so that tooth stress will not be greatly increased by a bad tooth contact with the mating gear.

Oral Discussion

H. F. Moore:[1] I have not had a chance to put my discussion of this paper into writing, but I want to ask one or two questions in order to make the procedure carried out in the tests a little plainer to my own mind.

The first question is—approximately what load in the tests described was applied as compared with the maximum service load which might have been expected? In general, in repeated-stress phenomena, short-time tests have proven rather unreliable as an index of behavior under service load. As has been pointed out by the previous discusser, this is due to the changing importance of different factors, notably strength and ductility, and I would like to have the author explain in his closure whether the test loads were much above ordinary service loads, or whether they were slightly above such loads, perhaps about maximum load which might be expected in service.

The second comment I would like to make is a reinforcement of the comment of the last speaker. The evaluation for service of the gear both in this paper and in the other paper mentioned was necessarily based to a certain extent upon the life of the gear under test. I want to emphasize the point made by the last speaker, that a considerable increase in test life is nowhere near as significant as the same proportionate increase in stress. In the fatigue testing of metals an increase of life of 100 per cent between two specimens would not be viewed as anything very remarkable. An increase of life of four or five times would be of interest, and a ten-fold increase of life would be regarded as distinctly significant. I merely mention this item from the viewpoint of a man interested in the fatigue testing of metals, wondering how far the results obtained in fatigue tests could be used in connection with this test.

Above all, I wish to say I am very glad indeed to see papers like this one and the other one referred to, throwing new light on the various effects of repeated stress. Nothing could be worse for either the laboratory or the service practice than worshipping any one test for strength under repeated stress, and I am very glad to see various test methods presented and discussed.

Author's Closure

The data presented by Mr. Smart are a valuable addition to the paper.

[1]Research Professor of Engineering Materials, University of Illinois, Urbana, Illinois.

Since our findings are quite well in agreement no further comment is necessary except to thank him for presenting that data and for the interest shown in the paper.

The writer agrees with Mr. Davis that the maintenance of correct tooth form is of great importance to the endurance. Many times cracks follow wear and change of tooth form but fatigue failure may progress in some different manner depending upon the design of the gear teeth. The pinion teeth in the tests cited failed by wear and pitting along the root since the tooth form was such that tension stresses at the root were not high enough to produce cracks. Passenger car ring gears with 14½ degree pressure angles tend to crack along the root of the teeth while truck gears with 20 degree pressure angles are less apt to fail in that manner since contact pressures are directed more toward the body of the gear and set up lower bending stresses at the root of the teeth.

Gears which have a soft skin produced by decarburization during reheating, or as Mr. Davis mentioned, in the carburizing process, score more readily. Gas carburizing with prepared mixtures is very apt to produce decarburized surfaces especially where heavy deposits of adherent coke are produced. For successful gas carburizing for such applications as gears where the original surface must be file hard it appears that the work must remain reasonably clean and free from adherent coke deposits yet without the gas mixture becoming too lean to produce the desired carbon content. A difference of opinion exists as to the file hardness of austenite or austenite-martensite mixtures. File hardness is greatly dependent upon carbon content and perhaps the soft skin is the result of partial decarburization on the very surface. Some steels are more prone to form the soft skin on direct quenching than others. The soft skin on direct quenched chromium-vanadium steels appears to be connected with the layer of spheroidized excess carbide which forms in the surface layers and crumbles away under the file.

Since the preservation of the outer surface is of prime importance for certain applications it becomes desirable to prevent decarburization by regulating furnace atmospheres, keeping the temperature as low as possible in reheating, by using a direct quench, avoiding unfavorable gas reactions in carburizing and to vary the heat treatment to produce the microconstituents most resistant to wear and tempering in the surface layers of the particular steel being used even at the sacrifice of the best core properties and over-all strength and toughness.

Mr. Horger states that conditions of the tests did not simulate service conditions. This of course is true to a certain extent as it is imposible to duplicate those conditions. The test conditions imposed on the axles were those arrived at during years of testing under various procedures as giving the most nearly comparable results with similar gears in actual service. Other loads have been tried (but not on this particular series) and loads have been increased in steps from zero up to failure without better correlation with service results being obtained. Momentary stresses in service from shock loads, sudden shifting of gears, etc., are not determinable. The test load used was an estimate of the maximum that might occur in service. There is no reason to believe that the deflection of the gear and mountings should not be the same under equal test and service loads. There was no vertical weight load on the

rear axle as in service but the axles tested were full floating and the effect of weight should be minimized. The kind and amount of lubricants were identical to those used in service and the temperature was kept approximating that found in service. More variation in temperature and viscosity of lubricant would occur in service because of stopping and starting again when cold. Shock loading did not occur in the tests but shock is largely absorbed in propeller and axle shafts, tires, etc. Almen and Boegehold[2] state that tooth failure in rear axle gears never occurs from shock. The appearance of the failed gears was quite similar to gears which failed in service.

I agree that it would be desirable to make tests at several different loads to establish an S-N curve. However, such a curve would not necessarily follow the S-N curve from standard laboratory test specimens of the same material due to change in tooth contact from deflection and wear, tempering operation, etc. The tests of full sized units are expensive ones to make and many tests of long duration would reach a prohibitive cost unless the volume of production was very large. A relatively few tests on full sized parts and units under conditions approaching as closely as possible those in service give far better indications of the service life of those parts than a large number of laboratory test specimens tested under more theoretically ideal conditions. This is not meant as a criticism of laboratory tests since both procedures have their proper field. Much preliminary work can be accomplished with laboratory specimens to point the way to final tests. Unsuspected factors enter into service failures and those factors are not imposed upon the laboratory test specimens but more of them enter as test conditions approach more closely to actual service.

In reply to Mr. Boegehold's comments concerning lack of correlation of laboratory flexural tests with rear axle tests, it can be noticed the conclusion of the paper states that agreement between the two methods as to load carrying capacities of the steels existed only when axle tests created conditions similar to those of the laboratory tests. Agreement in strength was good when bend test results were compared with ring gear life when the latter was not influenced by pinion failure. It was further pointed out that bend tests and pinion failures did not correspond because the additional factors of wear and temperature effects entered into pinion failure.

The writer agrees that distortion from heat treatment would affect the results the same as any other factor disturbing proper tooth contact. Several reasons may be pointed out to indicate that heat treatment distortion did not have a major influence on results. As to uncarburized S.A.E. 4340 steel less distortion would occur during heat treatment than in case hardened steels. More might be expected when that steel was case hardened, but all gears and pinions were matched and lapped together prior to the tests and passed as satisfactory for production by the regular inspector, thus eliminating the possibility of a great amount of heat treatment distortion being present. The values on case hardened S.A.E. 4340 steel given in Table I are averages of three or more tests. Unrepresentative values should be at least partially eliminated. The ranges of values were 15,000 to 63,000 cycles for 400 degrees Fahr. draw-

[2] "Rear Axle Gears: Factors Which Influence Their Life." A paper presented at the A.S.T.M. Convention in Detroit, June 24-28, 1935.

ing temperature, 34,000 to 41,000 for 600 degrees Fahr, and 46,000 to 59,000 for 800 degrees Fahr. This greater uniformity of results with increasing drawing temperature might be expected by decreasing the brittleness, but it does not seem that distortion should be greatly affected. The S.A.E. 4340 gears with the higher draws gave as good uniformity as case hardened gears. If much more distortion existed it might be expected that more variation would have been found in the former.

The tooth distortion produced during the actual gear tests as shown in the paper cited by Mr. Boegehold is far greater than would pass inspection if produced during heat treatment. Even for equal amounts of distortion from the original tooth form as cut the internal stresses from heat treatment are probably much less than those from the external load since part of the heat treatment distortion probably occurs in the plastic stage and cannot therefore account for a major portion of the stresses. It is even possible that heat treatment distortion producing a toe bearing with a light load might give better stress distribution along the tooth under heavy loads than would no distortion at all. The matching and inspection of gears for the tests makes it appear probable to the writer that heat treat distortion was not a deciding factor. Scratches and other mechanical defects have an influence on fatigue life and I believe that the distortion of the parts and mountings during operation have a very decided effect. These effects should be more or less averaged in a number of tests and leave other large and consistent variations rather difficult to explain if metallurgical differences are not to be considered.

In reply to Dr. Moore, it is rather difficult to compare stresses in a test of this nature with actual service. There are conditions, such as when a truck gets in a mud-hole, where shifts are made from low to reverse, so that momentarily a much higher load would be built up than occurred from the steady stresses in the dynamometer test. Therefore, it seems reasonable that the maximum stresses at least might be somewhere close to those actually obtained in service. The load applied in the tests was 60 per cent above full motor torque developed in low gear by the truck motor designed to be used with the axles.

Ordinary fatigue tests on standard specimens would probably compare with results of the tests where initial failure occurred in the ring gear since those results were related to the strength shown by the bend tests. Pinion failure which in several cases occurred first probably would not check very closely with standard fatigue specimens since partial lubrication permitted temperature rise at contact areas with softening and weakening of the structure, and wear—factors not entering into standard fatigue tests. Wear which changes the location of tooth contacts; deflection which separates the gear and pinion from normal positions and throws the point of load application nearer the top of the tooth and thus increases bending stresses at the root; and deflection of the teeth themselves shifting the load from toe to heel along the tooth face; all enter into gear life. The fiber stresses in the gear teeth may not therefore be entirely proportional to the measured input or output torque of the dynamometer tests and it might be expected that a stress-cycle curve would differ somewhat from that obtained on standard specimens even if the effect of tempering did not enter into either test.

THE EFFECT OF DEOXIDATION ON THE RATE OF FORMATION OF FERRITE IN COMMERCIAL STEELS

By D. L. McBride, C. H. Herty, Jr., and R. F. Mehl

Abstract

The rate of precipitation of ferrite from austenite at constant temperatures between A_3 and A_1 was studied in a series of nine commercial steels, including silicon-killed and aluminum-killed steels. The isothermal decomposition curves obtained can be described by the equation for a first order chemical reaction, and the reaction rate constant in this equation taken as a measure of the reactivity of the steel. A steel treated to give different austenite grain sizes gives different reaction rate constants for one temperature of precipitation; when, however, these are divided by the grain surface area they become equal. The rate of ferrite precipitation in aluminum-killed steels is greater than that of silicon-killed steels at low degrees of undercool, but less at high degrees of undercool, thus showing a smaller dependence on temperature. The amount of ferrite formed on normalizing compared to that formed on annealing was found to be dependent only on the mass of the specimen, which determines the cooling rate, and the austenite grain-size, increasing linearly with increasing austenite grain surface area per unit volume of specimen.

THE rate of decomposition of austenite has been studied by many workers, particularly Bain[1] in this country. These studies have

[1] E. S. Davenport and E. C. Bain, "Transformation of Austenite at Constant Sub-Critical Temperatures," *Transactions*, American Institute of Mining and Metallurgical Engineers, Iron and Steel Division, 1930, p. 117; E. C. Bain, "On the Rates of Reaction in Solid Steel," ibid, 1932, p. 13; E. C. Bain, "Factors Affecting the Inherent Hardenability of Steel," Transactions, American Society for Steel Treating, Vol. 20, 1932, p. 385; E. S. Davenport and E. C. Bain, "General Relationship Between Grain Size and Hardenability of Steels," Transactions, American Society for Metals, Vol. 22, 1934, p. 861.

This article is an abstract of a thesis submitted by D. L. McBride to the Carnegie Institute of Technology in partial fulfillment of the requirements for the degree of Doctor of Science.

A paper presented before the Seventeenth Annual Convention of the Society held in Chicago the week of September 30 to October 4, 1935. Of the authors, D. L. McBride is Metallurgical Advisory Board Fellow and Graduate Student, Department of Metallurgical Engineering, Carnegie Institute of Technology, Pittsburgh; C. H. Herty, Jr., formerly Director of Research, Metallurgical Advisory Board, Carnegie Institute of Technology, Pittsburgh, and since September, 1934, Research Engineer, Bethlehem Steel Co., Bethlehem Pa.; and R. F. Mehl is Director, Metals Research Laboratory and Professor of Metallurgy, Carnegie Institute of Technology, Pittsburgh. Manuscript received June 8, 1935.

been limited to decompositions which take place below the eutectoid temperature A_1, and are chiefly restricted to the formation of pearlite, though in some cases preliminary formation of ferrite and cementite have been observed, especially at higher temperatures. The rate of formation of ferrite alone, however, either at temperatures just below A_1, or at temperatures between A_1 and A_3 (where nothing but ferrite can form) has not been studied. Information on the rate of ferrite formation at these higher temperatures is of interest and of importance, particularly with respect to the operations of normalizing and annealing and also, though less directly, with respect to the operation of quenching.

Deoxidation alters steel in a number of ways: It eliminates free or dissolved iron oxides to a greater or lesser degree dependent upon the strength of the deoxidizer employed and the amount of deoxidizer added; it leaves in the steel the excess of unused deoxidizer as a metallic alloyed impurity; and it creates in the steel a dispersion of deoxidation products, chiefly oxides. Different deoxidizers affect steel in different ways with respect to the residual deoxidation products. SiO_2 is a relatively low melting constituent which fluxes and agglomerates readily with iron oxide and thus possesses the quality of self-elimination by levitation from the steel bath when sufficient time is provided; Al_2O_3, however, has a high melting point and very low fluxing capacity for iron oxide and thus tends to remain in the steel in the form of a fine dispersion widely distributed.

This fine dispersion of Al_2O_3 likely is the cause for the relatively high austenite coarsening temperatures characteristic of aluminum-killed steels. Silicon-killed steels, on the other hand, show a relatively low austenite coarsening temperature. Thus at intermediate temperature ranges similar heat treatments will produce large austenite grains in silicon-killed steels and small grains in aluminum-killed steels. The size of the austenite grain is an important factor in determining the rate of decomposition, for these reactions proceed chiefly by rejection of the transformation product at the grain boundary or surface, and the rate is thus dependent upon the area of the grain boundary surface; thus small-grained steels which possess large grain surface areas per unit volume react more rapidly than large-grained steels which possess small grain surface areas.

It is known that transformation processes in alloys operate by the formation of nuclei and the subsequent growth of these nuclei. Evidently any influence which changes either of these factors will

alter the rate of transformation. Apart from the influence of deoxidation on grain-size, the effect of the deoxidation products as possible nuclei for initiating the transformation process is therefore important.

It must be remembered that other factors affect the rate of decomposition of austenite, particularly elements in solid solution in austenite. For the steels studied here only metallic alloyed deoxidizer and dissolved oxygen need be considered; the exact role played by these is not now certain and seems difficult to study. It does not seem likely that either metallic alloyed deoxidizer or dissolved oxygen in the very small concentrations obtaining here can sensibly affect the rates of decomposition measured.

The present study is an effort to determine the influence of common deoxidation practices upon the rate of formation of ferrite at temperatures between A_1 and A_3. For this purpose nine commercial steels, deoxidized with manganese, silicon, and aluminum, and roughly divisible into silicon and aluminum-killed steels, were procured. Samples of these were annealed at various temperatures within the austenite range to produce various austenite grain sizes (in order later to permit a quantitative evaluation of the effect of grain size on the rate of decomposition) and then quenched to a series of temperatures between A_3 and A_1 and held there for various periods of time; the extent of reaction after various time periods was measured by a planimetric evaluation of the ferrite areas developed. This is the sub-critical isothermal transformation technique so extensively employed by Bain[1]. In an extension of this work, the relative amounts of ferrite developed on normalizing and annealing for samples of different masses were determined planimetrically, and finally the depth of hardening on water quenching was determined in the usual way on the same steels.

Materials

Twelve steels were studied in the several parts of this work. The compositions of these steels are shown in Table I. Except for steel AX, all fall between 0.33 and 0.50 per cent carbon. These steels may be classed as either silicon-killed or aluminum-killed steels; they all are commercial steels, made in conjunction with the work of the Metallurgical Advisory Board of the Carnegie Institute of Technology. The compositions of the deoxidizers used are

given in Table II, and the deoxidation treatment in Table III. It will of course be noted that the steels designated as "aluminum-killed" had actually been deoxidized also with silicon and manganese; in conformity with usual nomenclature the term "aluminum-killed" simply designates a steel during the deoxidation of which aluminum was used.

Table I
Compositions and Ar_3 Temperatures of Steels Used

Designation	Per Cent C	Mn	P	S	Si	Metallic Al	Ar_3 °C.	°F.
D*	0.44	0.64	0.039	0.028	0.157	0.010	740	1364
J	0.39	0.73	0.016	0.031	0.073	none	740	1364
X	0.33	0.44	0.011	0.029	0.163	none	771	1420
Y	0.41	0.62	0.021	0.034	0.191	none	757	1395
Z*	0.405	0.58	0.018	0.031	0.183	0.016	761	1402
AD	0.41	0.81	0.034	0.039	0.169	none	755	1391
AE*	0.50	0.83	0.021	0.040	0.170	0.012	730	1346
AP*	0.48	0.74	0.022	0.030	0.205	0.020	745	1374
AR*	0.37	0.62	0.016	0.035	0.197	0.013	760	1400
AS*	0.45	0.71	0.013	0.031	0.138	0.009	742	1367
AT*	0.40	0.56	0.021	0.030	0.127	0.009	765	1409
AX	0.21	0.43	0.016	0.043	0.111	none	798	1469

*Aluminum-killed steels

Table II
Composition of Deoxidizers

	Per Cent Mn	Si	Al	C
Common spiegel	20	1.5	....	4.0
High silicon spiegel	21	4.0	....	4.25
Silicospiegel	30	7.0	....	3.5
Silicomanganese	69	15.5	....	2.5
Mn-Si-Al alloy	67.5	16.2	4.0	1.35
Ferromanganese	80.0	0.6	....	6.50
Ferrosilicon	....	50.0	....	....
Alsifer	....	40.0	20.0	....
Aluminum	....	....	98.0	....

The Rate of Formation of Ferrite

Methods. Samples were cut in the form of ¼ or ½ inch cubes, taken from the outer surface of billets and axle stock in order to obtain material from what was originally the surface of the ingot, thus avoiding regions of extensive segregation. The analyses given in Table I were procured from samples taken from a similar location.

The cube samples were annealed in air in an electric muffle furnace at various temperatures above A_3 for various periods of time in order to homogenize them and to develop different austenite grain-sizes. After this treatment they were transferred to a salt bath

Table III
Methods of Deoxidation

Designation of Steel	Added in Furnace	Added in Ladle
D	Silicospiegel Ferromanganese	Alsifer—Ferrosilicon Coal
J	High silicon spiegel Ferromanganese	Ferrosilicon
X	High silicon spiegel Ferromanganese	Ferrosilicon Coal
Y	High silicon spiegel Ferromanganese	Ferrosilicon Coal
Z	Common spiegel	Alsifer—Ferrosilicon Ferromanganese
AD	High silicon spiegel Ferromanganese	Ferrosilicon
AE	Common spiegel	Alsifer—Ferrosilicon Ferromanganese
AP	Silicomanganese	Alsifer—Coal
AR	Ferromanganese Mn-Si-Al alloy	Ferromanganese Ferrosilicon—Coal
AS	Ferromanganese Mn-Si-Al alloy	Ferromanganese Ferrosilicon—Coal
AT	Silicospiegel Ferroaluminum	Ferromanganese Ferrosilicon—Coal
AX		Ferromanganese Ferrosilicon

maintained at a constant temperature between A_3 and A_1 and held there for various periods of time, and then quenched in water. In order to soften the samples for ease in grinding and machining and to produce contrast in the final photomicrograph by converting the martensite to troostite or fine sorbite, they were later reheated to 400 degrees Cent. (750 degrees Fahr.).

Early experiments showed an induction period — an initial period in which apparently no ferrite formed — varying from 5 seconds to 30 seconds. Much of this period was accounted for by the time required for the temperature of the sample to reach the subcritical temperature chosen for the reaction. The quenching temperatures varied between 850 and 1000 degrees Cent. (1560-1830 degrees Fahr.), temperatures above the A_3 temperatures of roughly 100 to 250 degrees Cent.; the transformation temperatures chosen were never more than 50 degrees Cent. below the A_3 temperature, so that most of the time of cooling was consumed in traversing the austenite range where no reaction could take place. In later experiments the samples were more leisurely transferred to the

salt bath, the operation taking from 15 to 30 seconds. Using this technique no incubation period was observed. All reactions shown in the following figures thus begin at zero time. Any inaccuracies introduced by this method cannot be important, because in the worst case the true induction period — if it exists — can be a matter of only a few seconds whereas the reactions studied last from minutes to hours.

The cubes treated as described above were polished, etched with picric acid in alcohol, and finally photographed. The amount of ferrite formed during the chosen reaction period was then evaluated by the planimetric method previously employed by Herty and Lightner[2]. This method consists in superimposing a transparent grid with 400 unit squares per square inch upon the photomicrograph, and counting the number of unit squares occupied by the ferrite areas. Tests have shown this method to be accurate to within $\pm$ 2 per cent of the measured area.

It will be necessary later in the work to calculate the grain surface areas in order to compare the reactivities of the various steels upon a common basis. This calculation was made as follows: The approximate shape of the grains in these steels as seen on the photomicrograph is a circle; in three dimensions the grain is thus a sphere. If r is the radius of the average grain, G the number of grains per square inch as seen on the photomicrograph at 100 diameters, then $G^{3/2}$ is the number of grains per cubic inch at 100 diameters. Since $\frac{1}{G} = \pi r^2$, then $r = \sqrt{\frac{1}{\pi G}}$; and since $4\pi r^2$ is the grain surface per grain (the area of the surface of a sphere), then $4\pi\left(\frac{1}{\pi G}\right) = \frac{4}{G}$ = grain surface per grain, and accordingly the grain surface area $S = \frac{4G^{3/2}}{G} = 4\sqrt{G}$. This method of calculation must be regarded as an approximation only, since it involves the assumption that the grains are actually spheres and that the grains are all of one size, neither assumption being strictly true. The data obtained in this investigation, plotted according to the grain surface area calculated in this way, however, are greatly simplified, as will be seen, and the calculation therefore seems amply justified.

[2]C. H. Herty, Jr. and M. W. Lightner, "The Transverse Impact Strength of Plain-carbon, Normalized Steels," Cooperative Bulletin No. 59, Metallurgical Advisory Board to the Carnegie Institute of Technology, 1932.

Results

The data obtained in the manner described for the steels listed in Table I are given in Tables IV and V, Table IV listing silicon-killed steels and Table V aluminum-killed steels. These tables also list the austenite grain-sizes, the temperatures to which the steel was quenched for reaction, and the degrees of undercool — the difference between A_3 and the quenching temperature.

Table IV

Per Cent Ferrite Formed at Various Times after Quenching into Salt Bath, Silicon-killed Steels

Steel	Steel J		Steel X					Steel AD		
Grains per sq. inch at 100X	5.3	3.3	12.1	8.8	32.5	3.3	8.2	2.4	110	1.7
Quenching Temp. Degrees C.	676	707	697	707	717	750	753	707	717	734
Undercool °C.	64	33	73	63	53	21	18	48	38	21
Minutes after Quench	PER CENT FERRITE									
1	1.8	..	5.7	...	1.7	Trace	...	...	...	...
2	...	0.8	18.6	17.3	11.7	0.8	0.7	2.3	8.0	...
3	...	...	27.7	...	25.9	...	...	...	12.3	...
4	23.2	3.5	37.9	28.1	31.9	6.3	...	5.4	...	...
5	...	...	48.0	...	41.1	...	5.7	...	15.5	Nil
6	24.0	7.1	...	39.0	...	9.5	...	8.5	16.0	...
7	...	...	...	...	...	...	14.0	...	...	...
8	26.1	...	...	...	...	13.3	...	...	...	...
10	27.8	...	53.3	43.2	39.2	16.7	17.0	11.6	...	Nil
12	...	...	...	...	...	19.1	...	...	...	...
15	...	11.7	...	...	...	...	21.1	14.8	...	Nil
20	...	...	53.3	...	...	24.1	20.7	...	...	0.1
25	...	...	...	...	...	23.9	...	...	...	0.2
30	...	17.0	...	44.4	...	...	...	18.9	...	1.0
45	...	...	...	...	...	...	...	...	...	5.3
60	...	22.0	...	44.0	...	...	...	21.0	...	8.9
120	...	23.9	...	...	...	...	...	21.9	...	...

Steel	Steel Y							Steel AX		
Grains per sq. inch at 100X	4.8	32.5	3.0	32.5	32.5	2.3	2.3	7.0	7.0	12.5
Quenching Temp. Degrees C.	698	697	707	707	717	719	732	730	747	774
Undercool °C.	59	60	50	50	41	38	25	68	51	24
Minutes after Quench	PER CENT FERRITE									
1	...	2.5	...	...	...	...	...	7.2	19.4	1.0
2	..	15.0	4.8[a]	9.6	5.0	...	...	36.0	29.0	9.2
3	...	24.0	...	...	...	...	...	...	...	...
4	...	32.9	8.9[a]	19.5[a]	13.0	...	...	42.6	35.7	19.8
5	18.8	35.4	...	...	16.0	2.5	2.5	...	...	...
6	...	38.8	11.7[a]	27.8[a]	21.0	...	...	45.2	46.9	27.3
7	...	39.0	...	...	23.4	...	...	...	...	...
8	...	...	...	29.2	...	...	...	45.2	46.9	29.6
10	...	39.0	17.1[a]	...	...	9.6	4.0	...	...	...
12	...	...	...	...	26.4	...	...	...	...	...
15	36.0	...	20.2[a]	...	...	...	6.4	58.7	46.6	32.3
20	...	...	...	31.4	...	16.9	8.5	...	...	...
30	36.0	...	25.3	29.6	...	23.1	12.0	58.0	46.6	31.1
45	36.0	...	...	...	...	...	15.3	...	...	...
60	36.0	...	28.5	30.0	...	...	15.1	58.0	...	32.0
120	...	...	32.0	30.0	...	24.9	15.0	...	...	...

a = average of two or more values

Fig. 1 shows the type of structures obtained, and illustrates the progress of ferrite formation, for the steel designated AD. It may be seen in these photomicrographs that the ferrite forms nearly exclusively at grain boundaries. The ferrite thus outlines the original austenite grains, enabling the observer readily to determine their size.

As the reaction proceeds to completion, ferrite begins to form spines or "needles" projecting from the grain boundary toward the center of the grain. At this point, obviously, any calculation of rate of reaction on the basis only of grain surface area begins to lose all significance. This, however, happens only near the completion of the reaction and does not invalidate any calculations made for the first part of the reaction. An evaluation of the relative amounts of intercrystalline or grain boundary ferrite and intracrystalline ferrite was made on steel Y (which may be taken as typical in this respect), and the results plotted as reaction-time curves. These are shown in Fig. 2 where it may be seen that the intracrystalline ferrite becomes appreciable only after the reaction is 50 per cent complete.

Table V
Per Cent Ferrite Formed at Various Times after Quenching into Salt Bath, Aluminum-Treated Steels

Steel	Steel Z						Steel D			Steel AE		Steel AP	
Grains per sq. in. at 100×	3.5	80.0	80.0	4.6	80.0	3.3	1.9	1.6	1.6	120	4.6	108	2.1
Quenching Temp. Degrees C.	696	697	707	707	717	747	707	717	728	701	702	669	702
Undercool °C.	65	64	54	54	44	14	33	25	12	29	28	76	43
Minutes after Quench	PER CENT FERRITE												
0.25	...	Nil	...	...	Nil	...	...	...	...	...	...	...	...
0.50	...	Nil	...	...	Nil	...	...	...	...	...	...	...	...
1.0	5.0	4.4	...	...	0.4	...	...	...	...	...	...	16.3	...
1.5	...	...	...	...	2.7	...	...	...	...	...	...	...	...
2.0	...	15.9[a]	9.4	21.6	7.3[a]	Nil	1.5	0.5	Nil	15.1	0.5	34.0	1.0
2.5	...	20.5	...	...	13.7	...	...	...	...	...	...	...	...
3.0	15.4	31.5	...	25.6	19.1	...	...	...	...	...	...	39.0	...
3.5	...	...	...	...	21.0	...	...	...	...	...	...	...	...
4.0	...	37.5	13.5	28.5	...	...	4.5	1.6	0.1	15.1	1.8[a]	...	8.2
5.0	...	40.3	...	...	...	8.0	...	...	...	...	...	...	...
6.0	29.1	40.0	19.1	...	...	...	9.2	4.4	0.8	...	5.5[a]	...	9.2
8.0	...	...	...	30.8	...	...	...	...	...	...	11.0	...	13.9
10.0	43.0	40.0	...	...	26.9	...	13.0	7.8	2.8[a]	...	...	39.8	...
12.0	...	...	...	...	...	...	...	...	...	...	14.7	...	16.3
15.0	...	...	29.4	...	...	8.3	18.1	...	5.9	...	...	...	...
20.0	...	...	...	...	...	...	19.7	14.5	5.8	...	14.8	...	...
30.0	43.0	...	29.5	29.5	...	...	22.0	...	9.0	...	...	...	...
60.0	43.0	...	29.5	29.2	...	8.3	28.4	20.8	...	...	15.0	...	...
120.0	...	...	...	...	...	...	32.0	21.9	...	...	...	...	...

a = average of two or more values

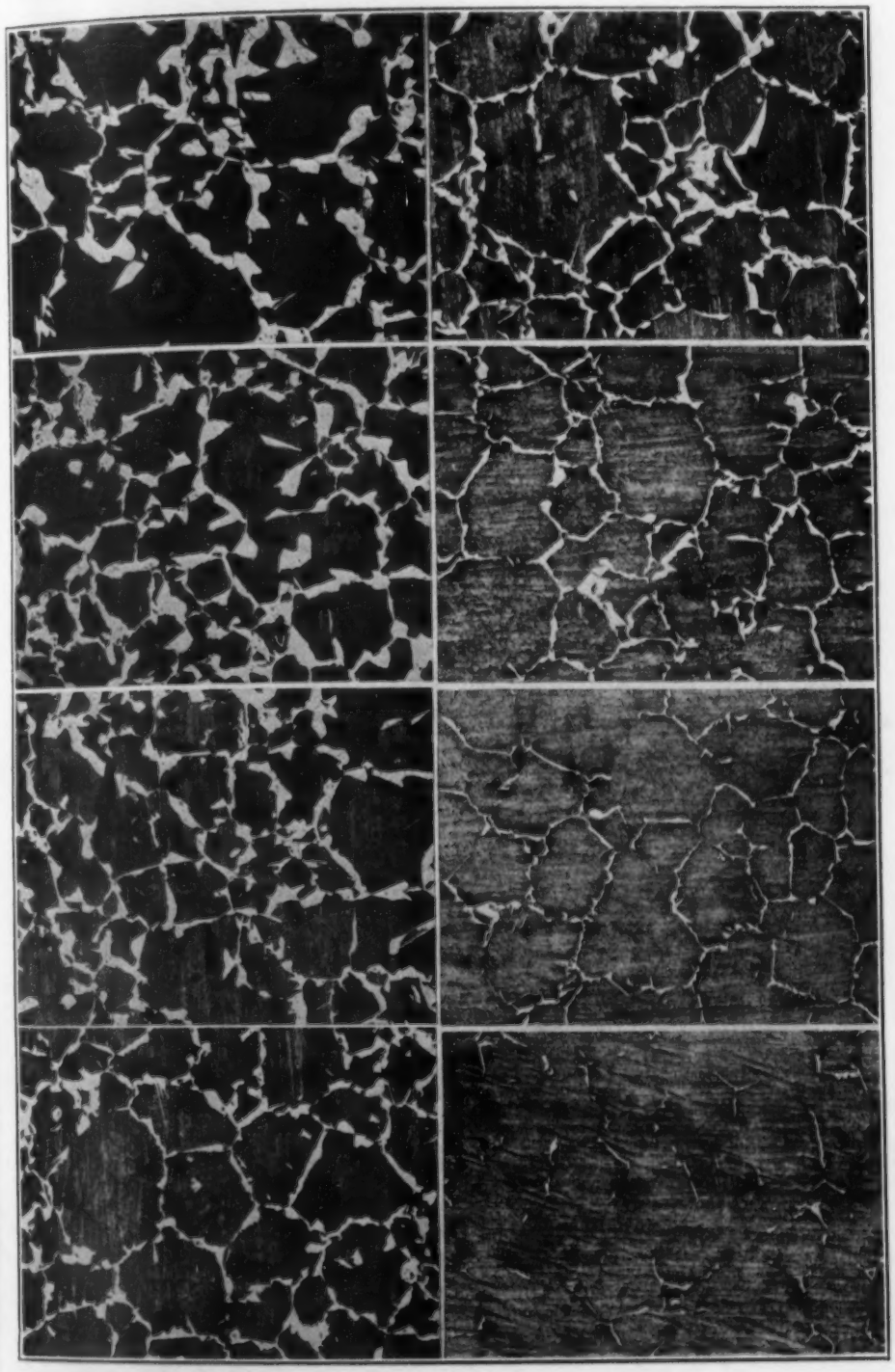

Fig. 1—Ferrite Formation in Steel AD at 707 Degrees Cent. (T = 48 Degrees Cent.) Magnification, × 200. (Reduced One-Half in Printing.)

Time After Quench	Per Cent Ferrite	Time After Quench	Per Cent Ferrite
2 minutes	2.3	15 minutes	14.8
4 minutes	5.4	30 minutes	18.9
6 minutes	8.5	60 minutes	21.0
10 minutes	11.6	120 minutes	21.9

In basing calculations of rate of reaction upon the grain surface area it must also be appreciated that the progressive formation of ferrite at grain boundaries progressively decreases the grain surface area by simple shrinkage of the grain which is rejecting ferrite. These several considerations must be kept in mind in considering the results

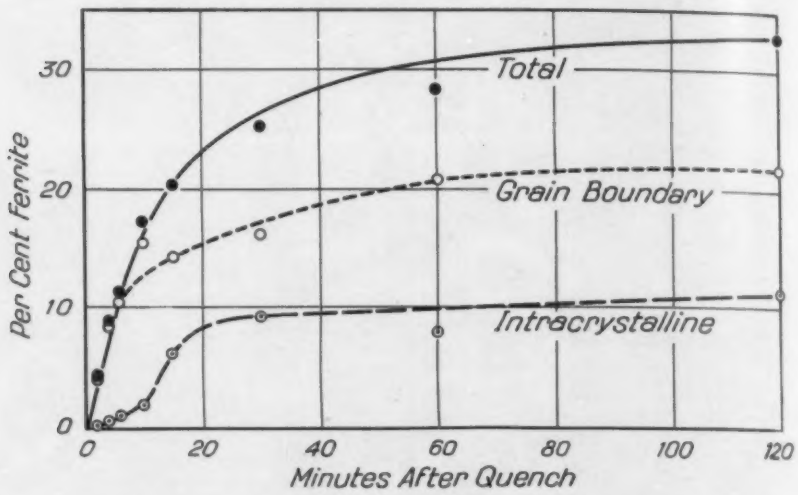

Fig. 2—Grain Boundary and Intracrystalline Precipitation of Ferrite in Steel Y, 50 Degrees Cent., Undercool.

of the present study; in general they tend to decrease the precision with which the data may be treated, but evidently not seriously, as will be seen.

A consideration of the iron-carbon system will show that the total amount of ferrite formed at constant temperatures between A_3 and A_1 will be dependent upon (1) the composition of the steel, insofar as it affects the A_3 and (to a lesser extent) the A_1 temperatures, and (2) the temperature of precipitation or, stated in a different way, the amount of undercool. In both cases, when the full course of the critical temperature curve A_3 is known, the total or equilibrium ferrite can be calculated by simple application of the familiar lever-arm principle. Conversely, if the equilibrium amount of ferrite is determined by experiment, the position of the A_3 curve may be fixed (if the obviously small solubility of carbon in alpha iron between A_3 and A_1 is neglected, as it has been in this work). The A_3 temperatures listed in Table I were determined in this way.

The results of these sub-critical isothermal decomposition studies, listed in Tables IV and V, are plotted in Figs. 3, 4, 5, and 6. These figures are simple rate curves, in which the percentage of total

ferrite is plotted against elapsed time. In each case the temperature of decomposition is noted, and in several cases two curves are given for the same temperature, applying respectively to steels possessing coarse and fine austenite grains. It will be seen that the rate of ferrite formation is the slower in the coarse-grained steels. It will also

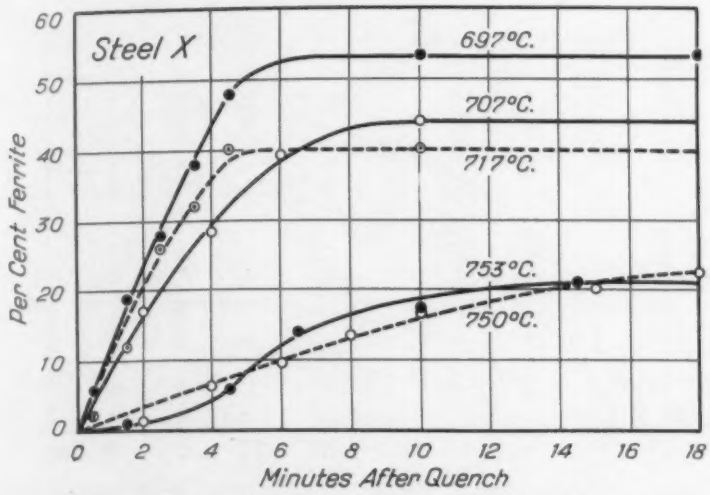

Fig. 3—Rate of Ferrite Formation on Steel X, Silicon-Killed.

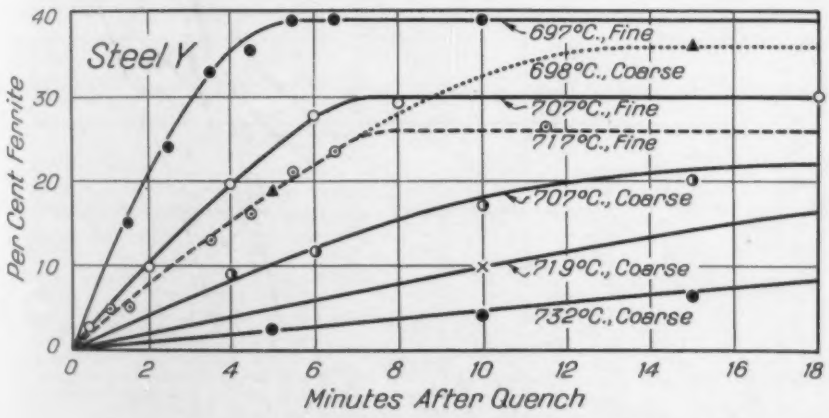

Fig. 4—Rate of Ferrite Formation on Steel Y, Silicon-Killed.

be seen that the rate of ferrite formation increases as the temperature of formation decreases. In plotting these figures one-half minute was deducted from the data listed in Tables IV and V for the steels X, Y, and Z at the temperatures 697 and 717 degrees Cent. (1285-1320 degrees Fahr.) in order to correct for the time of cooling or quenching; this has been discussed under "Methods." With this correction, no induction period is represented, all curves show-

ing ferrite formation beginning at the origin. It will be noted that Figs. 3 and 4 are for silicon-killed steels, and Figs. 5 and 6 for aluminum-killed steels. These figures do not represent all of the data obtained in this study, but may be taken as sufficiently representative for the present purpose.

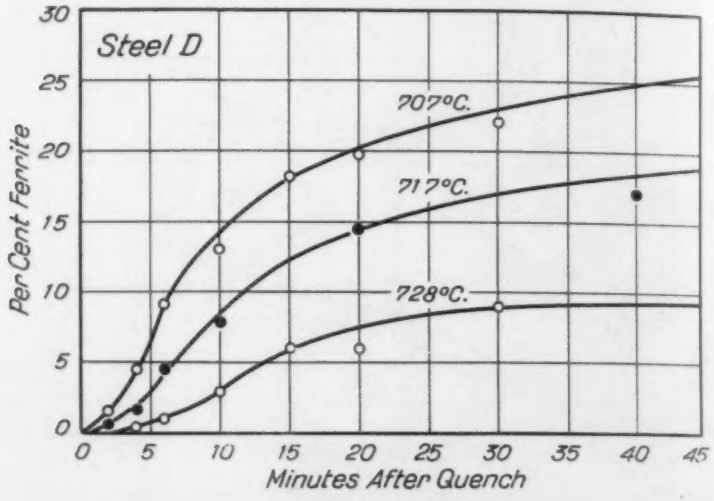

Fig. 5—Rate of Ferrite Formation on Steel D, Aluminum-Treated.

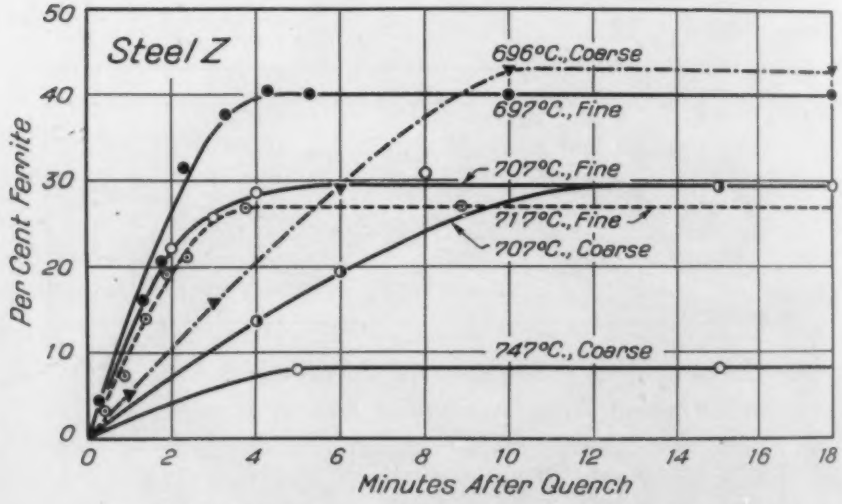

Fig. 6—Rate of Ferrite Formation on Steel Z, Aluminum-Treated.

Discussion of Results on the Rate of Formation of Ferrite

As stated in the introduction, reactions such as these proceed by the formation of nuclei and the subsequent growth of these nuclei to

form visible grains of the product. It has been suggested by a number of workers that these reactions may be represented as first order reactions, so familiar to the physical chemist.[3] The basis for this lies in the fact that much of the reaction curve conforms to the mathematical equation which characterizes first order reactions. This, however, is true only in the middle section of the curve, the beginning and end sections generally showing marked deviations.

There seems to be little real justification for considering solid-solid reactions as first order chemical reactions. Since the reaction is known to proceed by nuclei formation and subsequent growth of these nuclei (a mechanism having nothing in common with the conditions of true concentrations and effective collisions of real first order chemical reactions), it would seem much more useful to analyze the reaction into these terms, and to study the effect of composition, temperature, etc., upon these two controlling factors.[4] It is not yet possible to perform such analysis because of the difficulties involved in the experimental determination of the rate of nuclei formation and the rate of crystal growth.[5]

Admitting the artificiality in the analysis of these reactions as first order reactions (and the desirability of a more precise analysis), it is quite possible to compare the reactivities of several steels upon the basis of the constants which pertain to first order reactions. Upon this basis, the rate of precipitation of ferrite may be represented by the expression:

$$\frac{d\,Fe}{dt} = K\,(\text{austenite} - \text{ferrite}) \quad \ldots\ldots\ldots\ldots\ldots (1)$$

In this expression $\frac{d\,Fe}{dt}$ represents the rate of formation of ferrite, the expression in parentheses represents the difference between the amount of the original austenite (which is unity) and ferrite at any time period (in the present application these are not truly concen-

[3]Ref. 1; also: W. Fraenkel and W. Goez, "Kinetic Studies on Solid Metals. Decomposition of the Compound Al_2Zn_3," *Zeit. f. Metallkunde*, Vol. 17, 1925, p. 12 (also later papers by Fraenkel: ibid Vol. 19, 1927, p. 58; Vol. 22, 1930, p. 162.

[4]This matter has been discussed by R. F. Mehl, TRANSACTIONS, American Society for Metals, Vol. 22, 1934, p. 720.

[5]These difficulties originate in the opacity of metals; it is impossible to appraise the true size of any metal crystal upon a plane of polish because of the uncertainty in the location of that plane in the crystal. This affects alike the determination of nuclei number and crystallization velocity. It seems likely that indirect and statistical methods alone will be of help in this problem. Such an analysis is now in progress and will shortly be published.

trations as they are in reactions in gases or liquids, but merely fractions of the total mass) and K is the reaction rate constant, which we will designate as the reactivity constant or the specific reaction rate. This equation integrates to:

$$\ln \frac{1}{1-Fe} = Kt \quad \ldots\ldots\ldots\ldots\ldots\ldots\ldots\ldots\ldots\ldots (2)$$

The quantity K should be constant throughout the course of the reaction. In the application of the equation to the present data, however, K was observed not to be constant in several cases, which demonstrates the uncertainty in applying the first order reaction equation to data like these. However, those reaction rate curves which extrapolate smoothly to zero time will yield fairly constant values for K. The data obtained from steel Y, in the coarse-grained condition, at a temperature of 707 degrees Cent. (1305 degrees Fahr.), as shown in Table VI, may be taken as an example of close conformity to the requirements of equations (1) and (2). In this case, the precipitation of ferrite was essentially complete after thirteen minutes, and for this reason the value of K from this point on apparently rapidly decreased, though obviously there is nothing anomalous in this. Similar treatment of the data from steel D, however, gave values for K which were far from constant, these values first rising rapidly to a maximum and then decreasing gradually; in this case, and others like it, an average value for K was obtained by simple averaging of the calculated values over the fulltime curve. Nothing

Table VI

The Reactivity Constant for Steel Y at 707 Degrees Cent.

Coarse-grained Sample

Minutes After Quench	Per Cent Ferrite	$2.3 \log \frac{1}{1-Fe}$	K
1	2.0	0.0198	0.0198
2	4.0	.0412	.0206
3	5.8	.0601	.0200
4	7.8	.0817	.0204
5	9.6	.1009	.0202
6	11.5	.1222	.0204
7	13.2	.1415	.0202
8	14.9	.1614	.0202
9	16.4	.1791	.0199
10	17.8	.1966	.0197
11	19.2	.214	.0196
12	20.3	.227	.0190
13	21.3	.240	.0185
		Average	0.0199

Table VII

Reaction Rate Constants for Isothermal Decomposition Curves

Steel	Ar_3 °C.	Quenching Temp. °C.	Undercool ΔT°C.	(5) Grain/in² at 100×	$S=4\sqrt{G}$ Grain Surface per in³ at 100×	Reactivity Constant	K/S	Log K/S
D*	740	707	33	1.9	5.5	15.0×10^{-3}	2.72×10^{-3}	−2.565
D*	740	717	23	1.6	5.1	8.54	1.67	−2.777
D*	740	728	12	1.6	5.1	3.42	.68	−3.169
J	740	676	64	3.3	7.3	64.2	8.80	−2.056
J	740	707	33	3.3	7.3	8.3	1.14	−2.943
X	770	697	73	12.1	13.9	138.0	10.00	−2.000
X	770	707	63	8.8	11.9	87.8	7.41	−2.130
X	770	717	53	32.5	22.8	112.5	4.94	−2.306
X	770	750	20	3.3	7.3	16.9	2.32	−2.635
X	770	753	17	8.2	11.4	21.0	1.83	−2.737
Y	757	697	60	32.5	22.8	123.0	5.40	−2.268
Y	757	698	59	4.8	8.8	40.4	4.60	−2.337
Y	757	707	50	32.5	22.8	52.0	2.28	−2.642
Y	757	707	50	3.0	6.9	19.9	2.78	−2.556
Y	757	717	40	32.5	22.8	41.0	1.80	−2.745
Y	757	719	38	2.3	6.0	9.9	1.65	−2.783
Y	757	732	25	2.3	6.0	4.7	.78	−3.108
Z*	761	697	64	80.0	35.7	157.0	4.40	−2.357
Z*	761	707	54	80.0	35.7	142.0	3.98	−2.400
Z*	761	707	54	4.6	8.6	37.7	4.38	−2.361
Z*	761	717	44	80.0	35.7	129.0	3.61	−2.442
Z*	761	747	14	3.3	7.3	21.6	2.97	−2.527
AD	755	707	48	2.4	6.2	13.3	2.15	−2.668
AD	755	717	38	110.0	42.0	42.2	1.00	−3.000
AD	755	734	21	1.7	5.3	.95	.18	−3.745
AE*	730	701	29	120.0	43.8	110.0	2.53	−2.597
AE*	730	702	28	4.6	8.5	22.2	2.61	−2.580
AP*	745	669	76	108.0	41.5	205.0	4.94	−2.306
AP*	745	702	43	2.1	5.8	19.3	3.33	−2.482
AX	798	730	68	7.0	10.6	217.0	20.5	−1.688
AX	798	747	51	7.0	10.6	151.0	14.2	−1.848
AX	798	774	28	12.5	14.1	50.7	3.6	−2.444

*Aluminum-killed steels

further is claimed for this method of treating the data as described in the above except that it offers a convenience in comparing the reactivities of different steels.

The calculated reaction rate constants are summarized in Table VII. It will be seen that widely divergent values are obtained for K for a given steel at the same reaction temperature. This difference originates in the difference in grain-size in the original austenite. Since, as shown in Fig. 1 and as discussed previously, the ferrite forms chiefly at the grain boundaries, we may adjust the values for K by dividing by the grain surface area, S. It will be

seen in Table VII that the values for $\frac{K}{S}$ are indeed constant, independent of the austenite grain-size.

The variation of $\frac{K}{S}$ with temperature may be expressed by the equation:

$$\log \frac{K}{S} = a + b \triangle T \quad \ldots\ldots\ldots\ldots\ldots\ldots\ldots\ldots (3)$$

Evidently $\log \frac{K}{S}$ is a linear function of $\triangle T$; this is illustrated for the data at hand in Figs. 7-13. The values[6] of the constants a and b for the different steels are listed in Table VIII.

Table VIII
Comparison of Composition and Method of Deoxidation with the Characteristic Constants

Steel	Per Cent C	Per Cent Mn	Characteristic Constants a	Characteristic Constants b
		Silicon-killed Steels		
AX	0.21	0.43	—2.951	0.0205
X	0.32	0.44	—2.961	0.0132
Y	0.39	0.62	—3.708	0.0240
J	0.40	0.73	—3.657	0.0216
AD	0.41	0.81	—4.572	0.0400
		Aluminum-killed Steels		
Z	0.39	0.58	—2.573	0.0033
AP	0.47	0.74	—2.741	0.0058
AE	0.50	0.83	—2.741	0.0058
D	0.45	0.64	—3.504	0.0291

It will be seen from Table VIII that the values for a are generally lower in aluminum-killed steels than for silicon-killed steels (steel

[6]The usual physico-chemical expression for the variation of a rate constant with temperature is $k = Ae^{\frac{-b}{T}}$, which in logarithmic form is $\ln k = \ln A - \frac{b}{T}$. Equation (3) differs from this in replacing $\frac{1}{T}$ with ΔT; equation (3) is therefore not an equivalent expression since T is not a linear function of $\frac{1}{T}$ and since ΔT is used instead of the absolute temperature. The empirical equation (3) doubtless has its foundation in the orthodox equation given above in this footnote; the linearity shown in Figs. 7-13 is doubtless more apparent than real, owing to the small temperature interval represented in the figures. The empirical equation (3) is used rather than the orthodox Arrhenius equation only for reasons of simplicity; it does not seem profitable to extend the present treatment along more orthodox physico-chemical lines.

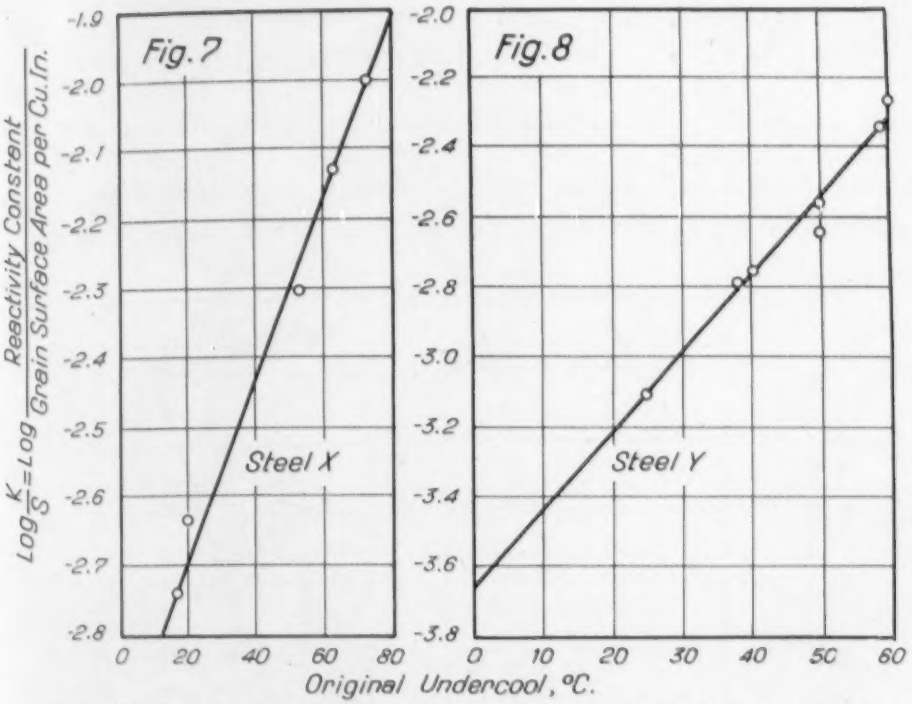

Fig. 7—Effect of Degree of Undercool on the Reactivity Constant of Steel X, Silicon-Killed.

Fig. 8—Effect of Degree of Undercool on the Reactivity Constant of Steel Y, Silicon-Killed.

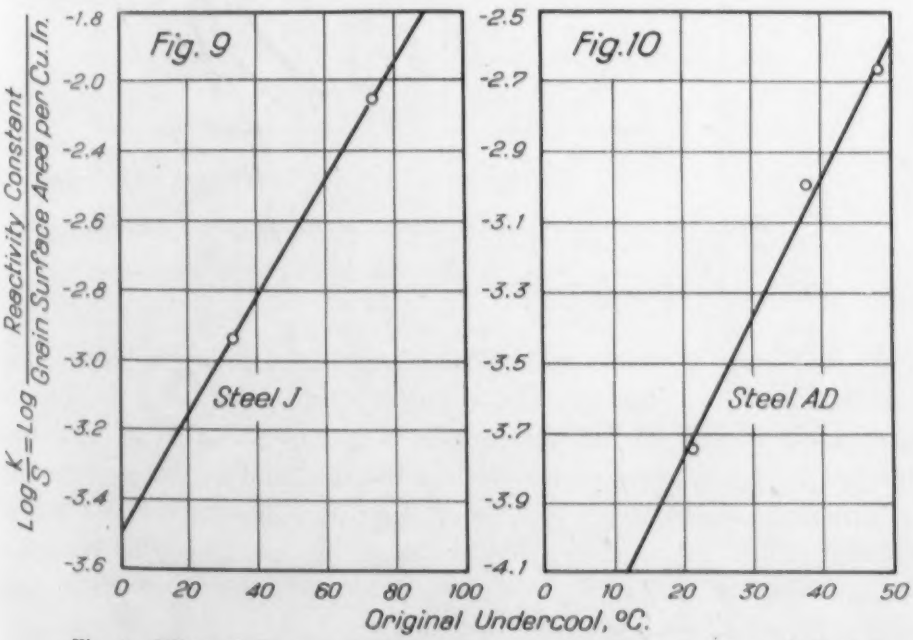

Fig. 9—Effect of Degree of Undercool on the Reactivity Constant of Steel J, Silicon-Killed.

Fig. 10—Effect of Degree of Undercool on the Reactivity Constant of Steel AD, Silicon-Killed.

D is an exception), and that b is also generally lower. In this connection it must be remembered that low values of a correspond to high values for $\frac{K}{S}$. Evidently a and b are both determined by the nature of the deoxidation practice, though it is impossible at this moment to attach any physical significance to the values of a and b.

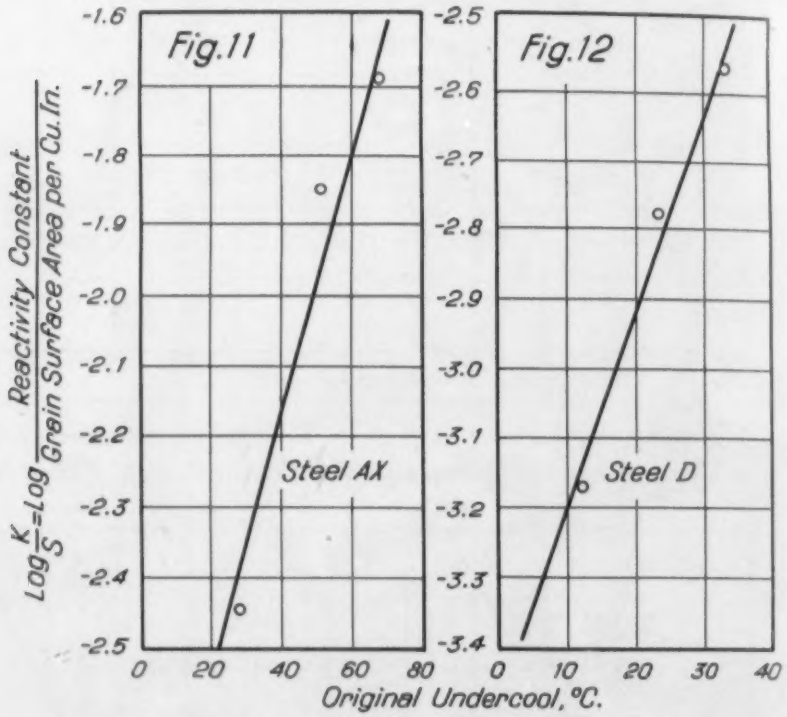

Fig. 11—Effect of Degree of Undercool on the Reactivity Constant of Steel AX, Silicon-Killed.

Fig. 12—Effect of Degree of Undercool on the Reactivity Constant of Steel D, Aluminum-Treated.

The difference in these values for a typical aluminum-killed steel (steel Z) and a typical silicon-killed steel (steel Y) is shown graphically in Fig. 14. In other words, it may be said that at high temperatures (low degrees of undercool) the rate of formation of ferrite in aluminum-killed steels is greater than that in silicon-killed steels, but that at low temperatures the reverse is the case. Judging from the present results, this may be expected to be generally true for all aluminum-killed and silicon-killed steels.

The increase in rate with decreasing temperature (increasing undercool) is more surprising than may appear at first sight. It

has been pointed out by Austin, arguing from Bain's data,[7] that the change to longer reaction times which on the average takes place at a temperature 150 degrees Cent. below A_1 may be explained as

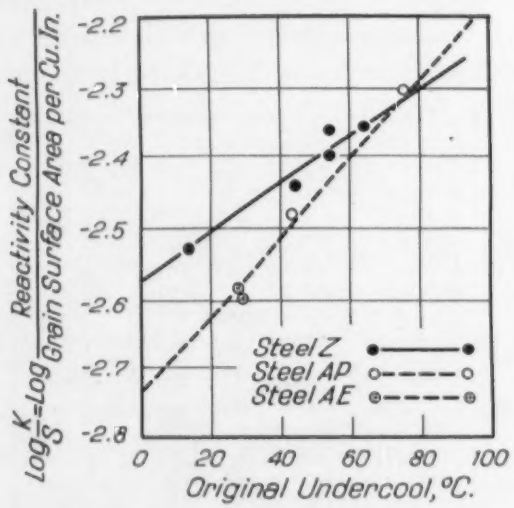

Fig. 13—Effect of Degree of Undercool on the Reactivity Constant of Steel Z, and Steels AE-AP, Aluminum-Treated.

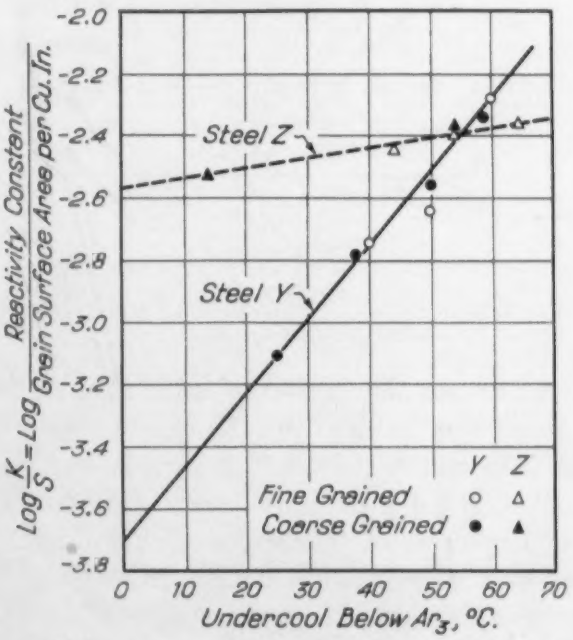

Fig. 14—Comparison of the Effect of Undercool on the Reactivity Constants of Steel Y (Silicon-Killed) and Steel Z (Aluminum-Killed).

[7] J. B. Austin, "Dependence of Rate of Transformation of Austenite on Temperature," Metals Technology, January 1935, American Institute of Mining and Metallurgical Engineers, Technical Publication No. 590.

a result of two competing factors, the first the free energy change which increases with increasing departure from A_1 and thus increases the tendency to transform and by inference the speed of reaction; and the second the viscosity of the system which progressively increases with decreasing temperature and retards the reaction; the first factor predominates between A_1 and the temperature 150 degrees

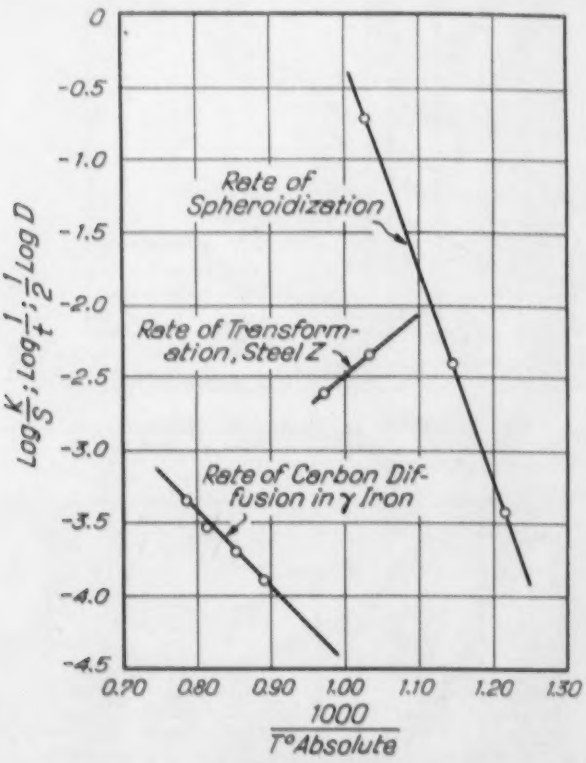

Fig. 15—Effect of Temperature on the Rates of Transformation, of Spheroidization and of Diffusion of Carbon in Gamma Iron.

Cent. lower, and the second factor predominates at lower temperatures. It was pointed out by Mehl in discussion that in all probability the first factor is in reality the tendency to nuclei formation and the second the rate of diffusion of carbon in gamma iron — not the viscosity. The observations of Tammann on the variation with temperature of the rate of nuclei formation from melts are consistent with the type of expression used by Austin for his first factor, and the variation with temperature of the rate of diffusion is consistent with the type of expression used by Austin for his second factor, this alternative method thus giving an entirely similar combined expression.

It may be concluded, therefore, that the rate of diffusion is not the controlling factor in the type of reaction discussed here, but that the rate of nuclei formation is, in all probability. We may see this somewhat more clearly in Fig. 15. It has been frequently observed that the rate of diffusion in solid metals is consistent with an expression of the form $D = Ae^{\frac{-b}{T}}$, or $\ln D = \ln A - \frac{b}{T}$. The logarithm of the diffusion coefficient of carbon in γ iron plotted against $\frac{1}{T}$ will thus give a straight line, as shown in Fig. 15, the data originating in the work of Bramley and Lord.[8] The transformation rate data for steel Z may be seen to have a slope of opposite sign, indicating that diffusion cannot determine the rate of ferrite formation. It is interesting that the rate of spheroidization of pearlite, as observed by Bailey and Roberts,[9] when plotted in this way likewise gives a straight line with a slope of the same sign as that for diffusion, which ostensibly is proof that this rate is determined by the rate of diffusion of carbon. The difference in slopes in the curves for spheroidization and diffusion originates in the fact that spheroidization involves diffusion in α iron, and also in the uncertainties inherent in determining the rate of spheroidization. Actually the curve shown represents the time for completion of spheroidization.

The Formation of Ferrite upon Normalizing

In a previous study on the effect of deoxidation on the transverse impact strength of normalized steels, it was found that the impact value was directly dependent upon the amount of ferrite formed during normalizing.[2] It was further found that steels of the same nominal composition gave widely different amounts of ferrite on normalizing. This seemed to be caused by the differences in the austenite grain-size which was determined by the type of deoxidation practice used in the preparation of the steel.

The difference between the behavior of silicon- and aluminum-killed steels is illustrated in Fig. 16, in which the fraction of the total

[8] A. Bramley and H. D. Lord, "The Gaseous Cementation of Iron and Steel, VI: The Nature of the Diffusion of Carbon in Iron," Carnegie Scholarship Memoirs, Vol. 18, 1929, p. 1.

[9] R. W. Bailey and A. M. Roberts, "Testing of Materials for Service in High Temperature Steam Plants," *Proceedings*, Institute of Mechanical Engineers, Vol. 22, 1932, p. 209.

(equilibrium) ferrite developed during normalizing is plotted against the percentage of carbon. The total or equilibrium ferrite is essentially that which is found on thorough annealing. With the size of the bar chosen, normalizing in still air developed all of the ferrite up to 0.45 per cent carbon, but above this, silicon-killed steels developed a decreasing fraction of the total ferrite while the aluminum-

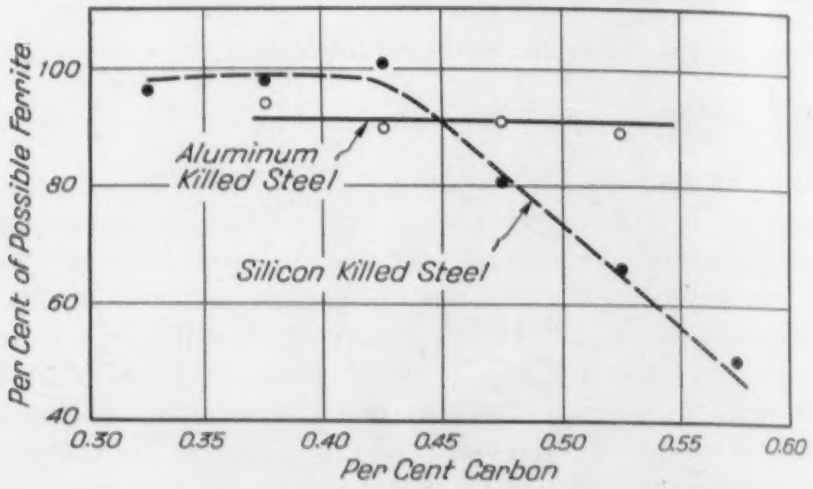

Fig. 16—Effect of Deoxidation on the Formation of Ferrite During Air-Cooling of ¾-Inch Bars.

killed steels developed essentially all of the ferrite throughout the carbon range shown.

It is not possible to predict the amount of ferrite developed on normalizing aluminum-killed and silicon-killed steels of the same grain-size from the data presented in the preceding section. As shown in Fig. 14, aluminum-killed steels form ferrite more rapidly at high temperatures than silicon-killed steels, and less rapidly at low temperatures; ferrite doubtless forms from austenite over a wide temperature range upon cooling during normalizing, and the relative amounts of ferrite formed at any one temperature (or small temperature interval) would be difficult to predict. An endeavor was therefore made to determine the relative amounts of ferrite formed during normalizing as compared to that formed during annealing for several of the steels listed in Table I, with proper regard for the effect of grain-size and for the mass of the sample.

Methods. Cubes were cut from stock of the dimensions ¼, ½, 1, and 2 inches. Different austenite grain-sizes were developed by heating the steels to different temperatures within the austenite

range; subsequent to this treatment all samples were allowed to cool in the furnace to 800 degrees Cent. (1470 degrees Fahr.) and left at this temperature for twenty minutes before being removed from the furnace and cooled in air. The amount of ferrite formed was determined by the method described in the preceding section, as was also the austenite grain-size.

Results

The results of this study are given in Table IX. The fraction of the total ferrite formed on normalizing is represented by the fraction $\frac{Fn}{Fa}$, where Fn = the amount of ferrite formed on normalizing and Fa = the amount of ferrite formed on annealing.

The data in Table IX are reproduced in Fig. 17, in which the fraction $\frac{Fn}{Fa}$ is plotted against the number of grains per square inch at 100 diameters. These curves are parabolic and extrapolate smoothly to the origin. When these results are plotted against grain

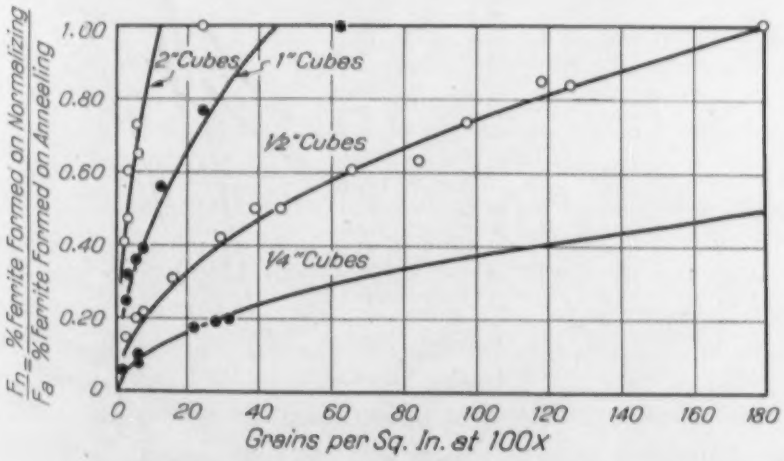

Fig. 17—Effect of Grain-Size and Mass on Ratio of Ferrite Formed During Normalizing and Annealing.

surface area instead of number of grains the curves are straight lines (it will be observed that the equation for the calculation of grain surface area given early in the paper is parabolic, so that this result is not surprising); this is illustrated in Fig. 18. This figure shows clearly that the grain surface area is the fundamental quantity gov-

Table IX

Per Cent Ferrite Developed on Normalizing Various Sizes of Cubes

Steel	Diameter of Cube	(Fa) Per Cent Ferrite on Annealing	(Fn) Per Cent Ferrite on Normalizing	Fn/Fa	(G) Grains/in² at 100×	(S) Grain Surface at 100×
AP*	¼ inch	39.8	2.2	0.06	2.1	5.8
AS*	¼ inch	45.9	3.8	0.08	6.1	9.9
AT*	¼ inch	49.6	4.0	0.08	5.7	9.6
AR*	¼ inch	52.3	5.3	0.10	6.1	9.9
AS*	¼ inch	45.9	7.8	0.17	22.0	18.7
AR*	¼ inch	52.3	10.0	0.19	28.0	21.1
AT*	¼ inch	49.6	10.0	0.20	31.8	22.5
AP*	¼ inch	39.8	22.2	0.56	220.0	59.3
AD	½ inch	46.8	4.6	0.10	2.2	5.9
AD	½ inch	46.8	6.9	0.15	2.7	6.5
Z*	½ inch	51.1	7.1	0.14	2.9	6.7
Y	½ inch	50.3	8.5	0.15	2.9	6.7
Y	½ inch	50.3	7.1	0.14	4.3	8.3
Y	½ inch	50.3	10.2	0.20	5.4	9.3
Y	½ inch	50.3	10.0	0.20	7.6	11.0
AD	½ inch	46.8	10.5	0.22	7.7	11.1
Y	½ inch	50.3	15.5	0.31	16.0	16.0
AL	½ inch	50.3	21.2	0.42	29.2	21.6
X	½ inch	60.1	29.8	0.50	39.6	25.2
Y	½ inch	50.3	25.3	0.50	46.0	27.1
J	½ inch	48.0	30.3	0.61	65.5	32.4
AD	½ inch	46.8	29.3	0.63	84.0	35.6
AE*	½ inch	35.8	26.0	0.73	97.2	39.4
Z*	½ inch	51.1	43.2	0.85	118.0	43.5
AE*	½ inch	35.8	30.0	0.84	126.0	44.9
AE*	½ inch	35.8	36.7	1.03	180.0	53.7
Z*	½ inch	51.1	51.5	1.01	182.0	54.0
J	1 inch	48.0	7.6	0.16	2.2	5.9
Y	1 inch	50.3	12.5	0.25	2.9	6.7
Z*	1 inch	51.1	16.2	0.32	3.4	7.4
J	1 inch	48.0	17.3	0.36	5.8	9.6
Y	1 inch	50.3	19.4	0.39	7.6	11.0
Y	1 inch	50.3	28.3	0.56	12.4	14.1
Y	1 inch	50.3	39.0	0.77	24.6	19.8
Y	1 inch	50.3	50.3	1.00	62.5	31.6
J	2 inch	48.0	19.5	0.41	2.2	5.9
Z*	2 inch	51.1	24.0	0.47	3.4	7.3
Y	2 inch	50.3	30.4	0.60	3.1	7.0
Y	2 inch	50.3	32.5	0.65	6.2	10.0
J	2 inch	48.0	35.0	0.73	5.8	9.6
Y	2 inch	50.3	50.3	1.00	24.6	19.8

*Aluminum-killed steels

erning the amount of ferrite precipitating, as it was also shown to be with isothermal transformations.

Inasmuch as data for both silicon-killed and aluminum-killed steels are plotted in Figs. 17 and 18 it is seen that the deoxidation practice is unimportant with respect to the fraction of ferrite formed on normalizing when comparisons are made on the basis of equal grain-sizes or equal grain surface areas; deoxidation practice is greatly important, however, in determining the austenite grain-size fixed by a given annealing treatment and thus for the absolute amount

of ferrite developed per unit mass of sample. Thus deoxidation practice affects the amount of ferrite formed on normalizing only insofar as it affects the austenite grain-size.

This similarity in the behavior of silicon-killed and aluminum-killed steels doubtless originates in the circumstance suggested at the beginning of this section, namely, that the higher rate of ferrite formation at high temperatures in aluminum-killed steels in comparison with silicon-killed steels is balanced by the lower rate at low

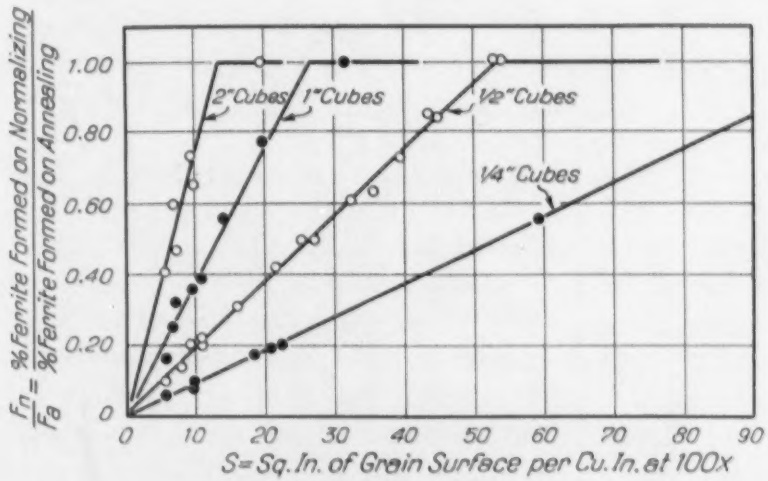

Fig. 18—Effect of Grain Surface and Mass on Ratio of Ferrite Formed During Normalizing and Annealing.

temperatures, so that there is no difference in the final amounts of ferrite developed on normalizing.

The value of the grain-size at which the full amount of ferrite forms on normalizing, when $\frac{Fn}{Fa} = 1$, is of practical importance, particularly since the amount of ferrite formed during this process controls the impact properties, and very likely other properties. Thus, if the maximum grain-size compatible with the full development of ferrite on normalizing is known for a given mass of steel, it might be possible to use simple heat treatments rather than to employ expensive deoxidizers to produce an excessively fine grain. With this thought in mind, Table X has been developed, listing the maximum grain-sizes for which the full amount of ferrite develops.

It is evident that the values given in Table X form a geometrical progression. The surface area and the mass (in volume) of the test piece must control the rate of cooling, and this rate must be pro-

Table X
Edge of Cube

	¼-inch	½-inch	1 inch	2 inches
S—Square inches of grain surface at 100 ×	107	53.5	26.8	13.4
G—Grains/in² at 100 ×	715	179.0	41.5	11.2

portional to the ratio of surface area to mass (or volume). This ratio for the sizes of cubes used is given in Table XI. Comparison of the ratio surface area/volume with the value for grain surface

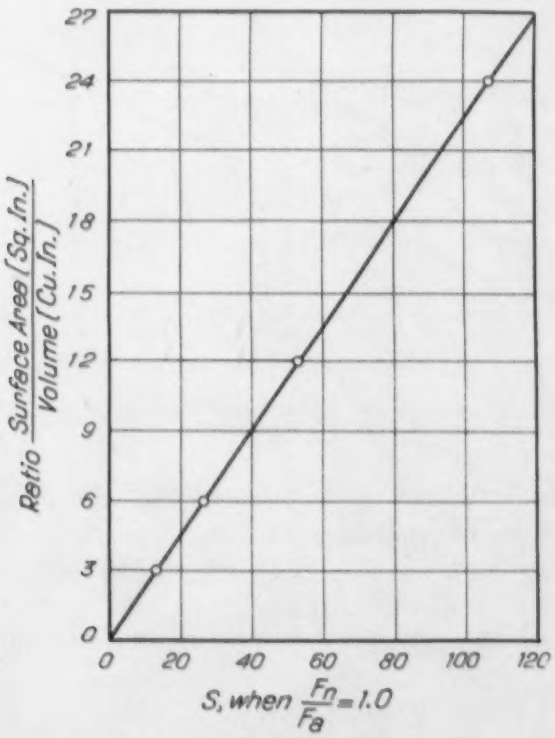

Fig. 19—Relation Between Specimen Size and Grain Surface Area Necessary for Complete Ferrite Formation.

Table XI
Relation Between Surface Area and Volume for Various Sizes of Cubes

Specimen Size	Surface Area Square Inches	Volume Cubic Inches	Surface Area / Volume
¼-inch cubes	0.375	0.015625	24
½-inch cubes	1.500	.125000	12
1-inch cubes	6.000	1.000000	6
2-inch cubes	24.000	8.000000	3

area S when $\frac{Fn}{Fa} = 1$, as given in Table X, shows that both are geometric progressions of the same type. Accordingly when these two quantities are plotted against each other, a straight line relationship obtains, as shown in Fig. 19. From this figure values for the grain surface area for the condition $\frac{Fn}{Fa} = 1$ may be read off for cubes of different sizes, and from the grain surface areas, the more usual quantity, grains per square inch at 100 diameters, may be calculated. Because of this, it is believed that Figs. 18 and 19 should prove of practical value.

Influence of Composition and Deoxidation Practice on Hardenability

The relationship between the hardenability and the composition and grain-size of a steel has been pointed out by Bain,[1] who has stated that the use of aluminum in deoxidation produces a highly reactive steel and therefore a shallow-hardening steel, primarily because of the effect of the small grain-size which characterizes this steel. Bain correlated the hardenability with the rate of pearlite formation, but a correlation of this sort may also be made with the rate of ferrite formation, for ferrite formation is frequently observed in hardenability tests on shallow-hardening steels. For this reason, hardenability tests were performed on three silicon-killed and three aluminum-killed steels for which data on the rate of ferrite formation had been obtained.

Methods. These tests were performed in the standard way on 1-inch rounds, four to five inches in length. In order to determine the effect of grain-size, three different test pieces were prepared of each steel, and single bars heated respectively to 800, 900, and 1000 degrees Cent. (1470, 1650, 1830 degrees Fahr.) for one hour. These were then cooled in the furnace to 800 degrees Cent. (1470 degrees Fahr.) and quenched in ice water. The quenched bars were then cut in half by a high speed cutter running in water, and Rockwell "C" hardness readings taken along three diameters on the sectioned faces, and finally the values at equal radii averaged.

Results

The data obtained in this way are given in Table XII and Fig.

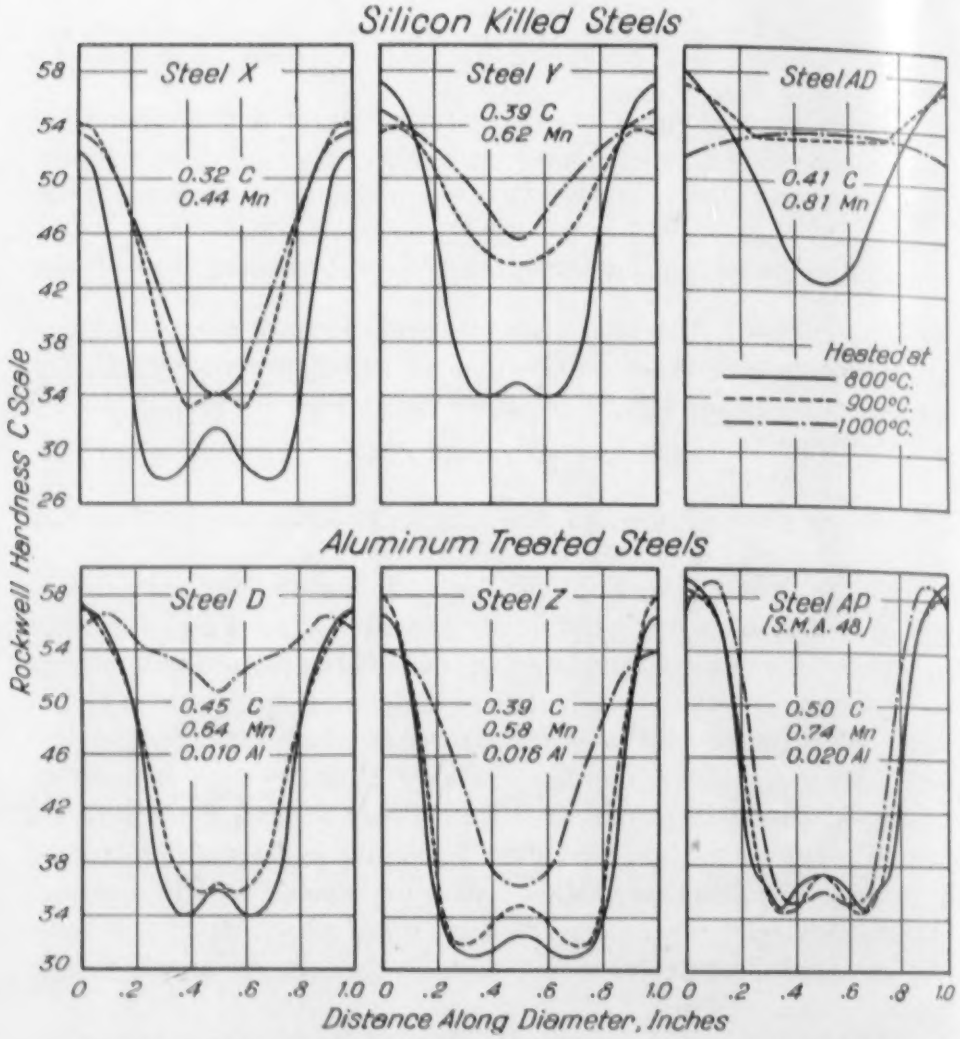

Fig. 20—Hardness Penetration in 1-Inch Round Bars Heated to Various Temperatures for 1 Hour and Water-Quenched from 800 Degrees Cent.

20. The hardenability of a steel is usually appraised by a visual inspection of curves such as shown in Fig. 20, or by a figure representing the depth of the hardened zone for a piece of a given diameter. This method is obviously satisfactory for practical purposes.

A semi-quantitative method of evaluating hardenability may be derived by calculating the relative areas (or volumes) of the hardened and the unhardened portions of the hardenability test specimens. This has been done for the tests reported here, by dividing the cross sectional area into a series of concentric rings and multiplying the area of each ring by the average hardness of the area. If we take the maximum hardness (developed on the surface) and

Table XII

Hardness Penetration in One-inch Round Bars, Heated to Various Temperatures for One Hour and Water-Quenched from 800 Degrees Cent.

Heating Temperature	Steel X			Steel Y			Steel AD		
	800°C.	900°C.	1000°C.	800° C.	900°C.	1000°C.	800°C.	900°C.	1000°C
Inches from Center	ROCKWELL "C" HARDNESS								
.50	52.2	54.2	53.6	57.2	53.4	55.2	58.1	57.2	51.8
.45	51.3	54.0	53.1	56.7	53.7	54.8	57.0	56.9	52.2
.40	46.4	51.9	52.0	54.8	53.5	53.9	55.1	55.9	52.8
.35	41.3	49.6	49.7	51.6	52.2	53.1	53.6	55.2	53.0
.30	32.6	46.6	46.8	46.5	50.4	52.0	52.4	54.3	52.9
.25	28.5	42.3	44.1	39.2	48.3	50.7	50.1	53.5	53.4
.20	27.9	38.2	41.5	35.9	46.6	50.1	48.2	53.2	53.5
.15	28.0	35.3	38.9	34.1	45.3	48.0	45.4	53.4	53.2
.10	29.0	33.1	36.0	33.9	44.5	47.2	43.6	53.2	53.8
.05	30.7	33.7	34.5	34.5	43.8	46.3	42.7	53.1	53.4
.00	31.6	34.0	34.0	35.0	43.8	45.6	42.4	52.9	53.5
	Steel D			Steel Z			Steel AP		
.50	57.0	57.2	55.6	56.5	58.0	54.0	59.2	58.4	57.3
.45	56.6	56.0	56.2	55.7	56.4	53.6	58.7	57.9	58.6
.40	54.6	54.1	56.7	50.9	50.8	53.0	56.9	56.9	59.1
.35	52.2	51.7	55.9	41.0	44.1	51.2	53.0	52.8	56.8
.30	47.6	48.5	54.7	34.4	35.4	48.7	43.5	45.3	52.6
.25	40.5	44.6	53.9	31.7	32.2	46.0	37.1	39.3	43.8
.20	35.9	40.4	53.5	31.5	32.0	43.0	36.0	35.6	38.3
.15	34.2	37.2	53.0	31.0	32.5	39.7	34.7	34.6	35.4
.10	34.1	36.1	52.4	31.6	33.6	37.4	36.3	34.8	35.1
.05	35.2	35.8	51.5	32.4	34.5	36.5	37.1	36.5	35.5
.00	36.0	36.4	50.8	32.5	35.0	36.3	37.2	37.2	36.2

Table XIII

Hardenability of One-inch Rounds in Terms of Percentage-hardness

Designation of Steel	Heating Temp. °C.	Area of Specimen	Maximum Rockwell "C"	Maximum Rockwell-Area	Observed Rockwell-Area	$\frac{\text{Observed}}{\text{Maximum}} \times 100$ Per Cent Hardenability
X	800	0.786	52.2	41.0	31.7	77.3
X	900	0.786	54.2	42.6	37.3	87.5
X	1000	0.786	53.6	42.1	37.7	89.6
Y	800	0.786	57.2	45.0	38.0	84.5
Y	900	0.786	53.4	42.0	40.0	95.3
Y	1000	0.786	55.2	43.3	41.4	95.5
AD	800	0.786	58.1	45.7	41.7	92.1
AD	900	0.786	57.2	45.0	43.4	96.5
AD	1000	0.786	53.6	42.1	41.6	99.0
D	800	0.786	57.0	44.8	38.3	85.5
D	900	0.786	57.2	44.9	39.0	86.8
D	1000	0.786	56.7	44.5	43.3	97.4
Z	800	0.786	56.6	44.5	33.9	76.2
Z	900	0.786	58.0	45.5	34.8	76.5
Z	1000	0.786	54.0	42.5	38.6	90.8
AP	800	0.786	59.2	46.5	38.5	82.8
AP	900	0.786	58.4	45.9	38.7	84.3
AP	1000	0.786	59.1	46.5	40.8	87.8

multiply it by the area of the test piece, we obtain a pure number which represents a completely hardening steel. If we now take the observed hardnesses multiplied by the areas in which they obtain—as described above — we obtain a result less than this, and the ratio of the observed to the maximum representing a perfectly hardening steel, we obtain a quality factor for hardenability, which we may call "percentage hardenability." The results of this calculation are shown in Table XIII, with the last column listing the "percentage hardenability."

A relationship between grain-size and percentage hardenability may be inferred from this table (the values in the last column increase with increasing heating temperature) but the data are too meager to attempt any quantitative evaluation.

It may be seen in the table that the silicon-killed steel X possesses the lowest percentage hardenability, but this steel is too low in carbon to be classed as a hardening steel. Excluding this steel, silicon-killed steels harden more completely than aluminum-killed steels. This is shown more clearly by comparing steel Y which was killed with silicon with steel Z which was killed with aluminum; these steels were nearly identical in composition, and when both were heated in the preliminary treatment to 1000 degrees Cent. (1830 degrees Fahr.) they were nearly identical in grain-size. The table shows the silicon-killed steel Y to be the most completely hardening.

A comparison of the percentage hardenability values given in Table XIII with the characteristic rate constants a and b given in Table VIII shows that low values of a and b run parallel to low values of percentage hardenability. It does not seem possible at the present time to attach any significance to this apparent relationship, chiefly because of the complex nature of the constants a and b.

Summary

The rates of precipitation of ferrite from austenite at constant temperatures between the A_3 and A_1 temperatures for different degrees of undercool have been measured for five silicon-killed and four aluminum-killed commercial steels ranging in carbon between 0.33 and 0.50 per cent. The method of manufacture and the compositions of these steels are given. These rates may be described by the equation for the rate of a first order chemical reaction, though this equation is not strictly applicable in this case. The effect of the

method of deoxidation upon the rate of precipitation of ferrite is entirely one of controlling the grain-size of the original austenite. When this grain-size is large the rate is small and when the grain-size is small the rate is large. On this basis, aluminum-killed steels, which possess a small austenite grain-size react more rapidly than silicon-killed steels which possess a large grain-size. When, however, the rate of the reaction is expressed in terms of equal grain surface areas, the rates are much the same for both silicon- and aluminum-killed steels. On this basis, the logarithm of the rate constant was found to be a linear function of the degree of undercool. The rate of precipitation of ferrite in silicon-killed steels showed a greater dependence upon degree of undercool than in aluminum-killed steels; the reason for this is not now clear. At low degrees of undercool the rate of ferrite formation is greater in aluminum-killed steels than in silicon-killed steels; while at greater degrees of undercool the reverse is the case. The mechanism of this type of reaction is discussed in detail. It seems certain that the rate is not determined by the rate of diffusion of carbon but by the rate of ferrite nucleation.

The ratio of the amount of ferrite formed on normalizing to the amount of ferrite formed on annealing has been determined for these steels. Differences between silicon- and aluminum-killed steels are entirely attributable to the effect of the austenite grain-size; equal grain surface areas in the two types of steel gave the same ratios. Data are given for the limiting austenite grain-sizes for the full development of ferrite on normalizing for cubes of different sizes.

Measurements on the depth of hardening on water quenching of 1-inch rounds of silicon- and aluminum-killed steels have been made. The effect of deoxidation on the austenite grain-size is shown to be the chief factor in determining the hardenability. Hardenability is calculated on the basis of hardness areas and the results expressed as "percentage hardenability."

DISCUSSION

S. L. Hoyt[1]: I should like to raise a question in relation to the term reactivity or specific reactivity. What is it in terms of some other constant like diffusion velocity or reaction velocity? If it could be defined in terms of some constant of that kind, it seems to me that it would make it a little easier to understand. As for the paper proper, it is extremely valuable to one who has

[1]Director of Research, A. O. Smith Corp., Milwaukee.

to deal with steel products, particularly if the treatments involve heating and cooling at various rates. Personally, I appreciate having the data that are given, and the very clear-cut way in which the problems involved are dealt with.

JOHN CHIPMAN:[3] I should like to express my admiration for this piece of work, and especially for the conclusion that the effect of deoxidation upon the rate of formation of ferrite is only that which is attributable to its influence on grain-size. That conclusion, I believe, differs from the point of view expressed in the recent Campbell Memorial Lecture, and also differs from what I would have anticipated. I think we can all accept this as a very important piece of work.

Reply to Discussion by D. L. McBride

The dimensions of the specific reactivity constant are per cent ferrite per minute per unit grain surface area per degree undercooled. As far as the numerical value is concerned it differs for different steels. Using the constant for comparative purposes alone, it does have some value, but its application to terms of absolute value has no significance. As to Dr. Chipman's comments that deoxidation has no effect upon the relative amount of ferrite formed, that is true for steels containing more than 0.30 per cent carbon and less than 0.55 per cent carbon. Going beyond that we find that the aluminum-killed steels do behave just as shown on these curves, even up to 0.55 or 0.60 per cent carbon, but beyond 0.60 per cent carbon silicon-killed steels begin to develop decreasing amounts of ferrite.

---

[3]American Rolling Mill Co., Middletown, Ohio.

EQUILIBRIUM IN THE REACTION OF HYDROGEN WITH FERROUS OXIDE IN LIQUID IRON AT 1600 DEGREES CENT.

By M. G. Fontana and John Chipman

Abstract

A careful experimental study of the reaction of hydrogen with dissolved ferrous oxide in liquid iron has led to the discovery and elimination of a source of error which had affected the accuracy of results previously reported. It is found that the equilibrium constant of the reaction is a true constant at all oxygen concentrations up to saturation. The results are used to obtain the free energy of ferrous oxide at 1600 degrees Cent. (2910 degrees Fahr.). Calculations show that the results of this investigation constitute a confirmation of Vacher's experiments on the iron-carbon-oxygen system.

THE reactions involving ferrous oxide in liquid steel are of sufficient importance to justify the expenditure of considerable time and effort in determining the exact behavior of this substance under conditions of equilibrium. A number of its reactions have been investigated in some detail and their equilibrium constants are now known with a fair degree of approximation. Among the simplest and most useful of these studies have been those in which the dissolved ferrous oxide was brought into equilibrium with a controlled gaseous atmosphere as illustrated in the following equations:

$$FeO\ (\text{in Fe}) + CO = Fe\ (\text{liq.}) + CO_2 \qquad (1)$$
$$FeO\ (\text{in Fe}) + H_2 = Fe\ (\text{liq.}) + H_2O \qquad (2)$$

Both of these reactions were investigated by Vacher (1)[1] and the second was studied in somewhat more detail by Chipman (2).

[1]The figures in parentheses refer to the bibliography appended to this paper.

A paper presented before the Seventeenth Annual Convention of the Society held in Chicago, September 30 to October 4, 1935. This paper is taken from a dissertation submitted by M. G. Fontana in partial fulfillment of the requirements for the degree of Doctor of Philosophy at the University of Michigan. Dr. Fontana is now assistant metallurgist with E. I. du Pont de Nemours and Company, Wilmington, Delaware. Dr. Chipman was Research Engineer, Department of Engineering Research, University of Michigan, and is now Associate Director of the Research Laboratories, Amercian Rolling Mill Company, Middletown, Ohio. Manuscript received May 31, 1935.

Although their results were qualitatively similar they left a good deal to be desired as to the numerical accuracy of their agreement. Moreover they were chiefly confined to low oxygen concentrations. The present experiments were undertaken for the purpose of finding the cause of the numerical discrepancies in these two sets of data and of extending the measurements on Reaction 2 up to the limiting solubility of ferrous oxide in liquid iron.

Method and Apparatus

The method employed was similar to that used in both of the investigations mentioned above. A controlled mixture of steam and

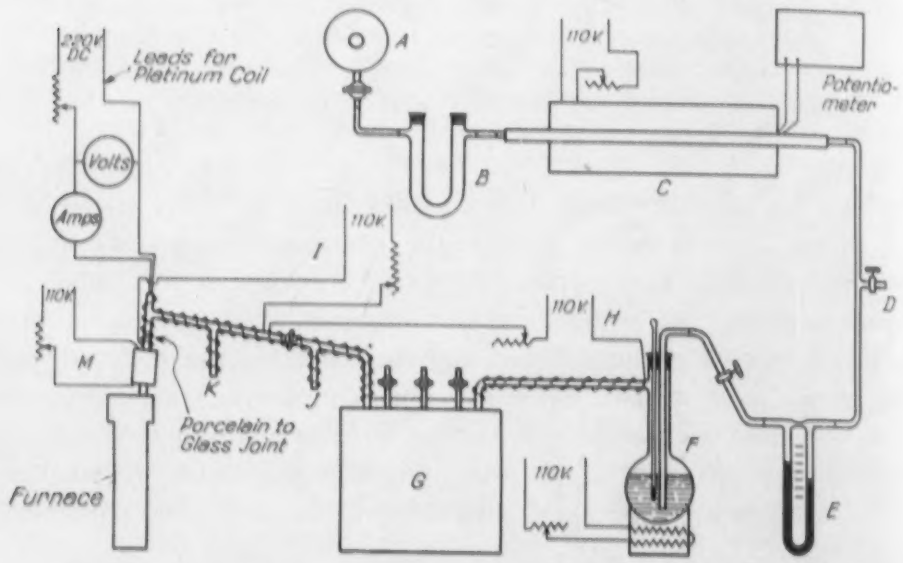

Fig. 1—Schematic Diagram of Apparatus Used in this Investigation. (A) Gas Tanks; (B) U Tube; (C) Furnace; (D) By-Pass Outlet; (E) Flow Meters; (F) Saturator; (G) Saturator; (H) Heater; (I) Heater; (J) Relief Outlet; (K) By-Pass Inlet; (M) Heater.

hydrogen was passed over the surface of a small melt of electrolytic iron in a closed induction furnace. After allowing sufficient time at constant temperature for the attainment of equilibrium the melt was cooled and analyzed for oxygen.

The apparatus is shown in Fig. 1. The hydrogen used was ordinary commercial hydrogen obtained in the usual tank cylinders. The gas flowed from the tank, A, through a U-tube, B, filled with ascarite and through a quartz tube, C, packed with platinized asbestos and heated to 500 degrees Cent. (930 degrees Fahr.) in order to

remove free oxygen. From this furnace the hydrogen passed through an orifice flowmeter, E, and then through the saturators and into the furnace. D is the by-pass outlet that was used while melting or heating the iron under hydrogen. In this case D was connected to the inlet K by means of rubber tubing which had a pinch clamp on it near D to regulate the flow of gas.

The preliminary saturator F consisted of a liter side-arm flask partially filled with water and heated by a resistance heater to approximately the same temperature as the saturator G. The latter consisted of three vertical towers, the first two packed with broken glass and the third empty to serve as an entrainment separator. This assembly was made of pyrex glass and was welded together so that no rubber connections were necessary. It was immersed in a thermostat consisting of a large battery jar, which was filled with transformer oil. The oil was vigorously stirred by means of an immersed paddle which was driven by an electric motor. The outside of the jar was well insulated to cut down the heat loss and to insure better temperature control. The heating coil had a variable resistance in series by means of which the temperature was manually controlled to less than $\pm$ 0.1 degree Cent. The temperature was measured by means of a 40-100 degrees Cent. (105-210 degrees Fahr.) thermometer calibrated against a standard thermometer from the U. S. Bureau of Standards.

The performance and efficiency of the saturator under various conditions were checked by passing the gas mixtures through a weighed tube containing dehydrite and phosphorus pentoxide to absorb water which was determined by the gain in weight. The hydrogen was collected over water and determined volumetrically. The saturator temperature, the flask temperature, the rate of hydrogen flow and the conditions in the entrainment chamber were varied. The results showed complete saturation under all of these conditions

Fig. 2 shows a section of the furnace set-up used in the equilibrium work. The silica tube was surmounted by a brass head which was cemented securely with zinc cement. The sight glass was of pyrex and was held loosely in position by means of a slit brass ring. One turn of previously burned asbestos cord served as a gasket. This arrangement also provided a safety valve to take care of any explosions that might have occurred in the furnace. The sight glass was raised from the furnace head proper by means of a brass tube extension which was water cooled to prevent fogging of the sight

glass which otherwise would have been a source of trouble. There was not sufficient cooling, however, to cause condensation of water vapor.

The iron was melted in a magnesia crucible which rested on a magnesia base. For certain runs in which the crucible containing the liquid iron was to be quenched directly into a bath of tin or water,

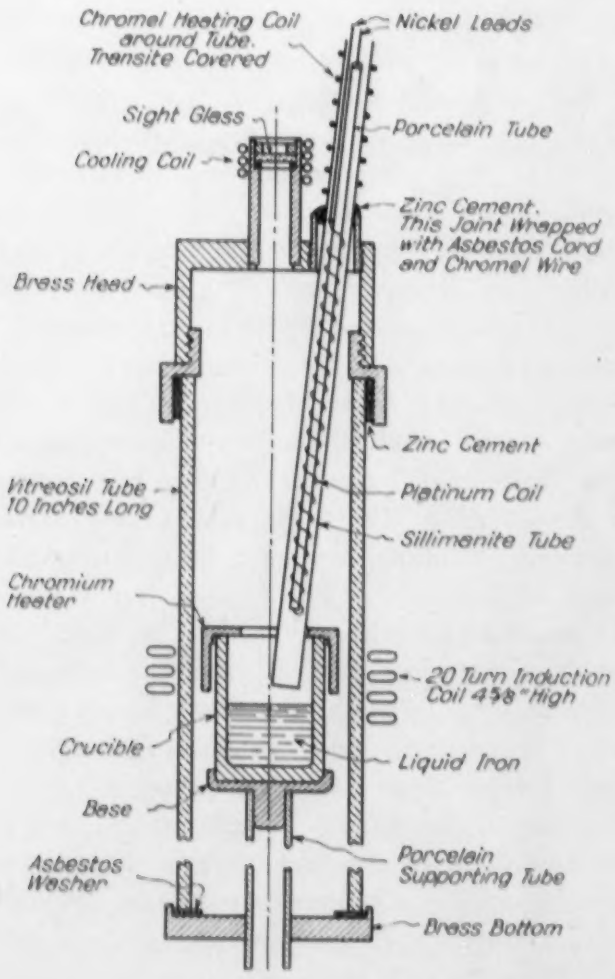

Fig. 2—Cross Section of Furnace Setup Used in this Investigation.

the base was not used. For these runs the crucible was formed with a lower projection which fitted directly into the supporting tube. A crucible of this type is shown in the extreme left of Fig. 3. A soft brick washer was used to separate the crucible from the porcelain tube to avoid overheating the latter and so that it would not crack

when it was immersed into the water. The base and several crucibles are shown in Fig. 3. The chromium heater, which will be discussed later, rested directly on the crucible as shown in Fig. 2. The heater had an elliptical hole in it through which the sillimanite inlet tube passed and through which the optical pyrometer was sighted. The whole internal furnace set-up was supported from the bottom by means of a porcelain tube. The seal between the furnace bottom and

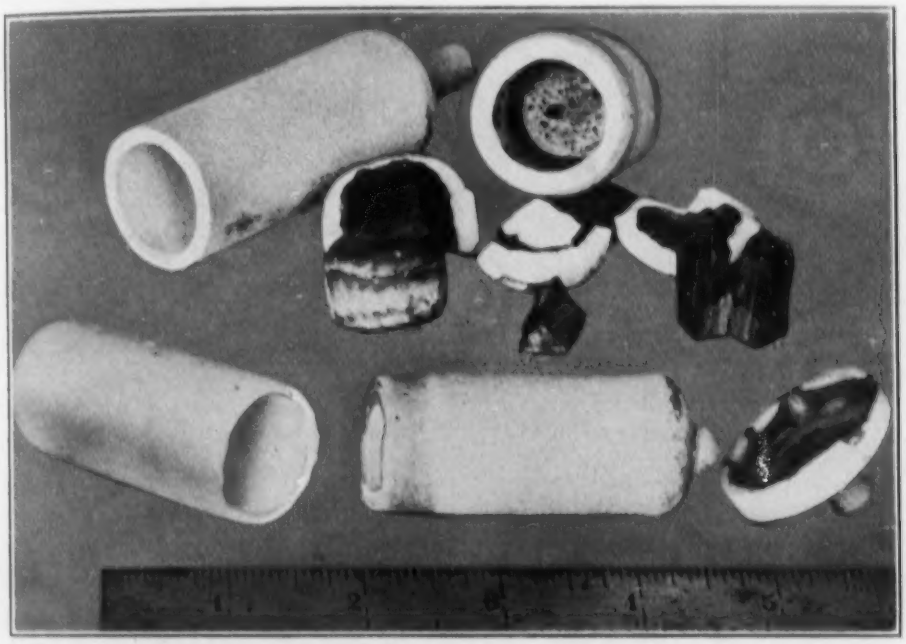

Fig. 3—Typical Crucibles and Ingots Used in this Investigation.

the supporting tube was made with asbestos cord. An asbestos washer was placed between the brass bottom and the quartz tube. The power for the 20-turn induction coil was furnished by a 35 Kva. high frequency converter. The temperature of the chromium heater was varied by raising or lowering its position with respect to the top of the induction coil.

Magnesium oxide was used for the manufacture of the crucibles because it is not easily reduced and possesses the very desirable property of absorbing several times its own weight of iron oxide without seriously impairing its use as a refractory. Beryllium oxide was tried and gave more satisfactory results than magnesium oxide but its high cost precluded its extensive use. A mix consisting of one part of ball-milled powder and two parts of 60-mesh yielded the

best crucibles. The crucibles were formed dry by tamping in a graphite mold around a steel core. After removing the core and covering each mold with a graphite top seven of the crucibles were simultaneously fired in an induction furnace to about 2000 degrees Cent. (3630 degrees Fahr.). Crucibles produced in this manner were easily made, were hard and dense, and possessed remarkable strength.

The electrolytic iron which was used throughout this investigation was first melted and cast into 0.9-inch round bars. Pieces of these bars weighing about 50 grams were each melted in a crucible under a pressure of 0.05 millimeters or less. The crucible containing its vacuum-melted charge was then used for an equilibrium run. The reasons for vacuum melting were to remove nitrogen and carbon and to prepare a charge of iron that could be readily melted down without great danger of bridging or of overheating the chromium heater. After the equilibrium run "pie slices" were cut from the ingot and analyzed for oxygen in an improved vacuum fusion apparatus. This is unquestionably the best method for determining oxygen in ingots of this type. Ingots and the manner of sampling are illustrated in Fig. 3.

The temperature of the liquid iron was measured by means of an optical pyrometer of the disappearing filament type which was sighted through a prism and the sight glass in the furnace head. This previously calibrated instrument was checked during each run by observing the melting point of iron by reducing the power input into the furnace so as to cause a slow solidification of the metal. The melting point of iron containing low oxygen was taken to be 1530 degrees Cent. (2785 degrees Fahr.) while that of iron saturated, or nearly saturated, with oxygen was assumed to be 1525 degrees Cent. (2775 degrees Fahr.) as reported by Tritton and Hanson (3). The measurement of the temperature of the liquid iron represents the greatest source of uncertainty in this work. The temperature of the melt was regulated by carefully controlling the power input to the furnace. Practically all of the experiments were made at 1600 degrees Cent. (2910 degrees Fahr.), but for those runs made in the neighborhood of that temperature the equilibrium constant was corrected to 1600 degrees Cent. (2910 degrees Fahr) by means of the approximate temperature coefficient for the reaction as observed by Chipman (2).

Early developments during this investigation indicated that the degree of preheating the gases had a decided effect upon the equi-

librium as will be explained below. The preheating arrangement is partially shown in Fig. 1. The first three heaters H, I, and M consisted of chromel wire wound around the tubing. M was covered with transite and kept at a red heat. The sillimanite inlet tube contained a platinum coil as shown in Fig. 2. The temperature of the coil was determined by measuring its resistance, and calibration by this method gave the average temperature of the coil. The chromium heater as shown in Fig. 2 heated the upper portion of the crucible and part of the exit end of the inlet tube. The temperature of the heater was estimated to be 1600 degrees Cent. (2910 degrees Fahr.) during the run. The gases were also preheated by radiation from the liquid metal itself.

Chromium was chosen for the construction of the heater because of its high melting point and good resistance to oxidation. Considerable trouble was encountered before a sound and easily machinable casting was produced. Several molds and molding materials were tried with poor success before the mold that yielded good castings consistently was devised. This consisted of a two-piece steel mold with an inverted magnesia crucible for a core. The crucible was held firmly centered by means of a screw and a hole in the mold allowed the expanding gases in the crucible to escape. Electrolytic chromium was used and it was melted in a 400-gram induction furnace constructed especially for that purpose. A graphite heater was first tried but it caused considerable fogging of the sight glass and also reacted with the water vapor present to form carbon monoxide. The absorption of this gas by the melt resulted in hollow ingots with low oxygen contents.

Procedure

The hydrogen train and the saturators were thoroughly flushed out with purified gas for about two hours before the power was turned on to the furnace. The furnace was flushed out with hydrogen for at least fifteen minutes before the heating of the metal began. The iron was sometimes melted under hydrogen and sometimes under saturated, or partially saturated, hydrogen. After the iron had completely melted, the power input was reduced and the melting point of the iron determined during its slow solidification. The power was then increased and the hydrogen was passed through the saturator at the desired rate of flow. The beginning of the run was marked by the time when the furnace temperature "settled

down" at 1600 degrees Cent. (2910 degrees Fahr.) and the run was continued for about 45 minutes.

The iron was cooled in position in the furnace by simply turning off the power or it was quenched for a more rapid rate of cooling. The time required for solidification in position was about fifteen seconds and most of the ingots were cooled in this manner. Several attempts were made to lower the crucible into a bath of liquid tin contained in the bottom of the furnace, but they were not completely successful. The most rapid cooling was obtained when the crucible was lowered directly into a large bath of water at the end of the run. The furnace power was not turned off during this operation and the time required to get the crucible completely immersed in water was only about one second. The crucible was lowered vertically into the water so that the metal would not run out.

Experimental Results

A total of forty ingots were prepared during this investigation and a summary of all of the data that are considered reliable is shown in Table I. Since a large part of this work was concerned with developing a furnace set-up and technique, some of the runs were made to determine the effects of variables in the procedure and their results are not included in determining the equilibrium constant. In addition, several ingots were rejected because of uncertain temperature measurement chiefly due to fogging of the sight glass. Several were discarded because of air leaks as evidenced by high nitrogen content (0.002 per cent or higher) of the ingot, and others because of carbon monoxide evolution resulting in hollow ingots in the runs wherein the graphite heater was used.

The second column of Table I gives the ratio of steam to hydrogen in the furnace as computed from the barometric pressure and the vapor pressure of water in the saturator, and corrected for the small deviation of steam from the ideal gas law. The third column gives the temperature during the final 30 to 45 minutes of each run. The fourth contains the average of duplicate or triplicate oxygen determinations.

The equilibrium constant of Reaction 2 may be most simply expressed by the following equation:

$$K' = \frac{(H_2O)}{(H_2)\ (\%\ O)}$$

The observed value of K′ is recorded in the fifth column of the table while the sixth shows the constant corrected to 1600 degrees Cent. (2910 degrees Fahr.) by means of the approximate temperature coefficient previously established (2). The 7th column contains data as to the method of preheating the gas stream which will be discussed in the following paragraphs.

Table I

Heats and Equilibrium Data

Heat Number	$\frac{H_2O}{H_2}$	Temp °C.	Per Cent Oxygen	K′ Observed	K′ 1600	Preheat
33	0.259	1620	0.061	4.25	4.58	None
34	0.259	1620	0.065	4.00	4.33	Pt. coil
35	0.259	1625	0.068	3.82	4.23	Pt. coil
37	0.124	1620	0.030	4.10	4.43	Pt. coil
40	1.021	1600	0.211	***	***	Pt. coil
51	0.263	1600	0.062	4.20	4.20	Coil + Cr heater
52	0.263	1590–95	0.063	4.16	4.04	Coil + Cr heater
53	0.263	1600	0.067	3.94	3.94	Coil + Cr heater
55	0.260	1600	0.060	4.31	4.31	Pt. coil
57	0.847	1605	0.222	3.82	3.90	Pt. coil
58	0.754	1600	0.184	4.10	4.10	Coil + Cr heater
59	0.723	1600	0.188	3.84	3.84	Coil + Cr heater
60	0.755	1600	0.190	3.98	3.98	Coil + Cr heater
62*	1.414	1600	0.215	***	***	Coil + Cr heater
63*	0.980	1600	0.196	***	***	Coil + Cr heater
64*	0.983	1600	0.200	***	***	Coil + Cr heater
67	0.671	1600	0.162	4.14	4.14	Coil + Cr heater
69	0.715	1595	0.196	3.66	3.58	Coil + Cr heater
70**	0.829	1605	0.209	3 96	4.04	Coil + Cr heater

*Quenched in tin.
**Quenched in water.
***See Fig. 4.

Effect of Preheating the Gases on the Equilibrium

The results of a series of experiments carried out during this investigation showed that the degree of preheating the gases had a decided effect upon the equilibrium. These experiments were prompted by the existence of several apparent anomalies. The first was that the preliminary runs at low oxygen concentration did not check the previous results obtained in this laboratory in that our new results showed appreciably lower values for the equilibrium constant. The second was that the observed ratio of steam to hydrogen was consistently higher than that calculated from the ratio CO_2:CO as found by Vacher and Hamilton (4) in equilibrium with iron of equal oxygen content. Our suspicions were further heightened by the surprising results reported by Emmett and Shultz (5) in which they observed a thermal separation of steam and hydrogen even in a flow-

ing system and at temperatures considerably below the melting point of iron.

The hypothesis presented by the writers (6) to explain the observed phenomenon is based on the well known concentration gradient that exists in solutions or gaseous mixtures when a temperature gradient is present. The heavier gas will be present in greater concentration in the cold region. The greater the ratio of the molec-

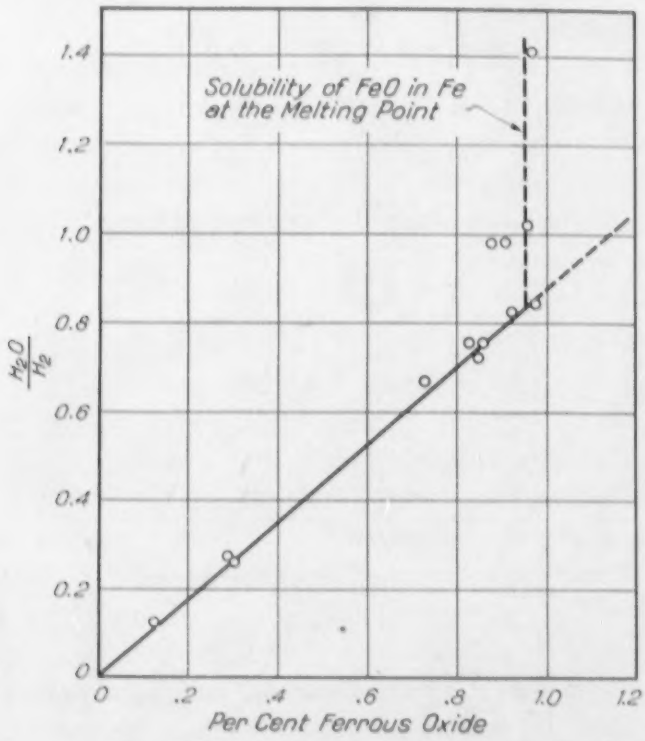

Fig. 4—Relationship Between Steam — Hydrogen Ratio and Oxide Content of the Melt.

ular weights of the gases mixed, the more pronounced the "segregation" should be for a given temperature gradient (7). This effect should be quite pronounced, therefore, in the system H_2-H_2O-liquid Fe but should not offer appreciable interference in the system CO_2-CO-liquid Fe. When the preheating of the gases is accomplished only by radiation from the liquid iron, a large temperature gradient will exist in the region adjacent to the iron and considerable thermal diffusion will occur. For a given ratio of H_2O:H_2 the concentration of H_2O will be greater in the colder region or the region further from the melt, whereas the hydrogen would tend to diffuse towards the liquid metal, and the ingot would, therefore, contain less oxygen

than it would contain if there were no "segregation" of the gases. The ideal conditions, or those which would be conducive to the existence of true equilibrium, would be attained if the gases were at the same temperature as the metal when they came in contact with the metal. Eastman and Ruben (8) have recently upheld our views on thermal diffusion in a dynamic system.

It should be possible to diminish the temperature gradient and thereby also the amount of thermal separation by preheating the gas stream as it approaches the hot metal surface. The preheating due to radiation from the liquid iron will be more efficient the lower the lineal velocity of the gases. The reason for the lower results in this work when compared to those previously reported for a given rate of flow and ratio $H_2O:H_2$, can thus be explained by comparing the sizes of the inlet tubes. In the former investigation a 3-millimeter diameter inlet tube was used, whereas we used a 7-millimeter tube, thus obtaining lower velocity of flow, better preheating of the gases and attendant higher oxygen contents of the ingots. Vacher used a lower rate of flow and a larger tube and obtained still higher oxygen contents.

The results of the heats which were made to determine the effect of preheating the gases are shown in Table II. The amount of preheat was varied by using the chromium heater described above and the platinum resistance heater inside the inlet tube. The temperatures of the chromium heater are estimates. The results indicate that the effect is greatest in the first stages as the preheating increases. Decreasing the rate of flow from 300 cubic centimeters of dry hydrogen per minute to 200 cubic centimeters has a slight effect upon the constant. It is believed that the preheating in experiments 52 and 53, especially the latter, has been sufficient to largely eliminate

Table II

Equilibrium at 1600 Degrees Cent and 0.065 Per Cent Oxygen

Heat Number	$\frac{(H_2O)}{(H_2) \times \% O}$	Flow cc/min.	Pt. Coil Temp. °C.	Preheat Conditions
1–18*	4.75	300	....	3 mm. tube
33	4.58	300	....	7 mm. tube
34	4.33	300	1170	No Cr heater
35	4.23	300	1320	No Cr heater
51	4.20	300	1170	Cr heater 1500° C.
52	4.04	300	1170	Cr heater 1600° C.
53	3.94	200	1170	Cr heater 1600° C.
55	4.31	450	1050	No Cr heater

*Reference (2).

the source of error due to thermal diffusion. Subsequent heats were made at a rate of flow of 200 cubic centimeters per minute or under conditions similar to heat number 53.

The Criteria of Equilibrium

In addition to reaching a constant value of K′ after sufficient preheating of the gases had occurred, another criterion of equilibrium was that the oxygen content of the iron reached a constant and reproducible value at a constant steam-hydrogen ratio. In the previous investigation it was found that 15 minutes was sufficient time to secure equilibrium for the oxygen concentrations of 0.01 and 0.11 per cent on which the effect of time was investigated. This rapid attainment of equilibrium is doubtless chiefly due to the fact that the iron is constantly and vigorously stirred in the high frequency induction furnace.

Most of the heats in this work were run for about 45 minutes under constant temperature, preheat, flow and steam-hydrogen ratio. At high concentrations of oxygen in the iron, the iron oxide reacts with the magnesia crucible and some of the oxygen is removed from the melt. This fact had to be considered in the ingots that were nearly saturated with iron oxide. An examination of the pieces of crucible in Fig. 3 will show the attack on the crucible by the oxide from the melt. If this reaction occurred continuously, equilibrium would never be obtained because oxygen would be continually removed from the metal. This condition, however, is not probable because of the sharp temperature gradient that exists between the liquid iron and the crucible. After some attack has occurred the outer surface of the slag layer solidifies and further slag formation is stopped. Examination of a high oxygen ingot after a run will support this contention. The surface of the crucible adjacent to the iron is bright and shiny and the ingot does not stick to the crucible wall.

Two runs were made to be sure that the attack on the crucible did not affect the equilibrium under the conditions of our experiments. Heat No. 69 was run for almost two hours and allowed to solidify in position in the furnace. This ingot contained about 0.2 per cent oxygen. Examination of Fig. 5 will show the results on this run. It will be noticed that the constant is below the line drawn for K′ thus indicating a higher oxygen content. This shows that

the effect of the crucible attack, which tends to lower the oxygen content, has not affected the result in this case and probably has been entirely eliminated in all of the heats made. Heat No. 70, which was quenched in water, was run for 1½ hours to yield an ingot of 0.21 per cent oxygen and also shows good agreement with the 45 minute runs.

The effect of the oxygen content of the charge on the equilibrium was investigated by approaching the equilibrium with higher oxygen and lower oxygen melts. This was done by subjecting the melt to

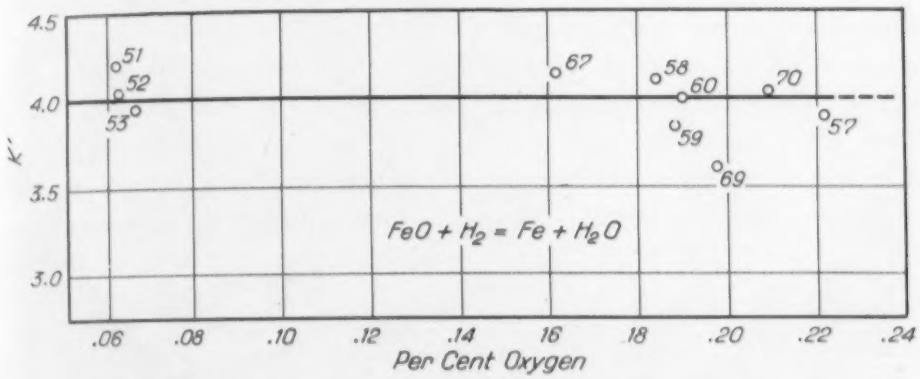

Fig. 5—Equilibrium Runs at Various Oxygen Concentrations.

a higher, or lower, steam-hydrogen ratio for some time before the desired ratio was maintained. Our experience showed that any effects due to this procedure were entirely eliminated during the 45 minutes allowed for each run under constant conditions.

Nature of the Solution of Oxygen in Iron

The completely straight line relationship between the steam-hydrogen ratios and the ferrous oxide content of the melt as shown in Fig. 4, affords a more rigorous proof than was formerly obtained that the oxygen dissolved in the liquid iron is present as an oxide containing one atom of oxygen. It also demonstrates that the solution of iron oxide in iron conforms more nearly to the ideal solution law than was previously reported.

An indication of the solubility of ferrous oxide in iron can be obtained from an examination of Fig. 4. At steam-hydrogen ratios higher than the ratio corresponding to about 1 per cent ferrous oxide, considerable ferrous oxide was ejected from the melt during solidification. Using ratios even as high as 1.4, the ferrous oxide

content of the ingot refused to exceed 1 per cent. The fact that the ferrous oxide content consistently stayed between 0.9 and 1.0 per cent may be considered as an indication of the maximum solubility of ferrous oxide in iron at the melting point. Tritton and Hanson (3) report 0.21 per cent oxygen (0.94 per cent FeO) as the solubility at the melting point. Herty (9) reports 0.22 per cent oxygen (0.98 per cent FeO). These figures are in good agreement with the data shown in Fig. 4. Herty reports the solubility of oxygen at 1600 degrees Cent. (2910 degrees Fahr.) as 0.305 per cent and Körber's (10) corresponding result is 0.325 per cent. This means that considerable ferrous oxide has to be thrown out of solution before the ingot solidifies in order to show only 0.21 per cent oxygen. The speed with which ferrous oxide is ejected as the melt cools is amazingly rapid since the time required for solidification of our ingots was very short as stated above. Confirmation of our conclusion that the excess ferrous oxide is thrown out of solution on cooling to the melting point was found in the microscopic examination of several of the ingots.

The Nature of Iron Oxide Inclusions in Iron

The large amount of ferrous oxide that is thrown out of solution as the melt cools, coalesces rapidly and tends to rise to the surface. Fig. 6 shows oxide inclusions near the top of heat 40. None of these large inclusions were found in the lower portion of the ingot, even though the time required for solidification from 1600 degrees Cent. (2910 degrees Fahr.) was only about twenty seconds. Note the very large inclusion that was trapped just as it reached the surface. Fig. 7 was taken on the middle of heat 70, and shows that the inclusions had formed but did not have time to rise to the surface. This ingot was quenched in water, and was probably completely solid in less than three seconds.

Although oxygen in liquid iron is always present as ferrous oxide, Figs. 6 and 7 show a duplex structure, which indicates the presence of another constituent. Chaudron (11) and Pfeil (12) have shown that ferrous oxide partially decomposes during cooling as follows:

$$4FeO = Fe_3O_4 + Fe$$

The ferrous oxide first becomes saturated with Fe_3O_4, and then ejects it as a separate phase as shown in the two figures. The dark

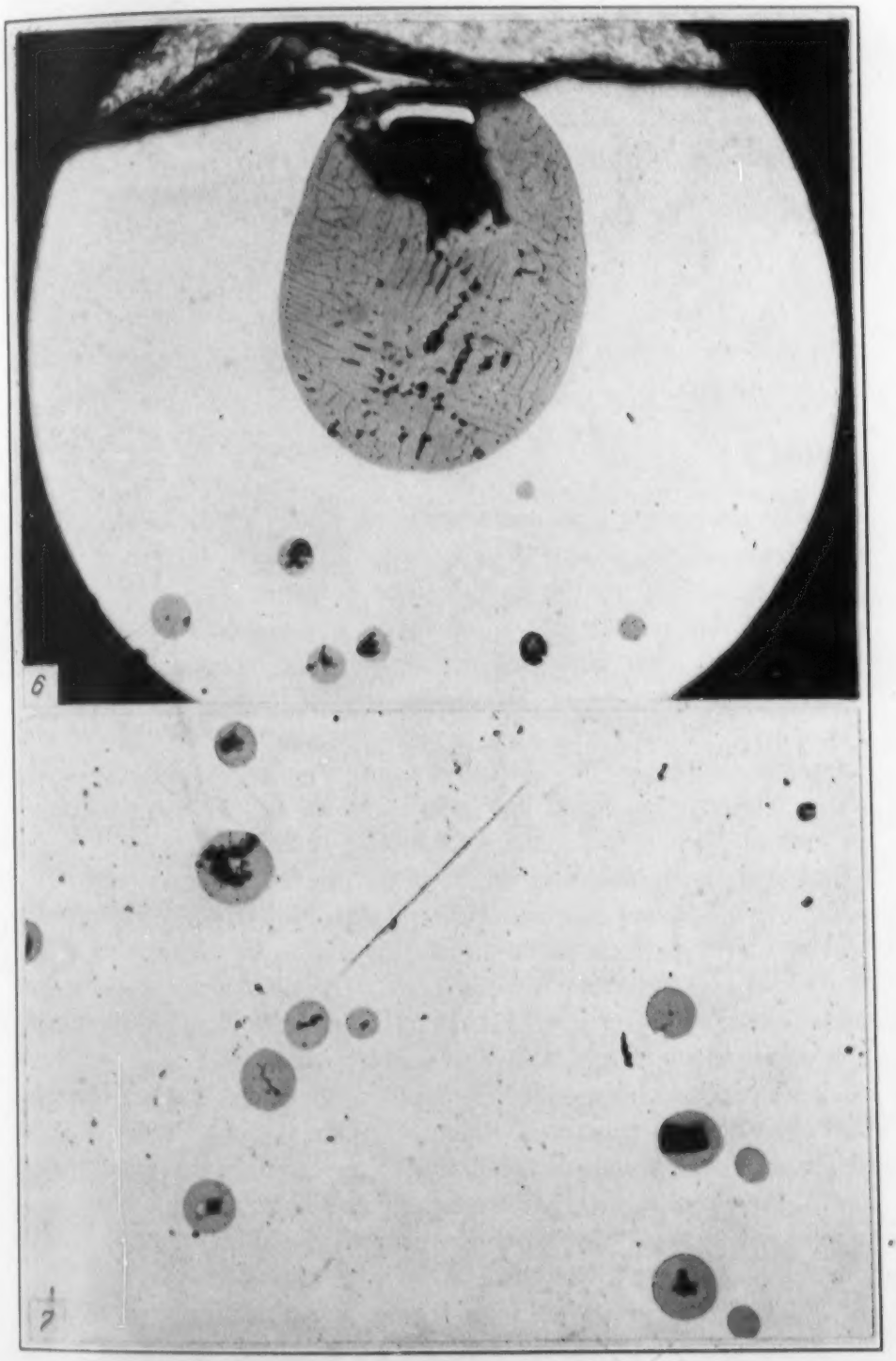

Fig. 6—Photomicrographs Showing Oxide Inclusions Near Top of Heat 40. ×100.
Fig. 7—Photomicrographs Taken Near the Middle of Heat 70 Showing that the Inclusions Had Formed but Did Not Have Time to Rise to the Surface. × 300. These Two Figures Show a Duplex Structure.

areas within the inclusions are probably Fe_3O_4 containing FeO and iron. The grey areas of the inclusions are probably FeO saturated with Fe_3O_4 and iron.

Thermodynamic Calculations

Effect of Oxygen Concentration on the Equilibrium and the Activity of Ferrous Oxide

Fig. 5 shows that the equilibrium constant for the reaction studied does not vary with the oxygen content of the iron. The constant plotted is:

$$K' = \frac{(H_2O)}{(H_2)\ (\%\ O)}$$

The line represents a value of 3.95 for K′ which was calculated as an average of the points shown except 51 which did not have sufficient preheating of the gases. The constant may be considered accurate to better than $\pm$ 0.2, or about $\pm$ 5 per cent.

The fact that K′ does not vary with oxygen concentration indicates that the reaction behaves according to the simple mass law. The activity of ferrous oxide is proportional to its concentration in the solution and this holds true not only in dilute solutions, as has been previously supposed, but also in all ranges of oxygen concentrations up to and including saturation. In the earlier work it was found that the equilibrium constant for the reaction decreased considerably with increasing oxygen concentrations indicating that the activity of the ferrous oxide did not increase as fast as the increase in ferrous oxide content of the melt. This apparent deviation of the behavior of the reaction from the laws of the ideal solution made it imperative, of course, that the activity of ferrous oxide, and not its concentration, be used when applying the mass law to reactions involving dissolved ferrous oxide. To facilitate this, a table of activity coefficients was deduced from the equilibrium measurements. Fig. 5, however, shows that the activity of ferrous oxide is equal to its per cent by weight at all concentrations. The per cent by weight will, therefore, be used in subsequent calculations.

Vacher (1) prepared four ingots by subjecting iron at 1580 degrees Cent. (2875 degrees Fahr.) to a mixture of steam and hydrogen. Our results, allowing for the difference in temperature, are well within the range of his observed equilibrium constants.

The Free Energy of Ferrous Oxide in Liquid Iron

From the equilibrium data obtained during this investigation, the free energy of ferrous oxide in liquid iron can be calculated. If we let the activity of liquid iron be equal to 1, and that of dissolved FeO be equal to its percentage, we may define the equilibrium constant for the reaction as

$$K = \frac{(H_2O)}{(H_2)\ (\%\ FeO)}$$

This constant is directly related to the standard change of free energy for the reaction. The relationship is:

$$\Delta F^\circ = -RT\ \ln K = -4.575\ T \log K$$

where ΔF° is the change in free energy in the reaction when each substance is in a standard state (that is, when its activity = 1), T is the temperature in degrees Kelvin (absolute) and ln K and log K are the natural and ordinary logarithms, respectively, of the equilibrium constant of the reaction.

The expression for K is similar to that used above for K′, except that we are now expressing oxygen content as per cent FeO instead of per cent oxygen. K is, therefore, equal to K′/4.49, the average value of which, as found in Table I, is 0.88 at 1600 degrees Cent. (2910 degrees Fahr.), or 1873°K. The change in free energy for the reaction is, therefore:

$$FeO\ (\%\ \text{in Fe}) + H_2 = Fe\ (l) + H_2O;\ \Delta F^\circ_{1873} = 480\ \text{cal.} \qquad (3)$$

The free energy of steam at this temperature quoted from the previously published work (13) is:

$$H_2 + \tfrac{1}{2}O_2 = H_2O(g):\ \Delta F^\circ_{1873} = -34260\ \text{cal.} \qquad (4)$$

By combining Equations 3 and 4, we obtain the free energy of formation of dissolved ferrous oxide at 1600 degrees Cent. (2910 degrees Fahr.):

$$Fe\ (\text{liquid}) + \tfrac{1}{2}O_2 = FeO\ (\%\ \text{in Fe});\ \Delta F^\circ_{1873} = -34740\ \text{cal.} \qquad (5)$$

The Free Energy of Liquid Ferrous Oxide

It is desirable to know the free energy of pure liquid ferrous

oxide for thermodynamic calculations on slag reactions. We may justly assume that the free energy of liquid ferrous oxide is approximately equal to its free energy in the saturated solution. The solubility of ferrous oxide in iron at 1600 degrees Cent. (2910 degrees Fahr.) from the data of Herty (9) and of Körber (10) is 1.35 per cent. The change in free energy in going from a 1 per cent solution to a 1.35 per cent solution is 4.575 T log 1.35. This may be represented as follows:

$$FeO\ (1\%\ in\ Fe) = FeO\ (1.35\%\ in\ Fe);\ \Delta F^\circ_{1873} = 1120\ cal. \qquad (6)$$

Now Equations 5 and 6 may be combined to obtain a figure which represents the free energy of FeO in the saturated solution, and which, therefore, is very close to the free energy of pure liquid ferrous oxide.

$$Fe\ (liquid) + \tfrac{1}{2}O_2 = FeO\ (liquid);\ \Delta F^\circ_{1873} = -33620\ cal. \qquad (7)$$

The Carbon-Oxygen Equilibrium in Liquid Iron

Because of its fundamental importance, the carbon-oxygen equilibrium has been the subject of many investigations. The reaction and its equilibrium constant are obtained by combining Equation 5 with the following equations and free energy values at 1600 degrees Cent. (2910 degrees Fahr.), which were derived in the previous work (13).

$$C\ (graphite) + \tfrac{1}{2}O_2 = CO;\ \Delta F^\circ_{1873} = -65{,}870\ cal. \qquad (8)$$

$$C\ (graphite) = C\ (\%\ in\ liq.\ Fe);\ \Delta F^\circ_{1873} = -12{,}340\ cal. \qquad (9)$$

The results of the combination are:

$$Fe\ (l) + CO = FeO\ (\%\ in\ Fe) + C\ (\%\ in\ Fe);\quad \Delta F^\circ_{1873} = +18{,}790\ cal. \qquad (10)$$

The equilibrium constant at 1600 degrees Cent. (2910 degrees Fahr.) is then:

$$\frac{(\text{per cent FeO})\ (\text{per cent C})}{(CO)} = 0.006$$

This result is in good agreement with Vacher's (1) experimentally determined value of 0.010 which perhaps represents the best experimental research on the carbon-oxygen equilibrium. It

is of interest to note that the calculated and experimental values of this constant are becoming more nearly equal. Of course, the experimental value should be given preference.

The Water Gas Reaction

The equilibrium constants for the reactions represented by equations (1) and (2) can be expressed respectively as follows:

$$K_1 = \frac{(CO_2)\ (Fe)}{(CO)\ (FeO)} \text{ and } K_2 = \frac{(H_2O)\ (Fe)}{(H_2)\ (FeO)}$$

If we divide K_2 by K_1, we get the equilibrium constant, K_3, for the water gas reaction thus:

$$CO_2 + H_2 = CO + H_2O;\ K_3 = \frac{(H_2O)\ (CO)}{(H_2)\ (CO_2)} \qquad (11)$$

The above constants are expressed differently than K′ in order that they may be directly compared to previously published data wherein the mol fractions of the reacting substances have been employed in the expressions for the equilibrium constants.

Let us calculate the equilibrium for reaction (11) using Vacher's data on the Fe-O-C system and the authors' data on the Fe-O-H system. Vacher reports 27.0 as his best value for K_1 at 1580 degrees Cent. (2875 degrees Fahr.) at which temperature his work was carried out. Since the temperature coefficient for this reaction is not well known in this range, we will convert the data for K_2 to 1580 degrees Cent. (2875 degrees Fahr.), using the temperature coefficient referred to above. The corrected value for K′ at 1580 degrees Cent. (2875 degrees Fahr.) is 3.62. When the ferrous oxide concentration is expressed as mol fraction rather than as per cent oxygen, the value for K_2 at 1580 degrees Cent. (2875 degrees Fahr.) then becomes 103.5.

Dividing K_2 by K_1, we get a value of 3.83 for K_3, the equilibrium constant for the water gas reaction. Bryant (14) reviewed all of the published data on this reaction and computed the equilibrium constants at temperatures up to 1527 degrees Cent. (2780 degrees Fahr.). Extrapolation of Bryant's data over the short interval to 1580 degrees Cent. (2875 degrees Fahr.) yields a value of 3.82 for K_3, which is in remarkably close agreement with the

value of K_3 calculated above directly from experimental data. However, Bryant has recently recalculated the values for K_3, using molecular heats calculated from spectroscopic data up to 2000°K. His new value for K_3 at 1580 degrees Cent. (2875 degrees Fahr.) is 4.07, which is entirely within the range of experimental error of this work. The agreement between the reported value for the water gas constant and that obtained from the experimental data of Vacher and of the authors, may be considered substantial evidence of the reliability of both investigations.

Summary and Conclusions

An experimental study of equilibrium in the reduction of dissolved ferrous oxide by hydrogen at 1600 degrees Cent. (2910 degrees Fahr.) has led to the following conclusions:

The equilibrium constant is independent of the oxygen concentration, and the activity of ferrous oxide dissolved in liquid iron is, therefore, proportional to its per cent by weight.

An unsuspected source of error in previous work has been discovered and corrected, thereby changing the value of the constant from 4.75 to 3.95.

The free energy of formation of ferrous oxide in a 1 per cent solution in liquid iron has been determined to be —34,740 calories at 1600 degrees Cent. (2910 degrees Fahr.).

The value of the carbon-iron oxide product at equilibrium in liquid iron has been calculated to be 0.006, which is considered a confirmation of the experimental value, 0.010.

The value of the constant of the water gas reaction found by combining the present data with Vacher's work is in agreement with that obtained from other sources.

References

1. H. C. Vacher, "The System Liquid Iron-Carbon Oxides," Bureau of Standards Journal of Research, Vol. 11, No. 4, 1933, p. 541.
2. John Chipman, "Equilibrium in the Oxidation of Liquid Iron by Steam and the Free Energy of Ferrous Oxide in Liquid Steel," *Journal*, American Chemical Society, Vol. 55, 1933, p. 3131-39.
3. F. S. Tritton and D. Hanson, "Iron and Oxygen," *Journal*, Iron and Steel Institute, Vol. CX, No. II, 1924, p. 90.
4. H. C. Vacher and E. H. Hamilton, "Carbon-Oxygen Equilibrium in Liquid Iron," *Transactions*, American Institute of Mining and Metallurgical Engineers, Vol. 95, 1931, p. 124.

5. P. H. Emmett and J. F. Schultz, "Gaseous Thermal Diffusion—The Principal Cause of Discrepancies Among Equilibrium Measurements on the Systems $Fe_3O_4 - H_2 - Fe\ H_2O$, $Fe_3O_4 - H_2 - FeO - H_2O$ and $FeO - H_2 - Fe - H_2O$," *Journal*, American Chemical Society, Vol. 55, 1933, p. 1376-89.

6. John Chipman and M. G. Fontana, "Thermal Diffusion of Gases Near a Hot Metal Surface," *Journal*, American Chemical Society, Vol. 56, 1934, p. 2011.

7. S. Chapman, "On Approximate Theories of Diffusion Phenomena," *Philosophical Magazine*, Vol. 5, 1928, p. 630-636.

8. E. D. Eastman and Samuel Ruben, "Influence of Thermal Diffusion in Certain Equilibrium Measurements," *Journal*, American Chemical Society, Vol. 57, 1935, p. 97.

9. C. H. Herty, Jr., and co-workers, "The Solubility of Iron Oxide in Iron," Carnegie Institute of Technology, Bulletin No. 34, 1927.

10. Friedrich Körber, "Untersuchungen über das Verhalten des Mangans bei der Stahlerzeugung," *Stahl und Eisen*, Vol. 52, 1932, p. 133-44.

11. Georges Chaudron, "Étude des Réactions Réversibles de l'hydrogène et de l'oxyde de Carbone sur les Oxydes Metalliques," *Annales de Chimie*, Vol. 16, 9 serie, 1921, p. 221-81.

12. L. B. Pfeil, "The Constitution of Scale," *Journal*, Iron and Steel Institute, Vol. 123, 1931, p. 237.

13. John Chipman, "Application of Thermodynamics to the Deoxidation of Liquid Steel," TRANSACTIONS, American Society for Metals, Vol. 22, 1934, p. 385.

14. W. M. D. Bryant, "Calculations on Water-Gas Equilibrium," *Industrial and Engineering Chemistry*, Vol. 23, No. 9, 1931, p. 1019.

DISCUSSION

Written Discussion: By H. C. Vacher, assistant scientist, National Bureau of Standards, Washington, D. C.

The authors have shown how careful and judicial experiments will lead ultimately to an explanation of numerical discrepancies. If this work had not been done the accuracy of the equilibrium constants for the reactions of ferrous oxide with carbon monoxide or hydrogen, reactions 1 and 2, page 313, would have been questionable and the choice of the best value would be a matter of opinion. As it is now, the equilibrium constants for both reactions are established firmly and in good agreement with reliable data for the water gas constant. The effect of thermal diffusion in gas mixtures within a temperature gradient on the values obtained for K′ is surprising and important. It means this source of error must be considered in future work where hydrogen is a reactant.

Written Discussion: J. B. Austin, Research Laboratories, U. S. Steel Corp., Kearny, N. J.

Of all the useful conclusions reached by Messrs. Fontana and Chipman, the most gratifying is that ferrous oxide forms an ideal solution in liquid iron, for it indicates that, just as in the case of gases, these metal systems approach ideality at high temperatures, a fact which greatly simplifies many calculations dealing with metallurgical reactions.

I should also like to comment on the unusual development of this con-

clusion. Ordinarily, the more refined the investigation of a system, the more evident becomes the deviation from ideal behavior, but in the present case the elimination of errors has revealed a closer approach to ideality, and the exceedingly careful work reported in this paper leaves no room to question the fact that the simple mass action law holds with considerable accuracy for the reaction between hydrogen and ferrous oxide.

Written Discussion: By D. L. McBride, Research Engineer, Bethlehem Steel Company, Johnstown, Pa.

The present paper makes a very significant contribution to Dr. Chipman's original paper on the "Application of Thermodynamics to the Deoxidation of Liquid Steel." Because of lack of data, it was necessary to assume perfect solution behavior in establishing several of the free energy equations and equilibrium constants. This assumption was unreliable in view of the fact that Dr. Chipman has found that a solution of FeO and liquid iron was not a perfect solution, but that the activity of FeO decreased with increasing concentration. It is indeed gratifying to find that Fontana and Chipman, by an improved experimental technique, have found that FeO and liquid iron form an ideal solution, and that the activity of FeO is equal to the mol fraction even up to saturation.

The correction introduced into the original equilibrium constants, involving the various deoxidizers and FeO, by the more accurate determination of the free energy of formation of FeO is not appreciable. The deoxidation constants, as given in the original paper, are not materially altered as may be seen by comparing the values for the carbon-FeO reaction given in the previous and present papers.

Previous Result .....(C) (FeO) 1600°C. = 0.005
Present Result .....(C) (FeO) 1600°C. = 0.006

The other deoxidation constants as originally given may be used without introducing any significant error.

However, in my mind, the importance of this work on the FeO-O-H system is not the accuracy of the results obtained but is the verification of the ideality of a solution of FeO in liquid iron. With this condition experimentally established, it is now possible to make calculations involving slag-metal reactions with a greater degree of reliability. It will now be possible to calculate the activity of the FeO in the slag from the activity of the FeO in the metal by means of the Nernst distribution coefficient according to the following relationship:

$$\frac{\text{a FeO in slag}}{\text{a Oxygen in metal}} = \frac{m}{N} = k$$

Since the value of k, the distribution coefficient, is known from the work of Herty,[1] it is readily possible to calculate the activity of the FeO in the slag if the concentration of the FeO in the metal is known. If the activity of the FeO in the slag can be determined in this way, it should be a simple matter to determine the effect of the various components of acid and basic slags on the activity of the FeO. Only when these effects and their temperature coeffi-

[1]Author's reference 9.

cients are known will the whole field of slag-metal reactions involved in ferrous metallurgy be on a precise and practical basis.

The authors are to be congratulated on their efforts to hasten the time when steel-making will be on a truly scientific basis.

Oral Discussion

DR. C. H. HERTY, JR.:[2] I do not believe it has been more than seven or eight years since the opinion was current at various metallurgical meetings that it was too much to expect that open-hearth slag-metal reactions could be attacked from the physico-chemical standpoint, because the slag was a concentrated solution, and the high temperatures involved made it extremely difficult to do proper experimental work. In this paper it is very interesting to know that Dr. Chipman and Dr. Fontana, by attacking the oxygen in iron problem from a gas metal reaction found a value of 0.95 per cent for the solubility of FeO in liquid iron at the melting point. Some time ago in our work at Pittsburgh, using a slag-metal reaction instead of a slag-gas reaction, we found a value of 0.94 per cent which is a remarkable check when you consider that two different methods of attack were used, and is indicative to me that we can go ahead without worrying about methods of attack.

Another example which comes closer home to the open-hearth man is this question of the carbon-iron oxide reaction. In 1929 at the Advisory Board Meeting in Pittsburgh, we gave a value for the carbon-FeO equilibrium in the open-hearth, as determined from carbon, and FeO determinations of the liquid steel during the refining period, of 0.011. Later on Vacher working with pure materials in an induction furnace arrived at a value of 0.010, and now Chipman and Fontana give us 0.006 as a value. In other words, all of this indicates that this business of trying to find out what is going on is not so very difficult after all, except that you have to be patient with these high temperature experiments.

Authors' Reply

By John Chipman

When discussing Wüstite we are dealing with a solid solution which is on the high oxygen side of FeO. It would be very difficult to estimate the activity of FeO in this solid solution. In the case of FeO dissolved in liquid iron we have shown (about two years ago) that the evidence available at that time indicated that the solute in liquid iron containing oxygen was either FeO, Fe_2O, Fe_3O or Fe_xO. There was no way at that time of distinguishing between them. The evidence which Dr. Fontana has obtained is even more conclusive to the same effect. We do not know whether it is FeO or Fe_2O but we do know that there is only one atom of oxygen in the molecule. Therefore, since we know that there is only one atom of oxygen, and it makes no difference how many atoms of iron are present, we call it FeO.

Regarding the application of this to the determination of the activity of iron oxide in slag, I will say that that is one of the important uses for the data obtained, but one must be very careful in making such an application to

[2]Research Engineer, Bethlehem Steel Co., Bethlehem, Pa.

insure that the slag and metal be actually in equilibrium with one another, otherwise the result would be a long way from correct.

The solubility of the simple diatomic gases in solid or liquid metals has been found to be proportional to the square root of the pressure. This is known as Sievert's law. It has been fashionable in the past to account for this well known behavior by the hypothesis that the dissolved gas exists in the atomic state. From the data which we have presented, it can be shown by simple mathematics that the system iron-oxygen at 1600 degrees Cent. (2910 degrees Fahr.) also conforms to Sievert's law, although the oxygen pressures are too small to permit direct determination. One could, therefore, account for the results by assuming that the solute in the liquid metal is atomic oxygen. This would not be impossible, but it seems extremely improbable, and is quite unnecessary. In all of the systems to which Sievert's law applies, it is reasonable to suppose that the solute is a compound whose molecule contains one atom of the gaseous element. In the case of nitrogen in liquid iron, I have shown that the solubility can be predicted approximately on the assumption that the solute is Fe_4N. In the case of sulphur, I will present at a later date some data which show that the solute is Fe_xS, probably FeS.

EFFECT OF CARBON, OXYGEN AND GRAIN-SIZE ON THE MAGNETIC PROPERTIES OF IRON-SILICON ALLOYS

By T. D. Yensen and N. A. Ziegler

Abstract

The paper is a continuation of the one presented a year ago on unalloyed iron and gives numerical relationships between carbon, oxygen and grain-size and the magnetic properties of iron-silicon alloys. Oxygen is without appreciable effect on the low density properties but affects the high density permeability considerably. The effect of carbon is generally less and the effect of grain-size is generally more (for low carbon contents) than the 1924 results indicated; but the effect of the various forms of carbon (solution or colloidal Fe_3C, free Fe_3C, pearlite, graphite) as shown in the 1924 paper has been confirmed.

THIS paper is a continuation of the one presented before this society a year ago on unalloyed iron,[1] and the methods there described for preparation, annealing and testing apply equally well in the present case. We shall, therefore, not repeat the details here, but only state that the alloys were prepared by melting electrolytic iron and 98 per cent silicon together with appropriate amounts of carbon and iron oxide in the "Bell Jar" high frequency vacuum furnace; that the ingots were forged into rods that were machined into rings 1 inch O.D. x ¾ inch I.D. x 1 inch long; that these were annealed either in hydrogen at 900 to 1400 degrees Cent. (1650 to 2550 degrees Fahr.) or in vacuum at 900 to 1100 degrees Cent. (1650 to 2010 degrees Fahr.) and slowly cooled (30 degrees Cent. per hour) to room temperature; and that after final magnetic testing the samples were analyzed for carbon, oxygen, nitrogen and hydrogen and for microstructure. This procedure was followed so that in every case there should be correspondence between the magnetic properties and the analysis, irrespective of the particular heat treatment used.

[1] T. D. Yensen and N. A. Ziegler, "Magnetic Properties of Iron as Affected by Carbon, Oxygen and Grain-Size," Transactions, American Society for Metals, Vol. 23, June 1935, p. 556.

A paper presented before the Seventeenth Annual Convention of the Society held in Chicago, September 30 to October 4, 1935. Of the authors, T. D. Yensen is manager of the magnetic division of Westinghouse Electric & Mfg. Co., E. Pittsburgh, and N. A. Ziegler formerly sales research engineer of West Penn Electric Co., Pittsburgh. Manuscript received June 28, 1935.

Table I
Chemical, Microscopic and Magnetic Properties of Specimens

Sample No.	Composition: %Si	%C	Oxygen: %O_2	Oxygen: Calc'd as SiO_2	%H_2	%N_2	Microanal.: N Grains per mm.^{2}	Remarks (See Key*)	Magnetic Properties: $\mu_{max.}$	$\beta_{min.} \times 10^5$	For B = 10000 Wb: H_c Oersteds	For B = 10000 Wb: Ergs/cc per Cycle	$\mu_{H=100}$: Orig.	$\mu_{H=100}$: Corrected to 3% Si	Point Notation
Group #1			C — .001 to .0015%		Ave C = .0012%										
I-31B	3.10	.0013	.006	.011	.0005	.0000	0.47	No Incl.	63000	1.59	.070	221	178.5	178.9	cross
I-32B	2.35	.0012	.040	.074	.0005	.0004	0.16	No Incl.	78400	1.27	.074	192	175.7	173.4	cross
F-24A	2.80	.0010	.053	.100	.0005	.0000	13.30		6160	16.20	.403	1074	171.9	171.2	cross
Group #2			C — .0015 to .0025%		Ave C = .0021%										
I-30E	2.87	.0025	.002	....	.0002	.0003	4.43	Veining	18715	5.34	.202	588	.....	.....	dot in circle
I-32C	2.35	.0020	.010	.018	.0011	.0000	0.11	No Incl.	73300	1.36	.048	162	180.0	177.7	dot in circle
I-31E	3.10	.0022	.007	.013	.0007	.0000	0.65	No Incl.	57300	1.95	.118	325	177.8	178.2	dot in circle
I-145C	2.51	.0021	.026	.048	.0007	.0000	0.92	Some gl Incl.	43250	2.31	.104	295	176.8	175.1	dot in circle
F-20B	3.08	.0025	.038	.072	.0006	.0000	0.58	No Incl.	52660	1.90	.061	212	174.2	174.5	dot in circle
F-29B	2.40	.0018	.049	.092	.0009	.0000	0.82		48700	2.05	.083	275	172.2	170.1	dot in circle
I-145A	2.51	.0019	.044	.082	.0005	.0004	7.20	Some gl Incl.	10420	9.58	.306	899	169.5	167.8	dot in circle
I-30B	2.87	.0020	.053	.099	.0008	.0002	0.97	No Incl.	42200	2.37	.119	365	177.0	176.6	dot in circle
F-25A	2.83	.0024	.049	.092	.0003	.0003	0.85	No Incl.	42750	2.34	.098	319	172.6	172.0	dot in circle
F-28A	2.80	.0023	.031	.058	.0004	.0003	0.92	No Incl.	43400	2.30	.098	328	173.0	172.3	dot in circle
F-21A	3.05	.0022	.036	.068	.0006	.0002	12.00		6570	15.20	.382	1129	173.0	173.2	dot in circle
F-22A	2.93	.0016	.043	.080	.0007	.0003	0.85	Some gl Incl.	47300	2.11	.101	324	172.4	172.2	dot in circle
Group #3			C — .0026 to .0033%		Ave C = .0029%										
I-31C	3.10	.0033	.001	.003	.0008	.0000	0.13	No Incl.	51750	1.94	.058	183	180.5	180.9	cross in circle
I-30C	2.87	.0032	.006	.012	.0005	.0002	0.17	No Incl.	50500	1.98	.074	237	178.5	178.1	cross in circle
I-32E	2.35	.0026	.022	.041	.0009	.0000	1.15		34000	2.94	.141	414	177.3	175.0	cross in circle
F-30B	2.56	.0026	.025	.046	.0009	.0000	5.25		13700	7.30	.205	656	175.5	174.0	cross in circle
F-23A	2.92	.0027	.029	.055	.0007	.0000	8.42		9200	10.85	.352	1054	175.3	175.0	cross in circle
F-30A	2.56	.0029	.028	.052	.0008	.0000	9.54		8040	12.43	.376	970	174.7	173.2	cross in circle

Table I (Continued)
Chemical, Microscopic and Magnetic Properties of Specimens

Sample No.	Composition %Si	%C	Oxygen %O_2	Oxygen Calc'd as SiO_2	%H_2	%N_2	Microanal. N Grains per mm.^{2}	Remarks (See Key*)	Magnetic Properties $\mu_{max.}$	$\mu_{min.} \times 10^5$	For B = 10000 He Oersteds	For B = 10000 W_h Ergs/cc per Cycle	$\mu_{H=100}$ Orig.	$\mu_{H=100}$ Corrected to 3% Si	Point Notation
Group #3			C — .0040 to .0042%			Ave C = .0041%									
I-33C	2.95	.0040	.000	.0016	.0006	.0003	0.21	No Incl.	48850	2.04	.076	218	183.8	183.6	cross in circle
F-31B	2.76	.0040	.026	.048	.0005	.0000	5.48		12750	7.85	.202	663	175.8	175.0	
I-145B	2.51	.0040	.023	.042	.0009	.0002	1.00	Some gl Incl.	33900	2.95	.138	386	176.0	174.3	
I-33D	2.95	.0041	.002	.004	.0007	.0002	0.25	sG No Fe_3C	47600	2.10	.074	247	178.7	178.5	
I-34B	3.19	.0042	.020	.038	.0011	.0000	1.65	No Incl.	29150	3.43	.168	499	175.5	176.2	
I-32D	2.35	.0042	.036	.067	.0005	.0003	0.14	sG No Fe_3C	68000	1.47	.056	198	176.2	173.9	
Group #4			C — .0045 to .0057%			Ave C = .0049%									
I-33B	2.95	.0046	.005	.009	.0007	.0002	0.48	No Incl.	42650	2.34	.107	331	177.9	175.6	dot in triangle
I-34D	3.19	.0051	.003	.006	.0011	.0000	0.22	sG No Fe_3C	42850	2.33	.086	278	177.6	178.3	
I-34E	3.19	.0045	.003	.006	.0011	.0000	1.47		21750	4.60	.193	526	178.3	179.0	
I-30D	2.87	.0047	.008	.014	.0006	.0002	0.43	G No Fe_3C	50000	2.00	.089	280	176.8	176.4	
I-34C	3.19	.0054	.009	.017	.0003	.0003	0.18	sG No Incl.	40000	2.50	.082	254	177.0	177.7	
F-26B	2.77	.0047	.029	.054	.0009	.0002	4.23		15150	6.66	.168	613	170.5	169.7	
F-27B	2.82	.0050	.032	.060	.0010	.0000	4.10		14500	6.90	.184	603	173.5	173.0	
I-31D	3.10	.0057	.026	.048	.0009	.0000	0.10	sG No Fe_3C	52700	1.90	.064	204	176.5	176.9	
I-33E	2.95	.0045	.025	.047	.0008	.0000	3.83		16600	6.03	.230	706	174.6	174.4	
Group #5			C — .0059 to .0079%			Ave C = .0069%									
F-21B	3.05	.0063	.032	.060	.0007	.0003	3.75		16950	5.90	.153	474	174.0	174.2	dot in square
F-23B	2.92	.0072	.071	.132	.0006	.0002	3.75		15300	6.53	.174	533	171.5	171.2	
F-25B	2.83	.0069	.045	.085	.0004	.0002	9.53		8515	11.73	.122	513	174.5	173.9	
F-22B	2.93	.0072	.054	.100	.0008	.0002	2.85		18970	5.27	.147	455	168.0	167.8	
F-24B	2.80	.0079	.043	.081	.0005	.0000	6.15		11500	8.70	.236	745	172.5	171.8	
F-28B	2.80	.0059	.049	.091	.0004	.0000	1.76		23300	4.29	.141	425	172.5	171.8	

Table I (Concluded)
Chemical, Microscopic and Magnetic Properties of Specimens

Sample No.	Composition					Microanal.		Magnetic Properties For B = 10000 Wb					
	% Si	% C	Oxygen % O_2	Calc'd as SiO_2	% H_2	% N_2	N Grains per $mm.^2$	Remarks (See Key*)	$\mu_{max.}$	$\rho_{min.}$ $\times 10^5$	He Oersteds	Ergs/cc per Cycle	$\mu_{H=100}$ Orig.	Corrected to 3% Si	Point Notation
Group #6			C — .13 to .16		Ave C = .140%										
I-35C	3.34	.153	.009	.016	.0005	.0000	abt 200	LP	2920	34.20	.970	3520	169.5	170.7	solid dot
I-36B	3.13	.135	.007	.013	.0007	.0003	21.70	LG	5080	19.65	.608	1658	168.0	168.5	
I-35A	3.34	.154	.038	.072	.0006	.0000	155	LP	3210	31.10	.980	3060	170.0	171.2	
I-35B	3.34	.153	.044	.083	.0008	.0000	23.50	LP	3280	30.50	.880	2995	171.2	172.4	
Group #7					Ave C = .294%										
I-36A	3.13	.292	.005	.010	.0009	.0002	18.60	LP & LG	1860	53.75	1.652	5000	164.0	164.5	solid square
I-36C	3.13	.296	.003	.006	.0004	.0000	abt 100	LP & LG	1490	67.10	1.86	5430	163.7	164.2	

*Key

Fe_3C = cementite
G = graphite
P = pearlite
SiO_2 = silica inclusions

g = grains
gb = grain boundaries
n = needles
Incl. = inclusions
Prec. = precipitate

gl = glassy
L = large amount
s = small amount
tr = trace

In Tables I, II and III are listed the samples of approximately 3, 4 and 5 to 6 per cent silicon respectively, together with the results of the chemical and microscopic analysis and of the magnetic testing. The samples are arranged in groups according to carbon content, the oxygen content increasing within each group.

The method of presentation will consist in using minimum reluctivity ($\rho_{min.} = \frac{1}{\mu max.}$) as a measure of the low density magnetic properties, and then when desirable, to convert to coercive force (H_c) and hysteresis loss (W_h) by means of appropriate conversion relations such as are obtained from Fig. 1 for 3 per cent silicon. These relations are listed in Table IV, including that for 0 per cent silicon as obtained from the previous paper. It will be noted that the ratio between H_c and $\rho_{min.}$ and between W_h and $\rho_{min.}$ decreases rapidly with increasing silicon content, being about one-half for 6 per cent silicon of what it is for 0 per cent silicon. In other words, for the same maximum permeability the hysteresis loss for 6 per cent silicon is about one-half that for 0 per cent silicon.

From the several hundred samples prepared a large number were discarded because of slight cracks and other imperfections. Even with this precaution, it is quite probable that there may be a small number of samples included in the final analysis that have hidden imperfections and that accounts for the scattering of the points. Another factor that contributes to the scattering is the fact that the microscopic analysis only covers one surface. In getting the grain-size one end of the ring was polished and etched, and the total number of grains counted at 100 diameters. Ruder's objection to the use of grain area rather than grain volume[2] may be valid in case of thin samples of varying thickness, but does not seem justified in the present case. If desired, grains per square millimeter (N_s) may be converted to grains per cubic millimeter (N_v) by the relation

$$N_v = N_s^{3/2}$$

Effect of Oxygen

The preliminary investigation revealed that small amounts of oxygen apparently have little if any effect on the low density properties of iron-silicon alloys containing 3 per cent silicon or more. This

[2] See discussion of previous paper referred to in footnote 1.

Table II
4 Per Cent Silicon Alloy

Sample No.	Composition: %Si	%C	Oxygen %O_2	Oxygen Calc'd as SiO_2	%H_2	%N_2	Microanal. N Grains per mm.^{2}	Remarks (See Key*)	Magnetic Properties: $\mu_{max.}$	$\mu_{min.} \times 10^5$	For B = 10000 H$_e$ Oersteds	For B = 10000 W$_h$ Ergs/cc per Cycle	$\mu_{H=100}$ Orig.	$\mu_{H=100}$ Corrected to 4% Si	Point Notation
Group #1		C — .0025 to .0045% Ave C = .0039%													
I-130B	3.96	.0041	.004	.007	.0007	.0002	1.11		23700	5.60	.153	400	175.5	175.4	cross
I-125C	4.78	.0042	.005	.009	.0013	.0002	4.22	No Prec.	16400	6.10	.116	346	172.0	174.8	
I-130C	3.96	.0039	.008	.015	.0009	.0003	0.30	No Incl. No Fe_3C	25000	4.00	.104	278	173.8	173.7	
I-126A	3.37	.0040	.014	.027	.0008	.0000	0.76	SiO_2,	27380	3.65	.159	473	174.8	172.6	
I-126C	3.37	.0027	.020	.038	.0003	.0005	0.38		33750	2.96	.138	415	174.0	171.8	
I-128A	4.00	.0045	.046	.085	.0005	.0000	4.12	No Incl. No Fe_3C	16000	6.25	.211	606	169.0	169.0	
Group #2		C — .0050 to .0065% Ave C = .0056%													
I-125A	4.70	.0051	.007	.012	.0013	.0000	4.38	No Incl. No Fe_3C	15710	6.36	.193	515	171.1	173.9	dot in circle
I-37C	4.12	.0054	.007	.013	.0007	.0000	13.85	sG	8650	11.55	.272	595	173.5	173.9	
I-127C	4.00	.0063	.014	.026	.0013	.0000	0.59	Fe_3C in gb, SiO_2	23420	4.27	.165	478	172.3	172.3	
I-37A	4.12	.0062	.016	.030	.0019	.0000	17.25	No Prec.	7045	13.40	.358	1655	172.0	172.4	
I-127B	4.00	.0052	.044	.082	.0008	.0000	1.40		22500	4.44	.171	461	169.2	169.2	
Group #3		C — .0070 to .0080% Ave C = .0074%													
I-130A	3.96	.0073	.005	.009	.0006	.0000	4.41	No Incl. No Fe_3C	14600	6.85	.214	589	175.0	174.9	cross in circle
I-126B	3.37	.0075	.019	.036	.0012	.0000	0.49	Fe_3C in gb, SiO_2	19900	5.03	.171	525	174.5	172.5	
Group #4		C — .010 to .0125% Ave C = .0111%													
I-125B	4.78	.0099	.032	.060	.0008	.0008	0.32	No Prec.	17850	5.60	.153	402	167.7	170.5	dot in triangle
I-37B	4.12	.0123	.004	.008	.0008	.0000	13.63	G	7750	12.90	.318	759	174.5	174.9	
Group #5		C > .015% Ave C = .062%													
I-38B	4.16	.0191	.027	.050	.0008	.0000	20.70	LG	5770	17.30	.557	1457	170.3	170.4	dot in square
I-38A	4.16	.0422	.025	.047	.0009	.0006	19.75	G	5780	17.28	.643	2423	170.1	170.7	
I-38C	4.16	.123	.050	.094	.0010	.0002	18.80	LG	5620	17.75	.566	1412	168.0	168.6	

*Key (see Table I).

*Key (see Table I).

Table III
5 to 6 Per Cent Silicon Alloy

Sample No.	Composition: %Si	%C	Oxygen: %O_2	Oxygen: Calc'd as SiO_2	%H_2	%N_2	Microanal.: N Grains per mm.^{2}	Remarks (See Key*)	Magnetic Properties For B = 10000: $\mu_{max.}$	$\rho_{min.} \times 10^5$	He Oersteds	W_h Ergs/cc per Cycle	μ_{100}: Orig.	μ_{100}: Corrected to 6% Si	Point Notation
Group #1		C — .0025 to .0045% Ave C = .0033%													
F-42A	5.30	.0042	.018	.034	.0004	.0000	8.74		9320	10.70	.245	683	168.0	165.6	cross
F-43A	6.34	.0032	.016	.031	.0000	.0000	1.15		33200	3.01	.128	480	163.6	164.8	cross
F-43B	6.34	.0033	.031	.058	.0012	.0000	0.23		38500	2.59	.074	224	161.9	163.1	cross
F-43C	6.34	.0026	.040	.075	.0009	.0000	0.89		41350	2.42	.055	154	161.0	162.2	cross
Group #2		C — .0050 to .0080% Ave C = .0069%													
F-54B	5.95	.0075	.018	.033	.0009	.0000	0.40	No Prec.	26400	3.78	.138	448	166.0	165.8	dot in circle
I-50A	5.95	.0068	.025	.046	.0010	.0000	2.70	No Prec.	16840	5.90	.175	510	164.2	164.1	dot in circle
I-54A	5.95	.0066	.021	.040	.0012	.0000	0.88	No Prec.	25000	4.00	.135	350	164.5	164.3	dot in circle
F-42B	5.30	.0052	.027	.051	.0008	.0000	2.51		18870	5.59	.107	336	168.0	165.6	dot in circle
I-53D	5.42	.0068	.036	.067	.0009	.0000	5.09	Tr. of Fe_3C	12220	8.17	.208	666	164.9	162.9	dot in circle
I-54D	5.95	.0079	.037	.070	.0004	.0000	1.21	No Prec.	23100	4.32	.095	267	161.8	161.6	dot in circle
F-40C	5.36	.0068	.037	.070	.0011	.0000	2.34		18800	5.31	.092	250	163.4	161.2	dot in circle
F-41C	5.96	.0070	.037	.070	.0004	.0003	0.22		28200	3.54	.067	180	159.0	158.9	dot in circle
I-50C	5.95	.0063	.040	.076	.0013	.0000	3.25	Fe_3C n & in gb	15770	6.33	.193	557	163.1	162.9	dot in circle
I-51C	5.67	.0068	.050	.094	.0009	.0000	2.25	Fe_3C in gb	17600	5.67	.194	568	162.3	161.1	dot in circle
F-40B	5.36	.0075	.047	.088	.0011	.0003	7.04		9470	10.55	.129	372	163.3	161.1	dot in circle
F-44C	5.59	.0076	.047	.088	.0007	.0000	0.33		26300	3.80	.061	177	162.2	160.8	dot in circle
Group #3		C — .0080 to .010% Ave C = .090%													
I-50B	5.95	.0097	.020	.037	.0013	.0000	0.63	tr of Fe_3C-n	22000	4.54	.122	320	166.0	165.8	cross in circle
F-42C	5.30	.0085	.029	.055	.0007	.0002	0.30		24800	4.03	.077	211	165.5	163.1	cross in circle
I-51D	5.67	.0096	.041	.078	.0006	.0000	2.34	tr of Fe_3C	15170	6.60	.113	338	161.0	159.8	cross in circle
F-44A	5.59	.0081	.042	.080	.0013	.0000	9.72		7290	13.70	.214	515	163.0	161.6	cross in circle

Table III (Continued)
5 to 6 Per Cent Silicon Alloy

Sample No.	Composition: %Si	%C	Oxygen: %O_2	Oxygen: Calc'd as SiO_2	%H_2	%N_2	Microanal.: N Grains per mm.^{2}	Remarks (See Key*)	Magnetic Properties For B = 10000: $\mu_{max.}$	$\rho_{min.} \times 10^5$	H_c Oersteds	W_h Ergs/cc per Cycle	$\mu_{H=100}$: Orig.	$\mu_{H=100}$: Corrected to 6% Si	Point Notation
Group #4			C — .010 to .015%		Ave C = .0117%										
I-51B	5.67	.0117	.018	.034	.0012	.0000	18.12	Fe_3C in gb	12150	8.22	.199	612	165.0	163.8	dot in triangle
I-55C	5.01	.0123	.005	.009	.0009	.0000	28.82	Fe_3C in gb sG	9340	10.72	.337	971	159.4	155.9	
I-54C	5.95	.0127	.011	.020	.0009	.0000	0.18	No Prec.	21400	4.66	.150	498	167.0	166.8	
I-51A	5.67	0102	.023	.043	.0012	.0000	29.66	Fe_3C in gb	9290	10.75	.248	717	163.5	162.3	
I-41A	5.96	.0102	.033	.061	.0000	.0000	8.92		17680	5.65	.184	559	163.9	163.8	
I-52D	5.68	.0143	.037	.070	.0007	.0002	11.59		14600	6.85	.116	358	163.8	162.7	
I-52B	5.68	.0118	.043	.082	.0010	.0000	16.88	G	12750	7.83	.205	551	164.0	162.9	
I-53B	5.42	.0105	.045	.084	.0008	.0000	0.63	sG in g & gb	26400	3.78	.138	448	164.2	162.2	
Group #5			C — .0170 to .0225%		Ave C = .0205%										
I-52A	5.68	.0176	.003	.006	.0012	.0005	22.79	Tr. of G	8660	11.52	.276	772	169.5	168.4	dot in square
I-50D	5.95	.0195	.039	.073	.0009	.0000	0.27	Tr. of Fe_3C	21150	4.72	.107	320	162.0	161.8	
I-52C	5.68	.0201	.064	.120	.0008	.0000	17.41	G	11830	8.45	.221	618	162.0	160.9	
F-40A	5.36	.0224	.046	.086	.0002	.0000	28.92		8700	11.49	.269	730	164.2	162.0	
I-53A	5.42	.0201	.020	.037	.0009	.0008	29.74	sG in g & gb	8050	12.41	.337	964	166.9	164.9	
F-41B	5.96	.0220	.047	.088	.0011	.0000	0.91		19940	5.01	.126	392	161.5	161.4	
I-53C	5.42	.0220	.053	.099	.0007	.0003	0.46	Tr. of Fe_3C	14210	7.02	.248	723	164.0	162.0	
Group 6#			C > .090%		Ave C = .173%										
I-55A	5.01	.276	.046	.087	.0012	.0000	abt 150	LG in g & gb	5550	18.00	.515	1352	162.2	158.7	solid dot
I-55B	5.01	.148	.055	.103	.0007	.0000	abt 50	LG in g & gb	6660	15.00	.435	1624	164.1	160.6	
I-55D	5.01	.095	.034	.064	.0006	.0000	abt 50	LG in g & gb	7160	13.95	.398	1103	161.0	157.5	

*Key (see footnote to Table I).

is shown in Fig. 2 where minimum reluctivity ($\rho_{min.}$) has been plotted against per cent oxygen for samples of nearly the same carbon content and grain-size. The reason for this is probably that the oxygen combines with the silicon, while the alloys either are in the molten state, or at a high enough temperature after solidification to permit

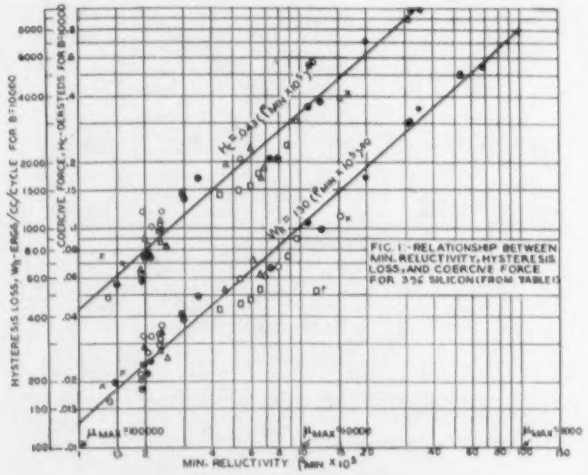

Fig. 1—Relationship Between Minimum Reluctivity, Hysteresis Loss and Coercive Force for 3 Per Cent Silicon Alloy.

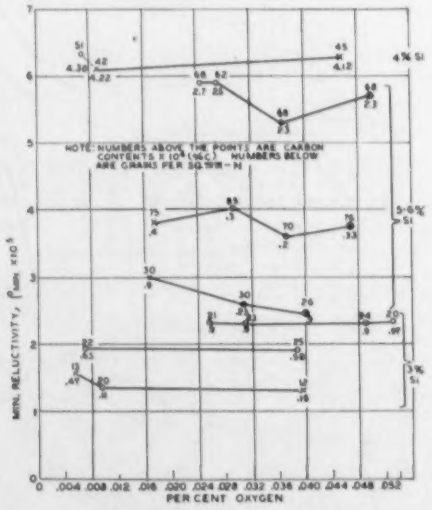

Fig. 2—Effect of Oxygen for Constant Carbon and Grain-Size of 3 to 6 Per Cent Silicon Alloy.

coalescing of the SiO_2 into large particles that have a relatively small aggregate effect on the lattice distortion. It will be recalled that with no silicon present the solubility of oxygen in iron increases rapidly

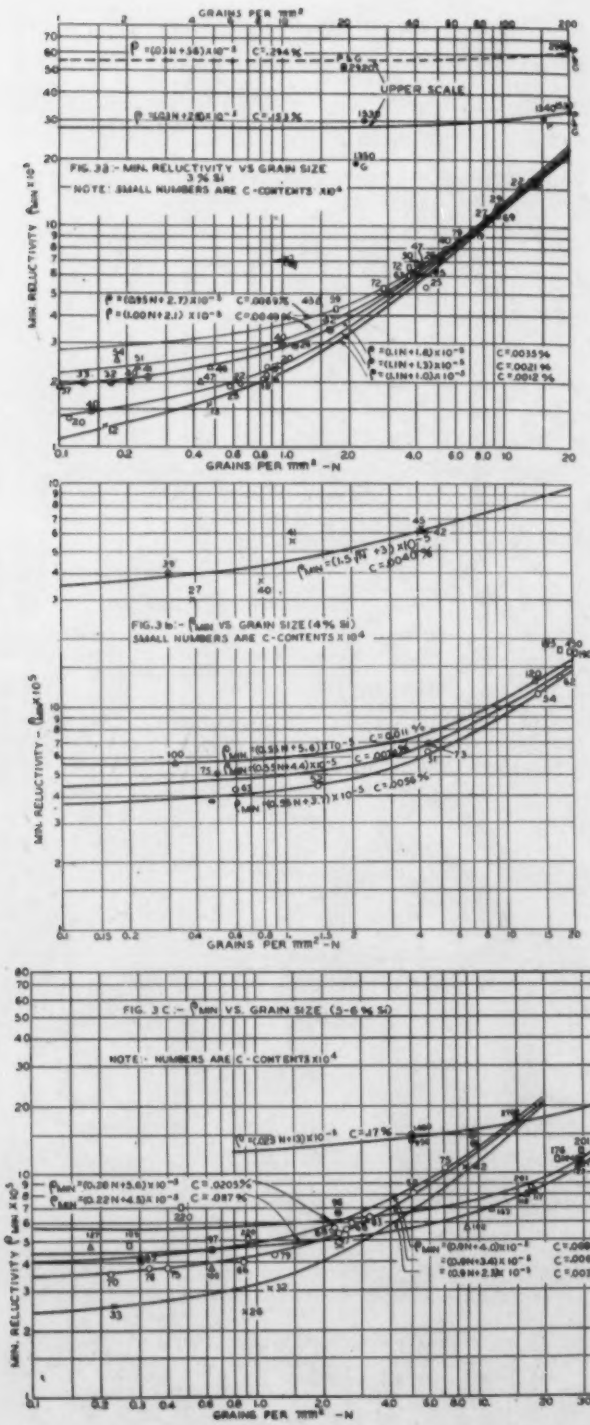

Fig. 3a—Minimum Reluctivity Versus Grain-Size of 3 Per Cent Alloy. Fig. 3b—ρ min Versus Grain-Size of 4 Per Cent Alloy. Fig. 3c—ρ min Versus Grain-Size of 5 to 6 Per Cent Alloy.

above 900 degrees Cent. (1650 degrees Fahr.)[8] reaching a value of 0.1 per cent. Most of this dissolved oxygen will precipitate as small (colloidal) particles during subsequent cooling and, thereby, cause considerable effect on the magnetic properties, as shown in the previous paper. While silicon thus prevents the bad effect of oxygen on the low density properties of iron, it will be shown later that it does not prevent oxygen from lowering the high density permeability.

Effect of Grain-Size and Carbon

The elimination of oxygen as a factor affecting the low density properties of iron-silicon alloys, simplifies the problem of ascertaining the effect of carbon and grain-size considerably. In Figs. 3a, 3b, and 3c the minimum reluctivity ($\rho_{min.}$) has been plotted against grain-size (N) for the various groups of constant carbon content. The plotting has been done on a double log scale because of the large range of both co-ordinates, and the necessity of plotting a large number of points in the lower range.

The relationship between N and $\rho_{min.}$ is so close to straight lines that straight lines have been drawn in all cases except one (4 per cent silicon with C = 0.004 per cent, Fig. 3c). The form of the equation is

$$\rho_{min.} = aN + b$$

in which "a" is the grain-size factor and "b" the effect of the particular silicon and carbon content for the group. The numerical values of "b" are obtained in the usual way by extrapolating to N = O. The results are tabulated in Table V. The grain-size factor ("a") has been plotted in Fig. 4, showing the decreasing effect of grain-size with increasing carbon. The values of "b" have been plotted all to the same $\rho_{min.}$ scale in Figs. 5a, 5b and 5c showing the effect of small amounts of carbon on single crystals of 3, 4 and 5 to 6 per cent silicon respectively. In Figs. 5d, 5e and 5f are shown the effect of higher carbon contents, but because of the great effect of carbon on the 3 per cent silicon the ordinate scale for this case is 4 times what it is for 4 and 6 per cent silicon. The curve for 4 per cent silicon is shown broken because of uncertainty due to insufficient grain-size data (Table II). Ordinates for H_c and W_h have been added in each case using the equations of Table IV. These curves show the net effect of carbon with all other factors presumably eliminated.

[8] N. A. Ziegler, "Solubility of Oxygen in Solid Iron," Transactions, American Society for Steel Treating, Vol. 20, July 1932, p. 73.

Table IV

Conversion Factors—$\rho_{min.}$ vs. H_c and W_h (for B = 10000)

0 Per Cent Silicon	$H_c = 0.054$	$(\rho_{min.} \times 10^8)$
	$W_h = 164$	$(\rho_{min.} \times 10^8)$
3 Per Cent Silicon	$H_c = 0.043$	$(\rho_{min.} \times 10^8)^{0.9}$
	$W_h = 130$	$(\rho_{min.} \times 10^8)^{0.9}$
4 Per Cent Silicon	$H_c = 0.040$	$(\rho_{min.} \times 10^8)^{0.9}$
	$W_h = 110$	$(\rho_{min.} \times 10^8)^{0.9}$
5-6 Per Cent Silicon	$H_c = 0.029$	$(\rho_{min.} \times 10^8)$
	$W_h = 80$	$(\rho_{min.} \times 10^8)$

Contrary to the 1924 results[4] the extrapolated curves of Figs. 5a, b, c do not go to zero for 0 per cent carbon, but cut the ordinate axis at increasingly higher values the higher the silicon. This indicates—what has already been anticipated for some time—that silicon in spite of its indirect beneficial effects has a disturbing effect on the magnetic properties.

In order to facilitate comparison Figs. 6a, 6b, 6c and 6d have been prepared showing $\rho_{min.}$ $\mu_{max.}$ H_c and W_h as functions of carbon content (0-0.014 per cent) for single crystals of 0, 3, 4 and 5-6 per cent silicon with all other factors presumably eliminated. Fig. 7 similarly shows the hysteresis loss for carbon up to 0.14 per cent from present data, and the 1924 curves are shown in fine lines for comparison.

The micro analysis shows that there are no Fe_3C or graphite precipitates visible at 100 diameters for carbon up to about 0.005 per cent. Fig. 8a for a 3 per cent alloy (I-31E) with 0.0022 per cent carbon is representative of this type. In some of the low carbon

Table V

Effect of Grain-Size: $\rho_{min.} = aN^m + b$

	Per Cent Carbon	$\rho_{min.} \times 10^8$
3 Per Cent Silicon	0.0012	$1.10N + 1.0$
	0.0021	$1.10N + 1.3$
	0.0035	$1.10N + 1.8$
	0.0049	$1.00N + 2.1$
	0.0069	$0.95N + 2.7$
	0.153	$0.03N + 28$
	0.294	$0.03N + 56$
4 Per Cent Silicon	0.0039	$1.5\ N^{1/2} + 3.0$
	0.0056	$0.55N + 3.7$
	0.0074	$0.55N + 4.4$
	0.0110	$0.55N + 5.6$
5-6 Per Cent Silicon	0.0033	$0.90N + 2.3$
	0.0069	$0.90N + 3.4$
	0.0090	$0.90N + 4.0$
	0.0117	$0.22N + 4.5$
	0.0205	$0.20N + 5.6$
	0.17	$0.025N + 13.0$

[4]T. D. Yensen, "The Magnetic Properties of the Ternary Alloys Iron, Silicon, Carbon," *Transactions*, American Institute of Electrical Engineers, Vol. 43, 1924, p. 145.

samples there are seen a few glassy inclusions that probably are SiO_2 or silicate particles. From 0.005 per cent up to about 0.05 per cent we find Fe_3C, with traces of graphite in the 4 to 6 per cent alloys (see Figs. 9a for I-127C, and 10a for I-50C). Here too we occasionally see glassy inclusions. Above 0.05 per cent the precipitate is pearlite for the 3 per cent alloy (Fig. 8b, c and d for I-35B and I-36A) and graphite for the 4 to 6 per cent alloys (Fig. 9b for I-38A and Fig. 10b and 10c for I-53A and I-55B). This accounts for the

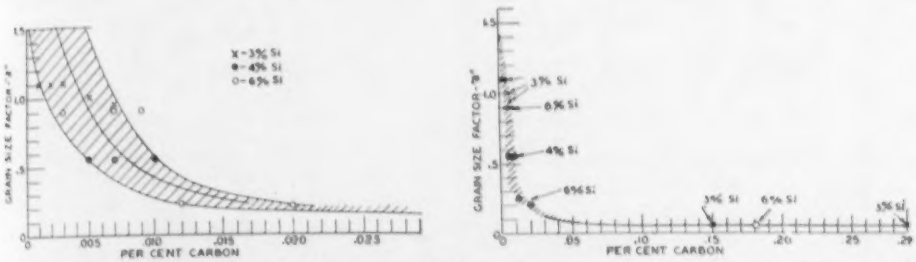

Fig. 4—Effect of Carbon on Grain Size Factor "a". ρ min = aN+b, Where N = grains per square millimeter and b = effect of carbon.

steep curve for the 3 per cent alloy (Fig. 7) corresponding very closely to the 1924 curves for 0 and 2 per cent silicon in which carbon was found to be precipitated as pearlite. However, the fact that in one 3 per cent sample carbon was found to be precipitated as graphite (see Fig. 8e) with correspondingly lower reluctivity (see Fig. 5d) indicates that it is possible by prolonged heating at lower temperatures to precipitate carbon as graphite also with 3 per cent silicon. If this were done the curves for 3 per cent silicon would correspond more nearly with those for 4 and 6 per cent silicon also for high carbon.

Attention is called to the crossing of the curves of Fig. 3c (5 to 6 per cent silicon), which means that for small grain-size it apparently should be possible with high silicon to decrease the minimum reluctivity values by increasing the carbon content from less than 0.01 per cent to more than 0.02 per cent. This is an anomaly that probably is due to the form in which carbon occurs in these alloys. It was shown above that with high carbon the precipitate in 4 to 6 per cent silicon is largely graphite while with low carbon the precipitate is Fe_3C. It is, therefore, conceivable that in two samples, A and B, A with 0.008 per cent carbon and B with 0.02 per cent carbon, sample A will contain more Fe_3C than sample B and consequently, other factors being equal, that B will have higher permeability than A in spite of the higher total carbon content. By proper heat treat-

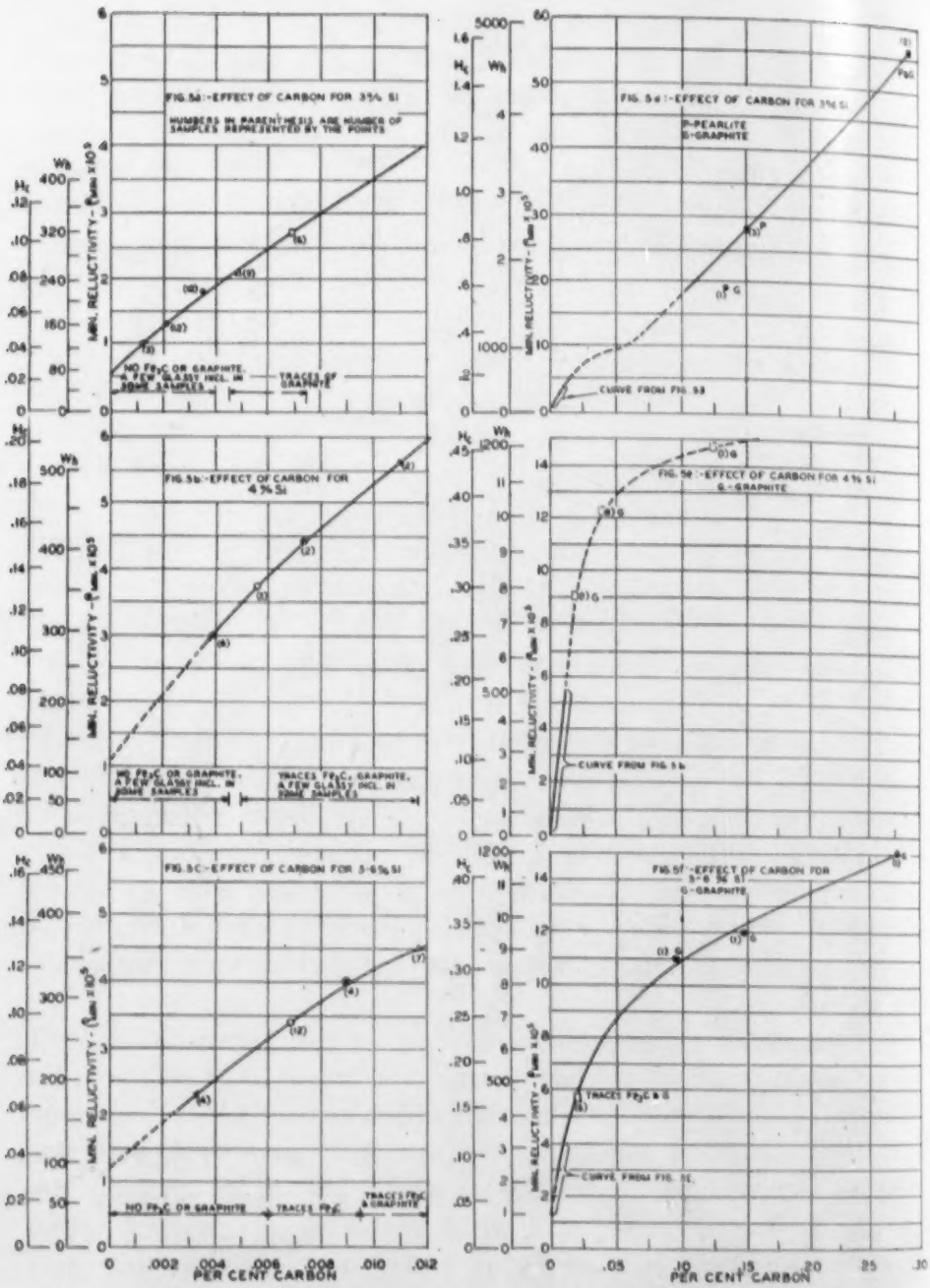

Fig. 5—Effect of Carbon for Single Crystals of 3 to 6 Per Cent Silicon Alloy.

ment, however, it should be possible to graphitize the carbon in both samples so that the permeability of A would be higher than that of B.

Comparing the present results with those of 1924 (Fig. 7) the new picture is not nearly as simple as the earlier one, although the

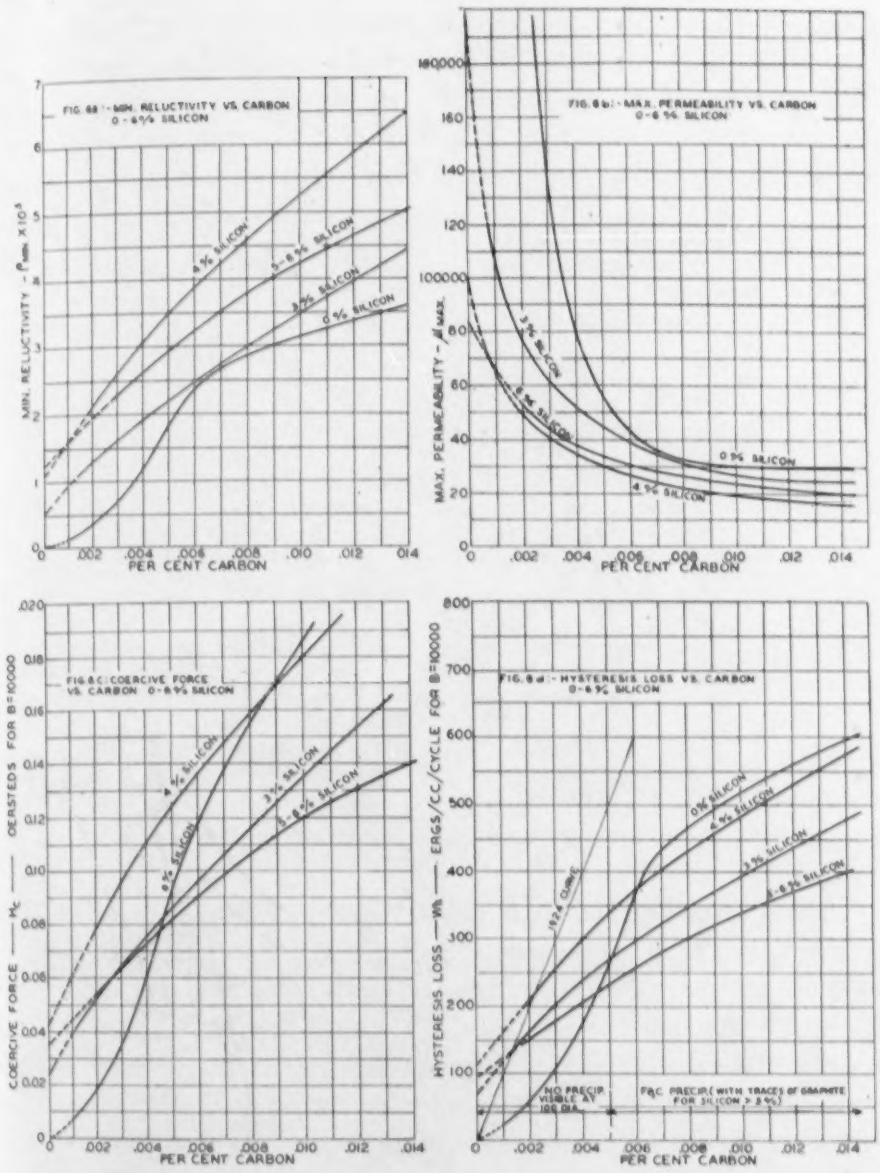

Fig. 6—Effect of Carbon on Magnetic Properties of Single Crystals of Iron-Silicon Alloys.

general tendency is about the same. The main point of divergence is that none of the curves coincide, and that they all lie considerably below the 1924 curve for low carbon contents, especially the 3 and 6 per cent curves. The 4 and 6 per cent curves cross the 1924 curves at 0.03 and 0.05 per cent silicon respectively and lie above these curves for higher carbon contents.

For 0 per cent silicon the divergence was explained in the previ-

ous paper (loc cit) on the basis of about 0.02 per cent O_2 being present in the 1924 samples, but any such explanation does not hold here, as the present data indicate no effect due to oxygen in the presence of more than 3 per cent silicon. The only explanation that can be offered is that the present data are more extensive and offer

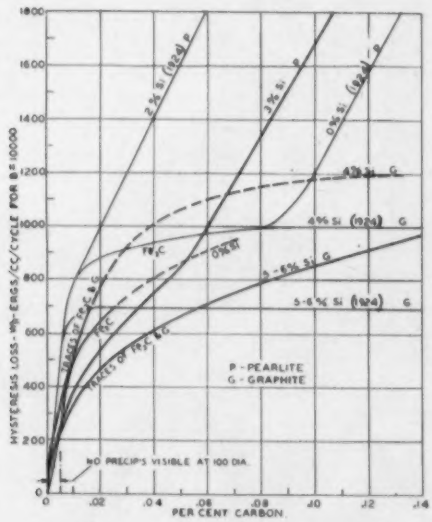

Fig. 7—Hyteresis Loss Versus Carbon on 0 to 6 Per Cent Silicon Alloy.

less chance for uncertain extra- and interpolations than in the previous case.

Effect of Grain-Size. In Table V and in Figs. 11a, 11b, and 11c, the effect of grain-size is recapitulated for the three silicon contents and these sets have been combined into one picture in Fig. 11d showing the effect on hysteresis loss. In the latter the 1924 and 1930[5] curves are shown broken. These curves represent the term aN^m in the equation $x = aN^m + b$, in which x is $\rho_{min.}$, W_h or H_c and "b" is a parameter depending on the carbon content as shown in Table V.

While the earlier results indicated a square root law ($W_h = 100\sqrt{N}$) for low carbon and a linear relationship for high carbon ($W_h = 3N$) the recent data point towards a linear relationship for all carbon contents. (Only in one case do we get a square root curve).

Effect of Oxygen and High Density Permeability

It was mentioned in the first part of the paper that oxygen, while apparently being without appreciable effect on the low density

[5]T. D. Yensen, *Metals and Alloys*, Vol. 1, May 1930, p. 493.

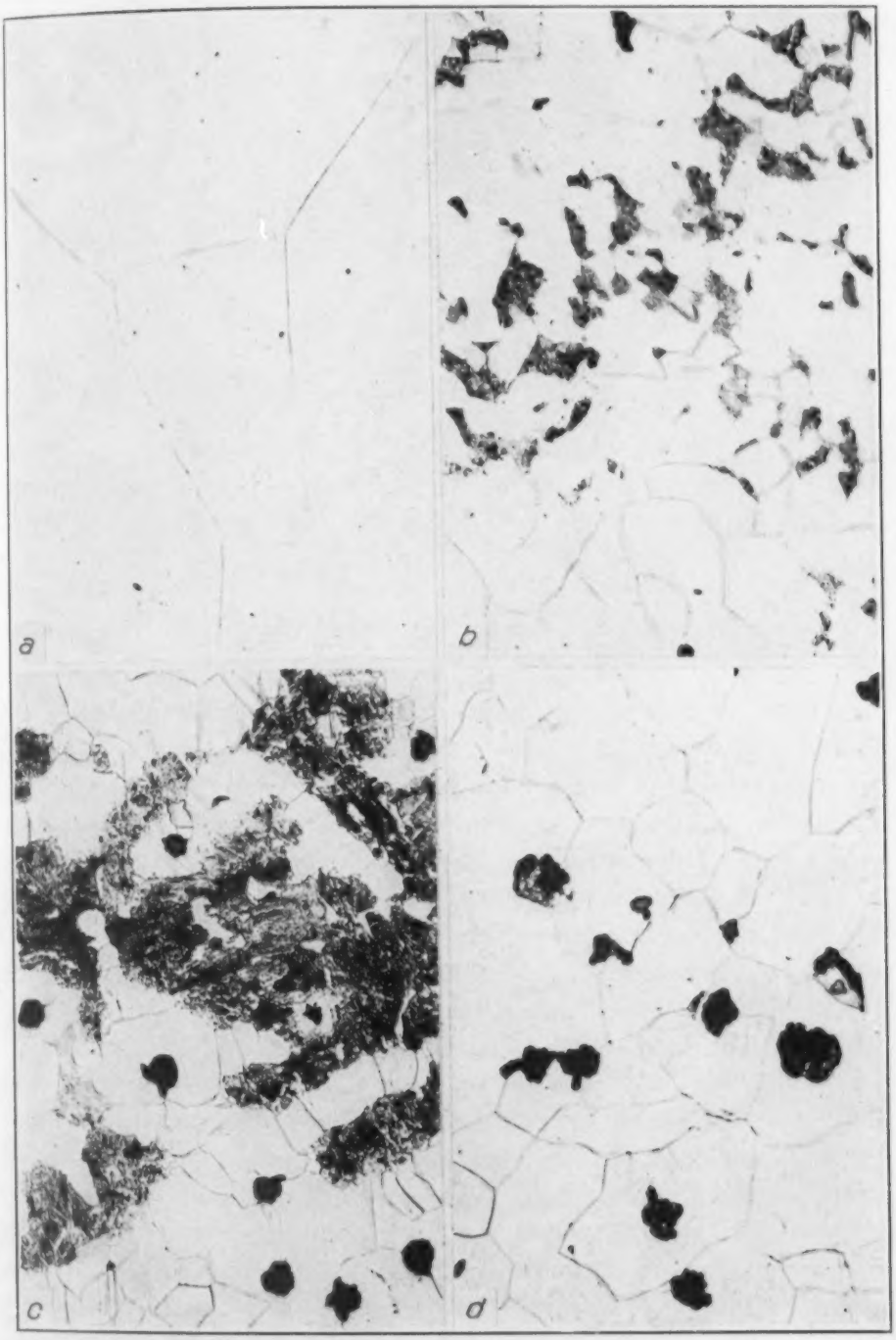

Fig. 8—Photomicrographs of 3 Per Cent Silicon Alloy. × 100. Fig. 8a—Alloy I-31E, 3.10 Per Cent Silicon. Fig. 8b—Alloy I-35B, 3.34 Per Cent Silicon. Fig. 8c—Alloy I-36A, 3.13 Per Cent Silicon. Fig. 8d—Alloy I-36B, 3.13 Per Cent Silicon.

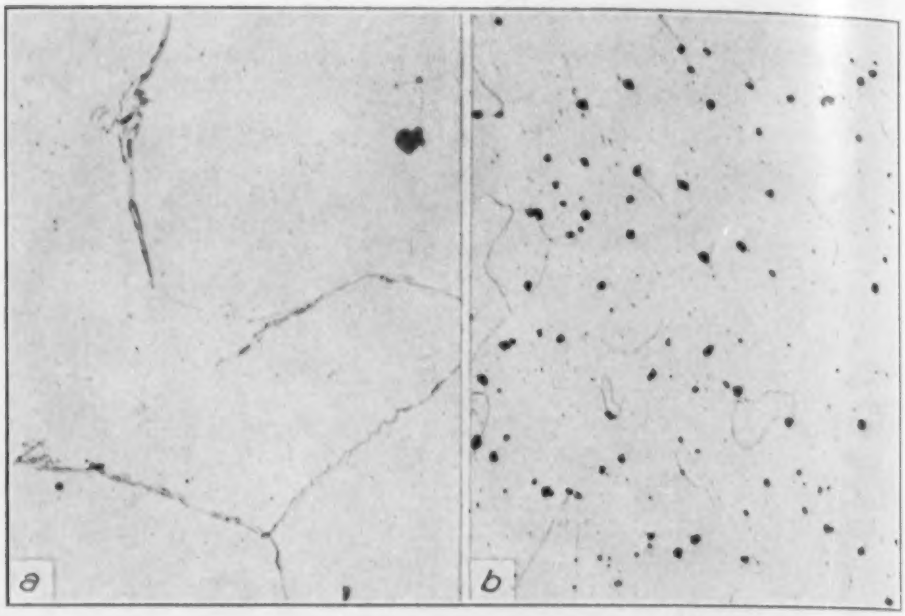

Fig. 9—Photomicrographs of 4 Per Cent Silicon Alloy. × 100. Fig 9a—Alloy I-127C, 4.00 Per Cent Silicon. Fig. 9b—Alloy I-38A, 4.16 Per Cent Silicon.

properties of iron-silicon alloys, does affect the high density permeability quite markedly.

In Tables I, II and III the permeability for H = 100 ($\mu_{H=100}$) has been tabulated. As the silicon-content varies considerably within each group of samples, and as silicon itself has a large effect on the high density permeability, it is necessary first to make corrections for the variation in silicon from the mean value (3, 4, and 6 per cent). This has been done by means of the solid curve of Fig. 12 obtained from the 1924 paper (loc cit). The values of $\mu_{H=100}$ thus corrected to correspond to 3, 4 and 6 per cent silicon are tabulated in Tables I, II, and III respectively and plotted on a log scale in Figs. 13a, 13b and 13c. The three curves (obtained by disregarding the points for high carbon) have been combined in Fig. 13d for comparison. Unfortunately, data were not obtained for 0 per cent silicon for H = 100 so that the corresponding curve for 0 per cent silicon could not be drawn directly, but by plotting the extrapolated values of $\mu_{H=100}$ for 0, 0.1, 0.2 and 0.5 per cent O_2 the broken curves of Fig. 12 are obtained, which, extrapolated give approximate values for 0 per cent silicon that are shown as the broken curve of Fig. 13d.

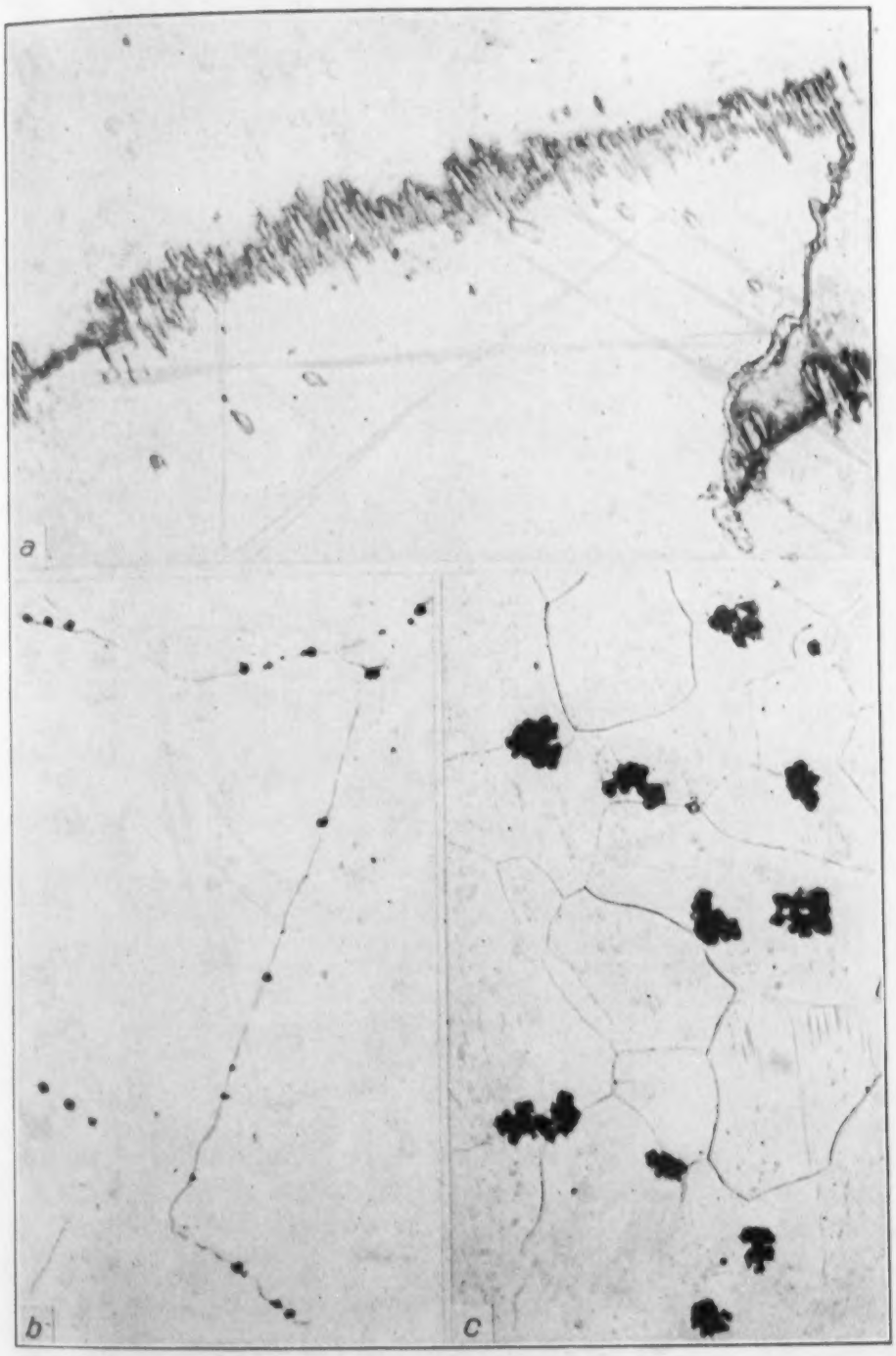

Fig. 10—Photomicrographs of 5 to 6 Per Cent Silicon Alloy. Fig. 10a—Alloy I-50C, 5.95 Per Cent Silicon. × 500. Fig. 10b—Alloy I-53A, 5.42 Per Cent Silicon. × 100. Fig. 10c—Alloy I-55B, 5.01 Per Cent Silicon. × 100.

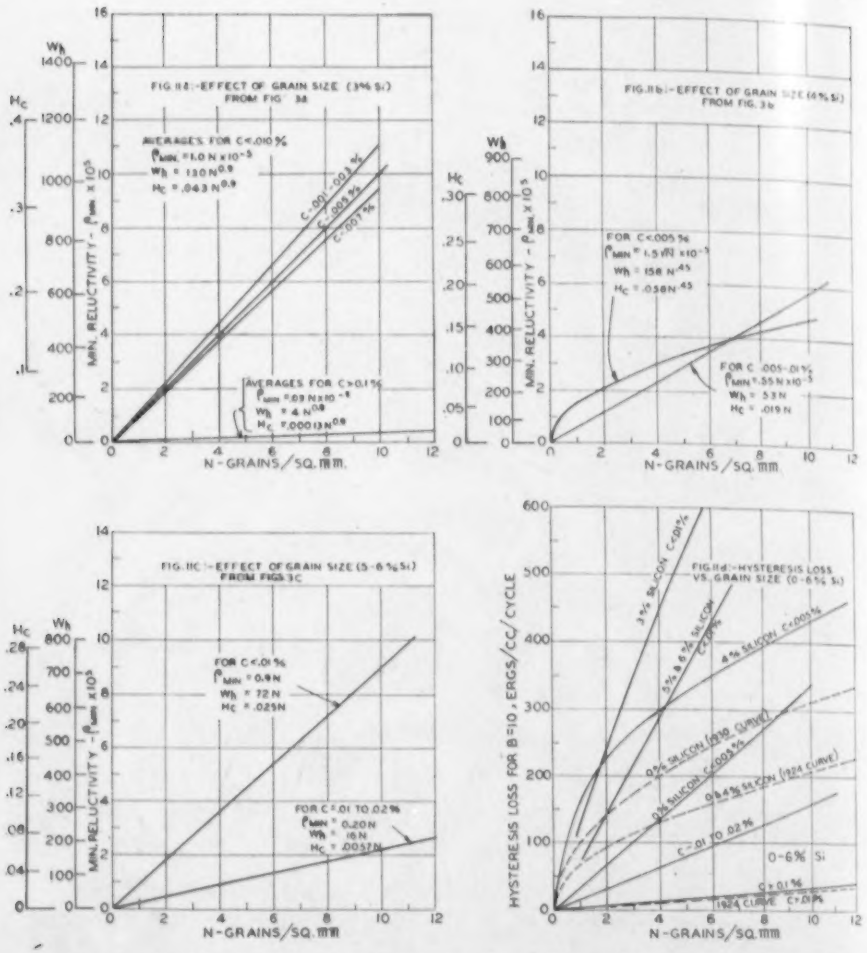

Fig. 11—Effect of Grain-Size (0 to 6 Per Cent Silicon Alloy). Curves Represent Term aN^b in Equation $X = aN^b + b$, where X is ρ min, W_h or H_c; b Increasing with Carbon Content.

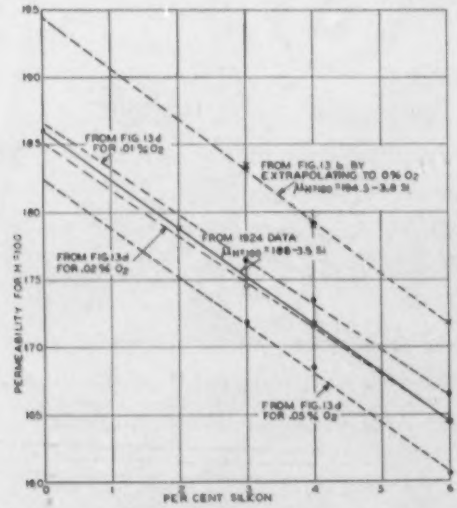

Fig. 12—Permeability for H = 100 Versus Per Cent Silicon for Randomly Oriented Grains.

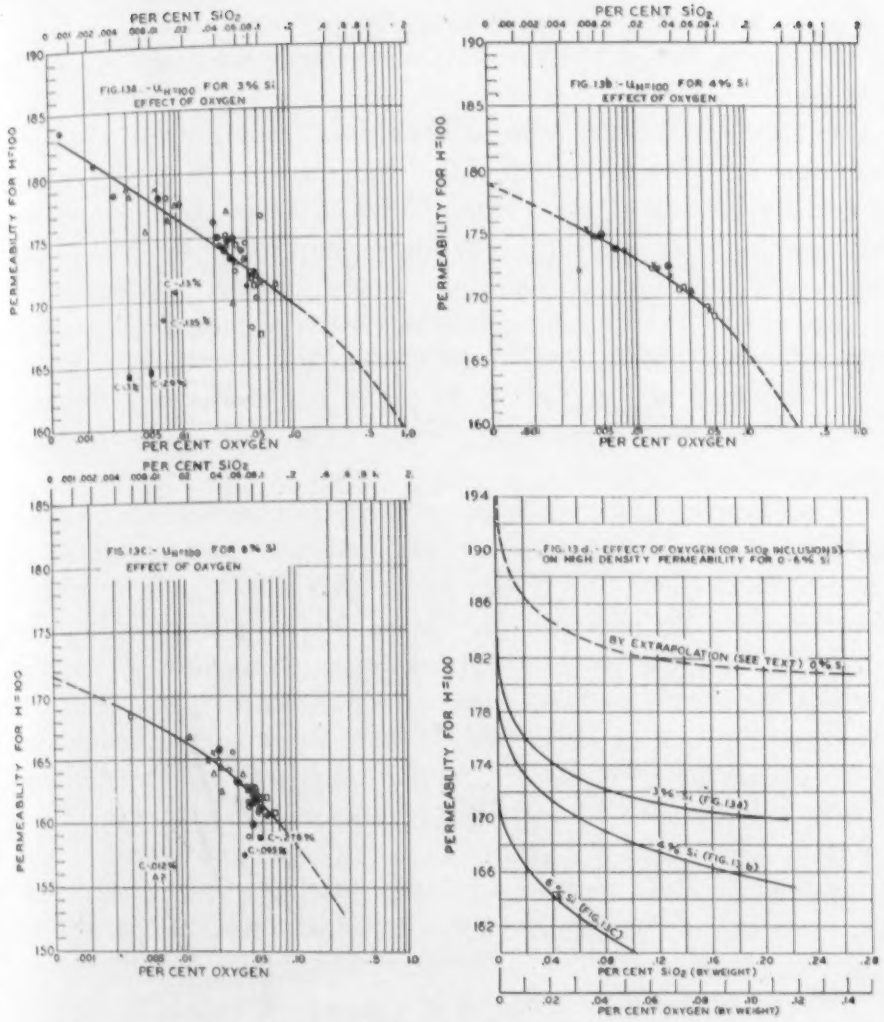

Fig. 13—Effect of Oxygen (SiO_2) on High Density Permeability — 0 to 6 Per Cent Silicon Alloy.

Summary and Conclusion

1. In the presence of 3 per cent silicon or more, small amounts of oxygen have no appreciable effect on the low density magnetic properties of iron-silicon alloys. However, oxygen does affect markedly the high density permeability as shown in Fig. 13d.

2. The large effect of carbon previously reported for iron-silicon alloys has been generally confirmed, but the effect for carbon less than 0.01 per cent is not as large as reported in 1924 and varies with the silicon content. It appears to be greatest for 4 per cent silicon.

3. For carbon less than 0.005 per cent no visible precipitate is

visible at 500 diameters, confirming the previous conclusion that in this low range carbon is either in solution or precipitated as colloidal particles.

4. Above 0.005 per cent carbon is precipitated in various forms, depending on the silicon and carbon contents, but there seems to be no definite boundary line. From 0.005 to about 0.05 per cent the precipitate is Fe_3C for 3 per cent silicon, and partly Fe_3C and partly graphite for 4 to 6 per cent silicon. Above 0.05 per cent carbon precipitates as pearlite for 3 per cent silicon after short annealing at high temperatures (1100 to 1200 degrees Cent.) (2010 to 2190 degrees Fahr.) but may be graphitized on prolonged heating at lower temperatures. For 4 to 6 per cent silicon carbon (above 0.05 per cent) is precipitated as graphite.

5. The effect of carbon above 0.005 per cent on the magnetic properties depends on the form of the precipitate, being greatest for pearlite, intermediate for cementite (Fe_3C) and least for graphite, thus confirming the previous conclusion. Fig. 7 gives a general view.

6. In regard to grain-size there can be no doubt as to the large effect of this factor, but again the effect varies with the silicon and carbon contents as shown in Fig. 11d. For low carbon contents the effect appears to be generally greater than was reported in 1924, while for high carbon contents the agreement is fairly good. Fig. 4 gives the variation of the grain-size factor as a function of the carbon content. The linear relationship between grains per square millimeter and $\mu_{min.}$ H_c, W_h holds in most cases rather than the square root law.

We regret that we are unable at the present time after ten years of work to express the relationship between the magnetic properties and the various factors affecting them in simpler and more general terms. We have no doubt that this will gradually be done, and it is with this expectation in mind and the hope that this interim report will assist in reaching the goal that we feel justified in publishing it.

In conclusion we wish to express our appreciation to the Westinghouse Electric and Manufacturing Company for permission to publish this report; to Wilson Scott for assistance in the preparation of samples, and for the carbon analysis, to A. A. Frey for most of the annealing; to S. L. Burgwin and H. B. Ikelman for the magnetic testing; to R. H. Wynne for the chemical analysis and to Miss Mildred Ferguson for the microscopic analysis and for the excellent photomicrographs.

ALLOYS OF IRON, MANGANESE AND CARBON—PART XV

The Ternary Diagram and General Summary

By F. M. Walters, Jr., and Cyril Wells

Abstract

This paper summarizes the work done in the Metals Research Laboratory of the Carnegie Institute of Technology reported previously in fourteen parts (1-14)[1] on the constitution and properties of high purity iron-manganese alloys (0-100 per cent manganese) and of high purity iron-manganese-carbon alloys (0-14 per cent manganese and 0.02-1.4 per cent carbon).

Various methods were employed in investigating the behavior of the alloys in the solid state: dilatometric, thermal, and thermomagnetic analysis, the variation of electrical resistance with temperature, parameter measurements by X-rays and the microscopic examination of suitably heat treated specimens.

The phases involved in this study are the alpha, gamma and epsilon phases in the iron-rich alloys and alpha, beta, and gamma phases in the manganese-rich alloys (see Fig. 2). In the ternary alloys studied, the carbide observed was cementite in which up to a fourth of the iron atoms were replaced by manganese atoms.

A binary iron-manganese phase diagram and several sections of the iron-manganese-carbon phase diagrams are presented as well as a three-dimensional diagram indicating the phase boundaries of the ternary alloys.

Introduction

AT THE time this investigation was undertaken, little was known about the effect of manganese on iron and iron-carbon alloys. The solidus and liquidus of rather impure iron-manganese alloys had been determined by Rümelin and Fick (15). Hadfield (16) had measured the mechanical and physical characteristics of iron-manga-

[1]The figures appearing in parentheses refer to the bibliography appended.

Of the authors, F. M. Walters, Jr., a member of the Society, formerly of the Metals Research Laboratory, Carnegie Institute of Technology, Pittsburgh, is now Research Engineer, Youngstown Sheet and Tube Company, Youngstown, Ohio, and Cyril Wells is associated with the Metals Research Laboratory, Carnegie Institute of Technology, Pittsburgh. The work of V. N. Krivobok, M. Gensamer, and John F. Eckel is included with that of the authors in this summary.

nese alloys of commercial purity, and some studies of high purity ternary alloys containing up to 2 per cent manganese and up to 1.6 per cent carbon had been made at the Bureau of Standards (17).

After this work was started, binary iron-manganese diagrams were proposed by Öhman (18), Ishiwara (19), and Gayler (20), and a number of sections of the ternary diagram were determined by Bain, Davenport and Waring (21). Of these investigators only Gayler used high purity alloys.

Preparation of Alloys. The binary alloys discussed in this paper were prepared from manganese distilled in vacuo, and electrolytic iron melted in vacuo with enough carbon to reduce the oxygen to a low value (1). To add carbon in the preparation of the ternary alloys, sugar charcoal was used. The alloys were melted in chemically pure magnesium oxide crucibles under argon at atmospheric pressure and cooled in the furnace. The binary alloy ingots containing up to 67 per cent manganese, and the ternary ingots up to 13 per cent manganese and 1.57 per cent carbon, were reduced about 90 per cent by forging. Alloys containing between 70 and 100 per cent manganese were quite brittle and could not be forged.

The material which was used in crucial experiments was heated for several hours at a temperature near the solidus to remove persistent dendritic segregation.[2] In the heat treatments and in the observations at elevated temperatures care was taken to preserve the purity of the alloys by conducting the heating in vacuo or in purified argon or helium.

Phases Present in the Binary and Ternary Alloys. The phases present in the iron-manganese alloys were identified in two series of X-ray measurements. In the first, cameras were employed which were suitable for the identification of phases but which were of only moderate accuracy in the determination of lattice parameters, (3) while in the second series, the use of a Sachs' back reflection camera gave results of a much higher accuracy (13).

In the binary system 6 phases are stable at room temperature or may be retained by quenching. They are solid solutions of the substitutional type, and the lattice parameters of the cubic forms increase as the manganese content is raised, except when other phases are present (Fig. 1). These phases are:

[2]As a result of this treatment the constituents were much more uniformly distributed in the alloys (as shown by the microscope), and the temperature ranges between the beginning and the end of transformations were reduced (as revealed by dilatometric studies). These facts indicate that the long time high temperature treatment greatly reduced dendritic segregation.

1. Alpha iron, body-centered cubic
2. Gamma iron, face-centered cubic
3. Epsilon, hexagonal close packed
4. Alpha manganese, complex cubic with 58 atoms in unit cell
5. Beta manganese, complex cubic with 20 atoms in the unit cell
6. Gamma manganese, face-centered tetragonal as quenched.

The phases observed in the ternary region studied were the alpha iron solid solution, the gamma iron solid solution, the epsilon solid solution, and cementite. The cementite in the iron-manganese-carbon alloys may have up to one-fourth of its iron atoms replaced by manganese. This observation is based not only on the results of chemical analysis (22) and of X-ray observations (23), but is fundamental to a consistent explanation of the behavior of the ternary alloys. For example, high manganese high carbon alloys annealed at 500 degrees Cent. (930 degrees Fahr.) to precipitate carbides show by their behavior on cooling that the matrix is lower in manganese as well as in carbon (7, 8). Apparently the manganese carbides Mn_4C and Mn_7C_3 do not occur in the ternary compositions studied.

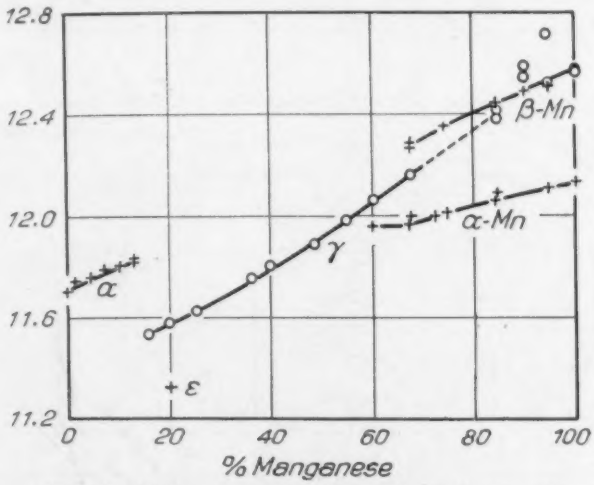

Fig. 1—Volume per Lattice Point of the Phases Stable at Room Temperature or Retained by Quenching.

X-ray observations were very useful in identifying the phases present in the binary alloys; in conjunction with microscopic observations, they served to determine the phase diagram for both the high manganese alloys and the low manganese alloys, and they also were essential to the interpretation of the dilatometric, thermal, microscopic and other data.

The gamma phase is face-centered cubic up to about 70 per cent

manganese, while from 70 to 94 per cent the alloys quenched from the gamma field are found to be face-centered tetragonal with an axial ratio decreasing from unity to 0.93 for manganese. One may assume that the tetragonal gamma is a transition phase formed on quenching a gamma phase which is cubic at high temperatures (13).

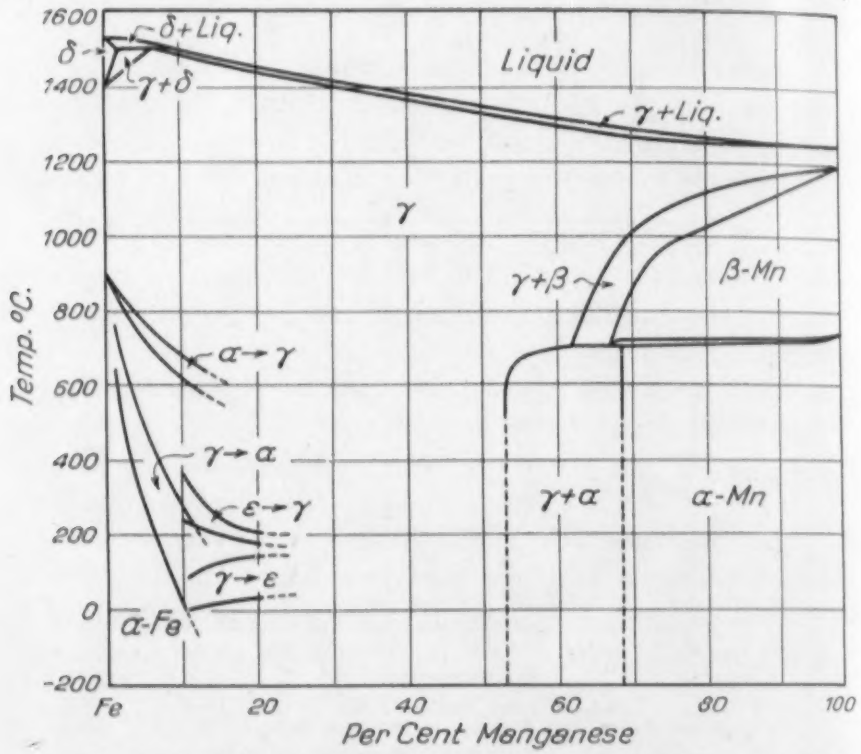

Fig. 2—Iron-Manganese Diagram. 0 to 50 Per Cent Manganese is Based on Dilatometric Observations, 50 to 100 Per Cent Manganese is Based on Microscopic and X-ray Examination of Quenched Alloys. The Delta Region and the Solidus-Liquidus are Redrawn from Gayler's Data[20].

No satisfactory experimental evidence has been presented for the existence of a two-phased region, gamma iron-gamma manganese. Gamma manganese is relatively soft, while alpha and beta manganese are hard and brittle as might be expected from their complex atomic arrangements.

Constitution of the Binary Alloys

There is a marked contrast between the iron and manganese side of the constitutional diagram (Fig. 2). High manganese gamma and beta phases may be retained at room temperature by quenching. Only that part of the diagram dealing with high manganese alloys is substantially an equilibrium diagram. Low manga-

nese alloys remain in the gamma state until a definite temperature is reached, at which they begin to transform. For example, the 7 per cent manganese alloy showed no evidence of transformation from gamma to alpha, when held at 630 degrees Cent. (1165 degrees Fahr.) (just below Ac) for 17 hours or at 400 degrees Cent. (750 degrees Fahr.) (just above Ar) for 41 hours. Accordingly the low manganese part of the diagram is a diagram representing transformations at prescribed heating and cooling rates rather than an equilibrium diagram.

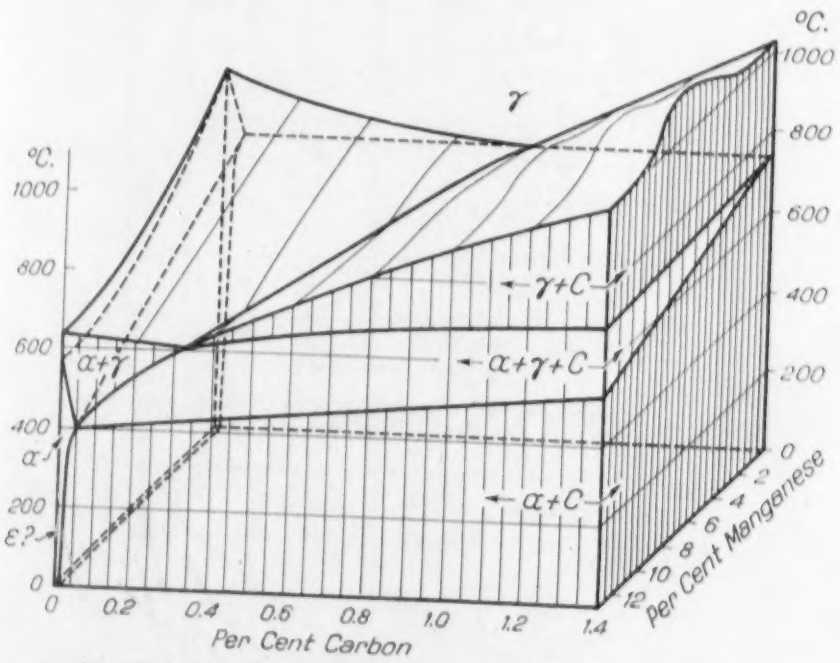

Fig. 3—Iron-Manganese-Carbon Ternary Diagram (0-1.4 Per Cent Carbon and 0-13 Per Cent Manganese).

Heterogeneity. The high degree of dendritic segregation and the slow rate of diffusion of manganese in iron in the solid state make it necessary to heat the alloys for a long time (8 to 24 hours) at temperatures just below the solidus in order to secure homogeneity. Such treatment definitely sharpens the alpha-gamma transformation range, but its effect is most marked on the epsilon transformation range which was narrowed from 100 degrees Cent. in alloys "as forged" to 10 degrees Cent. after homogenization (6).

The sharpness of the transformations in the binary alloys can be definitely disturbed and what may be called "transformational segregation" can be brought about by holding the 4 to 13 per cent

alloys just below or within the alpha to gamma transformation range (9). This "dispersion of composition" is readily removed by holding alloys a short time at 1000 degrees Cent. (1830 degrees F.).

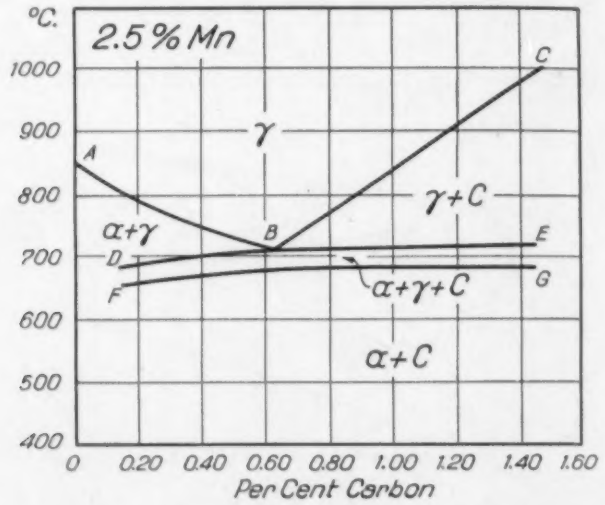

Fig. 4—Section of Iron-Manganese-Carbon Ternary Diagram—2.5 Per Cent Manganese (Gensamer).

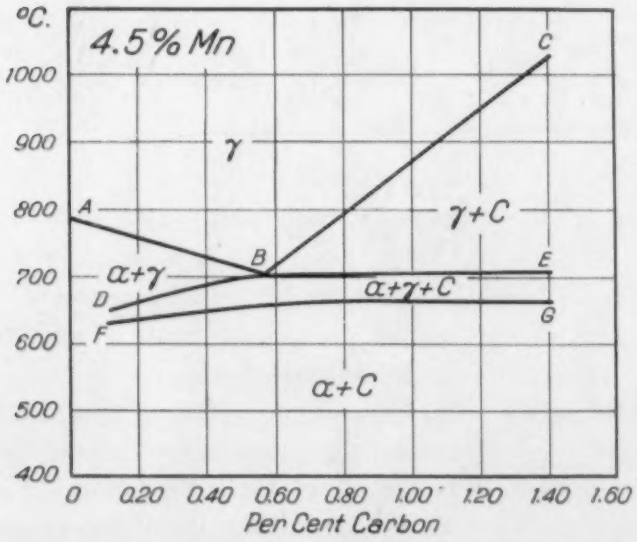

Fig. 5—Section of Iron-Manganese-Carbon Ternary Diagram—4.5 Per Cent Manganese (Gensamer).

The marked persistence of segregation in the gamma phase of the ternary alloys results primarily from the presence of manganese (not carbon) concentration gradients, since the rate of diffusion of carbon in gamma iron is many times faster than that of manganese. In alloys containing two or more phases, the con-

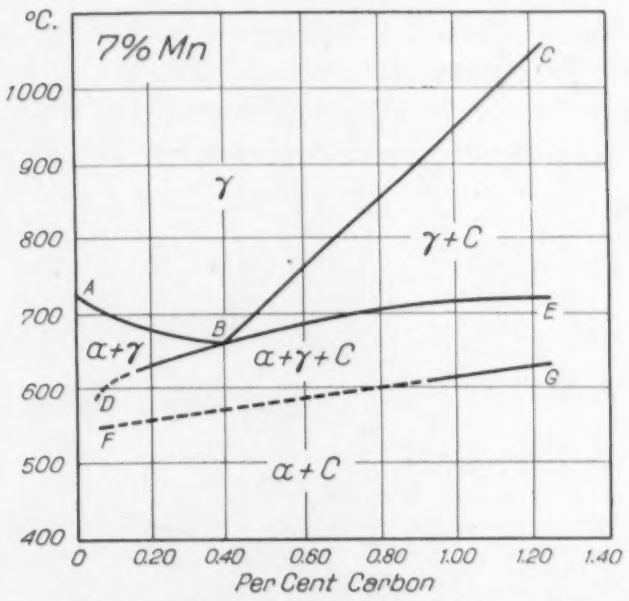

Fig. 6—Section of Iron-Manganese-Carbon Ternary Diagram—7.0 Per Cent Manganese.

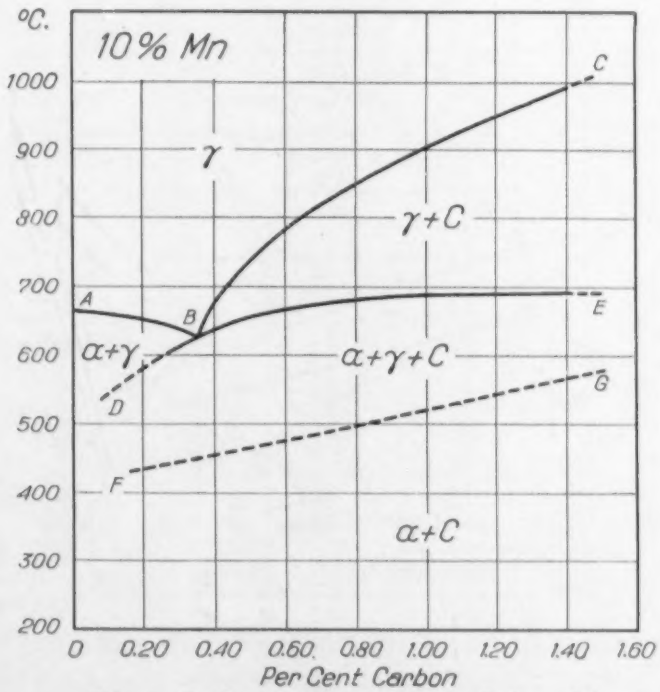

Fig. 7—Section of Iron-Manganese-Carbon Ternary Diagram—10 Per Cent Manganese (Eckel and Krivobok).

centration of manganese and carbon is highest in the carbide. Hence the presence or absence of a dendritic structure as outlined by the carbide indicates the presence or absence of dendritic segregation.

Dilatometric Analysis. The boundaries of the two-phase regions, alpha to gamma, gamma to alpha, epsilon to gamma, and gamma to epsilon, were determined from dilatometric observations

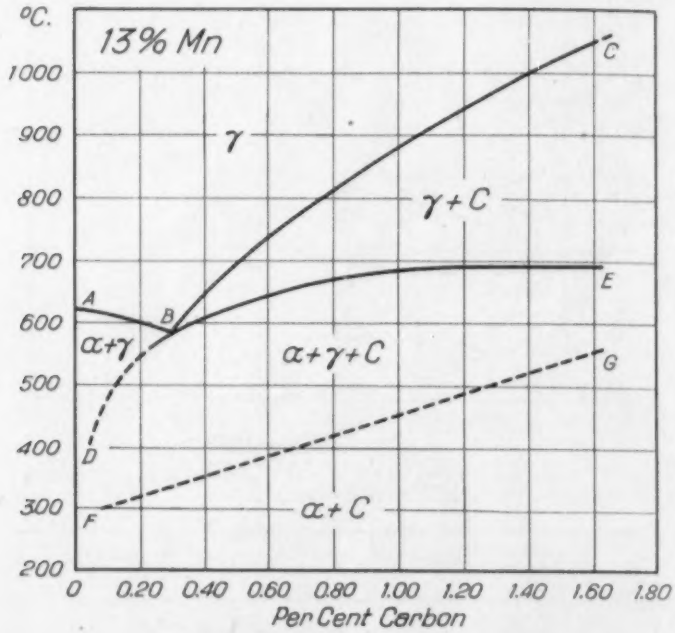

Fig. 8—Section of Iron-Manganese-Carbon Ternary Diagram—13 Per Cent Manganese.

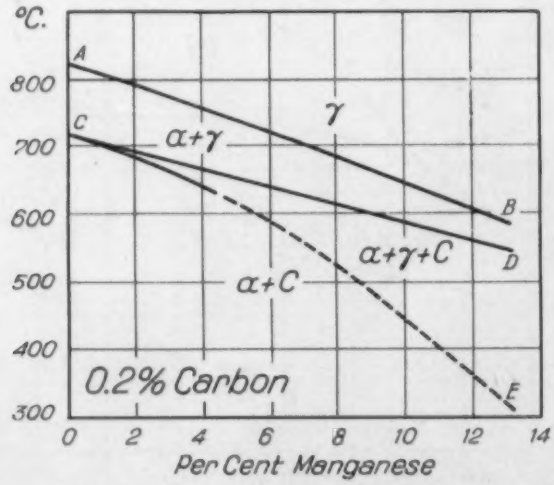

Fig. 9—Section of Iron-Manganese-Carbon Ternary Diagram—0.2 Per Cent Carbon.

on homogenized alloys. Heating and cooling rates of 6 or 12 degrees per minute were employed; slower cooling rates did not affect the temperature range of the gamma to alpha transformation, but slower heating rates resulted in the alpha to gamma transforma-

tion beginning at a lower and ending at a higher temperature (6).

It is shown by X-ray measurements that the transformation of gamma to epsilon is accompanied by a decrease in volume and the transformation to alpha by an increase. It was possible not only to

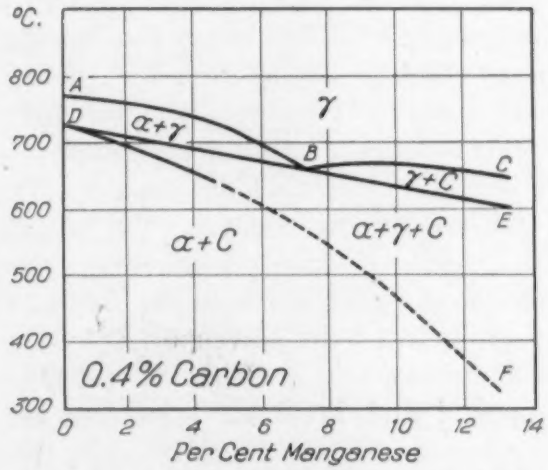

Fig. 10—Section of Iron-Manganese-Carbon Ternary Diagram—0.4 Per Cent Carbon.

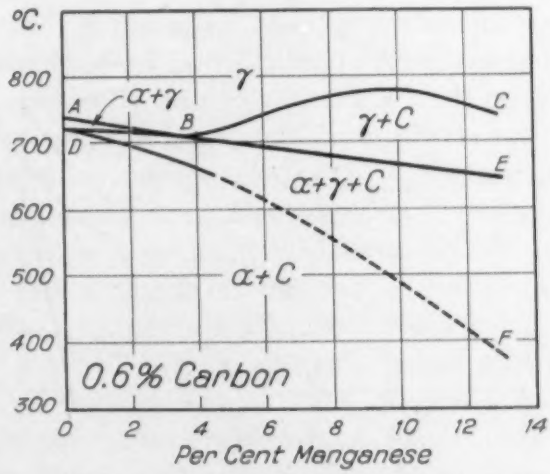

Fig. 11—Section of Iron-Manganese-Carbon Ternary Diagram—0.6 Per Cent Carbon.

identify these transformations, but to show that in the case of the 13 per cent alloy both transformations occurred: part of the gamma decomposing to epsilon, part to alpha and part being retained (4). From the anomalous length change accompanying a transformation, together with the lattice parameter measurements of the phases involved, an estimate may be made of the completeness of the transformation (6, 8).

Thermal Analysis. Dilatometric analysis not only confirmed the results of thermal analysis (2), but also served to explain them. For example, the gradual decrease in intensity of A_3, as the manganese increases, was shown to be due to the increasing range of temperature required for the transformation, not to its incompleteness (in alloys containing less than 10 per cent manganese). While the sharpness of the thermal disturbances due to the epsilon transformations showed them to be essentially different from those due to the alpha transformations, dilatometric observations combined with X-ray data definitely identified the reaction. A gradient furnace was used for the thermal analysis; the heating and cooling rates were about 15 degrees Cent. per minute.

The Epsilon Phase. This has been the subject of much speculation. Öhman (18), and Bain, Davenport and Waring (21), believe it to be a transition phase. Ishiwara (19) asserts it is an intermetallic compound and Mehl (25) suggests an intermediate phase formed by a peritectoid reaction. However, the point of view may be taken that for a limited range of manganese concentration, the gamma decomposes to a hexagonal close packed lattice rather than to the body-centered alpha (13). Epsilon is the closest packed of these three phases, and it is likely that its formation is favored by pressure. When the 16 and 20 per cent alloys were compressed slightly beyond the elastic limit, the transformation to epsilon was almost complete, whereas in unstressed specimens about 70 per cent of the gamma remained untransformed (6). Data obtained thermomagnetically may be interpreted as favoring a peritectoid reaction.

Epsilon is essentially a low carbon phase; it was not observed in the ternary alloys except after heat treatments which removed carbon from solution rather completely (7).

Variation of Magnetic Flux and Electrical Resistance with Temperature. The results of the thermomagnetic analysis (10) may be briefly summarized: the binary alloys are magnetic when in the alpha state and below the Curie point of iron. The magnetism of the alpha phase decreases with increasing manganese. No attempt was made to evaluate magnetic constants.

Manganese (like other elements in solid solution) was found to increase the electrical resistance of alpha iron and to decrease the temperature coefficient (11). A surprisingly small effect on the resistance of gamma iron was found. At 1000 degrees Cent. (1830 degrees Fahr.) the specific resistance of the 29 per cent manganese

was only 25 per cent greater than the resistance of iron, while at 24 degrees Cent. the specific resistance of the 10 per cent alloy was four times as great as that of iron.

The thermal hysteresis of the alpha-gamma transformation

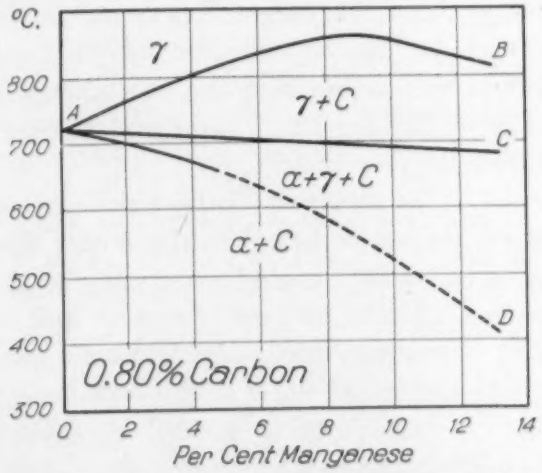

Fig. 12—Section of Iron-Manganese-Carbon Ternary Diagram—0.8 Per Cent Carbon.

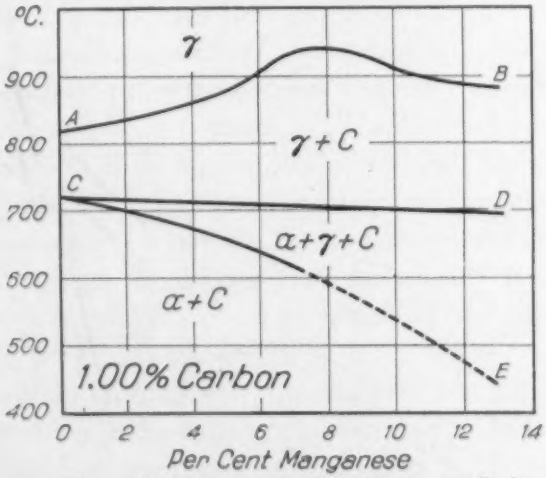

Fig. 13—Section of Iron-Manganese-Carbon Ternary Diagram—1.0 Per Cent Carbon.

was shown by the variation of magnetism and of electrical resistance with temperature, though not as precisely as by the dilatometric observations.

The High Manganese Alloys. The epsilon transformation does not occur in alloys containing more than 32 per cent manganese. Between this composition and 54 per cent, at which alpha manganese is found, no evidence for transformations in the solid state was found by thermal, dilatometric, X-ray or microscopic examination.

The diagram for the manganese-rich alloys is based on microscopic and X-ray examination of quenched specimens. In many cases equilibrium was approached from two directions. The temperature of the eutectoid ($\beta Mn \rightleftarrows \alpha Mn + \Upsilon$) was confirmed dilatometrically. The authors' diagram differs from that of Öhman (18) and Gayler (20) chiefly in the omission of the two-phase region, gamma iron-gamma manganese and the accompanying peritectic at 1270 degrees Cent. (2320 degrees Fahr.) and the eutectoid at 1030 degrees Cent. (1885 degrees Fahr.).

Microstructure. The structure characteristic of pure metals and single phase solid solutions is found in the binary alloys containing 0 to 2 per cent when slowly cooled, in those containing 32 to 54 per cent under all conditions of heat treatment and in higher manganese alloys after quenching drastically from the gamma field (5).

After any heat treatment the 7 and 10 per cent alloys have a fine duplex structure with a poorly defined Widmanstätten pattern. This structure is also characteristic of the rapidly quenched alloys of lower manganese content.

Alloys containing 13 to 32 per cent manganese possess, regardless of heat treatment, a fine duplex structure with well defined Widmanstätten patterns. This well defined pattern is the result of the low temperature transformation of gamma to epsilon. When gamma transforms to alpha the martensitic structure is observed. This difference in Widmanstätten pattern resulting from the decomposition of gamma is due not only to the expansion accompanying the formation of alpha and the contraction accompanying the epsilon transformation, but also to the character of the Widmanstätten mechanism involved (24).

In both the gamma to alpha and the gamma to epsilon transformations, the octahedral planes of the gamma phase are planes for precipitation. The (111) planes of gamma are parallel to the (110) planes of alpha in the one transformation and to the (00.1) planes of epsilon in the other. The matching of the hexagonal atomic arrangement of gamma (111) and epsilon (00.1) planes is better than that of gamma (111) and alpha (110) planes; there are probably 24 possible orientations of alpha that may form on a single gamma grain, but only 4 of epsilon. This reasonably accounts for the more poorly developed Widmanstätten pattern resulting from the gamma to alpha than from the gamma to epsilon transformation.

The manganese-rich alloys have a coarse duplex structure with

the phases distinctly separated into grains large enough to be identified easily at moderate magnification. There is an increasing tendency toward Widmanstätten patterns with higher manganese. For example, on cooling the 67 per cent alloy, the beta manganese result-

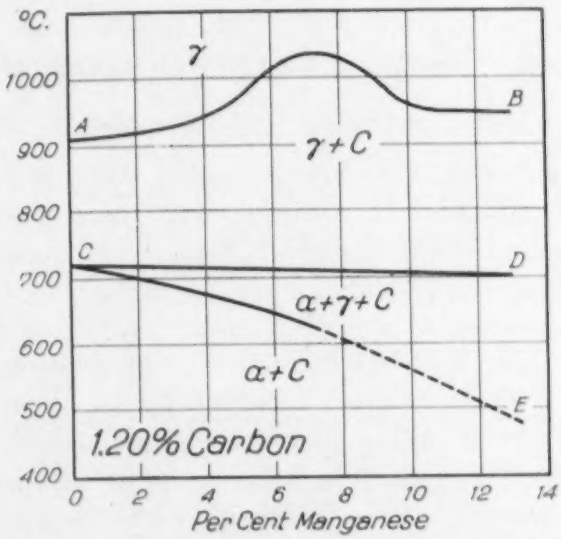

Fig. 14—Section of Iron-Manganese-Carbon Ternary Diagram—1.2 Per Cent Carbon.

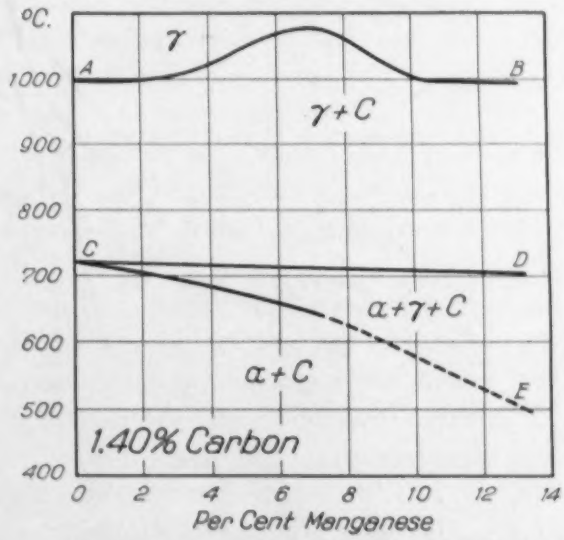

Fig. 15—Section of Iron-Manganese-Carbon Ternary Diagram—1.4 Per Cent Carbon.

ing from the decomposition of the gamma phase is almost all formed at the gamma grain boundaries, giving a cellular structure, whereas in the 90 per cent alloy, the beta and the remaining gamma reveal a well developed Widmanstätten pattern.

The effect of carbon on the temperatures of stability and on the rate of decomposition of the iron-manganese gamma solid solution makes it possible by a suitable choice of heat treatment and composition to produce in iron-manganese-carbon alloys practically all the slight variations in microstructure that have been observed in steels. (Proeutectoid carbide or ferrite in the gamma grain boundaries and within the grains, pearlite, sorbite, troostite, martensite, austenite).

Constitution of the Ternary Alloys

The constitution of the ternary alloys (0.02 to 1.4 per cent carbon and 0 to 13 per cent manganese has been determined by the microscopic examination of quenched specimens, previously brought to equilibrium at crucial temperatures (7, 8, 12, 14).

For the purpose of a general understanding of the constitution of the alloys as a whole, the diagram of Fig. 3 has been drawn. At temperatures just above those indicated by the upper surfaces only the gamma phase is stable. Below these surfaces the stable phases are as designated and occur between limits indicated by the limiting boundaries. The line at the intersection of the upper two surfaces represents the upper eutectoid compositions and temperatures (720 degrees Cent. and 0.80 per cent carbon for pure iron-carbon alloys and 600 degrees Cent. and 0.30 per cent carbon for 13 per cent manganese ternary alloys). The space indicated by epsilon is limited but has not been determined in this investigation. The results of Bain, Davenport and Waring (21) relating to the constitution of commercial-ternary alloys show that the diagram of Fig. 3 represents, at least approximately, the constitution of commercial alloys as well as those of high purity.

Manganese in iron-carbon alloys makes possible the co-existence of three phases, alpha, gamma and carbide, in equilibrium. This is indicated in Fig. 3 and more specifically in the constant manganese and constant carbon sectional diagrams. As carbon is added to iron-manganese alloys of constant manganese content, the upper and lower temperature limits at which the three phases can exist in equilibrium are raised.[3] (Figs. 3 to 8). The effect of manganese on the temperature zones of stability for the phases in alloys of constant car-

[3]When an alloy in the three-phase region is in equilibrium, the concentration of manganese and of carbon is highest in the carbide, intermediate in the gamma, and lowest in the alpha phase. Due to this distribution of components in the phases, an increase in carbon in iron-manganese-carbon alloys of constant manganese content results in a decrease of manganese in the gamma in equilibrium with alpha and carbide phases at the upper and lower temperature limits of the eutectoid reaction and therefore in a raising of the upper and lower temperature limits of the three-phase zone.

bon content is indicated in Figs. 9 to 15. These diagrams were derived from the data given in Figs. 4 to 8.[4]

The upper temperature limit of the eutectoid reaction as indicated by B (Figs. 4 to 8) is lowered by manganese (Fig. 16) and

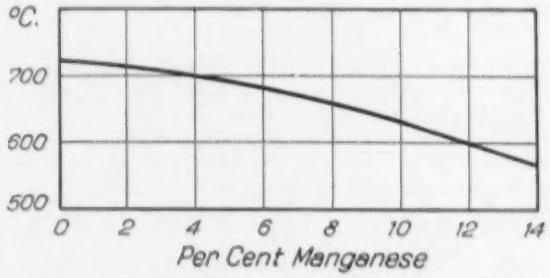

Fig. 16—Effect of Manganese on Upper Eutectoid Temperature Limit in Alloys of Eutectoid Composition.

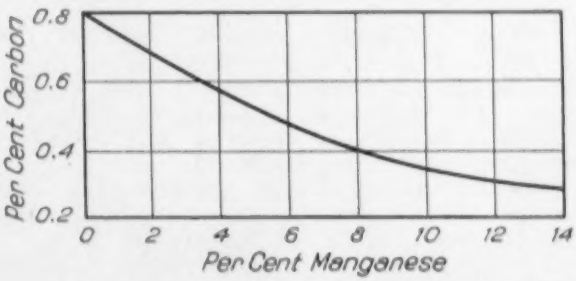

Fig. 17—Effect of Manganese on Carbon Concentration in Alloys of Eutectoid Composition.

the carbon concentration of the eutectoid composition is also lowered with increase of manganese (Fig. 17).

References

1. Walters, "Alloys of Iron, Manganese and Carbon—Part I. Preparation of Alloys," TRANSACTIONS, American Society for Steel Treating, Vol. 19, 1932, p. 577.
2. Walters and Wells, "Alloys of Iron, Manganese and Carbon—Part II. Thermal Analysis of the Binary Alloys," TRANSACTIONS, American Society for Steel Treating, Vol. 19, 1932, p. 590.
3. Gensamer, Eckel and Walters, "Alloys of Iron, Manganese and Carbon—Part III. An X-ray Study of the Binary Iron-Manganese Alloys," TRANSACTIONS, American Society for Steel Treating, Vol. 19, 1932, p. 599.
4. Walters and Gensamer, "Alloys of Iron, Manganese and Carbon—Part IV. A Dilatometric Study of Iron-Manganese Binary Alloys," TRANSACTIONS, American Society for Steel Treating, Vol. 19, 1932, p. 608.
5. Krivobok and Wells, "Alloys of Iron, Manganese and Carbon—Part V.

[4]Since the sectional diagrams presented are neither binary nor pseudo-binary diagrams, they give no indication of the proportions or compositions of two or more phases co-existing in equilibrium. Until such time that the chemical compositions of each phase in equilibrium with the other phases are known, only an incomplete knowledge of the ternary diagram is possible. At present few data of this kind are available.

Microscopic Studies of Binary Iron-Manganese Alloys," TRANSACTIONS, American Society for Steel Treating, Vol. 21, 1933, p. 807.
6. Walters, "Alloys of Iron, Manganese and Carbon—Part VI. Transformations in the Binary Iron-Manganese Alloys," TRANSACTIONS, American Society for Steel Treating, Vol. 21, 1933, p. 821.
7. Wells and Walters, "Alloys of Iron, Manganese and Carbon—Part VII. Influence of Carbon on Thirteen Per Cent Manganese Alloys," TRANSACTIONS, American Society for Steel Treating, Vol. 21, p. 830.
8. Eckel and Krivobok, "Alloys of Iron, Manganese and Carbon—Part VIII. Influence of Carbon on Ten Per Cent Manganese Alloys," TRANSACTIONS, American Society for Steel Treating, Vol. 21, p. 846.
9. Walters, "Alloys of Iron and Manganese—Part IX. Transformations and Heterogeneity in the Binary Alloys of Iron and Manganese," TRANSACTIONS, American Society for Steel Treating, Vol. 21, p. 1002.
10. Walters and Eckel, "Alloys of Iron and Manganese—Part X. Thermomagnetic Analysis of the Binary Alloys of Iron and Manganese," TRANSACTIONS, American Society for Steel Treating, Vol. 21, p. 1016.
11. Walters and Wells, "Alloys of Iron and Manganese—Part XI. The Variation of Electrical Resistance with Temperature in Binary Alloys of Iron and Manganese," TRANSACTIONS, American Society for Steel Treating, Vol. 21, p. 1021.
12. Gensamer, "Alloys of Iron and Manganese—Part XII. Alloys of Iron and Carbon with 2.5 and 4.5 Per Cent Manganese," TRANSACTIONS, American Society for Steel Treating, Vol. 21, p. 1028.
13. Walters and Wells, "Alloys of Iron and Manganese—Part XIII. The Constitution of the Binary Alloys of Iron and Manganese," TRANSACTIONS, American Society for Metals, Vol. 23, p. 727.
14. Wells and Walters, "Alloys of Iron, Manganese and Carbon—Part XIV. Iron-Carbon Alloys Containing Seven Per Cent Manganese," TRANSACTIONS, American Society for Metals, Vol. 23, p. 751.
15. Rümelin and Fick, "Beiträge zur des Systems Eisen-Mangan," *Ferrum*, Vol. 12, 1914-15, p. 41.
16. Hadfield, "Alloys of Iron and Manganese Containing Low Carbon," *Journal*, Iron and Steel Institute, Vol. 115, 1927, p. 297.
17. Neville and Cain, "Effects of Carbon and Pure Manganese on the Mechanical Properties of Pure Iron," Bureau of Standards, Scientific Papers, Vol. 18, 1923, p. 411.
Rawdon and Sillers, "Effect of Manganese on the Structure of the Alloys of the Iron-Carbon System," Bureau of Standards, Scientific Papers, Vol. 18, 1923, p. 637.
18. Öhman, "Röntgenographische Untersuchungen über das System Eisen-Mangan," *Zeitschrift für Physikalische Chemie*, Vol. 8, 1930, p. 81.
19. Ishiwara, "On the Equilibrium Diagrams of Al-Mn, Cu-Mn and Fe-Mn," *Science Reports*, Tohoku University, Vol. 19, 1930, p. 499.
20. Gayler, "The Constitution of the Alloys of Iron and Manganese," *Journal*, Iron and Steel Institute, Vol. 128, 1933, p. 499.
21. Bain, Davenport and Waring, "The Equilibrium Diagram of Iron-Manganese-Carbon Alloys of Commercial Purity," *Transactions*, American Institute of Mining and Metallurgical Engineers, Vol. 100, 1932, p. 228.
22. Arnold and Reed, "Chemical and Mechanical Relations of Iron, Manganese and Carbon Alloys," *Journal*, Iron and Steel Institute, Vol. 38, 1910, p. 169.
23. Westgren and Phragmen, "The Crystal Structure of Cementite," *Journal*, Iron and Steel Institute, Vol. 105, 1922, p. 255; Vol. 109, 1924, p. 159.
24. Mehl and Co-authors, "Studies Upon the Widmanstätten Structure," *Transactions*, American Institute of Mining and Metallurgical Engineers, 1930-34.
25. Mehl. Discussion of the Progress Report on "The Alloys of Iron-Manganese and Carbon," presented at the Fourth Open Meeting of the Mining and Metallurgical Advisory Boards, Pittsburgh, Oct. 17, 1930.

X-RAY INVESTIGATION OF THE IRON-CHROMIUM-SILICON PHASE DIAGRAM

By A. G. H. Andersen and Eric R. Jette

Abstract

Applying only the methods of X-ray crystal structure analysis, the authors have determined a large portion of the phase diagram of the ternary system, iron-chromium-silicon. By making accurate measurements of lattice constants and applying the methods of interpolation and extrapolation developed in a previous article, and by making use of the clear-cut identification of the phases present in an alloy, which is a characteristic feature of the X-ray method, it was possible:—(1) to study the equilibrium relations between the alpha-phase and three other phases which are based respectively on the binary phases Fe_3Si_2, Cr_3Si and FeCr, (2) to determine the alpha-phase boundaries with respect to these three phases at three temperatures 1000, 800 and 600 degrees Cent. (1830, 1470 and 1110 degrees Fahr.), (3) to construct the parametric surfaces (i.e., the relation between the lattice parameter and composition) for the major portion of the ternary alpha-phase alloys and for the adjacent two-phase regions, and (4) to indicate the more important features of the greater portion of the remainder of the ternary system. Since the three binary systems involved had previously been studied by X-ray methods, it was possible to secure this large quantity of information with the use of only seventy ternary alloys.

Previous Work

ALLOYS of iron in which both chromium and silicon enter as the only main alloying elements are at present used for corrosion and heat resistant materials (3).[1] The recent Engineering Foundation monograph by Greiner, Marsh and Stoughton (4) describes a number of alloys of iron with silicon as well as alloys of iron with chromium and silicon. The various collections of alloy

[1]The figures appearing in parentheses refer to the bibliography appended to this paper.

This paper is part of a thesis submitted by A. G. H. Andersen in May 1935 to the Faculty of Pure Science of Columbia University in partial fulfillment of the requirements for the degree of Doctor of Philosophy.

Of the authors, A. G. H. Andersen is with the Phelps Dodge Corporation, Research Department, and Eric R. Jette is Associate Professor of Metallurgy, School of Mines, Columbia University, New York City. Manuscript received February 14, 1936.

patents (5, 6) contain a large number of compositions of alloys of iron with chromium and with silicon and with both elements in combination. The claims put forth for many of these alloys appear to have been made on the basis of meagre information and on researches which appear to be insufficient to justify their widely inclusive claims and ranges.

The iron-chromium-silicon system has been investigated by Denecke (7) by means of melting point arrests and microscopic investigation. This investigator reported the binary eutectic of iron solid solution and FeSi at approximately 20 per cent silicon, and showed a eutectic curve going from the binary point and into the ternary regions. A minimum is shown on the binary iron-chromium melting curve at 14.3 per cent chromium; this point is at about 10 per cent less chromium than the minimum given by several other authors. The minimum is continued as a curve on the ternary melting point surface. Denecke also shows the peritectic reaction on the iron-silicon binary, by which FeSi and Fe solid solution react to form Fe_3Si_2 and alpha solid solution. This reaction is followed far into the ternary regions, and the reaction is said to be promoted by increase in chromium. The approximate position of the alpha solid solubility boundary was shown, without indication of the various abutting phase regions which have been determined in the present work. The characteristic contour of this phase boundary was therefore missed. This undoubtedly was due to the fact that he did not recognize the presence of two phases in addition to Fe_3Si_2 which enter into equilibrium with the alpha phase.

The alloys of iron with silicon have been the object of numerous investigations (8-12). The Engineering Foundation monograph (4) is a summary and critical review of data published before 1933. Jette and Greiner (1) investigated a part of the iron-silicon diagram by means of X-rays. Addition of silicon to iron was found to cause a contraction of the iron lattice constant. Up to about 9 atomic per cent silicon, the contraction amounts to 0.00065 Ångstrom units per atom per cent and above 9 atom per cent, it is 0.00209 Å. per atom per cent. Two straight lines which may intersect in a point, or possibly be connected by a short curved section, according to the authors, fit the experimental data.

Researches on the iron-chromium alloys have been reported by many investigators. Adcock (15) gives a bibliography on the system, from the early investigations of Treitschke and of Tammann

(13), 1907 and up to 1931. R. H. Greaves (30) in his monograph "Chromium Steels" reviews the literature for the entire field up to December 1933. Only such parts of the previous work which are directly concerned in the present investigation will be mentioned here. Kinzel (18) has studied the critical points of iron-chromium alloys by means of a telescopic dilatometer, and found the existence of a gamma loop the widest range of which was at 12.2 per cent chromium, a width which has substantially been checked by Adcock (15) but has been questioned by Hicks (19). Preston (20) investigated the lattice parameters of the iron-chromium system. Iron and chromium form one unbroken series of solid solutions, starting with body-centered iron and ending with body-centered chromium. Additions of chromium expand the iron lattice. A rather flat S-shaped curve results when the lattice constants are plotted as a function of the composition, but portions of the range may be represented by straight lines within the experimental error of the measurements. The connections between the various straight portions may be made by small curved sections similar to the case mentioned under the iron-silicon system. F. Wever and W. Jellinghaus (32) describe the occurrence of a secondary solid solution in the binary iron-chromium system. Neither the range of composition nor of temperature was established with any certainty. This phase occurs in the neighborhood of the composition FeCr and apparently forms from the simple alpha solid solution somewhere between 925 and 1000 degrees Cent. (1700 and 1830 degrees Fahr.) and is stable at the lower temperatures.

The existence of this phase has recently been confirmed by S. Eriksson (33). Apparently the homogeneity range of the secondary solid solution is generally separated from that of the alpha solid solution range by a fairly wide two-phase region. At the high temperature limit between 925 and 1000 degrees Cent. (1700 and 1830 degrees Fahr.) the homogeneous alpha and secondary solid solution fields meet. The two articles disagree as to the extent of the two-phase field. Eriksson claims that he has observed X-ray photogram lines due to the secondary solid solution at chromium contents as low as 30 per cent at 630 degrees Cent. (1165 degrees Fahr.). Wever and Jellinghaus, however, give a diagram showing that the first appearance of this phase as part of a two-phase field, at this temperature, is at about 40 per cent. The structure of this secondary solid solution evidently is very complex. Eriksson hazards the guess that it is either of monoclinic or triclinic symmetry.

The chromium-silicon system was investigated by Frilley (21) by means of density measurements. This investigator inferred the existence of the following compounds: Cr_3Si, Cr_2Si, Cr_3Si_2 and CrSi.

Borén (22) recently investigated the chromium-silicon system by means of X-rays, and found that chromium dissolves up to 8 per cent silicon and forms intermediate compounds Cr_3Si, Cr_3Si_2, CrSi and $CrSi_2$. He does not confirm the existence of Frilley's compound Cr_2Si. Silicon is said probably to dissolve little or no chromium. The structure of the compound Cr_3Si was determined by Borén who ascribes to it a comparatively simple cubic structure. It is, however, entirely different in structure and X-ray diffraction pattern from both alpha-iron and the superstructure in the iron-silicon solid solutions. He further states that Cr_3Si_2 is probably orthorhombic, and CrSi cubic and isomorphic with FeSi. $CrSi_2$ is said to be hexagonal.

The melting point of pure chromium has been the object of numerous investigations, and figures ranging from 1513 to above 1900 degrees Cent. (2755 to above 3450 degrees Fahr.) have been published. The discrepancies have been ascribed to contamination with crucible material, oxygen, carbon and especially nitrogen. Adcock, (15) who determined the complete iron-chromium liquidus, gives the figure of 1830 degrees Cent. (3325 degrees Fahr.) for the melting point of pure chromium as the result of very careful work.

Outline of Experimental Procedure

The experimental work which is recorded and interpreted in the following chapters included the following steps: Melting a number of ternary alloys; annealing of the ingots in order to insure uniform distribution of constituents; chemical analysis of the annealed ingots; preparation of metallic powders; sealing of the powders in evacuated glass or silica tubes; heat treatment and quenching of the tube-enclosed powders; preparation of X-ray specimens from the quenched powders; and the procurement of powder photograms of the crystal structures of their constituent phases; measurements of the photogram lines obtained and calculation of their $\sin^2 \theta$ values and further identification of phases.

Raw Materials

The alloys which were used in the present investigation were

prepared by melting together silicon, electrolytic chromium and carbonyl iron. The silicon was a refined product, supplied through the courtesy of the Electro-Metallurgical Company, New York. Analysis of this metal, reported by the producer, is given in Table I.

Table I
Chemical Analysis of Refined Silicon and Carbonyl Iron

	Silicon Per Cent		Carbonyl Iron Per Cent
Silicon	99.84		0.004
Carbon	0.025		0.007
Iron	0.020		
Aluminum	0.016		
Calcium	0.005		
Manganese	0.001		Trace
Nitrogen	0.006	S	0.004
Oxygen	0.034		
Hydrogen	0.006	P	nil
Total	99.953		

Chromium was likewise supplied by the Electro-Metallurgical Company. It was an electrolytic product from the same lot as that supplied for the work of Jette, Nordstrom, Queneau and Foote on the nickel-chromium system (34). The carbon content of such chromium is below 0.02 per cent and usually runs not much above 0.01 per cent. Chemical tests had previously revealed 0.04 per cent iron and 0.017 per cent sulphur with a trace of silicon, and spectroscopic tests showed no other elements present.

A standard grade of carbonyl iron was bought from the I. G. Farbenindustrie, Oppau Works. The analysis is included in Table I.

Melting Practice and Ingot Treatment

Most of the alloys were melted under vacuum in a high frequency furnace. The charges were accurately weighed out on an analytical balance. The charges usually weighed about 33.3 grams. A few slightly smaller charges were also melted. Alundum crucibles, Norton's # 6457, were used. These invariably showed signs of slight reaction with the charge, presumably due to slagging action of small amounts of oxides known to be present in the raw materials.

The vacuum was controlled by means of a closed end mercury manometer; hydrogen was used repeatedly to flush out the silica tube before the final evacuation. It was often found necessary to raise the temperature of the charge considerably above the apparent melting point of the alloys in order to get the chromium to melt. Occasionally some of the chromium would float on top of the molten metal

Table II
Chemical Analysis of Alloys

Weight Per Cents

Alloy No.	Analysis Cr	Si	Alloy No.	Analysis Cr	Si	Fe
A-1	2.28	0.05	G-33	29.38	5.42	.....
A-2	4.42	0.05	G-34	16.50	2.97	.....
A-3	6.61	....	G-35	28.14	5.11	.....
A-4	8.79	....	B-36	18.03	9.62	.....
A-5	11.81	0.02	B-37	20.67	11.00	.....
B-6	1.01	0.48	G-38	23.93	4.43	.....
B-7	1.74	0.82	C-39	8.38	8.90	.....
B-8	2.54	1.34	C-40	15.58	16.20	.....
B-9	3.58	1.89	C-41	16.63	.....	65.60
B-10	5.59	2.86	G-42	44.76	7.58	.....
B-11	8.36	4.67	C-43	24.02	....	49.45
B-12	11.43	6.08	F-44	2.41	....	76.85
B-13	14.86	6.51	E-45	4.42	....	77.85
B-14	15.83	7.96	D-46	7.40	....	76.53
B-15	19.09	10.80	E-47	2.45	....	88.22
C-16	15.28	15.20	S-48	33.15	....	34.75
B-17	20.16	10.37	49	32.19	4.46	.....
C-18	12.28	12.82	50	22.90	6.28	.....
D-19	7.93	16.83	C-51	6.64	6.58	.....
E-20	6.43	23.15	E-52	4.94	16.02	.....
F-21	2.64	16.16	53	11.71	15.85	.....
E-22	5.15	18.97	54*	35.70	15.30	.....
F-23	3.15	26.53	55*	50.70	15.30	.....
B-26	24.93	14.35	71	48.52	0.086	.....
D-27	4.71	11.57	72	34.21	1.21	.....
E-28	3.72	13.92	73	39.44	1.51	.....
F-29	1.09	15.63	74	44.99	3.96	.....
B-30	21.76	13.15	75	46.76	1.81	.....
B-31	16.86	9.11	76	57.28	1.51	.....
G-32	49.99	9.89				

*Not analyzed.

and dissolve in the melt only after prolonged heating. Chromium readily evaporated under the existing conditions and some was almost invariably lost. Silicon was lost by spattering. During the heating up of the charge the silicon metal, which was in the form of fine grains, would often be thrown upwards, and attach itself firmly to the sides of the crucible and silica tube. The silicon losses were regularly smaller than the chromium losses. The alloys were generally held above the fusion temperature for several minutes after all the metal had dissolved, and allowed to cool in the crucibles.

Table II gives the alloy numbers and the results of the chemical analysis.

The location of the alloys on a triangular co-ordinate system may be seen in Fig. 1. All analyzed alloys are given by their chemical analysis, and indicated in circles of single line. A few alloys which were not analyzed, but prepared by melting together weighed portions of analyzed alloys, are given by the composition of their charges, and indicated in double line circles. The proper alloy numbers have

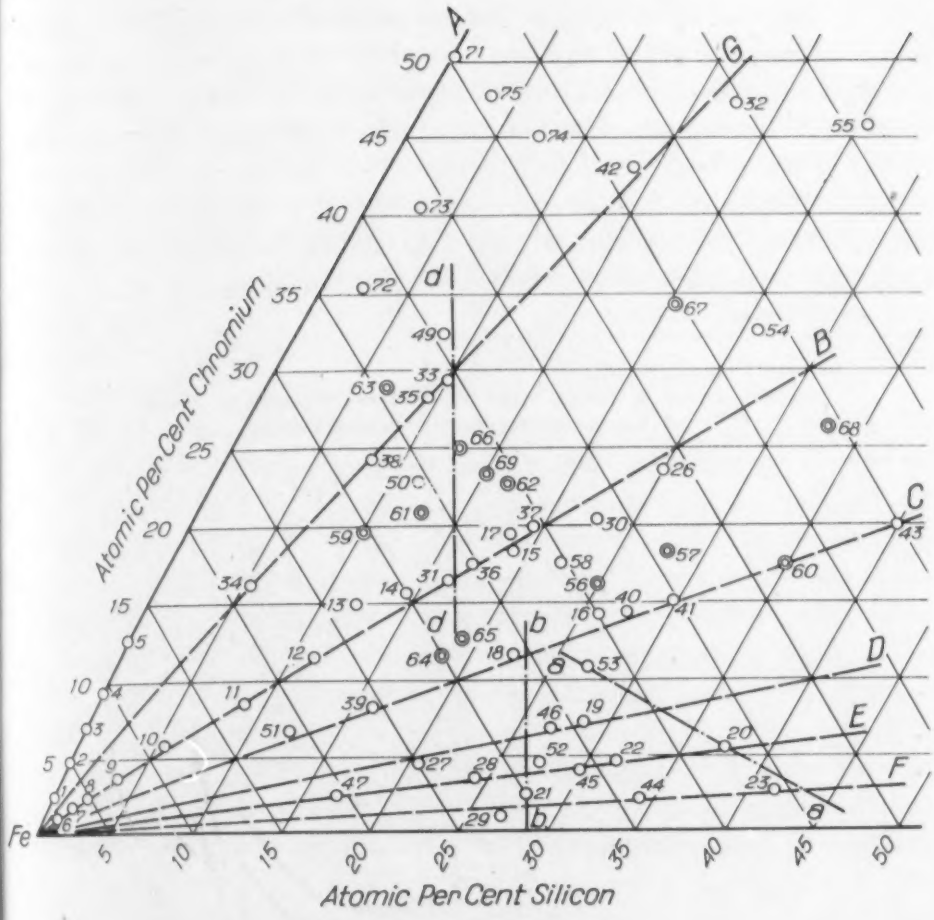

Fig. 1—Alloy Location Diagram.

been placed alongside the indicated alloy compositions. The letters A, B, C, etc., indicate the section lines on which it was aimed to place the alloys.

The alloys which were not analyzed, excepting Nos. 54 and 55, viz., all those indicated by numbers 56 to 69 inclusive, were melted in $\frac{3}{16}$-inch bore evacuated silica tubes in a gas-oxygen blast lamp. The charges for these alloys were made up from weighed portions of pairs, and in a single instance three, of the analyzed alloys. Their computed gross compositions are given in Table III. The temperature of the flame was raised until the silica tubes would collapse around the charges, and the tubes were heated at this temperature for three or four minutes and cooled slowly during about ten minutes. It was possible to obtain one continuous ingot in nearly every instance. Failing in this the ingot was discarded and a new charge made up.

In the cast condition the ingots possessed rough dark colored surface films where the ingot had touched the crucible. The top of the ingots usually had smooth, transparent oxide films. These were removed by grinding. The annealing was done in an evacuated and sealed silica tube about ¾ inch bore. All heating was performed in nichrome-wound resistance furnaces, which were brought up to 1000 degrees Cent. (1830 degrees Fahr.) and held for one week, whereupon they were allowed to cool down with their contents.

Table III

Compositions of Alloys Made by Melting Mixtures of Alloys of Known Composition in Sealed Tubes

Alloy No.	Composition Weight Per Cent		
	Per Cent Fe	Per Cent Cr	Per Cent Si
56	68.04	17.44	14.52
57	63.65	19.95	16.40
58	68.70	18.62	12.68
59	75.13	19.40	5.47
60	57.65	20.47	21.78
61	72.00	20.98	7.02
62	66.77	23.90	9.33
63	67.84	28.43	3.68
64	77.75	11.96	10.29
65	76.27	13.08	10.65
66	67.85	25.00	7.15
67	51.75	36.45	11.80
68*	45.6	28.4	26.0
69	61.52	23.36	15.12

*Approximate.

Chemical Analysis

After the anneal, the ingots showed more or less discolored surfaces, generally greenish. These surface films were removed by grinding. From those ingots which were machinable, turnings were obtained, while those which were not, were broken up and a portion for analysis was crushed. Crushing was done in a steel mortar, followed by grinding in an agate mortar to 100 mesh.

The large majority of the alloys were analyzed for chromium and silicon, and a few determinations of iron were made.

Hydrochloric acid would readily dissolve all but a few of the alloys; a few could be dissolved only after prolonged boiling with concentrated hydrochloric acid. Generally the higher the amount of alloying elements the less easily could the alloys be dissolved. More trouble was caused by high silicon than by high chromium content. Alloy No. 42 which corresponds nearly to the composition Cr_3Fe_3Si went into solution with extraordinary rapidity in finely powdered

form when warm concentrated hydrochloric acid was poured over it. This is the more remarkable since subsequently it was found that neither concentrated hydrochloric acid nor aqua regia would etch a polished surface of the same specimen, and this had to be accomplished by means of a mixture containing hydrofluoric acid. Sulphuric acid could be used to bring those alloys containing the lesser amounts of alloying elements into solution, while nitric acid even in mixtures with other acids showed a strong tendency to render the alloys passive. A few alloys were dissolved in hydrochloric acid mixed with a smaller portion of hydrofluoric acid; no silicon determinations, of course, were made on such solutions.

Silicon was determined by the sulphuric acid evaporation method described by Lundell, Hoffman and Bright (23) and by Hillebrand and Lundell (24). Chromium was determined by the ferrous sulphate—permanganate titration method, after oxidation of the chromium solutions by ammonium persulphate, described by the same authors. Determinations on three samples were made by two different analysts, giving a check on the general method of analysis for these elements. The results of all these determinations are given in Table II. Carbon determinations by the total combustion method were made on four samples, one of which was a mixture of portions from all samples except the other three analyzed. These determinations are due to the courtesy of the Union Carbon and Carbide Research Laboratories, Inc. The results are given in Table IV. Mr. Walter Crafts who reported these results states that they are based on single determinations on 10 factor weights.

Table IV

Carbon Analysis on Alloys

Sample	Carbon Per Cent
G-35	0.011
G-38	0.018
D-39	0.010
Composite	0.014

Powders for X-ray Exposures

Those alloys which could be reduced by crushing were reduced to 200 mesh in an agate mortar. Two to three gram portions were taken from each of the previously mentioned 100-mesh samples also used for chemical analysis. Alloys which were too tough to be

crushed were ground down on small alundum wheels. The metal dust obtained was magnetically separated from admixtures of impurities from the grinding wheel. About 90 per cent of this powdered metal could be passed through a 200-mesh screen, and the bulk of the remaining 10 per cent went through a 100-mesh screen.

As needed, small portions of these samples were sealed up in evacuated tubes of ⅛ to ¼ inch bore. Silica tubes were used for treatment temperatures exceeding 800 degrees Cent. (1470 degrees Fahr.), Jena glass for powders treated between 600 and 800 degrees Cent. (1110 and 1470 degrees Fahr.), and Pyrex glass for powders at lower temperatures.

The sealed up powders were heated in a vertical nichrome-wound resistance furnace, the arrangement of which has previously been described.[2]

This type of furnace and the technique used provides a practically instantaneous quench. In order to secure a reasonable approach to equilibrium at the lower temperatures, the alloys were heated to at least 800 degrees Cent. (1470 degrees Fahr.), furnace cooled to the desired temperature, and retained at this point for sixteen to forty-eight hours. The powders were pasted on paper strips by means of Duco-cement in as thin and even layers as possible.

A special thermocouple was built and standardized for use with the quenching furnace. It was checked at four points against a U.S. B.ofS. thermocouple. The checking was repeated after the completion of the whole series of heat treatments; it was found that the temperature—e.m.f. relation had remained virtually unchanged.

X-ray Apparatus and Technique

The powder method was employed. All but a few of the exposures were taken in focussing cameras designed by Phragmén. A description of this type of camera was recently given by Westgren (2). These cameras were calibrated with a number of pure metals using lattice constant data determined by Owen and Yates (35). The results of these authors have been closely checked by investigations recently reported from this laboratory. [See Jette and Foote (36).] Part of the work was done with a Siegbahn tube and part with tubes designed by M. W. Cohen (31). With the Siegbahn tube the exposure times were generally seven to eight hours in the inner

[2]Ref. (34) page 373.

and outer range cameras and three hours in the middle range camera. With the Cohen tube, the times were respectively three and two hours. However, some powders, particularly of alloys 49 and 50, required longer exposures. Both iron and chromium radiation $K\alpha_1$, $K\alpha_2$ and $K\beta$ were used. The wave lengths employed were those given by Siegbahn in 1933; for Cr, $K\alpha_1 = 2.28503$, $K\alpha_2 = 2.28891$, $K\beta = 2.08060$, and for Fe, $K\alpha_1 = 1.932076$, $K\alpha_2 = 1.936012$, $K\beta = 1.753013$. On alloys high in chromium content, iron radiation

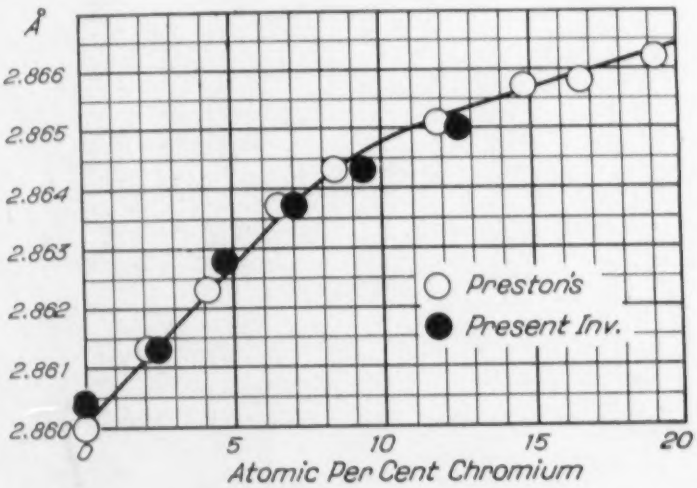

Fig. 2—Iron-Chromium System; Lattice Parameters Versus Composition, Angstrom Units Versus Atom Per Cent Chromium.

produced poor reflection lines due to the proximity of the wave lengths of iron radiation to the absorption edges of chromium. The reflecting crystal planes for iron radiation $K\alpha_{1,2}$ were the (220) planes and for $K\beta$ the (310) planes; with chromium radiation the reflecting planes were the (211) planes for all three wave lengths.

In Table V the results of the film measurements in the form of values for a_0 for those alloys which yielded lines of the alpha phase are recorded, together with the composition in terms of atomic per cent. They are arranged in consecutive order of alloy numbers. The values given are average values of lattice parameters computed from the outer two or three lines of films exposed in the outer camera. In many cases the figures given are the results from several films, the individual values of which have been averaged. In a few cases these averages are based on exposures of individual samples separately heat treated for various lengths of time. All lattice parameters are stated in Ångstrom units, (1 Å = 10^{-8}cm.). The Roman

Table V

Experimental Results

Alloy No.	Composition At. Per Cent Fe	Composition At. Per Cent Cr	Composition At. Per Cent Si	Lattice Parameter a_0; A	Quenching Temperature	Phase Region
A-1	97.46	2.44	0.10	2.8613	600	I
A-2	95.17	4.73	0.10	2.8628	600	I
A-3	92.84	7.06	0.10	2.8637	600	I
A-4	90.52	9.38	0.10	2.8643	600	I
A-5	87.35	12.60	0.05	2.8650	600	I
B-6	97.97	1.08	0.95	2.8603	600	I
B-7	96.56	1.85	1.95	2.8604	600	I
B-8	95.31	2.37	2.32	2.8595	600	I
B-9	92.61	3.76	3.63	2.8594	600	I
B-10	88.68	5.81	5.51	2.8589	600	I
B-11	82.64	8.53	8.83	2.8561	1000	I
B-12	77.19	11.48	11.33	2.8524	1000	I
"	.....	.....	.....	2.8533	600	I
B-13	73.10	14.83	12.07	2.8526	1000	I
"	.....	.....	.....	2.8522	580	II
B-14	69.92	15.59	14.49	2.8481	950	I
"	.....	.....	.....	2.8475	800	II
"	.....	.....	.....	2.8442	600	II
"	.....	.....	.....	2.8437	450	II
B-15	62.55	18.28	19.17	2.8385	1000	II
"	.....	.....	.....	2.8372	806	II
C-16	59.84	14.12	26.04	2.8259	1000	VIII
"	.....	.....	.....	2.8261	800	VII
"	.....	.....	.....	2.8226	600	VII
"	.....	.....	.....	2.8225	540	VII
"	.....	.....	.....	2.8212	450	VII
B-17	62.17	19.37	18.46	2.8391	1000	II
"	.....	.....	.....	2.8375	803	II
"	.....	.....	.....	2.8361	605	II
C-18	65.93	11.61	22.46	2.8312	1002	I
"	.....	.....	.....	2.8315	580	I
D-19	64.17	7.26	28.57	2.8192	1010	II
"	.....	.....	.....	2.8216	800	II
"	.....	.....	.....	2.8226	600	II
"	.....	.....	.....	2.8223	450	II
E-20	57.10	5.57	37.33	.....	...	VIII
F-21	69.88	2.44	27.68	2.8162	1004	VIII
"	.....	.....	.....	2.8185	800	VIII
"	.....	.....	.....	2.8182	800	VIII
"	.....	.....	.....	2.8192	450	VIII
E-22	63.67	4.64	31.69	2.8168	997	VIII
"	.....	.....	.....	2.8188	800	VIII
"	.....	.....	.....	2.8200	600	VIII
"	.....	.....	.....	2.8200	450	VIII
F-23	55.75	2.68	41.57	.....	997	X
Y-24	0.0	22.50	77.50	.....	992	binary
Y-25	0.0	50.00	50.00	.....	994	binary
B-26	51.49	23.47	25.04	2.8299	996	VI
"	.....	.....	.....	2.8289	806	VI
"	.....	.....	.....	2.8267	603	VI
D-27	74.88	4.53	20.59	2.8321	997	I
E-28	72.18	3.54	24.28	2.8243	996	I
F-29	72.07	1.01	26.92	2.8185	996	I
B-30	56.77	20.39	22.84	2.8326	994	II
"	.....	.....	.....	2.8326	805	VI
"	.....	.....	.....	2.8294	605	VI
B-31	67.13	16.43	16.44	2.8441	1000	II
"	.....	.....	.....	2.8413	800	II
"	.....	.....	.....	2.8417	642	II
"	.....	.....	.....	2.8407	600	II
"	.....	.....	.....	2.8411	450	II
G-32	35.36	47.29	17.35	.....	...	IV
G-33	60.55	29.35	10.10	2.8569	1000	II
"	.....	.....	.....	2.8574	800	II
"	.....	.....	.....	2.8579	600	II
G-34	78.35	16.23	5.42	2.8602	1000	I
G-35	62.30	28.20	9.50	2.8598	1000	II

Table V (continued)

Alloy No.	Composition At. Per Cent Fe	Composition At. Per Cent Cr	Composition At. Per Cent Si	Lattice Parameter a_0; A	Quenching Temperature	Phase Region
G-35	62.30	28.20	9.50	2.8577	793	II
"	.....	.....	.....	2.8581	600	II
B-36	65.24	17.48	17.28	.....	...	..
"	.....	.....	.....	2.8456	990	II
"	.....	.....	.....	2.8404	812	II
"	.....	.....	.....	2.8394	642	II
B-37	60.62	19.91	19.47	2.8379	990	II
"	.....	.....	.....	2.8355	803	II
"	.....	.....	.....	2.8346	600	II
"	.....	.....	.....	2.8344	450	II
G-38	67.45	24.25	8.35	2.8590	1000	I
"	.....	.....	.....	2.8586	807	II
"	.....	.....	.....	2.8590	580	II
C-39	75.60	8.22	16.18	2.8423	1000	I
C-40	58.21	14.28	27.51	2.8253	985	VIII
"	.....	.....	.....	2.8274	1000	VIII
"	.....	.....	.....	2.8242	964	VIII
"	.....	.....	.....	2.8257	797	VII
"	.....	.....	.....	2.8239	588	VII
"	.....	.....	.....	2.8223	540	VII
C-41	55.22	15.00	29.77	2.8251	1000	VIII
"	.....	.....	.....	2.8257	797	VII
"	.....	.....	.....	2.8229	588	VII
"	.....	.....	.....	2.8226	450	VII
G-42	43.37	43.01	13.62	.....	800	XI
C-43	Fe2	Cr	Si2	.....	800	XII
F-44	63.66	2.15	34.19	2.8143	985	VIII
"	.....	.....	.....	2.8168	800	VIII
"	.....	.....	.....	2.8191	600	VIII
"	.....	.....	.....	2.8180	450	VIII
E-45	66.03	4.03	29.94	2.8170	985	VIII
"	.....	.....	.....	2.8187	795	VIII
"	.....	.....	.....	2.8200	600	VIII
"	.....	.....	.....	2.8202	450	VIII
D-46	66.24	6.84	26.92	2.8217	985	VIII
"	.....	.....	.....	2.8221	800	VIII
"	.....	.....	.....	2.8230	600	VIII
"	.....	.....	.....	2.8222	450	VIII
E-47	80.60	2.40	17.00	2.8393	800	I
48	Fe	Cr	Si2	.....	800	XIII
49	59.33	32.36	8.3	2.8608	975	II
"	.....	.....	.....	2.8600	900	II
"	.....	.....	.....	2.8605	797	II
"	.....	.....	.....	2.8601	592	II
"	.....	.....	.....	2.8596	450	II
50	65.64	22.78	11.58	2.8541	1000	II
"	.....	.....	.....	2.8545	900	II
"	.....	.....	.....	2.8538	797	II
"	.....	.....	.....	2.8539	600	II
"	.....	.....	.....	2.8544	450	II
C-51	81.12	6.66	12.22	2.8500	900	II
E-52	68.01	4.56	27.43	2.8198	985	VIII
"	.....	.....	.....	2.8200	818	VIII
"	.....	.....	.....	2.8208	600	VIII
"	.....	.....	.....	2.8206	450	VIII
53	62.16	10.78	27.06	2.8245	986	VIII
"	.....	.....	.....	2.8242	818	VIII
"	.....	.....	.....	2.8249	600	VII
"	.....	.....	.....	2.8248	450	VII
54	41.60	32.54	25.85	2.8301	800	VI
55	28.60	45.79	25.61	2.8303	800	VI
56	58.83	16.19	24.98	2.8275	997	I
"	.....	.....	.....	2.8258	600	VI
57	54.08	18.20	27.72	2.8271	998	VIII
"	.....	.....	.....	2.8240	594	VII
58	60.30	17.55	22.15	2.8345	988	II
"	.....	.....	.....	2.8319	600	VI
59	69.17	16.15	14.68	2.8541	993	I

Table V (continued)

Alloy No.	Composition At. Per Cent Fe	At. Per Cent Cr	At. Per Cent Si	Lattice Parameter a_0; A	Quenching Temperature	Phase Region
59	69.17	16.15	14.68	2.8559	808	II
"	.....	.....	.....	2.8546	600	II
60	47.60	17.50	34.90	.....	991	XIII
61	66.34	20.76	12.90	2.8526	998	II
"	.....	.....	.....	2.8524	800	II
"	.....	.....	.....	2.8529	596	II
62	60.15	23.12	16.73	2.8406	1000	II
"	.....	.....	.....	2.8391	795	II
"	.....	.....	.....	2.8371	595	II
63	64.19	28.88	6.93	2.8613	988	I
"	.....	.....	.....	2.8611	808	II
"	.....	.....	.....	2.8607	600	II
64	70.00	11.56	18.44	2.8378	1010	I
"	.....	.....	.....	2.8377	826	I
"	.....	.....	.....	2.8385	621	I
65	68.40	12.60	19.00	2.8382	1010	I
"	.....	.....	.....	2.8385	820	I
"	.....	.....	.....	2.8385	621	II
66	62.30	25.00	12.70	2.8536	1000	II
"	.....	.....	.....	2.8535	795	II
"	.....	.....	.....	2.8539	595	II
67	45.25	34.25	20.50	2.8353	975	V
"	.....	.....	.....	2.8339	807	V
"	.....	.....	.....	2.8348	620	V
68	41.25	26.25	32.50	2.8279	975	VII
69	61.50	23.40	15.10	2.8488	975	II
"	.....	.....	.....	2.8485	802	II
71	49.58	50.25	0.17	2.8694	1032	I
"	.....	.....	.....	.....	775	II*
72	62.27	35.41	2.32	.....	975	I
"	.....	.....	.....	2.8663	755	II
73	56.56	40.56	2.88	.....	1000	II
"	.....	.....	.....	.....	775	XI
74	47.61	45.04	7.35	.....	1032	XI
"	.....	.....	.....	.....	768	XI
75	48.87	47.71	3.42	2.8665	1000	I
"	.....	.....	.....	.....	768	XI
76	38.98	58.17	2.85	2.8697	1000	I
"	.....	.....	.....	.....	770	II

*Probably not in equilibrium.

numbers in the last row of the table indicate the phase fields in which the alloys are located on the diagrams, Figs. 14 and 15.

In order to compare the lattice parameter measurements of this work with those of Preston in his investigation of the iron-chromium binary (20) six alloys of this binary series were made, analyzed and their parameters measured. In Fig. 7 the results of five of these determinations and the corresponding ones of Preston have been plotted on the same diagram. Preston's results appear on the plot as open circles. It may be seen that the two sets of values agree within the accuracy of the experiment, which may be stated to be $\pm$ 0.0005 Å. The sixth result is for alloy 71, for which the lattice constant is 2.8694, while Preston's curve gives the same value.

The Gamma Region

Alloys Nos. 1-9 were quenched from above 1000 degrees Cent. (1830 degrees Fahr.). Photogram lines of these powders were indistinct and broad. Quenched from 600 degrees Cent. (1110 degrees Fahr.) their lines were sharp. This undoubtedly was due to the well known effect of the gamma-alpha transformation, which it has been found impossible to arrest by quenching in many ferrous alloys. It was estimated that the boundary line of the stability field of the gamma phase at 1000 degrees Cent. (1830 degrees Fahr.) passes near alloy No. 9. On the diagram of Fig. 12, this line has been shown in dashes. The endpoint on the iron-chromium binary is taken from the work of Kinzel (18) and that on the iron-silicon binary from Wever and Giani (25). This ternary boundary is obviously only a rough estimate.

Variation of Lattice Parameters with Composition in the Alpha Solid Solution Region

A plot giving the relations between the atom per cent iron and the measured lattice parameters in the alpha phase region is reproduced in Fig. 3. The iron-silicon binary of Jette and Greiner (1) and the iron-chromium binary of Preston (20) have been plotted together with five sections obtained in the present investigation; the

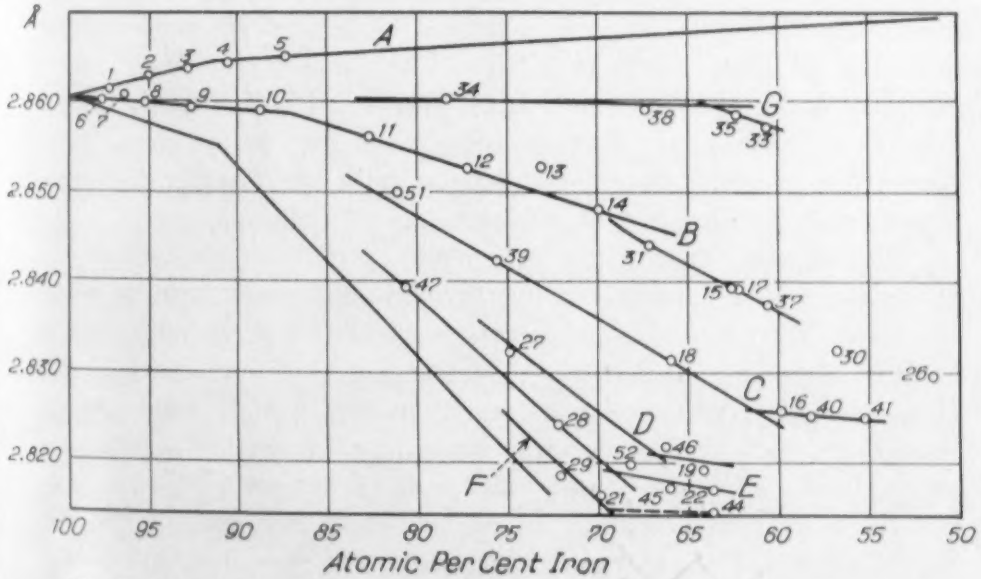

Fig. 3—Lattice Parameters, Alpha Solid Solution Range; Angstrom Units Versus Atom Per Cent Iron.

experimental results on which the latter are based are given in Table V. From the plot it may be seen that these relations correspond nearly with straight lines. The section marked B shows a similar break or bend as those previously noted for each of the two binaries. There are not sufficient alloy points on sections F and D for laying down the sections, and these have been found by interpolation from Figs. 9 and 10. It will be noted from the location diagram, Fig. 6, that many of the alloys are off the section lines by considerable distances. These five sections are, therefore, not suited for direct location of the phase boundaries.

Fig. 4 shows sections of constant atom per cent of iron drawn through each of the alloy compositions of the solid solution range. In the preparation of these sections use was made of an auxilliary plane, the trace of which is marked B on the location diagram, Fig. 1, and on Fig. 4. The perpendicular distances of each alloy from this trace was measured on Fig 1. These distances were laid out perpendicularly from the line B on the diagram, Fig. 4, and each distance was marked by a point and annotated with its proper alloy number. Through each of these points lines were drawn parallel to B. The lattice parameters of the various alloys were then taken from Table V and marked on these parallels as ordinates.

Each of the lines which were drawn perpendicular to B through any alloy on Fig. 1, represents a trace of a section of constant iron content. These traces were produced until they intersected the iron-chromium binary and the iron-silicon binary. The perpendicular distances of these intersections from the line B on Fig. 1 were similarly laid out from B on Fig. 4, and parallels to B were drawn. The lattice parameters corresponding to these binary points were read from Preston's diagram and from Jette and Greiner's diagram respectively, and marked on the parallels as ordinates.

In this way, three points were generally obtained on each section of constant iron content passing through any given ternary alloy. On some sections additional points were obtained by interpolation between alloys on the sections shown in Fig. 3. The points on any given section of constant iron content in Fig. 4 were connected by smooth curves. Each curve was made to conform to the shape of its neighbors, so that none of them would intersect.

As a final step, a diagram of horizontal sections, or isoparametric curves of the parametric surface, was prepared and this is reproduced in Fig. 5. The process of preparing the latter diagram

was as follows: The trace B was drawn in on Fig. 5 and the constant iron sections passing through each alloy were marked on lines perpendicular to B. It is seen that on diagram 4 any chosen lattice parameter intersects the various constant iron sections[3] at distances which may be measured out from trace B. By actually measuring these distances and laying them out on diagram 5 from the trace B on their proper constant iron sections, a number of points of identical lattice parameters and varying compositions were obtained.

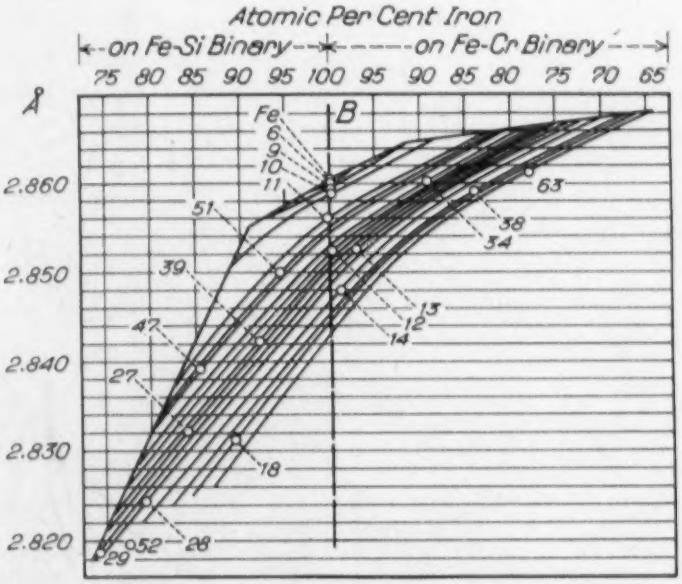

Fig. 4—Parametric Surface; Stage in Development. Sections of Constant Iron Content. Angstrom Units Versus (Atom Per Cent Cr) + (Atom Per Cent Si).

These points were then connected by a smooth curve and yielded an isoparametric curve. Such isoparametric curves were laid down spaced 0.001 Å apart. The process had to be repeated for each isoparametric curve. Figs. 3 and 4 show diagrams which essentially are stages in preparation for the final diagram of isoparametric curves shown in Fig. 5. Sections from these preliminary stages will therefore not be used in any subsequent work, but new sections obtained from the final diagram, Fig. 5, are to be employed. It may be noted that all the measured parameters fall within the experimental error of 0.0005 Å in their appropriate places with reference to the isoparametric curves shown on the diagram.

[3]Each curve represents an intersection between the parametric surface and a vertical section at constant iron content.

Variation of Lattice Parameters with Quenching Temperature

It has been mentioned that lattice parameters are functions of temperature measurable in terms of the coefficients of expansion of the phases under consideration.[4] In the present section, however, we are not concerned with this kind of temperature variation; all the lattice parameter measurements used were measured at substan-

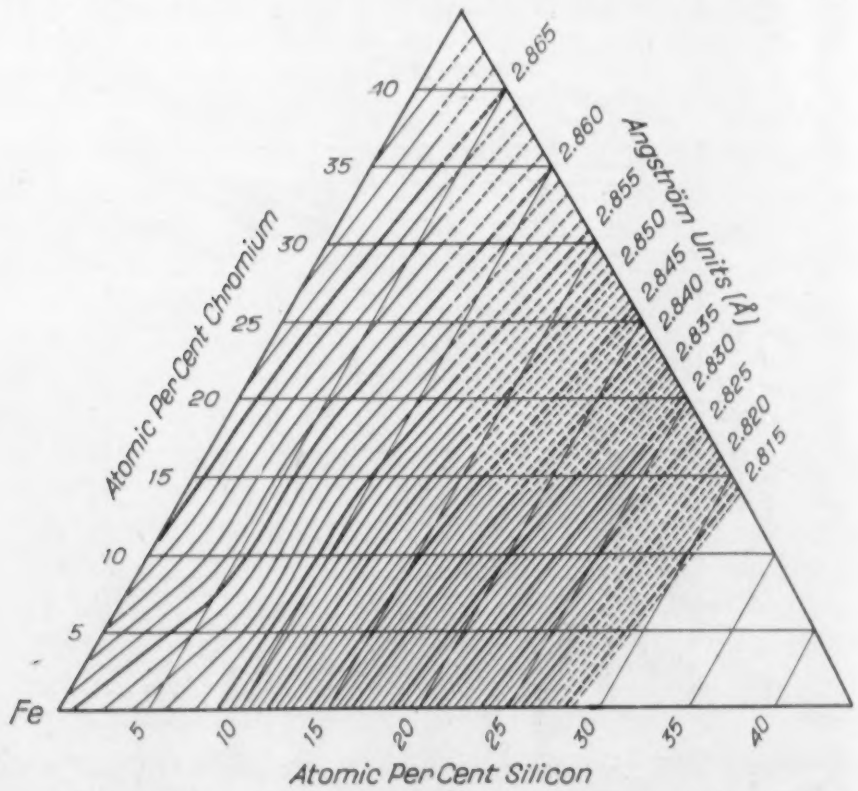

Fig. 5—Parametric Surface; Isoparametric Curves in the Alpha Solid Solution Region; Room Temperature; Atom Per Cent.

tially the same temperature, i.e., room temperature. The variations here considered are due to the changes in the compositions of the phases of the system with temperatures of quenching and are, under proper conditions, essentially a measure of these changes in compositions. In the following diagrams (Figs. 6 and 7) the variation with quenching temperature of lattice parameters in the three two-phase regions which have been found in this system is illustrated.

The abscissae give the lattice parameters in Ångstrom units, and the ordinates indicate the exact temperatures of heat treatment

[4]See also Reference 37.

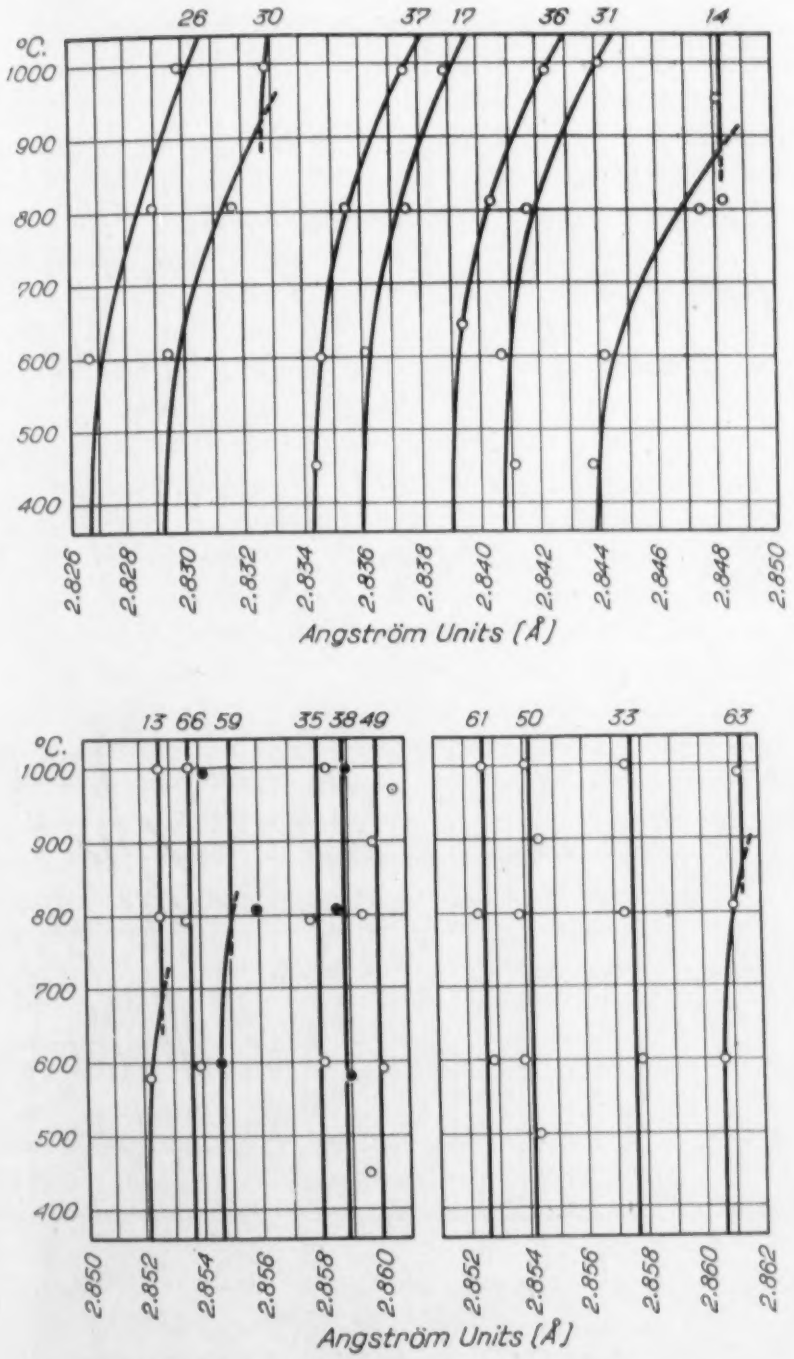

Fig. 6—Lattice Parameters Versus Quenching Temperature; Regions II and VI. Angstrom Units Versus Degrees Centigrade.

as measured from time to time and immediately before quenching. Four temperature levels, viz. 1000, 800, 600 and 450 degrees Cent.

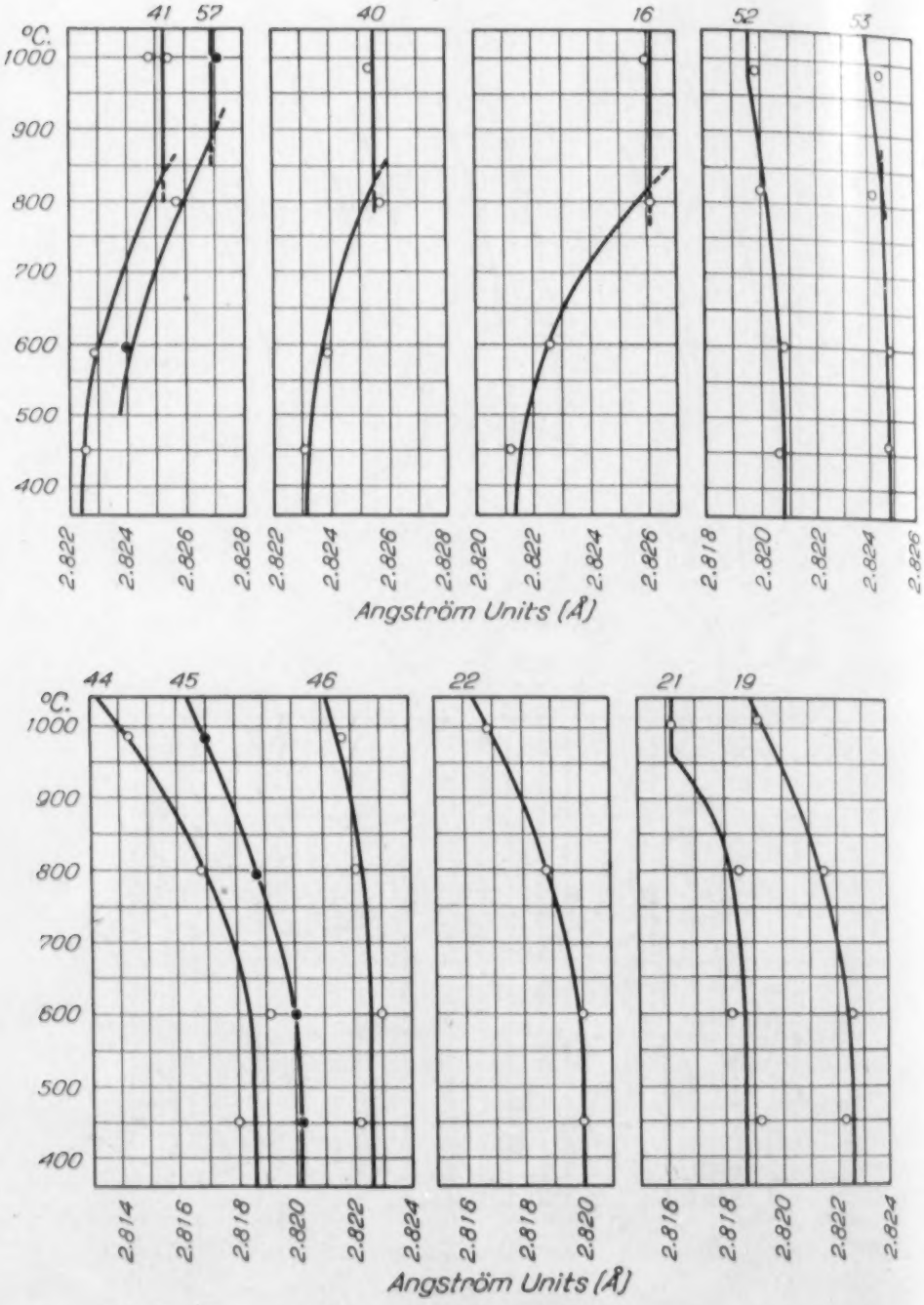

Fig. 7—Lattice Parameters Versus Quenching Temperature; Region VIII. Angstrom Units Versus Degree Centigrade.

(1830, 1470, 1110, 840 degrees Fahr.), were those generally employed. The figure at the head of each curve indicates the number of the alloy to which the data applies.

The curves have been drawn in between the plotted points in such a manner that alloys which at the temperatures employed remain continuously within one of the phase regions are represented by continuous curves, while those which exist in different phase regions at different temperatures are represented by two intersecting curves, each of which corresponds to a separate phase region. To accomplish this it was necessary not only to measure the lattice parameters of the alpha phase, but also to identify each of the phases appearing on the various films. This at times required the use of the middle and inner range cameras where the most characteristic lines of the individual phases occur.

Reference to the diagrams shows that practically all of the points fall within 0.0005 Å. of the curves. This consistency of the results may be taken as an indication that a reasonable approximation to equilibrium conditions has been reached. This is further borne out by the fact that powders which were given a long time anneal before quenching check well with those given a short time anneal.

It may also be seen that though the measured parameters at 600 and 450 degrees Cent. (1110 and 840 degrees Fahr.) agree in size within 0.0005 Å., there is a distinct trend in many of the curves at the lower temperatures.

Three separate two-phase regions yielding lines of the alpha phase have been found; it will be convenient to observe their locations on diagrams 14 and 15 and their notations: II, VI, and VIII.

The Alpha Plus Sigma Region

This is the region annotated II on diagrams 14 and 15. The composition of the secondary phase, sigma, will later be shown to be variable. It is a solid solution, based on the binary phase FeCr of Wever and Jellinghaus, (32), and in the ternary system it contains silicon over a fairly wide range of compositions. The range of composition over which the sigma phase is homogeneous has not been determined accurately.

Alloys No. 13, 14, 59 and 63 yield films showing one phase at higher temperatures and two at lower temperatures. The parameters vary with the quenching temperature in such a manner that each may be represented by a plot having a vertical portion in the higher temperature range and a curve below this range. The vertical portions correspond to the lattice parameters of the single-phase region, invariant with quenching temperatures. Alloys No. 17, 31, 36 and

37 all yielded films showing two phases at all temperatures employed. They are all represented by curves having approximately the same curvature, showing a trend of gradually decreasing parameters with decreasing quenching temperatures.

Alloys No. 33, 35, 38, 49, 50, 61 and 66 all yield lines of two phases, but their lattice parameters show no variations exceeding the experimental error of ± 0.0005 Å., with the quenching temperatures. The plots have consequently been drawn in as straight lines; these, however, do not indicate constant solubility with varying quenching temperatures, as will be shown later. The possibility of such cases occurring has been discussed in another article. (Ref. 37).

Alloys No. 14 and 59 show altogether three plotted points lying off the curves with a distance larger than the experimental error of 0.0005 Å.; this, however, need not be disturbing among such a large number of measurements. The probable error on the respective curves is less than 0.001 Å., and on the interpolation and averaging processes to be described later, the effect of these somewhat large deviations will be negligible.

The Alpha Plus $(Fe,Cr)_3 Si_2$ Region

This region has been annotated VIII on the diagrams of figures 14 and 15. Photograms of alloys No. 19, 22, 44, 45 and 46 indicate that they lie within the two-phase region at all temperature levels. All show distinctly the lines of both phases. The curves representing the relation between lattice parameters have, therefore, been drawn in as continuous ones. It may be seen from the plots that the experimental points are distributed about the curves with deviations well within the experimental error.

It may be mentioned here that the films which show the lines of the compound which later will be identified as $(Fe,Cr)_3Si_2$ also give more or less distinct lines of a structure identical with the FeSi structure described by Phragmén (12).

We have here three phases, one of which at least has a composition which varies with the gross composition of the alloy. As the third compound is very persistent and cannot be brought to disappear by any reasonable time of anneal the conclusion must be made that we have not reached equilibrium. Since diagrams 14 and 15 will be used for the determination of phase boundary lines in the following, it may be noted that the third phase disappears more and more completely as the composition of the alloys approaches the phase

boundary. Its presence will, therefore, not affect the location of the phase boundary by a measurable amount.

At 1000 degrees Cent. (1830 degrees Fahr.) alloys No. 21 and 52 show lines of the alpha phase region alone. At the lower temperature levels lines of the secondary phase also appear. This would indicate that these alloys consist of one phase at 1000 degrees Cent. (1830 degrees Fahr.) and of two phases at lower temperatures.

Alloys No. 16, 40, 41 and 57 show at 1000 degrees Cent. (1830 degrees Fahr.) photogram lines of the alpha phase and the $(Fe,Cr)_3Si_2$ phase. At lower temperatures a third phase, which at first it was thought might be the FeSi structure discussed above, was found to be present. It was noticed, however, that the first seven alloys, 19, 21, etc., yielded parameters which unmistakably increased with decreasing quenching temperatures, whereas the latter four, Nos. 16, 40, etc., decreased with decreasing temperatures. It was further noticed that alloy No. 16 yielded lattice parameters at 600 and 450 degrees Cent. (1110 and 840 degrees Fahr.) which were lower than that of the isoparametric line of the alpha phase region which passes through the point indicating the composition of No. 16. The observed inclination of the parametric surface is such that the parameters increase with increasing iron content, as shown on the diagrams of Fig. 5, and, therefore, the observed low values of the parameters of No. 16 could not be possible in the two-phase region. Close scrutiny of the films, however, revealed that the lines from the third phase in alloys No. 16, 40, 41 and 57 were not identical with those of the FeSi structure previously found in the alloys 19, 21, 44, etc. Later, these new lines were found also in alloys No. 26, 30, 54 and 55, and finally, they were identified from Borén's published data (22) as belonging to the compound Cr_3Si.

The phase region in which these four alloys occur below 800 degrees Cent. (1470 degrees Fahr.) is, therefore, a three-phase region composed of alpha solid solution, the $(Cr,Fe)_3Si_2$ phase and the compound Cr_3Si. At 1000 degrees Cent. (1830 degrees Fahr.) only the two former phases are present. The curves have, therefore, been drawn in with a vertical portion, representing the parameters of the two-phase region with no noticeable change in size at high temperature and a curved portion representing the lattice parameters at lower temperatures in the three-phase region. From data presented in a later section, it may be seen that alloy No. 53 falls within the two-phase area at 1000 degrees Cent. (1830 degrees Fahr.), but only

slightly below this temperature it passes into the three-phase region. It is, therefore, also represented by discontinuous curves.

Alloy No. 26 gives lines of two phases throughout the temperature range, viz., the alpha solid solution and the compound of the Cr_3Si structure; its lattice parameters are therefore represented by one continuous curve (Fig. 6). Alloy No. 30 (Fig. 6) shows the alpha solid solution and the sigma structure at 1000 degrees Cent. (1830 degrees Fahr.); at lower temperatures it shows the structures of the alpha phase and the Cr_3Si phase. The lattice parameter versus temperature relation for this alloy has consequently been drawn in as two intersecting curves. Alloy No. 58 for which no parameter measurement at 800 degrees Cent. (1470 degrees Fahr.) was obtained has not been plotted; it is, however, similar to alloy No. 30.

Location of the Phase-Boundary of the Alpha Plus $(Fe,Cr)_3Si_2$ Region

The two-phase region which is dealt with in the present section is that marked VIII on the diagrams 14 and 15. The general method employed consists in finding the intersection of the two parametric surfaces over the abutting phase regions, essentially as described in another article (Ref. 37). A number of sections of constant chromium content were chosen so that each one would pass through as many of the location points of alloys in the two-phase region as possible. These were chosen without regard to single-phase alloy location points, since sections of the parametric surface in the single-phase region could be obtained from the diagram shown in Fig. 5. As the alloy location points were not available close enough to any sections that could be chosen, interpolations had to be resorted to. This was done by a method similar to that used for determining the parametric surface of the alpha phase region as shown in figures 3, 4 and 5. Sections of constant silicon content were passed through each of the alloy location points in the two-phase region as shown in Figs. 8b, d, f, and interpolated values of lattice parameters from these sections were then used for drawing up the constant chromium sections, Figs. 8a, c and e. This method was employed for three temperature levels in each of the two major two-phase regions. A detailed description will be given for the 1000 degrees Cent. (1830 degrees Fahr.) level in the phase regions at present under consideration. It is important to note that all the diagrams employed for the

determinations of the solid solubility limits were laid out to exactly the same scales with respect to composition and to lattice parameters, respectively. The scales used were 0.01 Å = 50 mm and 1 atom per cent = 10 mm.

Referring to the location diagram, Fig. 1, lines were passed through each two-phase alloy location point parallel to the iron-chromium binary line until they intersected the reference line marked

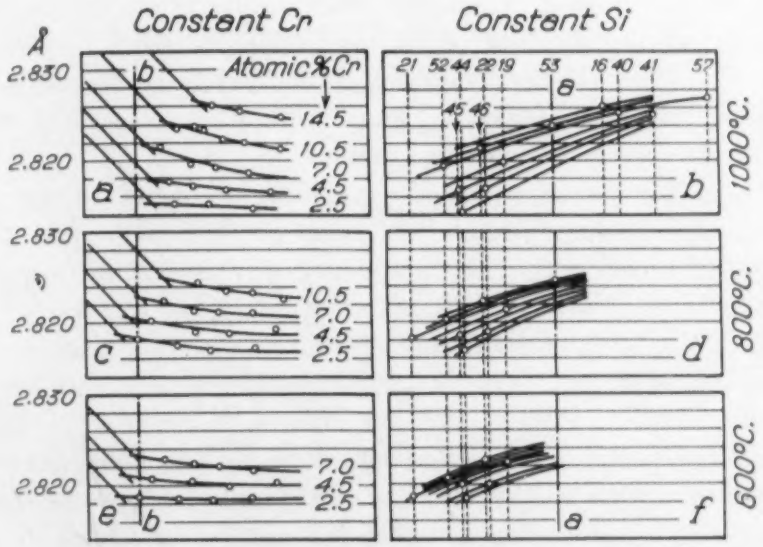

Fig. 8—Lattice Parameters Versus Composition in the (Alpha Plus $(Fe,Cr)_3Si_2$) Region. Angstrom Units Versus Atom Per Cent.

(a) Section of Constant Chromium Content, 1000 Degrees Cent.
(b) Section of Constant Silicon Content, 1000 Degrees Cent.
(c) Section of Constant Chromium Content, 800 Degrees Cent.
(d) Section of Constant Silicon Content, 800 Degrees Cent.
(e) Section of Constant Chromium Content, 600 Degrees Cent.
(f) Section of Constant Silicon Content, 600 Degrees Cent.

"a-a." The individual distances from each alloy point to this line were then laid out to scale in a horizontal direction on a separate diagram and perpendiculars erected from each point and marked with appropriate alloy numbers, as shown in Fig. 8b. The lattice parameters at 1000 degrees Cent. (1830 degrees Fahr.) were then read off the diagram on Fig. 7 and set off on its appropriate perpendicular. A number of points on various sections parallel to the iron-chromium base line on the parametric surface in the two-phase region were thus obtained. The various section lines could then easily be drawn in through their appropriate points by making each line conform to the general trend of its neighbors.

A number of constant chromium sections of the single-phase parametric surface, viz., 2.5, 4.5, 7 and 10.5 atomic per cent chromium were made. They are shown in Fig. 8a where they are represented by the highly inclined lines; they were constructed from diagram Fig. 5 by means of a reference plane, the horizontal and vertical traces of which are annotated *"b-b"* on the location diagram, Fig. 1, and on Fig. 8a, respectively.

In the two-phase region, the parameter of any alloy located exactly on a constant chromium section line could be plotted by measuring off the distance of its location point from the reference line *"b-b"* on the location diagram, and transferring this distance to Fig. 8a, setting it off out from line *"b-b"* as abscissae with the lattice parameter of the alloy as ordinate.

Those alloy points which are not located exactly on the section lines were interpolated along their constant silicon lines to the desired chromium section. The procedure was as follows, using as a specific example the 4.5 atomic per cent chromium section.

Alloy No. 45 is considerably off this section line and the interpolated value is sought. On the location diagram, Fig. 1, the distance from *"a-a"* to 4.5 atomic per cent chromium section is measured along the constant silicon section which passes through No. 45, and this distance is then laid out horizontally from *"a-a"* on the diagram of Fig. 8b. A perpendicular is erected until it intersects the same constant silicon section and the correct interpolated lattice parameter, 2.8172, is read off. This interpolated value can then be used exactly as the alloy points which are located exactly on the section, by transference to Fig. 8a, as already explained. The number of points thus obtained on each constant chromium section were then connected by smooth curves as shown in Fig. 8a, and the intersection of these curves with the single phase curves are points on the intersection lines between the two parametric surfaces, that is, they are points on the phase boundary at 1000 degrees Cent. (1830 degrees Fahr.). The solubility limits at 800 and 600 degrees Cent. (1470 and 1110 degrees Fahr.) were obtained in the same way. Since some of the alloys, which at 1000 degrees Cent. are in the two-phase range, become three-phase alloys at lower temperatures, there will be fewer alloys and fewer sections the lower the temperature. Finally, the points on the phase boundary were transferred to the horizontal sections shown in Fig. 12. Points on the Fe-Si binary line were obtained from Greiner (26).

Location of the Phase Boundary of the Alpha Plus Sigma Region

The solid solubility limits between the alpha plus sigma and the alpha regions, which are annotated II and I, were determined by exactly the same procedure; in Fig. 9 and 10 diagrams showing constant silicon sections and constant chromium sections have been shown. The shape of the curves in this case is seen to be quite different from those of the region first treated. The intersecting curves on the constant chromium sections which yield the solubility limits at the higher chromium contents meet at very obtuse angles. Under such conditions the accuracy of the determination must necessarily

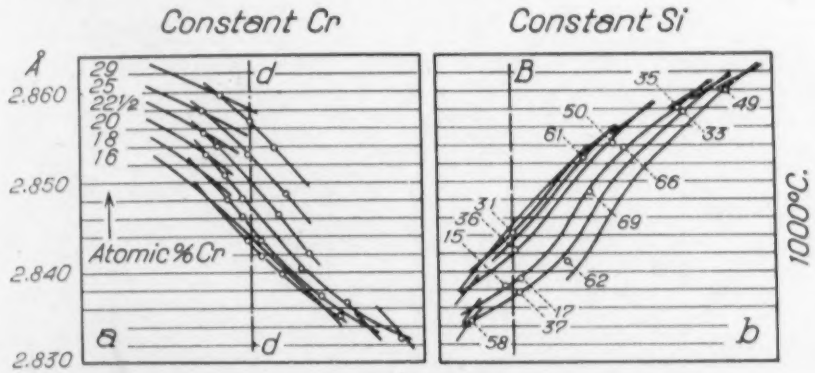

Fig. 9—Lattice Parameters Versus Composition in the (Alpha Plus Sigma) Region. Angstrom Units Versus Atom Per Cent.
(a) Sections of Constant Chromium Content, 1000 Degrees Cent.
(b) Sections of Constant Silicon Content, 1000 Degrees Cent.

remain low. Points on the 600 degrees Cent. (1110 degrees Fahr.) isotherm above 22 atom per cent chromium, and on the 800 degrees Cent. (1470 degrees Fahr.) isotherm above 25 atom per cent chromium are considered to be unreliable, and have been disregarded in drawing up the isotherm of the phase boundaries in Fig. 12. Fig. 11 shows a section of constant ratio of Cr:Si. The ordinates are Ångstrom units and the abscissae are atom per cent iron. This is the section marked B in Fig. 8. The lattice parameters in the solid solution range were obtained by construction from Fig. 4, and the lattice parameters of the alloys in the two-phase region were obtained from Fig. 6. Values of the lattice parameters of those alloys which are off the B-section have been corrected by interpolation. The lattice parameters of any alloy in the two-phase region are seen to be smaller, the lower the temperature. The points of each temperature level have been connected with smooth curves which intersect the single-phase sections. The iron contents of these intersec-

tions increase as the temperature decreases. These curves intersect at angles large enough to give good accuracy on the determinations.

Location of the Phase Boundary of the Alpha Plus Cr_3Si Region

This region, which in the diagram has been annotated VI, is very narrow and is wedged in between two three-phase regions, those marked V and VII, respectively, and bounded by the alpha solid solution. Reference to Figs. 5 and 14 will show that the tie-lines in this

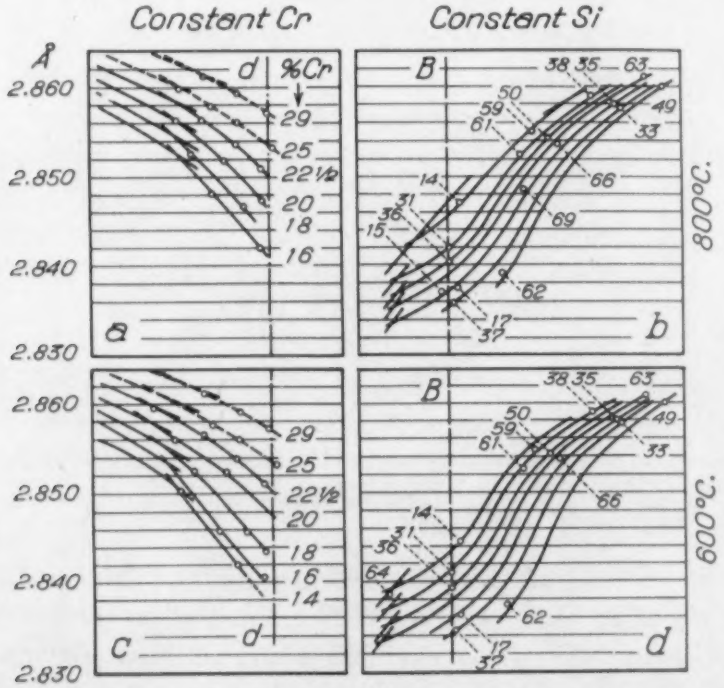

Fig. 10—Lattice Parameters Versus Composition in the (Alpha Plus Sigma) Region. Angstrom Units Versus Atom Per Cent.

(a) Sections of Constant Chromium Content, 800 Degrees Cent.
(b) Sections of Constant Silicon Content, 800 Degrees Cent.
(c) Sections of Constant Chromium Content, 600 Degrees Cent.
(d) Sections of Constant Silicon Content, 600 Degrees Cent.

region form very obtuse angles with the isoparametric lines, a fact which makes the method of sections unsuitable for the determination of these solubility limits.

It is possible, however, to determine the triple points of the three-phase regions at the terminals of the two-phase boundary lines. The triple point of the region V lies on the intersection of the boundaries of regions II and VI with I. The alpha-phase lattice parameter

in the three-phase region V was measured and the corresponding isoparametric curve of the single phase region was sought out on the diagram of Fig. 5. The intersection of this isoparametric curve with the phase boundary of region II must also be that point on the boundary between I and VI where both two-phase boundaries meet and terminate. One alloy was available in the three-phase region V, viz., No. 67 with a parameter of 2.835 Å. As the uncertainty in the measure of the parameter is ± 0.0005 Å and as the isoparametric lines of the region intersect the alpha plus sigma solubility boundary, region II, at obtuse angles, the precision of the determination is not high.

The same procedure was followed in the VII region. At 1000 degrees Cent. (1830 degrees Fahr.) we have in this region alloy No.

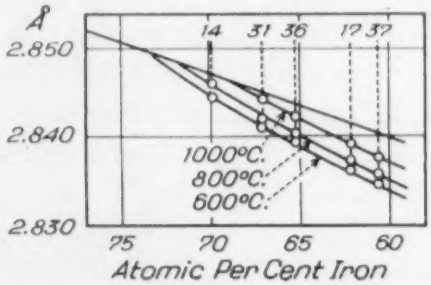

Fig. 11—Lattice Parameters Versus Composition in the (Alpha Plus Sigma) Region. Angstrom Units Versus Atom Per Cent Iron. Section B of Constant (Atom Per Cent Cr) : (Atom Per Cent Si) Ratio. 1000, 800 and 600 Degrees Cent.

68 with a lattice parameter of 2.828 Å. At 800 degrees Cent. (1470 degrees Fahr.) we have alloys No. 40, 41 and 16 in the three-phase region with an average parameter of 2.826 Å.; at 600 degrees Cent. (1110 degrees Fahr.) we have alloys No. 57, 41, 40, 16 and 53, with an average parameter of 2.824 Å.

The respective intersections of the corresponding isoparametric lines with the phase boundary between VIII and I were sought out and marked. Some indication of the course of the boundary between the terminal points was established from alloy No. 26, which at all three temperatures falls within the Cr_3Si plus alpha region, and from No. 54 and 55 at 800 degrees Cent. (1470 degrees Fahr.), of No. 30 at 800 and 600 degrees Cent. (1470 and 1110 degrees Fahr.), and of No. 58 at 600 degrees Cent. (1110 degrees Fahr.). Since the phase region is very narrow, an estimate could be made of the directions of the tie-lines and their intersections with the correspond-

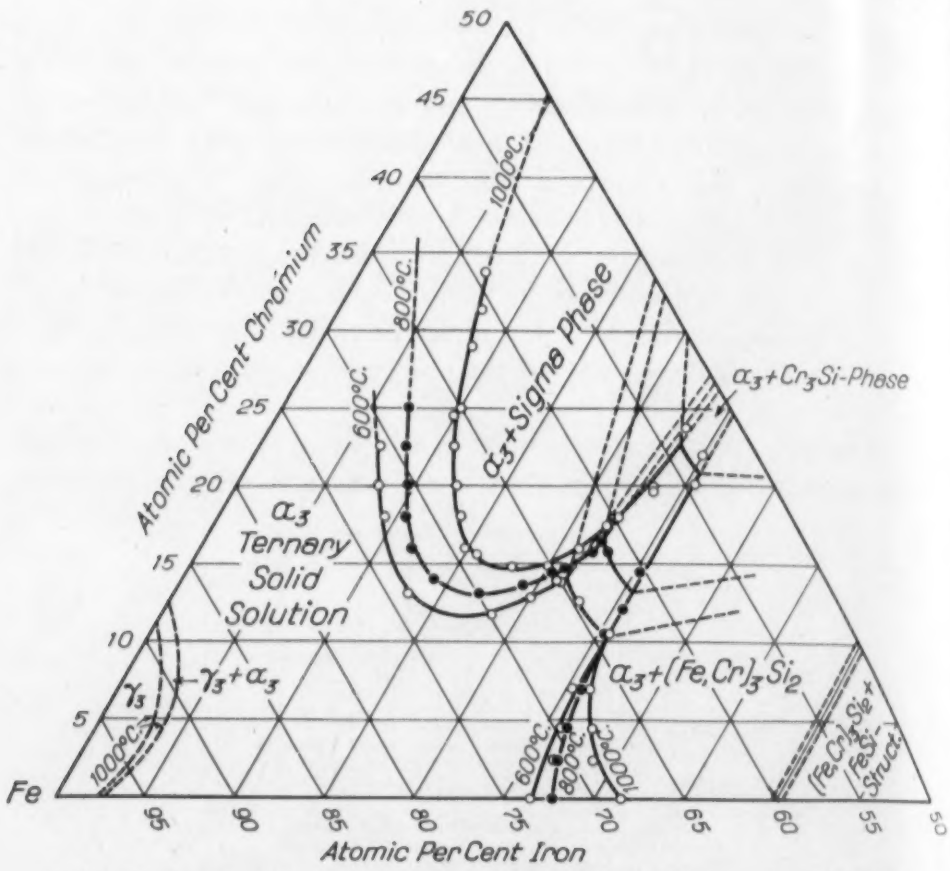

Fig. 12—Iron-Chromium-Silicon System; Constitutional Diagram of the Iron-Rich Solid Solution Range. Atom Per Cent.

ing isoparametric lines of the solid solution region could be roughly determined. The boundary lines for the various temperatures were then drawn in with regard to all points located and also with regard to the other two-phase boundaries. The disappearing phase criterion also assisted in placing the lines and finally the curves for the three temperature levels were made to conform to each other in general shape and direction. The accuracy which it was possible to obtain was certainly much less than that obtained for the other two-phase regions.

The Secondary Phases

(a) The Sigma-Phase. The alloys in the phase region marked II on the diagrams gave photograms which possess a large number of lines besides the lines of the body-centered alpha phase. This phase is hard and very brittle. A record of its $\sin^2 \theta$ values is presented in Table VI. (Cf. Refs. 32 and 33). It may be noted that very few

beta lines are observed. There is also a conspicuous absence of lines in the middle of the range.

The photograms of alloy No. 32 show the lines of this phase and those of a phase which has lines identical with those of Borén's Cr_2Si structure (22). On the other hand alloys No. 33 and 35 show the lines of the alpha phase and the unknown phase; the iron content of this must therefore lie between those of alloys No. 32 and 33.

The isoparametric lines of the alpha phase in the two-phase region were laid out from the diagrams of Figs. 9 and 10. These do not intersect in a point, but they all pass through a fairly narrow region which includes the stoichiometrically simple composition Cr_3Fe_3Si. Alloy No. 42 has approximately this composition; its photograms show only the lines of the new phase. Moreover, the lines of this phase shift by small amounts in the various alloy photograms, thus indicating that its composition is variable. The alloys in region II were deliberately placed near the alpha phase boundaries, which are far removed from the homogeneity region of the sigma phase.

Considerable interpolation and extrapolation are required in order to extend the isoparametric lines to the neighborhood of the homogeneity region, and their convergence is therefore subject to uncertainties. They are, therefore, only of qualitative value as indicators of the stability range of the phase, but they would indicate that the composition of the compound may vary considerably.

Alloy No. 71 on the binary gives a line pattern identical with those found for the ternary alloys. There can thus be little doubt that the sigma phase is a secondary solid solution of three components based on the secondary solid solution of the iron-chromium binary, the FeCr phase (see below). The existence of this phase in the Fe-Cr binary has been the subject of some controversy [see Greaves (30)], which we cannot discuss here. We may note, however, that we have observed that the presence of even a small amount of silicon, such as was used in alloys, numbers 71, 72, 73 and 76, seems to accelerate the precipitation of the sigma phase from the alpha phase. Number 71, which contained only 0.09 weight per cent of silicon was distinctly slower in reaching equilibrium even at 775 degrees Cent. (1425 degrees Fahr.).

The homogeneity range of the sigma phase may be represented as a roughly lens-shaped volume within the triangular base prism on

which temperature is represented as the vertical direction. Two possibilities exist: 1) the sigma phase is based on the binary compound FeCr, in which case its stability region continues over to the binary. 2) The binary compound FeCr is non-existent and the stability region of the sigma phase is separated by a single phase region from the binary. The width of this single phase region cannot be more than 0.09 per cent silicon at approximately 50 per cent chromium. At present, we are not prepared to decide which of these two possibilities actually exist.[1] Therefore when we use the term binary compound FeCr and binary of iron and chromium, it is with the reservation that a pseudo-binary with 0.09 per cent silicon may be more correct. The Fe-Cr binary intersects this lens in such a way that the maximum temperature on the binary lies between 925 and 1000 degrees Cent. (1700 and 1830 degrees Fahr.), and probably closer to the lower limit. With increasing silicon content the maximum temperature increases well above 1000 degrees Cent. (1830 degrees Fahr.). The 1000 degrees Cent. isothermal section of the ternary system intersects this lens in such a way as to yield an area of homogeneous sigma phase which is well removed from the binary. It may extend a few per cent beyond this composition but its extent has, however, not been determined. Since it is established that above about 925 degrees Cent. (1700 degrees Fahr.) the sigma phase recedes from the binary, isotherms above this temperature will show a terminal solid solution phase continuously from the Cr-Si binary to the Fe-Si binary. Below this temperature there are isotherms on which the sigma phase field and its two-phase field separate two portions of this range. The notations used here, II and II′, actually denote one region, but on some isotherms it will appear separated by the sigma region.

(b) The $(Fe,Cr)_3Si_2$-phase. The alloys located in the phase region marked VIII on the diagrams yielded lines identical with the lines of the Fe_3Si_2 phase which have been described by Phragmén (12). The structure has not been solved.

The lines on the photograms of the ternary alloys vary somewhat with gross alloy composition, and therefore it is certain that the pure binary compound does not exist in ternary alloys. The isoparametric lines of the alpha-phase in the two-phase region do

[1]Added in proof: Further work by Jette, Foote, and Andersen has shown beyond reasonable doubt that this phase does exist in binary Fe-Cr alloys with Si contents as low as 0.003 per cent. The transformation temperature for a 50.6 atomic per cent Cr alloy was found to be between 775 and 800 degrees Cent. (1427 and 1472 degrees Fahr.).

Table VI
$\sin^2\theta$ Values of the Sigma Phase of Alloy No. 42

Intensity		$\sin^2\theta$	Cr-rad.	Intensity	$\sin^2\theta$	Cr-rad.
m	No. 49	0.1248*	a			
w	50	0.1361*	a	m	0.8647	a_1
w	32	0.1480*	a	w	0.8683	a_2
w		0.2082	a	m	0.8700	a_1
vw		0.2335	a	w	0.8732	a_2
m		0.2410	b	sm	0.8814	a_1
s		0.2502	a	mw	0.8849	a_2
w		0.2560	a b	sm	0.9047	a_1
vw		0.2640	b	m	0.9085	a_2
w		0.2775	b	m	0.9162	a_2
vs		0.2900	a b	m	0.9192	a_2
s		0.3070	a b	m	0.9330	a_1
s		0.3180	a b	w	0.9362	a_2
vs		0.3360	a	s	0.9503	a_1
vs		0.3525	a	w	0.9622	a_2
vs		0.3690	a	vs	0.9673	a_1
m		0.3865	a	s	0.9705	a_2
w		0.4210	a			
vw		0.4875				
vw		0.6770	a_1			
vw		0.6794	a_2			
vw		0.6887	b			
vw		0.6937	a_1			
vw		0.6959	a_2			
w		0.7063	b			
vw		0.7177	a_1			
vw		0.7214	a_2			
w		0.7452	a_1			
vw		0.7467	a_2			
vs		0.8308	a_1			
s		0.8339	a_2			
s		0.8526	a_2			
m		0.8560	a_2			

Legend

vs	very strong
s	strong
sm	strong to medium
m	medium
mw	medium to weak
w	weak
vw	very weak
a	alpha = a_1 and a_2
a_1	alpha 1
a_2	alpha 2
b	beta

*These lines could not be found on films of alloy No. 42, but occurred on films of several alloys in this region. They may be quantitatively somewhat different from the corresponding lines of alloy 42.

not intersect in a point but spread out, fanshape, upwards from the alpha solid solution boundary. This would indicate a homologous series with chromium atoms replacing iron atoms in the structure.

Photograms of alloys No. 20 and 60 which are located to the left of the 40 atom per cent silicon section show lines including those of the alpha solid solution. Photograms of alloy No. 23 to the right of this section show no alpha iron lines. They do, however, show strong lines of FeSi. Alloy No. 43 is located approximately on the 40 atom per cent silicon section line and its photograms show only Fe_3Si_2 lines with traces of FeSi lines. All this bears out nicely the theory that this section is a semi-binary with the terminal compounds Fe_3Si_2 and Cr_3Si_2. It has also been noted that the tie-lines show a curvature, so that although they start out as straight lines from the solubility limit of the alpha-phase, they show a convexity towards the center of the diagram. This indicates a lack of equilibrium since the tie-lines in equilibrium must be straight lines. (See Ref. 37). This

lack of equilibrium may be due to very slow reaction rates. It is well known that Fe_3Si_2 is formed at a temperature variously stated to be between 1015 and 1030 degrees Cent. (1860 and 1885 degrees Fahr.) by a peritectic reaction between saturated alpha solid solution and FeSi. It is thus likely that this type of reaction takes place in the ternary system (cf. Denecke Ref. 7), between the saturated ternary solid solution and a compound having the same structure as FeSi, which in turn may be a homologous series of FeSi and CrSi. The final products of the reaction must be a two-phase equilibrium between saturated ternary alpha solid solution and the $(Fe,Cr)_3Si_2$ phase.

Evidence from the photograms shows further that the unstable FeSi structure is present only in the two-phase region, and is absent in the adjacent three-phase region. As the FeSi structure is not found in stable equilibrium with the primary phase, we are not directly concerned with it here. It was, however, identified by comparison with photograms available in this laboratory.

(c) The Cr_3Si Phase. This phase, as has been noted, has a cubic structure and it was identified from Borén's published $\sin^2\theta$ values (28). The lattice parameter of this compound was computed from the photograms of alloys No. 54 and 55. The value obtained was $a_0 = 4.4539$ Å., whereas the value published by Borén is $a_0 = 4.4555$ Å., thus indicating that in the ternary alloys the pure binary compound may not exist, but is replaced by a solid solution series in which iron is probably substituted for chromium.

The Alpha Phase Boundary

In Table VII a number of points of compositions on the phase boundaries of the alpha region are given. These points were read off the diagram, Fig. 12, and may be used for purposes of reproducing this diagram. These figures are, therefore, subject to the uncertainties stated on page 416. The points marked with asterisks are triple points. A few points on the two- and three-phase boundaries are also given. These are only very roughly determined. Points in other portions of the diagram will not be given as these are not known with sufficient precision.

Further Extension of the Ternary Diagram

While the object of the present series of experiments was pri-

Table VII

The Limits of Solid Solubility—Compositions of Selected Points on the Phase Boundaries

Phase Boundaries	Compositions					
	1000°C		800°C		600°C	
	at.% Cr	at.% Si	at.% Cr	at.% Si	at.% Cr	at.% Si
I-II	35.0	6.9	....	....	....	....
	30.0	8.2	....	....	....	....
	25.0	9.8	25.0	7.1	....	....
	20.0	12.2	20.0	9.5	20.0	7.9
	17.0	14.1	16.5	11.6	16.0	10.5
	16.0	15.0	15.0	12.8	14.5	11.6
	15.0	16.4	13.5	15.0	12.0	15.0
	14.6	18.0	13.0	17.0	11.6	17.0
	15.0	19.8	13.4	19.0	12.5	19.5
	17.5	22.0	15.0	21.2	14.0*	21.4*
	20.5	23.0	16.4*	22.2*	12.5	22.7
	22.8*	23.3*	15.0	23.4	11.0	24.5
	20.7*	25.4*	13.2*	25.4*	10.3*	25.4*
I-VIII	17.0	25.4	17.0	25.4	....	....
	10.0	25.6	10.0	25.4	10.0	25.4
	7.5	26.2	7.5	25.7	7.5	25.5
	5.0	27.2	5.0	26.3	5.0	25.8
	2.5	28.8	2.5	27.1	2.5	26.1
	0.0	31.5	0.0	26.7	0.0	26.4
II-V	35.0	18.0	35.0	16.9	35.0	16.2
VII-VIII	20.6	30.0	14.0	30.0	11.5	30.0

marily the determination of the limits of the iron-rich solid solutions, enough data was incidentally obtained to make possible a layout of a large portion of the ternary diagram.

Fig. 14 shows such a diagram in atom percentages at 1000 degrees Cent. (1830 degrees Fahr.). From this diagram, conversions of atom percentages into weight percentages were made and the diagram drawn up in weight percentages, as shown in Fig. 15. The 800 and 600 degrees Cent. (1470 and 1110 degrees Fahr.) sections could as well be drawn, but inasmuch as the temperature variation of only the iron-rich solid solution region has been definitely established, as shown in the diagrams of Figs. 12 and 13, there would be little point in doing this.

The solid solubility limits have been determined up to about 35 atom per cent chromium and the 1000 degrees Cent. (1830 degrees Fahr.) isotherm extrapolated into the chromium-silicon binary. Borén's value of the solubility of silicon in chromium, about 13.8 atom per cent (22) silicon, has been used. The extrapolated portion is shown in dotted line, since beyond the sigma solid solution region it is based largely upon conjecture.

However, in the neighborhood of this region a few alloys, viz., Nos. 71 to 76, inclusive, may facilitate extrapolation of the

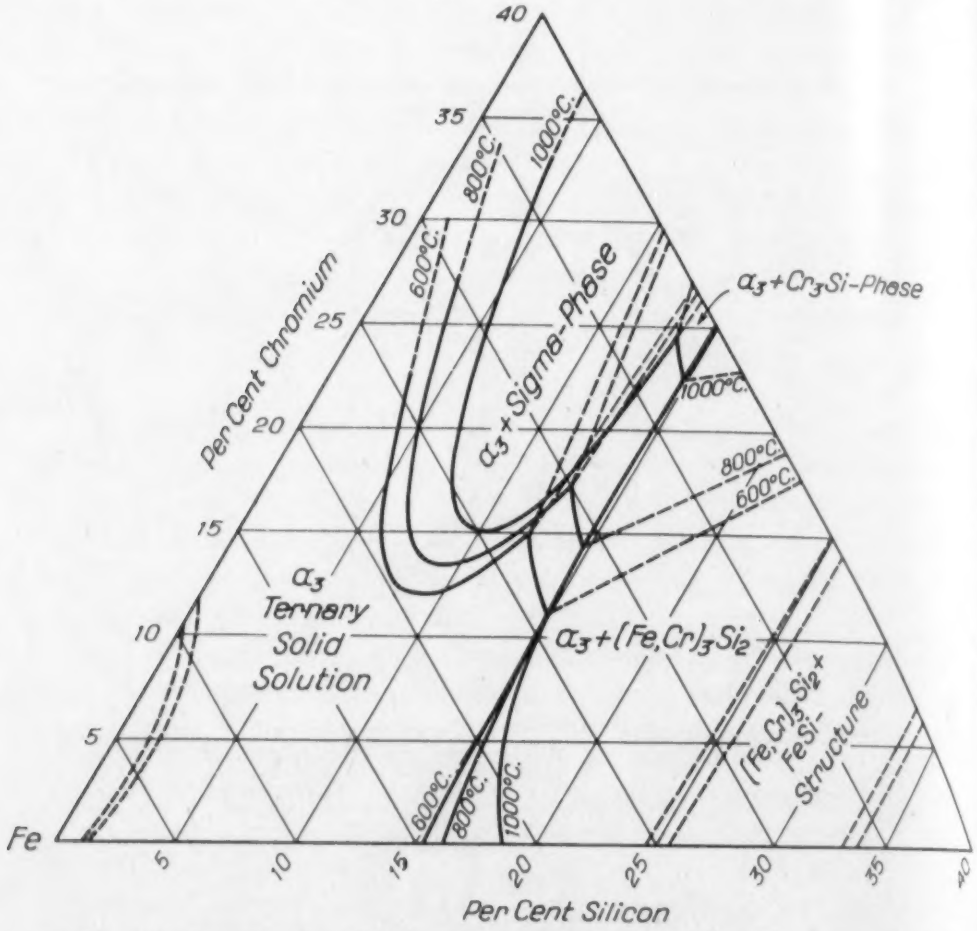

Fig. 13—Iron-Chromium-Silicon System; Constitutional Diagram of the Iron-Rich Solid Solution Range. Weight Per Cent.

solubility limits towards the iron-chromium binary. The phases present were identified by the photogram lines, and the parameters were computed for four of these alloys. A study of the results given in Table V shows that the 1000 degrees Cent. (1830 degrees Fahr.) isotherm between region I and II must run between alloys Nos. 74 and 75 and exclude alloys Nos. 72 and 73 from the two-phase region. The homogeneous sigma region at this temperature must include alloys Nos. 74 and 42, and exclude alloys Nos. 76, 32 and 67. The relations between these phases at low temperatures have not been represented on the diagrams because the available data were insufficient.

The ternary sigma phase is shown by a small ellipse marked XI, but its area bears no exact relation to the extent of the single phase homogeneity range of the compound, which is unknown.

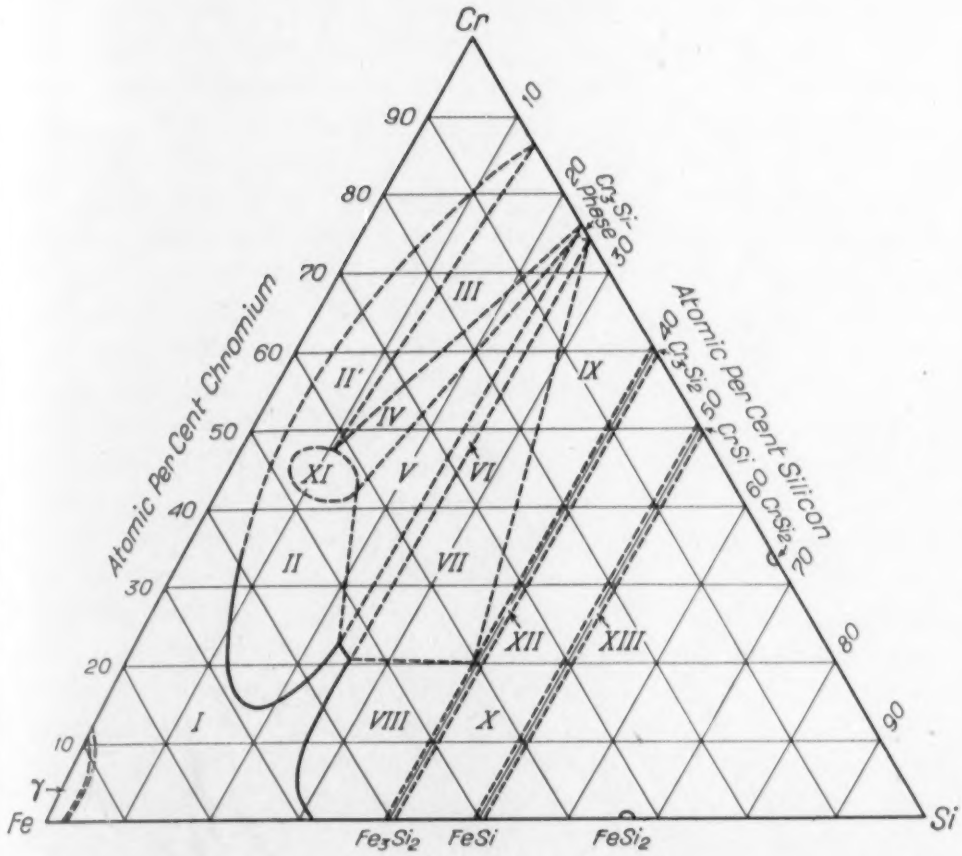

Fig. 14—Tentative Diagram of the Iron-Chromium-Silicon System; Atom Per Cent, 1000 Degrees Cent.

There must be two triple points in the boundary region of this phase. Since only three phases can exist in equilibrium at arbitrary temperature levels (excluding the case of a theoretically possible invariant quadruple point), these points must be separated by a two-phase range. Alloy No. 32, located in this range, yielded diffraction lines of both the sigma structure and the Cr_3Si structure, which are very distinctive. This field, which is marked IV, thus proves to be a two-phase field containing these two phases in equilibrium.

The three-phase field, shown on the high chromium side, contains sigma plus Cr_3Si plus the saturated binary solid solution of silicon in chromium. As no alloy was placed in this region, no direct verification has been obtained. Theoretically, it would be possible for this field to be subdivided into several phase regions. This, however, is improbable and in this tentative diagram the simplest possible case is shown. This region is marked III.

Region	Phases
I	α_3 solid solution
II	$\alpha_3 + \Sigma$
III	$\Sigma + Cr_3Si +$ Cr solid solution
IV	$\Sigma + Cr_3Si$
V	$\alpha_3 + \Sigma + Cr_3Si$
VI	$\alpha_3 + Cr_3Si$
VII	$\alpha_3 + Cr_3Si + (Fe,Cr)_3Si_2$
VIII	$\alpha_3 + (Fe,Cr)_3Si_2$
IX	$(Fe,Cr)_3Si_2 + Cr_3Si + Cr_3Si_2$
X	$(Fe,Cr)_3Si_2 +$ (Fe,Cr) Si
XI	Σ
XII	$(Fe,Cr)_3 Si_2$
XIII	(Fe,Cr) Si

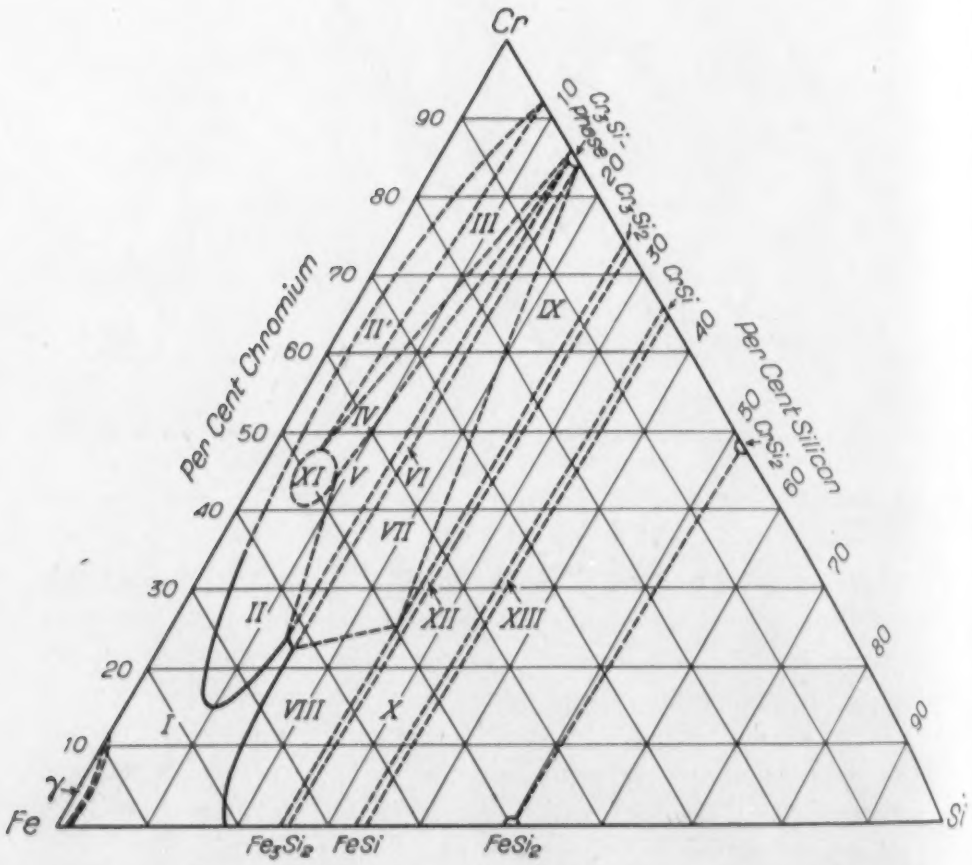

Fig. 15—Tentative Diagram of the Iron-Chromium-Silicon System; Weight Per Cent, 1000 Degrees Cent.

The field annotated V contains sigma plus Cr_3Si plus saturated ternary alpha solid solution. Photograms of alloy No. 67 gave very good lines of all three of these phases.

The compound Cr_3Si is shown by a half circle which indicates a composition range, but must not be considered as specifying its ex-

tent. Adjoining it is shown the two-phase region VI, separating throughout its extent the two three-phase regions, V and VII. The alloys Nos. 55, 54 and 26 are located in this region at 1000 degrees Cent. (1830 degrees Fahr.); at lower temperatures, Nos. 30, 56 and 58 are also included.

Region VII contains the phases Cr_3Si plus $(Fe,Cr)_3Si_2$ plus a saturated alpha solid solution; all three structures are represented by sharp lines on the photograms of alloy No. 68. The exact composition of the Cr_3Si phase is unknown; it may in this region possibly reach several per cent out into the field, or it may be a pure binary compound. Likewise the composition of the $(Fe,Cr)_3Si_2$ phase present in this field is unknown. The two distinct boundary lines going out from this compound are, therefore, not known with certainty.

The region annotated IX must be a two-phase region unless one complicates the matter by subdivision into several regions. No alloy was placed in this region. As shown, it would consist of the homologous series $(Fe,Cr)_3Si_2$ plus the Cr_3Si phase which here may be the pure binary or its isomorphic solid solutions, according to its appearance in region VII. The triple point on the $(Fe,Cr)_3Si_2$ semi-binary has been only approximately located. Since alloy No. 68 is definitely of three phases and alloy No. 60 shows two phases only, the phase boundary must run somewhere between these two alloys.

Since the location of the triple points of the compounds Cr_3Si and the sigma-phase are known only approximately, the phase boundaries going out from these points cannot be definitely placed. All these phase boundaries may be subject to temperature variation, as indeed has been definitely proven for the four lines going out from the triple points located on the alpha solid solution boundaries.

According to the phase rule, the triple point on the 40 atom per cent Si section must be abutted by a single phase region and, as the binary terminal compounds also must possess some degree of solubility, the semi-binary has been shown as double lines throughout its length enclosing a narrow solid solubility area.

On the 50 atom per cent silicon section one alloy, No. 48, which has not been analyzed, was located. Its photograms yield lines apparently identical with the FeSi structure, together with some faint lines which may be due to traces of $(Cr,Fe)_3Si_2$. This indicates that a homologous series may be formed by the two isomorphic terminal compounds FeSi and CrSi.

Between these two semi-binaries, alloy No. 23 is located. Photograms of this alloy show the lines of both the FeSi and the Fe_3Si_2 structures; a two-phase region consisting of the two homologous compounds is therefore indicated.

Beyond the 50 atom per cent silicon semi-binary line, the compounds $CrSi_2$ and $FeSi_2$ exist, and it is also mentioned by Borén (*22*) that silicon dissolves little or no chromium, while earlier iron-silicon diagrams indicate that silicon dissolves about 4 weight per cent iron.

The diagram is presented with the reservation that only the alpha solid solution boundaries shown in full lines have been definitely established. The other lines possess varying degrees of uncertainty up to roughly the 30 atom per cent silicon section. Beyond this section the phases and their boundaries shown are the most probable ones consistent with experimental results, which are not very extensive. They are, however, reliable for purposes of orientation and for planning of researches on the chromium and silicon ends of the system which were not objects of the present investigation.

Incidental Observations

The brittleness and hardness of the alloys in the cast condition increase with the alloy content. It has been established that many of the alloys can be hardened by quenching followed by aging at moderate temperatures, by which sigma phase is precipitated. An account of a few age-hardening tests will be published in another paper.

All alloys consisting preponderately of the alpha phase are strongly magnetic. The sigma-phase is nonmagnetic. Alloy No. 55 is magnetic but not so strongly, thus indicating that the Cr_3Si phase is nonmagnetic or only weakly magnetic. Alloy No. 23 which approximately has the composition $(Fe,Cr)_3Si_2$ is weakly magnetic.

The color of the alloys changes rather strikingly with composition. Those in the alpha region have the usual iron color. Alloys consisting primarily of the sigma phase and the Cr_3Si phase have a bright silvery luster. The alloys Nos. 43 and 23 having the $(Fe,Cr)_3Si_2$ composition were fairly bright and of a bluish tinge.

A number of samples were polished and the microstructures examined. The phases present in the various regions were recognized. Some of the alloys were difficult to etch. Alloy No. 42 was

etched by 50 per cent HCl containing some H_2F_2. The two alloys, Nos. 67 and 68, had previously shown the lines of three distinct phases. Under the microscope only two phases were at first visible. A combination of etching and polishing finally brought out three phases in No. 67, while so far no adequate technique for making visible the three phases in No. 68 has been found.

Accuracy of the Results

(a) Individual lattice parameters. The uncertainties which may cause constant errors are: 1) Impurities in raw materials; 2) Chemical analysis of alloys; 3) Calibration of cameras; 4) Calibration of thermocouples. A numerical estimate of these uncertainties is impossible. However, their combined effect on the lattice parameters can be neglected as far as comparison between determinations carried out with equal care in other laboratories is concerned. This is demonstrated by the fact that measurements of the lattice parameters of iron-chromium alloys in this investigation show no systematic deviation from those previously made by Preston (20). See Fig. 2.

A list of the possible sources of accidental errors is given in Table VIII, together with estimates of their magnitudes.

The probable error of determination of the individual lattice parameters may be stated to be $\pm$ 0.0006 Å. The interpolation methods used to obtain the isoparametric curves has tended to average out the errors on individual determinations. Errors due to reading and plotting may have counteracted this to some degree. No close estimate is possible, but considering the comparatively large number of alloys used and interpolations on sections of constant iron content and on horizontal sections, the isoparametric lines are probably correct within $\pm$ 0.0004 Å.

In the two-phase regions, the only error which will differ from those in Table VIII is $\triangle_3$; this is estimated to be approximately 0.0002 Ångstroms, in view of the care with which the alloys have been treated and the large number of alloys studied. When this is taken into account, the uncertainty becomes $\pm$ 0.0006 Ångstrom.

(b) Solubility limits. That the solubility limits as they were determined from the intersections of the parametric surfaces are essentially correct may be judged from the disappearing phase criteria. The reflection lines of any alloy correspond exactly to

Table VIII

Accidental Errors in Alpha-Phase Region

Source of accidental errors	Estimated value of individual errors in Angstroms
1) Impurities introduced in the various alloys	$\Delta_1 = .00025$
2) Chemical analyses on the individual alloys	$\Delta_2 = .0002$
3) Lack of equilibrium conditions in two and three phase alloys, segregation of constituents	$\Delta_3 = .0$
4) Errors of measurement of temperatures	$\Delta_4 = 0$
5) Readings of photograms, lines, shrinkage of films, and calculation of lattice constants	$\Delta_5 = .0004$
6) Temperature coefficient of the heat expansion of the unit cells	$\Delta_6 = .00025$
7) Effects of quenching	$\Delta_7 = 0$
8) Uncertainties of plotting, interpolations and extrapolations	$\Delta_8 =$ See text.

When the errors from sources 1 to 7, inclusive, are combined in the usual fashion without weighing, we have:

$$\Delta = \pm \sqrt{.00025^2 + .0002^2 + .0004^2 + .00025^2} = \pm .00058$$

as the uncertainty of an individual determination.

those which one would expect them to have, after observing the respective phase field in which they fall at any of the three temperature levels indicated in Figs. 12 or 13.

Since the intersection of the parametric surfaces can be determined with higher precision the less obtuse the angle of intersection and since these angles vary with composition and with temperature, a uniform precision over the whole field is probably not obtained. In the $(Fe,Cr)_3Si_2$ region the determined boundaries are probably very close to the true ones. An exception is, however, made for the region within two or three per cent of the iron-silicon binary at 1000 degrees Cent. (1830 degrees Fahr.), where the solubility changes very rapidly with temperature.

In the sigma-phase region the angles of intersection are better at 1000 than at 600 degrees Cent. (1830-1110 degrees Fahr.) where they become very obtuse. The 1000 degrees Cent. (1830 degrees Fahr.) boundary is probably better than those for the lower temperatures. The angles of intersection of the tie-lines in the Cr_3Si phase region and the isoparametric lines in the alpha region are very obtuse. The boundary between these regions is the one where the probable error is the largest.

In general, the shape of the solubility surfaces (or phase boundaries) is probably more correct than their absolute locations. A numerical calculation of the probable error of the determinations cannot be made, but it is estimated that as they stand they are on the average correct to $\pm$ 0.5 per cent.

Summary

The phase diagram of the iron-rich alloys of the iron-chromium-silicon alloys has been determined for the solid alloys by the use of X-ray crystal structure methods. During the course of this work, the methods of interpolation and extrapolation which are based upon orthographic projection and developed in a previous article have been applied to the determination of the surfaces which represent the variation of lattice parameter with composition (i.e. parametric surfaces) in one- and two-phase regions of the ternary system.

The parametric surface of the iron-rich solid solutions has been developed with considerable accuracy. This is apparently the first time that an extensive ternary parametric surface has been determined.

The range of compositions over which the alpha iron phase is homogeneous has been determined at three temperature levels, 1000, 800 and 600 degrees Cent. (1830, 1470, 1110 degrees Fahr.) in the range of 0 to about 35 per cent chromium. The alpha phase boundary consists of three sections. Over one section it is in equilibrium with a phase of the composition $(Fe,Cr)_3Si_2$ which is isomorphic with Fe_3Si_2. The next section is short, especially at high temperatures, and the phase in equilibrium with the alpha phase is isomorphic with Cr_3Si. Over the longest section of the boundary the second phase is a solid solution based on the compound FeCr, and it has been found to exist as a homogeneous phase over wide region in the ternary system. This last phase (sigma) dissolves considerable quantities of silicon up to perhaps 9 or 10 weight per cent.

The sigma phase forms by precipitation from the binary (Fe-Cr) and ternary alpha solid solutions. The alpha phase boundary in this region changes rather rapidly with temperature. Thus, there is a range of compositions in which precipitation hardening is possible. While this has been proved by experiment, the evidence is not presented here.

The various sources of error involved in the determinations of lattice parameters and solubility limits, and their effects on the accuracy of the results, has been estimated.

The general correctness of the stated phase regions of the iron-rich portion of the ternary diagram has been demonstrated by considerable exploration into the complete system. Tentative diagrams with compositions expressed in both weight per cent and atomic per cent have been drawn, which embody all the available information.

These diagrams cover the whole system below 50 atom per cent or 33 weight per cent silicon.

ACKNOWLEDGMENTS

We take this opportunity to make formal acknowledgment to:

Dr. F. M. Beckett of the Electro-Metallurgical Corporation for the highly purified silicon and chromium used in this investigation;

Dr. A. B. Kinzel and Mr. Walter Crafts for the analysis of a number of the alloys;

Mr. Earl S. Greiner, graduate student of the School of Mines, for the use of unpublished data on the iron-silicon system;

Mr. Frank Foote, research assistant in metallurgy at the School of Mines, for his helpful co-operation especially during the earlier stages of the experimental work and the reading of the proofs.

References

1. E. R. Jette and E. S. Greiner, "An X-Ray Study of Iron-Silicon Alloys Containing 0 to 15 Per Cent Silicon," *Transactions*, American Institute of Mining and Metallurgical Engineers, 1933, Vol. 105, p. 259.
2. A. F. Westgren, "X-Ray Determination of Alloy Equilibrium Diagrams," *Transactions*, American Institute of Mining and Metallurgical Engineers, 1931, Vol. 93, p. 13.
3. W. Campbell, Campbell's List of Alloys, American Society for Testing Materials, *Proceedings* (Part 1) Report of Committee B-2 on Nonferrous Metals and Alloys, (1927) Vol. 27, (1934) Vol. 34.
4. E. S. Greiner, J. S. Marsh and B. Stoughton, "The Alloys of Iron and Silicon," The Engineering Foundation, McGraw-Hill Book Co., 1933.
5. A Grützner, Eisen und Stahllegierungen: Patentsammlung, Verlag Chemie, Berlin, 1932-35.
6. Index to Iron & Steel Patents, Edition 2, V. E. Kinsey and T. E. Hopkins, American Compilation Co., Pittsburgh, 1931.
7. W. Denecke, Tabelle. (In his article: Über das Dreistoffsystem Eisen-Silicium-Chrom.), *Zeitsch. f. anorg. u. allg. Chemie*, 1926, Vol. 154, p. 180.
8. W. Guertler and Tammann, "Über die Verbindungen des Eisen mit Silicium," *Zeitsch. f. anorg. Chemie*, 1905, Vol. 47, p. 163.
9. N. Kurnakow and G. Urazow, "Toxische Eigenschaften des Ferrosiliciums des Handels," *Zeitsch. f. anorg. Chemie*, 1922, Vol. 123, p. 89.
10. M. G. Corson, "The Constitution of the Iron-Silicon Alloys, Particularly in Connection with the Properties of Corrosion-Resisting Alloys of this Composition," *Transactions*, American Institute of Mining and Metallurgical Engineers, 1928, Vol. 80, Iron and Steel Division, p. 249.
11. J. L. Haughton and M. L. Becker, Alloys of Iron Research, Part 9, "The Constitution of the Alloys of Iron with Silicon." *Journal*, Iron and Steel Institute, 1930, Vol. 121, p. 315.
12. G. Phragmén, "The Constitution of the Iron-Silicon Alloys," *Journal*, Iron and Steel Institute, 1926, Vol. 114, p. 397.
13. W. Treitschke and G. Tammann, "Über die Legierungen des Eisens mit Chrom.," *Zeitsch. f. anorg. Chemie*, 1907, Vol. 55, p. 402.
14. E. Jänecke, "Uber die Konstitution der Eisen-Chromlegierungen," *Zeitsch. f. Elektrochemie*, 1917, Vol. 23, p. 49.

15. F. Adcock, Alloys of Iron Research, Part X, "The Chromium-Iron Constitutional Diagrams," *Journal*, Iron and Steel Institute, 1931, Vol. 124, p. 99.
16. F. Adcock, "Alloys of Iron Research," Part 4, "The Effect of Nitrogen on Chromium and Some Iron-Chromium Alloys," *Journal*, Iron and Steel Institute, 1926, Vol. 114, p. 117.
17. F. Adcock, "Alloys of Iron Research," Part 5, Preparation of Pure Chromium, *Journal*, Iron and Steel Institute, 1927, Vol. 115, p. 369.
18. A. B. Kinzel, "Critical Points in Chromium-Iron Alloys," *Transactions*, American Institute of Mining and Metallurgical Engineers, 1928, Vol. 80, Iron and Steel Division, p. 301.
19. L. C. Hicks, "An X-Ray Study of the Diffusion Chromium Into Iron," *Transactions*, American Institute of Mining and Metallurgical Engineers, Iron and Steel Division, 1934, Vol. 113, p. 163.
20. G. D. Preston, "An X-Ray Examination of Iron-Chromium Alloys," *Philosophical Magazine*, Ser. 7, 1932, Vol. 13, p. 419.
21. R. Frilley, "Alliages de Chrome et de Silicium," *Revue de Métallurgie*, 1911, Vol. 8, p. 476.
22. B. Borén, "Röntgenuntersuchung der Legierungen von Silicium mit Chrom, Mangan, Kobalt und Nickel," *Arkiv for Kemie, Mineralogi och Geologi*, bd. 11A, No. 10, 1933.
23. G. E. F. Lundell, J. I. Hoffman and H. A. Bright, "Chemical Analysis of Iron and Steel," New York, 1931, John Wiley & Sons.
24. W. F. Hillebrand and G. E. F. Lundell, "Applied Inorganic Analysis," John Wiley & Sons, New York, 1929.
25. F. Weber and P. Giani, "Beiträge zur Kenntnis des Systems Eisen-Silizium," *Mitt. a.d. Kaiser-Wilhelm Institute, f. Eisenforschung zu Düsseldorf*, 1925, Vol. 7, p. 59-68.
26. E. S. Greiner and E. R. Jette, Unpublished results.
27. J. L. Burns, "Classification of Alpha Iron-Nitrogen and Alpha Iron-Carbon as Age-Hardening Alloys," *Transactions*, American Institute of Mining and Metallurgical Engineers, Iron and Steel Division, 1934, Vol. 113, p. 239.
28. J. B. Austin and R. H. H. Pierce, "The Linear Thermal Expansion and α-γ Transformation Temperature (A_3 Point)," TRANSACTIONS, American Society for Metals, 1934, Vol. 22, p. 447.
29. J. B. Austin and R. H. H. Pierce, "Linear Thermal Expansion and Transformation Phenomena of Some Low-Carbon Iron-Chromium Alloys," American Institute of Mining and Metallurgical Engineers, Technical Publication 589, January 1935.
30. R. H. Greaves, "Chromium Steels," His Majesty's Stationery Office, London, 1935.
31. M. W. Cohen, Dissertation, Columbia University, 1935.
32. F. Wever and W. Jellinghaus, "Zur Kenntnis des Zweistoffsystems Eisen-Chrom," *Mitt. Kaiser-Wilhelm Institute f. Eisenforschung zu Düsseldorf*, 1931, Vol. 13, p. 143.
33. S. Eriksson, "Röntgenundersökningar över Systemet Järn-Krom-Kväve," *Jernkontorets Annaler*, 1934, Vol. 89, p. 530-43.
34. E. R. Jette, V. H. Nordstrom, B. Queneau and F. Foote, "X-Ray Studies on the Nickel-Chromium System," *Transactions*, American Institute of Mining and Metallurgical Engineers, 1934, Vol. 111, p. 361.
35. E. A. Owen and E. L. Yates, "Precision Measurements of Crystal Parameters," *Philosophical Magazine*, Ser. VII, 1933, Vol. 15, p. 472.
36. E. R. Jette and F. Foote, *Journal Chem. Physics*, 1935, Vol. 3, p. 605.
37. A. G. H. Andersen and E. R. Jette, "X-Ray Methods for Ternary Systems," to be published in TRANSACTIONS of American Society for Metals, 1936.

OBSERVATIONS ON THE OXIDATION OF STEEL

By M. Baeyertz

Abstract

Plain carbon steels, S.A.E. 2330 and a series of commercial chromium and chromium-nickel stainless steels were oxidized at elevated temperatures. The oxidation was observed to take place in a discontinuous manner. This resulted from the preferential oxidation of silicon and chromium in advance of the oxidation of the iron in the alloy.

The stainless steels oxidized according to a general pattern in which similar oxide forms occurred in the different alloys. However these similar oxide forms occurred at different temperatures depending on the chromium content of the alloys. The shift of oxidation type with chromium content and temperature is consistent with the known limitation of the low chromium alloys to low temperature applications. The resistance of the stainless steels to oxidation at elevated temperatures appears to be due to the formation of two (possibly more) oxides high in chromium.

RECENT metallurgical literature has evinced the interest of numerous investigators in the rate of oxidation of pure iron and of steel at elevated temperatures. Besides the study of the rate of reaction, the oxidation of solid steel also affords an opportunity to study some of the characteristics of the products formed, the form in which they are precipitated and the order in which they separate from the metal. The formation of scale on steel at elevated temperatures differs from the oxidation of pure iron under like conditions. This is due to the additional elements and compounds which steel contains; e.g., silicon, manganese, nickel, chromium, carbides, etc.

The oxidation of steel was observed to take place in a discontinuous manner, as to be expected. The elements and compounds which constitute steel apparently oxidize in the order of increasing oxygen concentration required for the precipitation or liberation of the oxides formed. When the additional elements in steel react with oxygen more readily than iron does, oxidation results not only in

A paper presented before the Seventeenth Annual Convention of the Society held in Chicago, September 30 to October 4, 1935. The author, M. Baeyertz, is assistant research engineer, Carnegie-Illinois Steel Corp., South Works, Chicago. Manuscript received May 27, 1935.

the formation of a coating of scale, separate and distinct from the metal beneath it, but also in the precipitation of oxides within the steel adjacent to the coating of oxides which may be considered as the scale proper. The precipitation of such oxides in the steel is the result of preferential oxidation of the additional elements which are more readily oxidized than iron. As oxidation progresses, these oxides form part (or possibly in some cases all) of the scale. Exceptions to this are, of course, oxides which are volatile at the temperature of oxidation, e.g., carbon monoxide. The scale on steel may thus have a different mineralogical constitution than the scale formed on pure iron.

In the present study, metallographic evidence of the oxidation of both silicon and chromium in advance of the oxidation of iron was obtained. When silicon and chromium were present together in steel, there was also evidence that the silicon was preferentially oxidized before the chromium. Special attention was given to the oxides produced by heating low carbon iron-chromium and iron-nickel-chromium stainless steels in oxidizing atmospheres.

The steels studied were straight carbon, S.A.E. 2330 and a series of low carbon chromium and nickel-chromium stainless steels. The straight carbon steel samples were taken from forgings made from twenty-pound induction furnace ingots. The S.A.E. 2330 and the stainless steel samples were taken from commercial rolled stock. The analyses of these steels are listed in Table I. An identifying type name by which reference will be made is also given.

The steels were oxidized by heating small rectangular samples in an oxidizing furnace atmosphere for thirty minutes to twelve hours depending on the temperature and the chemical composition of

Table I
Chemical Composition of Steels Investigated

Number	Type	Per Cent C	Mn	P	S	Si	Ni	Cr	Mo	Cu
1	0.20 C	0.21	0.48	0.007	0.024	0.16	....	....	....	....
2	0.30 C	0.31	0.48	0.005	0.021	0.18	....	....	....	....
3	0.40 C	0.39	0.44	0.009	0.022	0.19	....	....	....	....
4	0.50 C	0.50	0.48	0.007	0.022	0.23	....	....	....	....
5	S.A.E. 2330	0.31	0.57	0.011	0.014	0.23	3.39	0.07	....	....
6	5 Cr	0.21	0.37	0.011	0.016	0.23	0.18	5.98	....	....
7	12 Cr	0.07	0.53	0.010	0.008	0.47	0.17	12.56	....	....
8	12 Cr	0.10	0.47	0.022	0.007	0.22	0.44	12.94	....	0.02
9	17 Cr	0.07	0.43	0.011	0.007	0.34	0.22	16.96	....	....
10	18-8	0.05	0.41	0.008	0.008	0.39	10.08	17.90	....	....
11	18-8	0.07	0.47	0.009	0.005	0.44	11.56	20.07	....	....
12	18-8-Mo	0.07	0.78	0.016	0.005	0.58	8.60	18.75	2.73	....
13	27 Cr	0.08	0.42	0.009	0.005	0.45	0.23	25.97	....	....

the steel. No long time scaling tests were made. The temperatures used were 1400, 1800, 2000, 2200, 2400 and 2475 degrees Fahr. (760, 980, 1095, 1205, 1315, 1355 degrees Cent.). After oxidation at these temperatures the samples were quenched in water. Above 1800 degrees Fahr. (980 degrees Cent.) the heating was done in a semi-muffle gas furnace. At 1800 degrees Fahr. (980 degrees Cent.) and below the samples were heated in an electric muffle. The oxidizing atmospheres were obviously different in the two cases. However, we believe that, since we were primarily interested in the mechanism and not the rate of oxidation, long time experiments with carefully controlled atmospheres would not change the general conclusions on the mechanism of the oxidation of the different steels.

The samples were polished at an angle to the scale surface. This method of preparation exposed sufficient metal and scale surrounding the scale-steel interface to permit study of the scale and steel immediately adjacent to the interface. It is important that the method of preparation of the samples should be kept in mind in examining the photomicrographs. The photomicrographs have been mounted so that the scale surface is always toward the top of the page, although frequently beyond the area shown in the photomicrograph.

The metal and scale adjacent to the scale-steel interfaces of a series of carbon steels and of S.A.E. 2330 were observed. The carbon steels were No. 1, to No. 4, inclusive, Table I. The S.A.E. 2330 was No. 5, Table I. These steels contained from 0.16 to 0.23 per cent of silicon and had similar manganese contents, namely 0.44 to 0.57 per cent. They did not differ one from the other in the appearance of the oxides produced by oxidation at each temperature from 1400 to 2475 degrees Fahr. (760-1355 degrees Cent.). At 1400 degrees Fahr. the inner oxide layer in these steels apparently consisted of a single phase, see Fig. 1. The dark spots in the oxide phase in Fig. 1 are pits. The oxide masses in the photomicrograph are projections from the inner ferrous oxide scale layer which were truncated by the polished plane examined under the microscope. There was no visible precipitation of silica or silicates ahead of the oxidation of iron to form the inner ferrous oxide layer of the scale.

At 2000 degrees Fahr. (1095 degrees Cent.) it was evident that the precipitation of oxides took place first along the grain boundaries, see Fig. 2. The first visible evidence of oxidation was the formation of a silicate phase, shown in the few dark rounded particles near the junction of the three grains at the bottom of Fig. 2. The

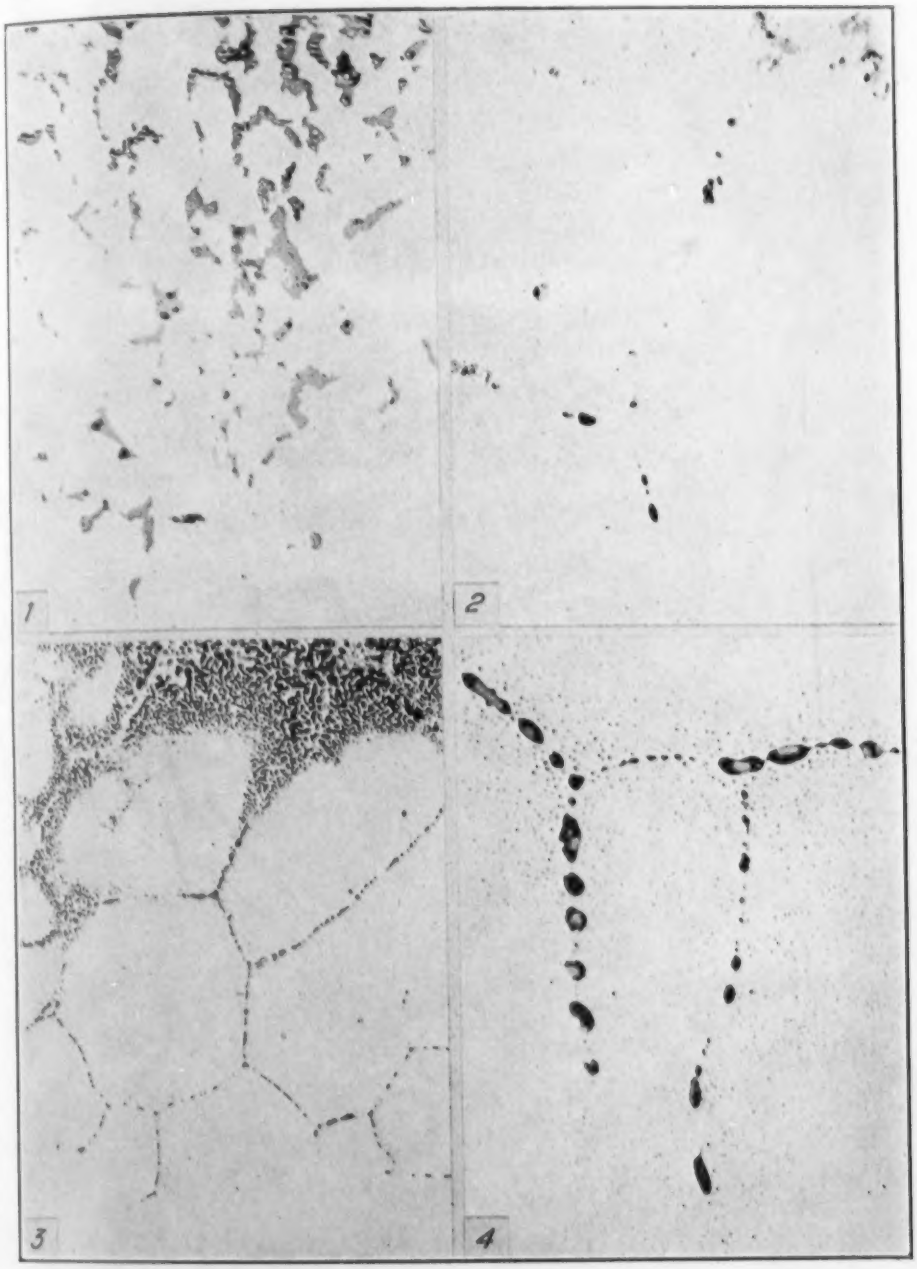

Fig. 1—Ferrous Oxide Produced by Oxidation of Steels No. 1 to 5 at 1400 Degrees Fahr. (760 Degrees Cent.). × 500.
Fig. 2—Silicate (Dark Rounded Particles) and Ferrous Oxide Produced by Oxidation of Steels No. 1 to 5 at 2000 Degrees Fahr. (1095 Degrees Cent.). × 500.
Fig. 3—Inner Scale and Oxides in Grain Boundaries Produced by Oxidation of Steels No. 1 to 5 at 2200 Degrees Fahr. (1205 Degrees Cent.). × 100.
Fig. 4—Detail of Area Similar to Fig. 3. × 500.

small masses of silicate were evidently incorporated in the ferrous oxide which formed along the grain boundaries later, shown in the

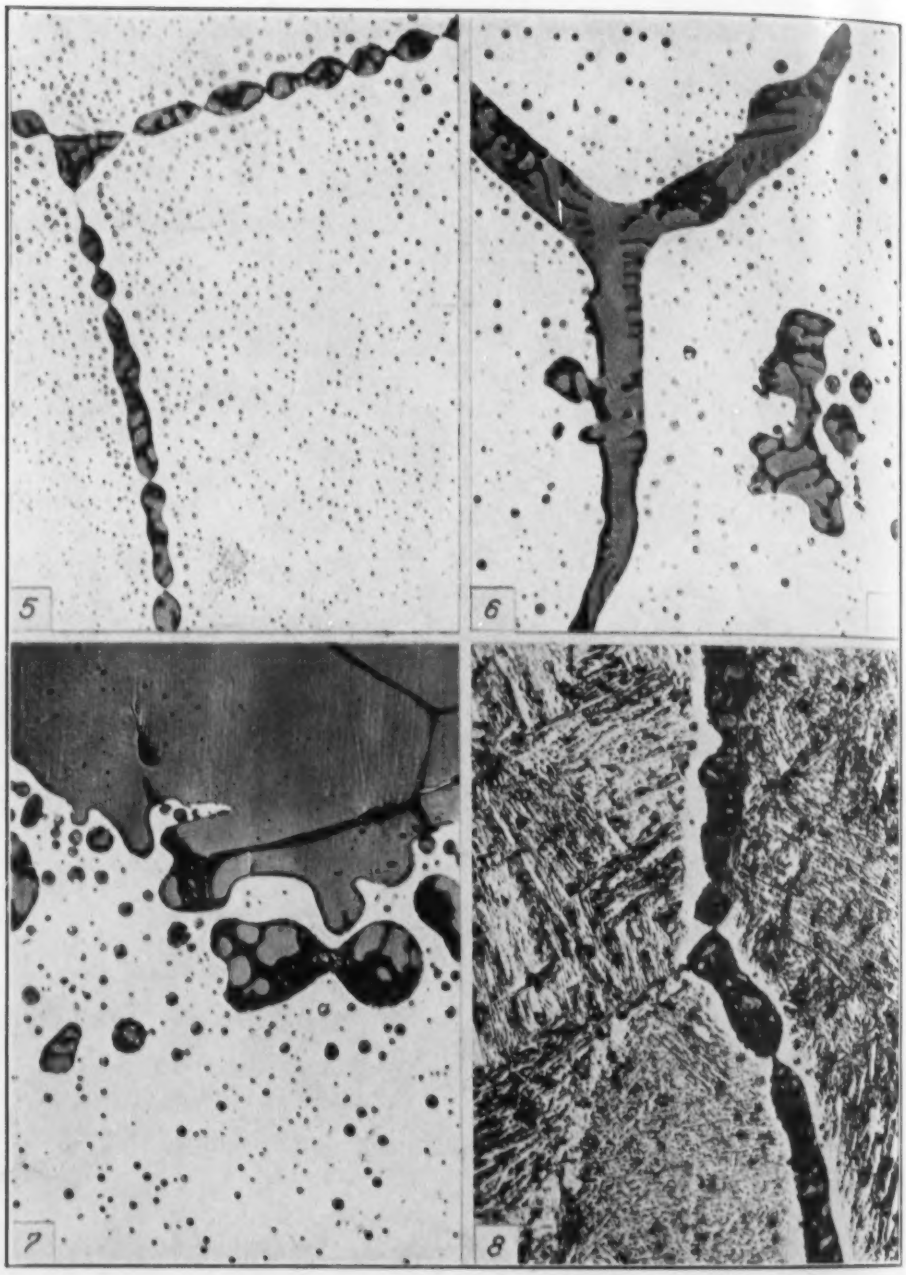

Fig. 5—Ferrous Oxide Dendrites in Silicate Produced by Oxidation of Steels No. 1 to 5 at 2400 Degrees Fahr. (1315 Degrees Cent.). × 500.

Fig. 6—Same as Fig. 5, Produced at 2475 Degrees Fahr. (1355 Degrees Cent.). × 500.

Fig. 7—Inner Scale and Area Similar to Fig. 6 after Etching for 5 Minutes in Boiling Alkaline Sodium Picrate Solution, Silicate Slightly Attacked. × 500.

Fig. 8—Area Similar to Fig. 6 after Etching for 10 Minutes in a Saturated Solution of Stannous Chloride in Ethyl Alcohol, Ferrous Oxide Deeply Attacked. × 500.

oxides in the grain boundary at the top of Fig. 2. In Fig. 2 a precipitate of fine nonmetallic particles, presumably oxides, may be observed within the grains. In case the boundaries of a grain contained precipitated oxides, the fine nonmetallic particles were observed to cover all or all but the centers of the grains. This is illustrated by the grain at the top of the left side of Fig. 2. In case the boundaries of a grain were only partly oxidized (as in the case of the other two grains in Fig. 2) the fine particles had precipitated along and just ahead of the oxidized boundaries of the grains but not in the rest of the grains. The preferential oxidation of silicon was more evident after heating at 2200 degrees Fahr. (1205 degrees Cent.) Figs. 3 and 4. At the first evident oxidation of the grain boundaries, (Fig. 4), the precipitated oxide phase was silicate (dark). Passing from the first precipitated oxide (at the bottom of Fig. 4) towards the scale (at the top and beyond the photograph in Fig. 4) the precipitated oxides also contained a small amount of ferrous oxide phase (medium grey). Between the oxides illustrated in Fig. 4 and the inner scale layer, the ferrous oxide phase became predominant. The inner scale layer may be seen at the top of Fig. 3. At 2400 degrees Fahr. (1315 degrees Cent.) the precipitated oxides resembled those observed at 2200 degrees Fahr. (1205 degrees Cent.) However, the precipitation of oxides in the grain boundaries had occurred to a greater depth in the metal than at 2200 degrees Fahr. (1205 degrees Cent.). As at 2200 degrees Fahr. (1205 degrees Cent.) the first oxidation was of silicon. In areas where the grain boundary oxides consisted of silicate plus ferrous oxide, there were indications that the ferrous oxide had separated from the silicate in dendrites, Fig. 5.

The formation of dendrites of ferrous oxide was even more evident at 2475 degrees Fahr. (1355 degrees Cent.), Fig. 6. This indicates that at the temperature of oxidation these oxides were in a solid plus liquid area of the phase diagram. Benedicks and Löfquist (1)[1] have sketched the liquidus area on which ferrous oxide or a series of solid solutions of manganous oxide in ferrous oxide are in equilibrium with liquid in the ferrous oxide-manganous oxide-silica system. According to the Campbell and Comstock-Wohrman (2) method for the identification of inclusions in iron and steel, the ferrous oxide phase in Fig. 6 was relatively low in manganous oxide since it was very slightly attacked after etching for 10 seconds

[1]The figures appearing in parentheses refer to the bibliography appended to this paper.

in a 10 per cent solution of nitric acid (sp. gr. 1.42) in ethyl alcohol and was not attacked after etching for 5 minutes in boiling alkaline sodium picrate solution (3). The latter is illustrated by Fig. 7 in which the silicate oxide phase (medium grey) has not been attacked while the ferrous phase (dark) has been slightly but definitely attacked. Attack by boiling alkaline sodium picrate indicates the presence of some manganese in the silicate. This etch also showed that the small oxide globules in the grains frequently consisted of two phases, evidently the same phases as existed in the grain boundaries in the same area. The intergranular network which the silicate formed in the inner ferrous oxide scale layer is also shown at the top of Fig. 7. After etching for 10 minutes in a saturated solution of stannous chloride in alcohol, the ferrous oxide was deeply attacked. Fig. 8. After etching for 10 minutes in an aqueous solution of hydrofluoric acid (1 part 48 per cent HF to 4 parts water by volume) the silicate phase was very deeply attacked.

To summarize briefly, it has been experimentally shown that the oxidation of steels containing 0.16 to 0.23 per cent of silicon differs visibly from the oxidation of pure iron at and above 2000 degrees Fahr. (1095 degrees Cent.). This difference is manifested by the oxidation of silicon in advance of the oxidation of the iron in the alloy accompanied by separation of aggregates of silicate or silicate plus ferrous oxide in the grain boundaries of the metal underneath the scale. The presence of manganese in the silicate phase was indicated. The silicate was evidently a liquid at high temperatures in the steels examined.

The chromium and nickel-chromium stainless steels were characterized by preferential oxidation of both silicon and chromium before the oxidation of iron in the alloy. At higher temperatures evidence of the preferential oxidation of silicon ahead of chromium was obtained. The temperature at which this became apparent was dependent on the silicon content of the alloy. The oxidation of chromium ahead of the iron was observed from 1400 to 2400 degrees Fahr. (760-1315 degrees Cent.). The oxide systems obtained were complex but were evidently composed of one or combinations of two or more of the following oxides; ferrous oxide, at least two oxides high in chromium and silica or silicate. Two oxides high in chromium were produced which resembled the oxides high in chromium previously described (4), (5) in general characteristics by reflected light and color by transmitted light. However, fundamental

Table II

Steel	Inner layer of green oxide high in chromium with adjacent layer of red oxide high in chromium	Inner layer of red oxide high in chromium with red or complex oxides high in chromium precipitated in the steel	Inner layer of ferrous oxide with red or complex oxides high in chromium precipitated in steel
5 Cr			1400 to 2400 degrees Fahr.
12 Cr		1400 degrees Fahr. (No oxide precipitated in metal.) 1800 degrees Fahr.	2000 to 2400 degrees Fahr.
17 Cr	1400 to 1800 degrees Fahr.	1800 to 2200 degrees Fahr.	2400 degrees Fahr.
18-8	1400 to 2200 degrees Fahr.	2000 to 2400 degrees Fahr. (plus Ni or Ni-Fe alloy in inner scale.)	
27 Cr	1800 to 2400 degrees Fahr.	2400 degrees Fahr.	

work on the system iron-chromium-silicon-oxygen is needed before a complete discussion of the oxidation of stainless steels could be attempted. Nevertheless, the few experimental observations recorded indicate the general mechanism of the oxidation of stainless steels, the reasons for the increased resistance to scaling due to the substitution of chromium for iron in the alloy and the mechanism which limits the low chromium alloys to the low temperature field.

In general the stainless steels studied (No. 6 to No. 13, inclusive, Table I) were characterized by scaling which assumed similar forms in the different alloys. However, the temperatures at which these similar forms occurred were dependent on the chromium content of the steels. This relationship as experimentally observed has been summarized in Table II.

5 Per Cent Chromium Steel (No. 6, Table I)

After oxidation at 1400 degrees Fahr. (760 degrees Cent.), the appearance of the precipitated oxides just within the metal near the scale-metal interface is shown in Fig. 9. The oxide occurred as outlining of the grain boundaries of the metal and as minute particles within the grains. The oxides were too finely divided to permit observation of their characteristics. The penetration of such oxidation into the metal underneath the scale was slight. Such sections had identical appearance after six hours and after twelve hours at temperature.

After oxidation at 1800 degrees Fahr. (980 degrees Cent.) the form of the precipitated oxides was intermediate between that just

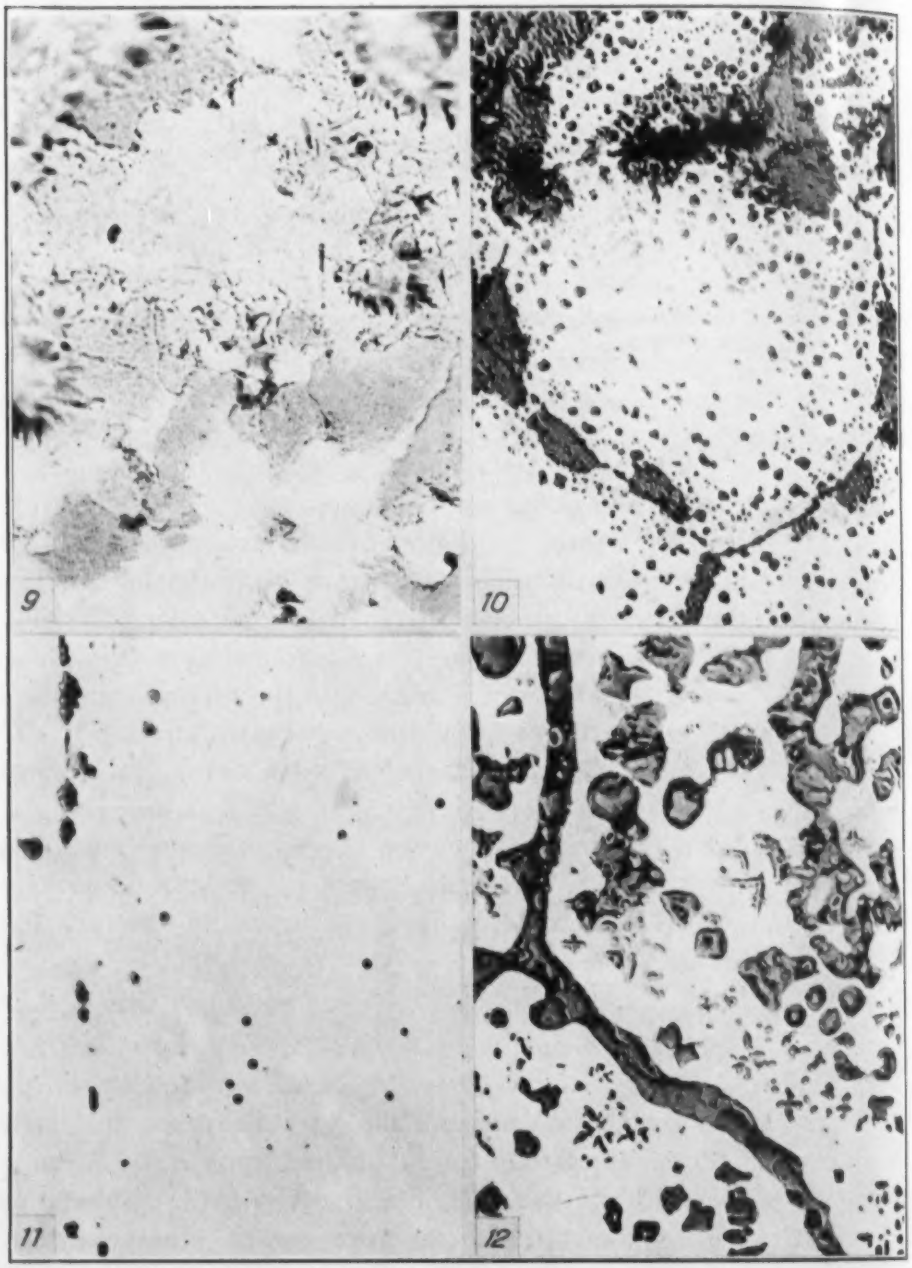

Fig. 9—Chromium Steel No. 6 Containing 5 Per Cent Chromium Oxidized at 1400 Degrees Fahr. (760 Degrees Cent.). × 500.
Fig. 10—Chromium Steel No. 6 Containing 5 Per Cent Chromium Oxidized at 2000 Degrees Fahr. (1095 Degrees Cent.). × 500.
Fig. 11—Chromium Steel No. 6 Containing 5 Per Cent Chromium Oxidized at 2400 Degrees Fahr. (1315 Degrees Cent.). × 500.
Fig. 12—Same as Fig. 11.

described for 1400 degrees Fahr. (760 degrees Cent.) and that to be described for 2000 degrees Fahr. (1095 degrees Cent.).

Fig. 10 shows a typical area in the steel just underneath the scale after oxidation at 2000 degrees Fahr. (1095 degrees Cent.). The innermost precipitation of oxide had taken place along the grain boundaries. This resulted in the formation of well defined crystals of an oxide high in chromium in the grain boundaries of the metal. By darkfield illumination these crystals were bright red, i.e., their color by transmitted light was bright red. Next the red oxide crystals had formed within the grains, beginning close to the grain boundaries and finally dotting the whole grain. Apparently no ferrous oxide formed as a separate phase until after the major portion of the chromium had been oxidized. Ferrous oxide first formed as projections of the inner scale layer along the grain boundaries of the metal. The structure thus developed is that shown in Fig. 10. The red oxide was enveloped by the ferrous oxide of the inner scale without evident change in the appearance of the red oxide. There was a cellular network of red oxide in the inner ferrous oxide scale layer. This network corresponded to the grain-size of the steel at the time the red oxide was precipitated in the grain boundaries of the metal.

At higher temperatures the oxide which separated ahead of the scale-metal interface was less translucent and was apparently mixed with at least one other phase. Spheroids of silica or silicate also separated, Fig. 11. Between the area shown in Fig. 11 and the scale, the oxidation of the metal had resulted in the formation of at least two oxides high in chromium as well as a silicate phase (dark). (Fig. 12.) No ferrous oxide is present in this photograph.

12 Per Cent Chromium Steel (No. 7 and 8, Table I)

The oxides precipitated on oxidation of the two 12 per cent chromium steels were identical except for the amount of silica or silicate formed at high temperatures. This reflected the silicon analyses of the steels.

Fig. 13 illustrates the scale-metal interface in 12 per cent chromium steel after oxidation at 1400 degrees Fahr. (760 degrees Cent.). No precipitation of oxide in the metal near the interface was observed. The oxide which formed the inner scale layer gave some red internal reflections by darkfield illumination.

After oxidation at 1800 degrees Fahr. (980 degrees Cent.) the oxides precipitated in the metal near the scale are shown in Fig. 14. The form is intermediate between the forms which occurred in

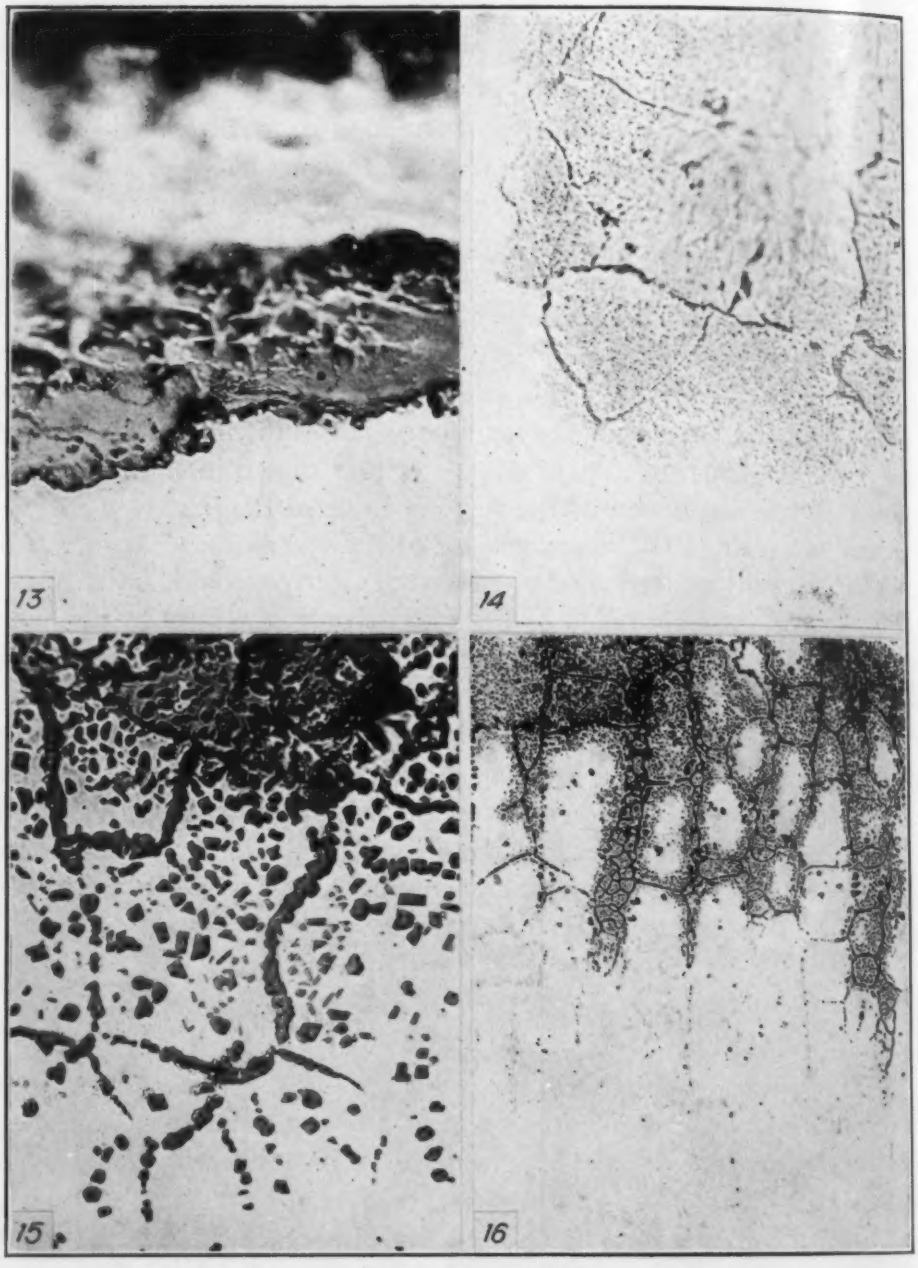

Fig. 13—Chromium Steel No. 7 Containing 12 Per Cent Chromium Oxidized at 1400 Degrees Fahr. (760 Degrees Cent.). × 500.

Fig. 14—Chromium Steel No. 7 Containing 12 Per Cent Chromium Oxidized at 1800 Degrees Fahr. (980 Degrees Cent.). × 500.

Fig. 15—Chromium Steel No. 8 Containing 12 Per Cent Chromium Oxidized at 2000 Degrees Fahr. (1095 Degrees Cent.). × 500.

Fig 16—Chromium Steel No. 7 Containing 12 Per Cent Chromium Oxidized at 2200 Degrees Fahr. (1205 Degrees Cent.). × 100.

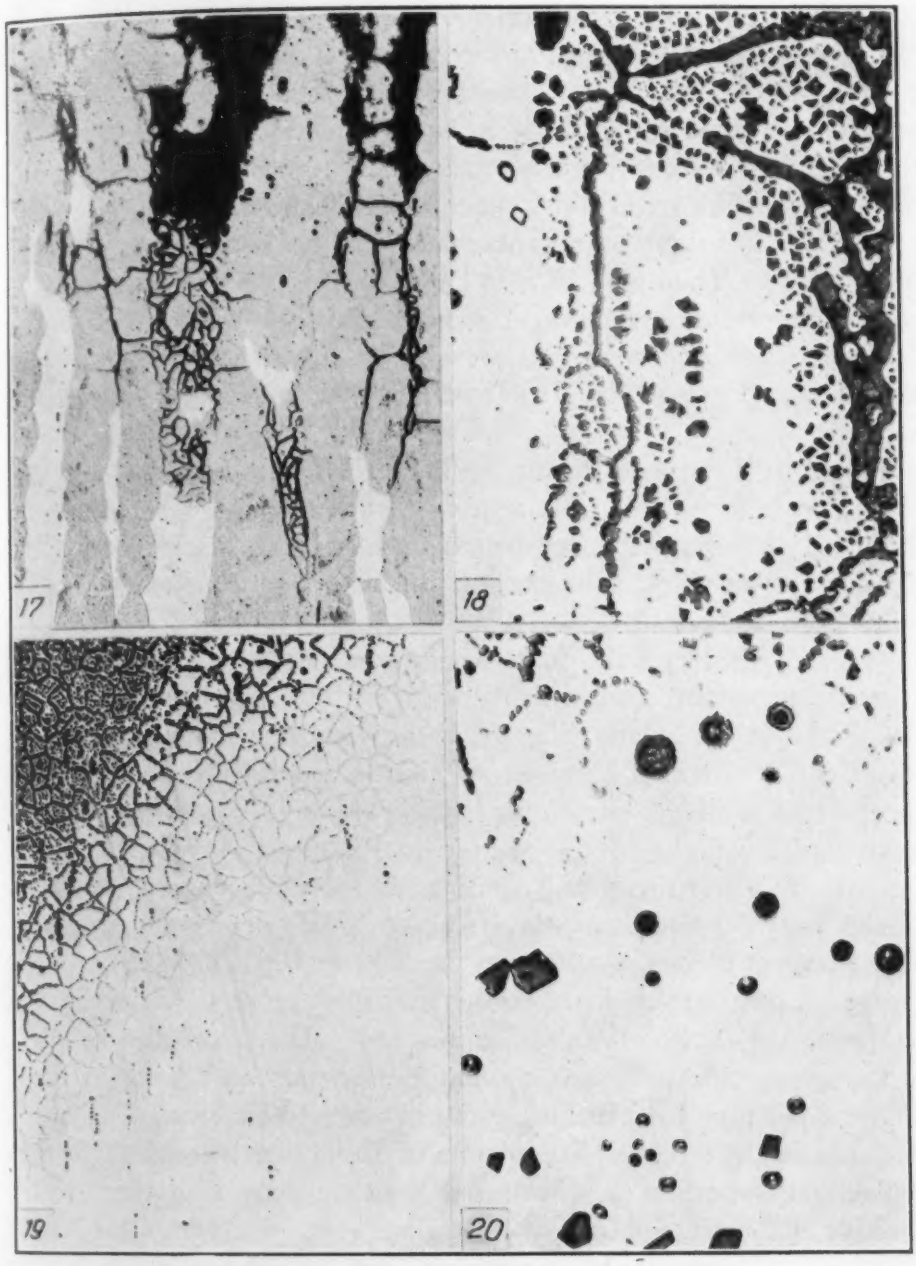

Fig. 17—12 Per Cent Chromium Steel Showing Area Similar to Fig. 16, Etched in Nital. × 100.
Fig. 18—Detail of Area Similar to Fig. 16. × 500.
Fig. 19—Chromium Steel No. 7 Containing 12 Per Cent Chromium Oxidized at 2400 Degrees Fahr. (1315 Degrees Cent.). × 100.
Fig. 20—Chromium Steel No. 8 Containing 12 Per Cent Chromium Oxidized at 2400 Degrees Fahr. (1315 Degrees Cent.). × 500.

the 5 per cent chromium steel at 1400 and 2000 degrees Fahr. (760 and 1095 degrees Cent.).

At 2000 degrees Fahr. (1095 degrees Cent.) the oxidation of 12 per cent chromium steel apparently took place in a manner analogous to the oxidation of the 5 per cent chromium steel at the same temperature except that a larger amount of oxide high in chromium precipitated in the steel, see Fig. 15. The amount of oxide high in chromium which precipitated in the metal appears to be a function of the chromium content of the steel. Compare Fig. 15 with Fig. 10. The oxide high in chromium, Fig. 15, gave some red internal reflections by darkfield illumination. As in the 5 per cent chromium steel, the red oxide was enveloped by the inner ferrous oxide scale (top of Fig. 15) without evident change in the red oxide.

Figs. 16, 17 and 18 illustrate the pattern of the precipitated oxides after oxidation at 2200 degrees Fahr. (1205 degrees Cent.). The pattern of the precipitated oxides was banded and was dependent in form on the coexistence of alpha and gamma bands in the steel. Figs. 16 and 17.

Fig. 19 illustrates the form of the precipitated oxides in the 12 per cent chromium steel which contained 0.47 per cent of silicon (No. 7, Table I), after oxidation at 2400 degrees Fahr. (1315 degrees Cent.). Strings of silica or silicate particles formed in advance of any visible separation of oxides high in chromium. Next the oxidation of chromium occurred. Oxides high in chromium precipitated in the metal and complex oxide-silica or oxide-silicate globules were formed from the strings of silica or silicate droplets. Various stages in this process may be seen in Fig. 20. This photomicrograph illustrates the transition from silica or very glassy silicate particles to the complex oxide-silica or oxide-silicate particles. Some silica or glassy silicate spheroids may be seen at the bottom of Fig. 20 (the small rounded particles with light concentric rings). As the chromium in the steel oxidized, some of the oxide formed evidently dissolved in the silica or silicate particles and saturated them with the oxide at the temperature of oxidation. On quenching, this solution of oxide high in chromium and silica or silicate broke down into a mixture of two phases. The beginning of this process may be seen in the round particle at the extreme right of Fig. 20. This particle has a glassy center and an outside rim of a fine mixture of oxide phases. In the three round particles at the top of the photomicrograph, the entire centers are composed of a mixture of oxide phases and the globules have a rim composed of crystals of oxide

high in chromium. This sample, Fig. 20, contained only 0.22 per cent of silicon. Due to the low silicon content, the oxidation of silicon and chromium was nearly simultaneous at 2400 degrees Fahr. (1315 degrees Cent.). In the 12 per cent chromium steel which contained 0.47 per cent silicon, there was sufficient silicon in the metal to form an appreciable amount of silica or silicate definitely in advance of the precipitation of oxide high in chromium as a separate phase. The precipitation of silica or silicate apparently maintains a concentration of oxygen (in the metal) which is too low to cause the separation of oxides high in chromium. Thus oxides high in chromium can precipitate only after the major portion of the silicon in the area has been oxidized. Increase in the silicon content of the alloy increases the amount of silicon, in any portion of steel sample, which must be oxidized before oxides high in chromium can precipitate. Hence the band, inside the scale proper, in which silica or silicate is precipitating widens as the silicon content is increased and the separation of silica or silicate ahead of the oxides high in chromium becomes readily discernible.

17 Per Cent Chromium Steel (No. 9, Table I)

In the 17 per cent chromium steel after oxidation at 1400 degrees Fahr. (760 degrees Cent.), the scale resembles that formed on the 12 per cent chromium steel at 1400 degrees Fahr. (760 degrees Cent.) (Fig. 13) except that traces of an inner layer of green oxide were observed. There was also in this steel (as in the 12 per cent chromium steels) a layer of oxide which gave some red internal reflections. The green oxide occurred as a very thin layer between the metal and the oxide which gave some red internal reflections. No precipitation of oxides in the metal near the interface was observed.

At 1800 degrees Fahr. (980 degrees Cent.) precipitation of red oxide in the metal had evidently begun, see Fig. 21, but occasional traces of the green oxide were still present.

At 2000 degrees Fahr. (1095 degrees Cent.) the inner layer of green oxide had disappeared. The oxides which had precipitated in the metal are shown in Fig. 22, which may be compared with Fig. 17 which shows oxides precipitated by oxidation of 12 per cent chromium steel at 1800 degrees Fahr. (980 degrees Cent.).

At 2200 degrees Fahr. (1205 degrees Cent.) well-formed crys-

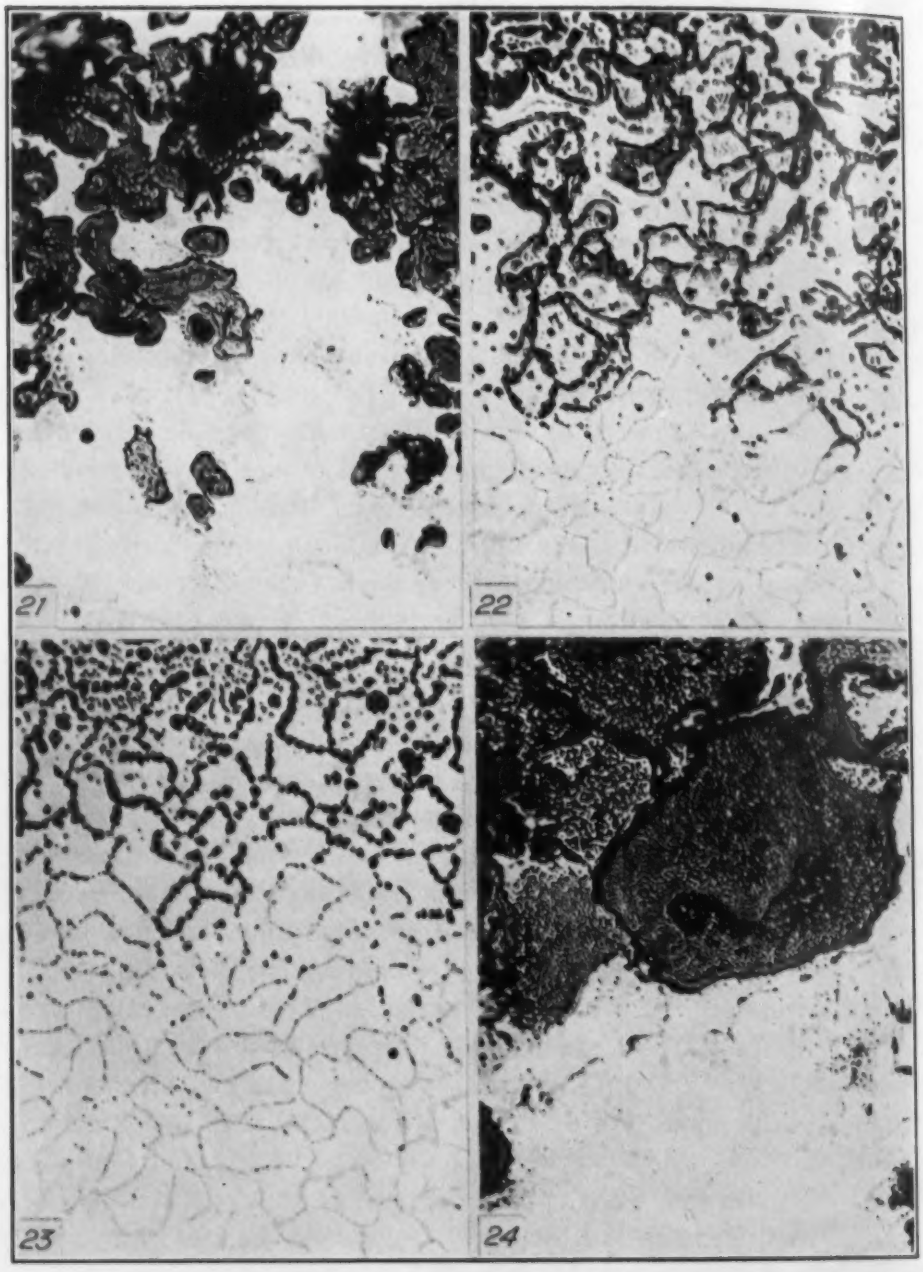

Fig. 21—Chromium Steel No. 9 Containing 17 Per Cent Chromium Oxidized at 1800 Degrees Fahr. (980 Degrees Cent.). × 500.

Fig. 22—Chromium Steel No. 9 Containing 17 Per Cent Chromium Oxidized at 2000 Degrees Fahr. (1095 Degrees Cent.). × 500.

Fig. 23—Chromium Steel No. 9 Containing 17 Per Cent Chromium Oxidized at 2200 Degrees Fahr. (1205 Degrees Cent.). × 500.

Fig. 24—Stainless Steel No. 10 (18-8) Oxidized at 1800 Degrees Fahr. (980 Degrees Cent.). × 500.

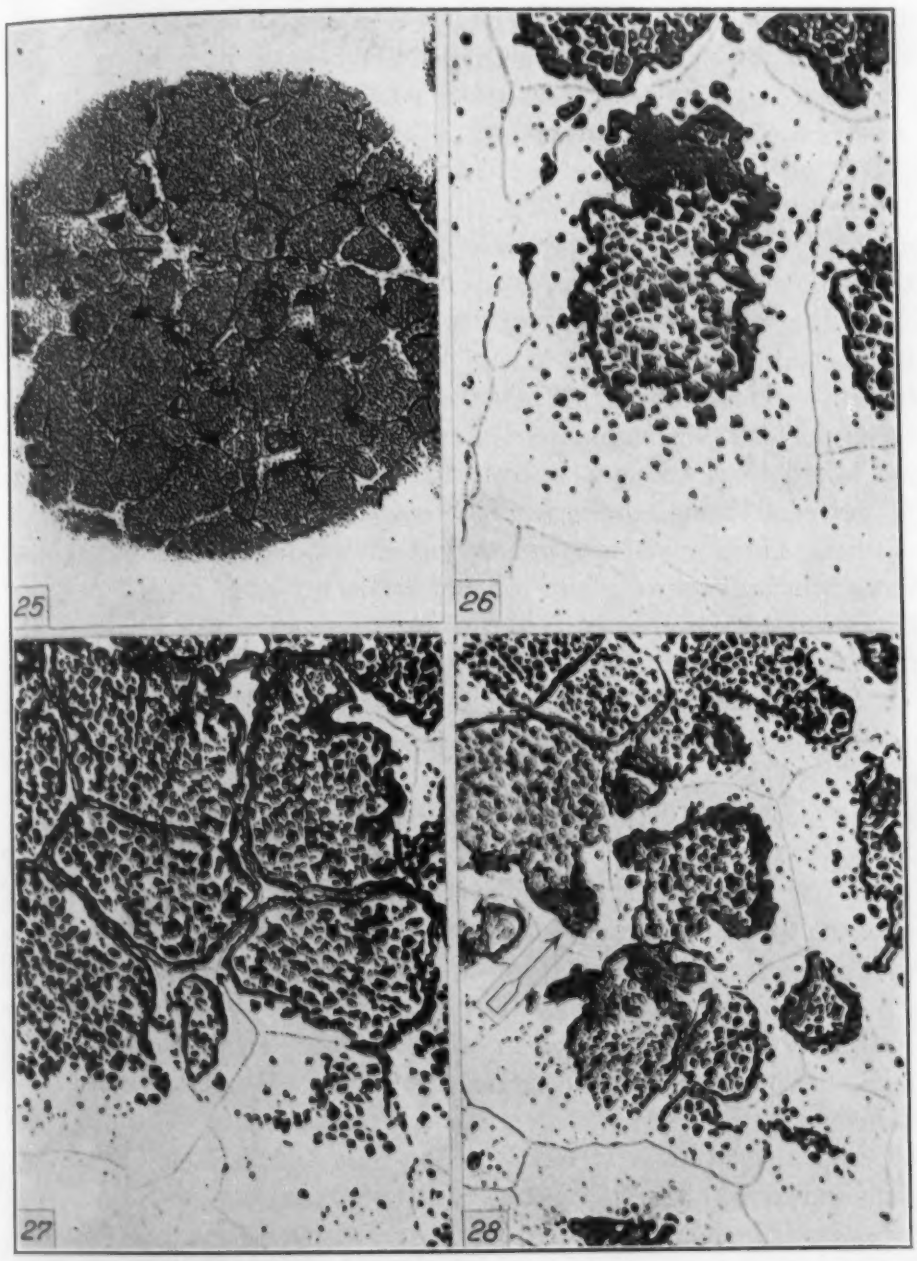

Fig. 25—Nodules of Accelerated Scaling on 18-8 Stainless Steel No. 10 Oxidized at 2000 Degrees Fahr. (1095 Degrees Cent.). × 100.
Fig. 26—Nodules of Accelerated Scaling on 18-8 Stainless Steel No. 12. × 500.
Fig. 27—Same as Fig. 26. × 500.
Fig. 28—Same as Fig. 26. × 500.

tals of oxide high in chromium precipitated in the metal. These resembled the oxide formed in the 12 per cent chromium steels at 2000 degrees Fahr. (1095 degrees Cent.). Compare Fig. 23 with

Fig. 15. Most of the oxide crystals in Fig. 23 appeared dark by darkfield illumination although occasional red internal reflections were observed. The loss of translucence of the red oxide with increase of the chromium content of the steel appears to be a true property of the oxide since the crystal size of the red oxide in the 5 per cent chromium steel (Fig. 10) and in the 17 per cent chromium steel (Fig. 23) were the same. For equally translucent crystals of the same size and shape, an equal amount of light should be reflected from the oxide-steel interfaces at the back and sides of the oxide crystals as they are observed in polished sections by darkfield illumination. However, in this case the oxide observed after oxidation of the 5 per cent chromium steel was bright red while only occasional red internal reflections were observed in the oxide precipitated in the 17 per cent chromium steel. This observed change in the character of the oxide crystals with increasing chromium content of the steel from which they were precipitated lends credence to the explanation suggested by Dayton (6) for his failure to observe red color by reflected light in an apparently similar oxide, in a sample of chromium, which he reported to be red when separated from the metal and examined by transmitted light.

18-8 Steels (No. 10, No. 11 and No. 12, Table I)

After oxidation at 1400 degrees Fahr. (760 degrees Cent.) the scale on all three steels contained a thin and apparently continuous layer of green oxide next to the metal. On the other side of the green oxide was a layer of oxide which gave some red internal reflections. As in the 17 per cent chromium steel, there was no visible precipitation of oxide in the metal near the scale-steel interface. At 1800 degrees Fahr. (980 degrees Cent.) the precipitated oxides (Fig. 24) resembled those produced by the oxidation of the 17 per cent chromium steel (Fig. 21) at the same temperature.

At 2000 degrees Fahr. (1095 degrees Cent.), however, localized nodules of scale formation were observed. They were apparently similar to those mentioned by Heindlhofer and Larsen (7). One of these is shown in Fig. 25. The nodules had more or less rounded outlines on the surface of the sample. The penetration of oxidation into the metal is deepest under the center of the nodules. Figs. 26, 27 and 28 illustrate the microstructure of these nodules on the 18-8-molybdenum steel (No. 12, Table I). Exactly the same char-

acteristics were observed in the nodules on the regular 18-8 steel (No. 10, Table I) and on the 18-8 steel with higher chromium and nickel analyses, (No. 11, Table I). The grain boundaries in the nodules were outlined with oxide. We believe that this oxide was silica or a silicate since at a somewhat higher temperature (2200 degrees Fahr.) the first oxide formed in the grain boundaries in these steels had the appearance and characteristics of silica or silicate, see Fig. 29. The centers of the grain in the nodules contain crystals of oxide high in chromium surrounded by a band of oxides high in chromium. These oxide bands sometimes form a double edge of the grain boundaries, see Fig. 27. The crystals of oxides high in chromium and most of the oxide bands between the crystals and the grain boundaries were dark with very few red internal reflections by darkfield illumination. Sometimes edges of green oxide occurred. One of these is indicated by an arrow in Fig. 28. The green oxide always occurred on the side of the oxide rim next to the grain boundary. The localized nodules of scale formation were present together with massive scale, illustrated by Fig. 30. In this scale the layer next to the metal was green by darkfield illumination. The other layer was similar to the red oxide layer observed on the 12 per cent chromium steel at 1400 degrees Fahr. (760 degrees Cent.). At 2200 degrees Fahr. (1205 degrees Cent.) the scaling had changed to the type produced on the 5 per cent chromium and 12 per cent chromium steels by oxidation at lower temperatures, i.e., the formation of oxides high in chromium along the grain boundaries and within the grains of the metal, see Fig. 31. We believe that the localized nodules of scale formation are a manifestation of the shift in the type of scaling from that produced on these steels at 1800 degrees Fahr. (green and red oxide layers) to that produced at 2200 degrees Fahr. (precipitation of oxides in the grain boundaries of the metal underneath the scale). The nodules are apparently caused by the failure of the green oxide layer to form in localized areas. This evidently permits oxidation in these areas to proceed at an accelerated rate. This shift in the scale type depends on the chromium content of the alloy. With 17 per cent of chromium (No. 9, Table I) precipitation of red oxide in the grain boundaries of the metal was observed after oxidation at 1800 degrees Fahr. (980 degrees Cent.) although some green oxide coexisted, but no green oxide was observed after oxidation at 2000 degrees Fahr. (1095 degrees Cent.). With 18 per cent of chromium (No. 10, Table I) the

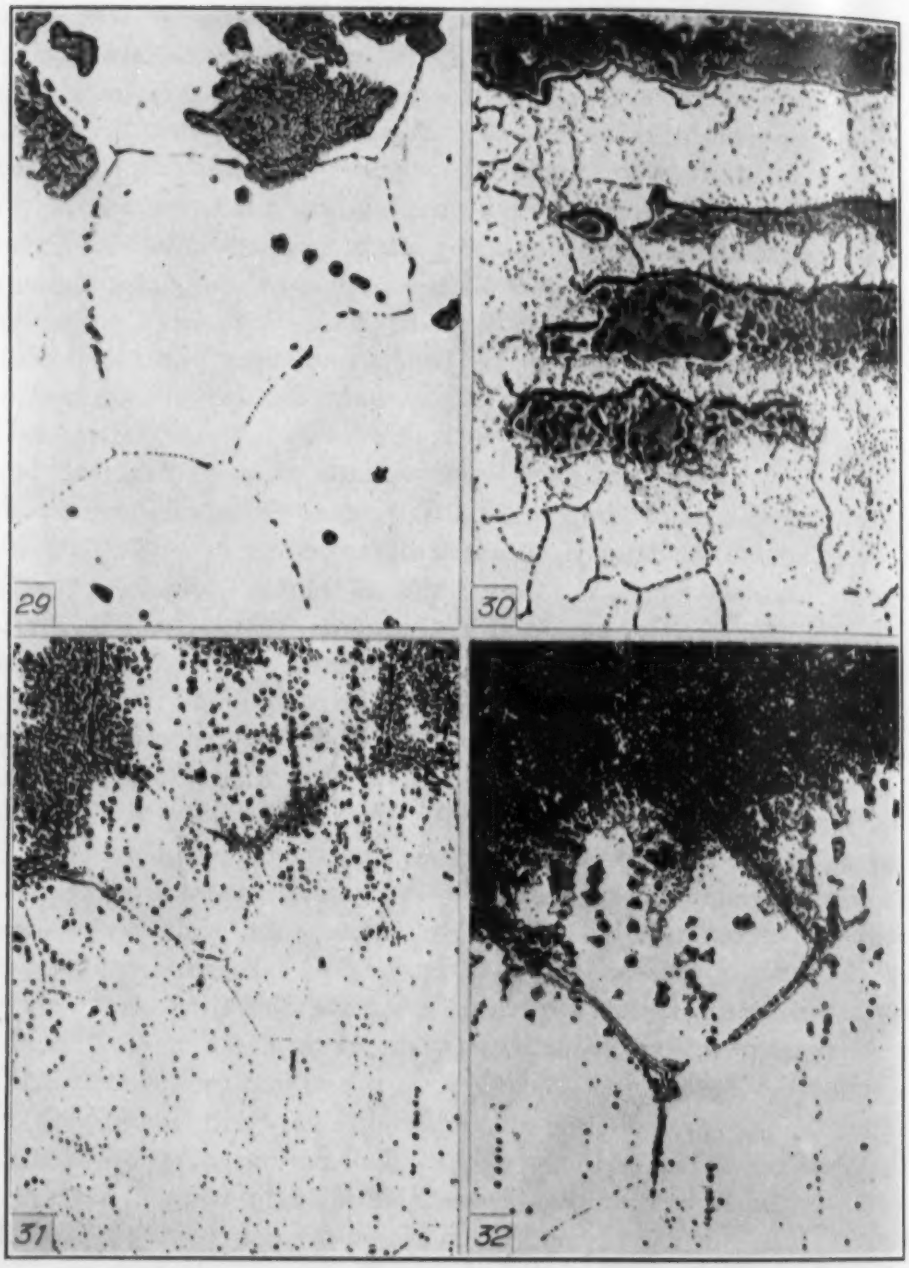

Fig. 29—Stainless Steel No. 12 (18-8) Oxidized at 2200 Degrees Fahr. (1205 Degrees Cent.). × 500.

Fig. 30—Stainless Steel No. 12 (18-8) Oxidized at 2000 Degrees Fahr. (1095 Degrees Cent.). × 500.

Fig. 31—Stainless Steel No. 12 (18-8) Oxidized at 2200 Degrees Fahr. (1205 Degrees Cent.). × 100.

Fig. 32—Stainless Steel No. 10 (18-8) Oxidized at 2400 Degrees Fahr. (1315 Degrees Cent.) Etched in Aqua Regia-Glycerine Reagent. × 100.

change in the type of oxidation occurred about 2000 degrees Fahr. (1095 degrees Cent.). In this steel some green oxide was observed after oxidation at 2000 degrees Fahr. but none after oxidation at 2200 degrees Fahr. (1205 degrees Cent.). With 20 per cent of chromium (No. 11, Table I) traces of green oxide were observed after oxidation at 2200 degrees Fahr. (1205 degrees Cent.) but none after oxidation at 2400 degrees Fahr. (1315 degrees Cent.). However, the particular form, i.e., nodules of accelerated scaling, observed on the 18-8 steels may be conditioned by the nickel in the alloy.

Figs. 32 and 33 illustrate the precipitated oxides produced by scaling at 2400 degrees Fahr. (1315 degrees Cent.). The samples were etched with aqua regia-glycerine reagent to show the extent of the separation of nickel or an alloy of iron and nickel as the chromium was oxidized and removed from the metal phase. The aqua regia-glycerine reagent attacks this residual alloy at a different rate than it attacks the original stainless alloy, see Fig. 33. Fig. 34 shows that oxidation of the chromium in the alloy left a similar metallic residue within and adjacent to the inner scale at 2000 degrees Fahr. (1095 degrees Cent.). Since this residue is obviously either nickel or an iron-nickel alloy and may have a different permeability for oxygen than the original stainless alloy and the oxides in the scale, it adds another factor to be considered in the scaling rate of the iron-nickel-chromium alloys. Such a metallic residuum was not present after oxidation of the chromium-iron stainless steels.

Fig. 35 illustrates the inner scale and the oxides precipitated in the adjacent metal after oxidation of the 18-8-molybdenum steel (No. 12, Table I) at 2400 degrees Fahr. (1315 degrees Cent.). This steel contained 0.58 per cent of silicon. It was evident from examination of the steel that the separation of silica or silicate particles generally occurred at the boundaries between the alpha phase and the gamma phase. This might be expected since silicon is more soluble in alpha iron than in gamma iron while oxygen is more soluble in the gamma phase. Fig. 36 is a detail of one of the groups of silica or silicate particles arrested, by quenching, in the process of taking oxide high in chromium into solution. Fig. 36 may be compared with Fig. 20 which showed a similar reaction in 12 per cent chromium steel. The alternate dark and bright bands in the large irregular silicate particle at the bottom of Fig. 35 are interference bands such as have been described by Benedicks and Löfquist (8).

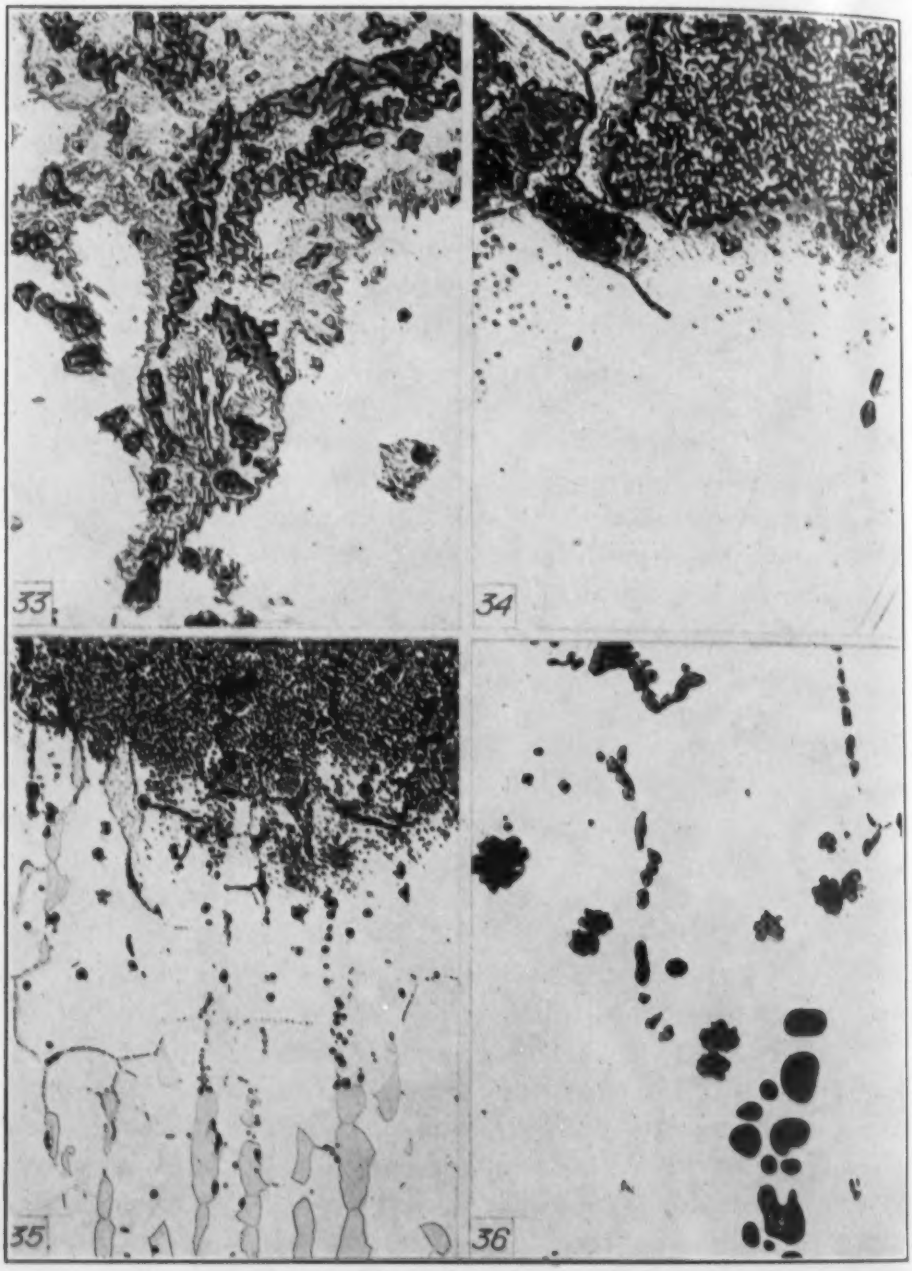

Fig. 33—Detail of Area of 18-8 Stainless Steels Similar to Fig. 32. × 500.
Fig. 34—Stainless Steel No. 11 (18-8) Oxidized at 2000 Degrees Fahr. (1095 Degrees Cent.) Etched in Aqua Regia-Glycerine Reagent. × 500.
Fig. 35—Stainless Steel No. 12 (18-8) Oxidized in Alpha Plus Gamma Temperature Range, Etched in Aqua Regia-Glycerine Reagent. × 100.
Fig. 36—Detail of Area Similar to Fig. 35. × 500.

27 Per Cent Chromium Steel (No. 13, Table I)

The scale was very slight on the 27 per cent chromium steel

after oxidation at 1800 degrees Fahr. (980 degrees Cent.). It resembled the scale shown in Fig. 37 (2000 degrees Fahr.) except that there was no observable precipitation of silica or silicate in the metal underneath the scale. The scale layer next to the steel gave green internal reflections and the next scale layer occasional red internal reflections. By heating at a higher temperature, see Fig. 38, it was evident that the oxide precipitated in the metal near the scale at 2000 degrees Fahr. was silica or a very glassy silicate. The two oxide layers in the scale may also be seen in Fig. 38. The scale and precipitated silica or silicate produced by oxidation at 2200 degrees Fahr. (1205 degrees Cent.) resembled the illustration in Fig. 38.

At 2400 degrees Fahr. the precipitation of oxides is illustrated by Figs. 39 and 40. Some of the oxide particles gave green internal reflection. In Figs. 39 and 41 it may be seen that oxidation of silicon and chromium occurred within the metal underneath the scale proper. The precipitation of oxides thus formed apparently followed chemical composition banding in the steel.

During the scaling at elevated temperatures of the series of iron-chromium and iron-nickel-chromium stainless steels listed in Table II, the following order of oxygen concentrations appears to be maintained by the precipitation of the various oxide phases in the steel. As long as there is sufficient silicon in or diffusing into the metal near the scale-steel interface to maintain the precipitation of silica or silicate, the oxygen content of the metal will be maintained at a value too low to permit the separation of other oxide phases. The silicon content required to effect this will, of course, depend on the rate at which oxygen is supplied to the metal from the scale. As already shown by Heindlhofer and Larsen (9) the rate of supply of a scaling agent to the metal is dependent on the thickness of the scale, its mineralogical character, the temperature and, in the earlier stages of scaling, on the concentration of the scaling agent in the furnace atmosphere. The effect of the precipitation of oxides high in chromium is analogous to the effect of the precipitation of silica or silicate from the metal. As long as sufficient chromium is present at or diffuses to the scale-steel interface, the green oxide will be precipitated to the exclusion of the formation of other oxide phases. When the concentration of chromium maintained in the metal at the interface is no longer sufficient to maintain the precipitation of the green oxide, then the oxygen concentration in the steel rises and

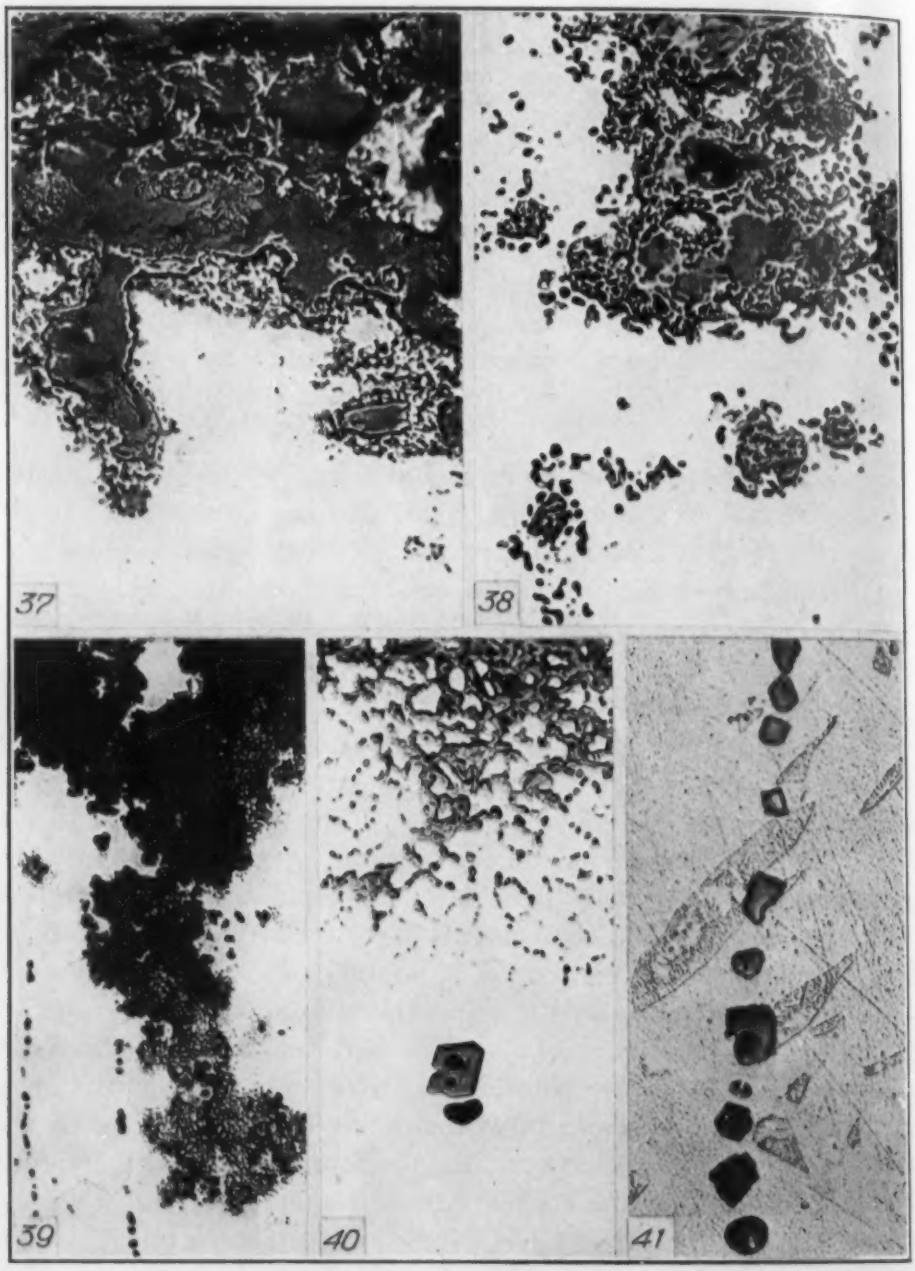

Fig. 37—Chromium Steel No. 13 Containing 27 Per Cent Chromium Oxidized at 2000 Degrees Fahr. (1095 Degrees Cent.). × 500.

Fig. 38—Area Similar to Fig. 37, Oxidized at Slightly Higher Temperature. × 500.

Fig. 39—Chromium Steel No. 13 Containing 27 Per Cent Chromium Oxidized at 2400 Degrees Fahr. (1315 Degrees Cent.). × 100.

Fig. 40—Detail of Area Similar to Fig. 39. × 500.

Fig. 41—Detail of Area Similar to Fig. 39, Etched in Aqua Regia-Glycerine Reagent. × 500.

precipitation of the red oxide occurs. The term, red oxide, as used in this and the following paragraphs includes those oxides which are indistinguishable by reflected light from the bright red oxide observed in the 5 per cent chromium steel after oxidation at 2000 degrees Fahr. (1095 degrees Cent.) but which are often darker when observed by darkfield illumination and at high temperatures are often composed of more than one oxide phase. These oxides have been lumped together for purposes of discussion since we do not know enough about these oxides to make finer distinctions and since the concentration of oxygen maintained by their precipitation appears to be greater than that maintained by the precipitation of the green oxide but less than that necessary to form ferrous oxide as a separate phase. Ferrous oxide appears to be precipitated only after the major portion of the silicon and chromium in the metal adjacent to the scale-steel interface has been oxidized.

In the 5 per cent chromium steel the chromium concentration was not high enough to maintain the precipitation of the red oxide at the scale-steel interface during oxidation at temperatures from 1400 to 2400 degrees Fahr. (760 to 1315 degrees Cent.) inclusive. The red oxide precipitated in the steel adjacent to the inner scale layer. The inner scale was composed of ferrous oxide containing a network of the red oxide.

In the 12 per cent chromium steels there was apparently sufficient chromium at and diffusing to the interface to maintain the precipitation of the red oxide at the interface at 1400 degrees Fahr. At 1800 degrees Fahr. and above the red oxide precipitated in the metal near the interface. At 2000 degrees Fahr. (1095 degrees Cent.) and above the inner scale layer was composed of ferrous oxide with a network of the red oxide.

In the 17 per cent chromium steel, precipitation of the green oxide was maintained at the scale-steel interface at 1400 degrees Fahr. (760 degrees Cent.) but not at 1800 degrees Fahr. (980 degrees Cent.). After oxidation at 1800 degrees Fahr. an occasional piece of green oxide could be observed but there was also some precipitation of red oxide in the metal. After oxidation at 2400 degrees Fahr. (1315 degrees Cent.) the inner scale layer contained some ferrous oxide phase. The 18-8 steels resembled the 17 per cent chromium steel except that the shift in oxidation type occurred between 2000 and 2200 degrees Fahr. (1095 and 1205 degrees Cent.) depending on the chromium content of each steel. Furthermore, no

ferrous oxide was observed in the inner scale layer after oxidation at 2400 degrees Fahr. (1315 degrees Cent.).

In 27 per cent chromium steel both the inner green and the adjacent red oxide layers were maintained during oxidation at temperatures up to and including 2200 degrees Fahr. (1205 degrees Cent.). After oxidation at 2400 degrees Fahr. (1315 degrees Cent.) there was precipitation of oxides in the metal. Both red and green oxides were present at 2400 degrees Fahr. (1315 degrees Cent.).

The formation of the observed two (or more) oxides high in chromium may well account for the low scaling rate of steels which contain chromium. The green oxide forms an inner layer of scale. The red oxide either forms an inner layer of scale or precipitates in the metal adjacent to the scale. In the latter case a continuous cellular network of red oxide is formed in the grain boundaries of the metal. When the inner scale layer is composed of ferrous oxide, this network of red oxide is incorporated in the inner scale layer and adds its effect to the rate of diffusion of oxygen through the scale. In steels which contain nickel, the continuous cellular network of red oxides is present and also a certain amount of nickel or nickel-iron alloy is retained in the inner scale layer. This residuum of nickel or nickel-iron alloy adds another factor in the rate of diffusion of oxygen through the scale. The summary of oxidation forms given in Table II indicates the reason for the limitation of the low chromium alloys to the low temperature field. This shift in oxidation type apparently fits the experimental data of Rickett and Wood (9). They determined the scaling rate of chromium steels at 980 degrees Cent. (1796 degrees Fahr.). They observed that the scaling rate dropped rapidly as the chromium content of the alloy was increased from 12 to 17 per cent.

The data from which Table II was assembled were obtained from samples subjected to comparatively short exposure to scaling conditions. Long time exposure at elevated temperatures might alter the oxidation type, i.e., such steels might scale according to Table II only for a limited time. The chromium concentration in the metal near the interface might be depleted by diffusion and oxidation until the oxidation type indicated in Table II could no longer be maintained and the oxidation type would shift to that of an alloy with lower chromium content. Such a condition was indicated by the scaling of the 18-8 steels at 2000 degrees Fahr. (1095 degrees Cent.). Again, since the rate of supply of oxygen to the metal from the scale

decreases as the thickness of the scale increases, the chromium concentration at the interface might become large enough (in relation to the concentration of oxygen supplied from the scale) to shift the oxidation type towards that maintained during the initial stages of scaling in an alloy containing more chromium. It would seem that these considerations might explain the sudden increase and later resumption of a lower scaling rate which were observed by Heindlhofer and Larsen (9) in the case of 27 per cent chromium steels during scaling at 1100 degrees Cent. (2010 degrees Fahr.). It is also possible that different furnace atmospheres would shift the temperature of occurrence of the various oxidation types which are listed in Table II.

To recapitulate, when silicon was present in stainless steels silica or silicate precipitated ahead of the oxides high in chromium provided that the temperature was high. In steels containing 0.4 to 0.6 per cent of silicon this was observed at 2200 degrees Fahr. (1205 degrees Cent.). When less silicon was present, 0.2 per cent, the separation of silica or silicate was not definite except at 2400 degrees Fahr. (1315 degrees Cent.). The separation of silica or silicate frequently occurred along chemical composition banding, grain boundaries or alpha-gamma phase boundaries in the steel near the scale-steel interface. The scaling of a series of stainless steels containing from 6 to 26 per cent of chromium conformed to a general pattern of oxide formation which assumed similar forms in different alloys. However, the temperatures at which these similar forms occurred depended on the chromium content of the steels, see Table II. The low scaling rate of the stainless steels appears to be due to the formation of two (possibly more) oxides high in chromium. The limitation of the low chromium alloys to the low temperature field is consistent with the shifts of oxidation type observed.

It is a pleasure to acknowledge the generous encouragement of Dr. M. A. Grossmann throughout the course of this work.

References

1. C. Benedicks and H. Löfquist, "Non-Metallic Inclusions in Iron and Steel," p. 101, New York, 1931.
2. A. S. M. National Metals Handbook, (1933 ed.) p. 636 and 637.
3. A. S. M. National Metals Handbook, (1933 ed.) p. 632, reagent 4a.
4. Stephen F. Urban and John Chipman, "Nonmetallic Inclusions in Steel," TRANSACTIONS, American Society for Metals, Vol. 23, 1935, p. 105.

5. M. Baeyertz, TRANSACTIONS, American Society for Metals, Vol. 22, 1934, p. 625.
6. R. W. Dayton, Technical Publication No. 593, American Institute of Mining and Metallurgical Engineers, 1935, p. 23 and 24.
7. K. Heindlhofer and B. M. Larsen, *Metal Progress,* September 1934, p. 34.
8. Benedicks and Löfquist, *Jernkontorets Annaler,* Vol. 117, p. 443-56, Sept. 1933. (Read in translation only.)
9. K. Heindlhofer and B. M. Larsen, TRANSACTIONS, American Society for Metals, Vol. 21, 1933, p. 865.
10. R. L. Rickett and W. P. Wood, TRANSACTIONS, American Society for Metals, Vol. 22, 1934, p. 358.

DISCUSSION

Written Discussion: By R. L. Rickett, Firestone Steel Products Co., Akron, Ohio.

Anyone who has made microscopic studies of scaled specimens can appreciate the large amount of careful work necessary to produce the results recorded in this paper. Fundamental information of this sort is greatly needed, and it is to be hoped that the author will continue her investigation and extend the methods used here to the whole cross section of scale produced under varying conditions of time, temperature, and alloy content.

Information regarding the reactions occurring at the scale-metal interface and within the metal is, of course, of considerable importance. Much more important, though, in the opinion of the present writer, is a knowledge of the constitution of the scale layer as it is first formed and the changes that take place as the scaling process continues. The metallographic method employed by the author is one method of attacking this problem, but one involving considerable difficulties in technique. Also, as mentioned by the author, more information regarding the systems composed of the principal alloying elements and their oxides would probably be necessary for a complete interpretation of the structures encountered.

The compounds formed at the scale-metal interface at any period in the scaling process depend upon the amount of scaling agent reaching this point through the scale, the composition of the alloy and the temperature. In this way some indirect information as to the rate of diffusion through the scale might be obtained when investigating the scaling of complex alloys. Identification of the two "oxides high in chromium" described by the author would be of great value in this respect, when studying the oxidation of iron-chromium alloys.

The order of precipitation of oxides within the scale as found by the author is interesting, but probably has little effect on the over-all scaling rate in the cases discussed. Reactions within the metal may, however, have considerable effect when there is rapid inter-granular penetration, as sometimes occurs in the presence of sulphur gases. In such a case a large amount of metal may be enclosed within a network of scale and the conversion of these "islands" of metal to scale may take place at a lower rate than the penetration of scale.

The order of oxidation of silicon and chromium within the metal as found

by the author is what might be expected from the results given by Chipman for the deoxidation of steel by these elements[1] bearing in mind, however, that Chipman's results as given apply to liquid steel at 1600 degrees Cent. (2910 degrees Fahr.). It might be surmised that aluminum in an alloy would be oxidized at a greater depth than silicon and chromium. The fact that silica or silicates were observed by the author only in the specimens oxidized at the higher temperature used may be because such temperatures are necessary for the particles to coalesce to a sufficient size to be easily visible. The fact that chromium is more readily oxidized than iron at low oxygen pressures was demonstrated by W. P. Wood and the present writer.[2]

The formation of nodules of scale on 18 per cent chromium-8 per cent nickel alloys at temperatures of about 1095 degrees Cent. (2000 degrees Fahr.) has also been observed by W. P. Wood and the writer. They found, too, that the oxidation rate of such alloys was quite variable at this temperature, indicating that it is probably a region of rapid change in the temperature-rate of scaling relationship for the alloys.

The author concludes that the formation of two or more oxides high in chromium at the scale-metal interface and within the metal may account for the behavior of the series of chromium alloys towards oxidation. It is the view of the present writer that the formation of these oxides and the rate of scaling both depend upon a common factor, that is the amount of metal and of oxygen diffusing counter-currently through the scale. This factor, in turn, depends upon the type of scale initially produced and the changes that take place in the scale during the course of the scaling process.

Written Discussion: By H. A. Schwartz, Manager of Research, National Malleable & Steel Castings Co., Cleveland.

While the author has concerned herself mainly with the oxides formed in alloys of iron with chromium and silicon, it may not be inopportune to offer for record an observation as to the composition of oxide layers.

It was noted some years ago that annealing pots (used in the annealing of malleable castings) made of rather low carbon white cast iron containing some 14 per cent of chromium formed in use two layers of oxide. The outer layer whose fracture was bright and almost metallic in appearance, contained 63.7 per cent iron and amounts of chromium ranging from 0.6 per cent downward. An inner layer which was dull and earthy in fracture contained 44.8 per cent iron and 17.5 per cent chromium. No particular effort was made to secure complete analyses.

Written Discussion: By M. A. Scheil and S. L. Hoyt, Research Metallurgist and Director of Metallurgical Research, A. O. Smith Corp., Milwaukee.

During our investigation of various heat resisting alloys, we had occasion to study quite a few alloys of Fe-Cr compositions. We were interested in high temperature stability and made several accelerated life tests of a few pertinent compositions of these alloys. We found that the scaling or oxida-

---

[1]John Chipman, "Application of Thermodynamics to the Deoxidation of Liquid Steel," TRANSACTIONS, American Society for Metals, Vol. 22, 1934, p. 431.

[2]R. L. Rickett and W. P. Wood, TRANSACTIONS, American Society for Metals, Vol. 22, 1934, p. 376.

tion takes place similarly as the author has pointed out, and in this connection we would like to present a few observations that we have made using reflected polarized light on Fe-Cr alloys containing above 30 per cent chromium.

Observations of the scale formed or internal oxidation that takes place in these alloys was performed upon life tested wires. We used ⅛ inch diameter swaged wires which were heated electrically and intermittently in air to test temperatures above 2400 degrees Fahr. to accelerate scaling. Many of these test wires were cross-sectioned, polished and microscopically examined after life testing, and the following account is given of our observations.

An alloy wire of 58.0 per cent chromium, 0.08 per cent silicon, and 0.06 per cent carbon was heated over 2 hours at 2550 degrees Fahr. Due to a hot spot, the wire burned out in the life test, and an examination was made of it at this point. Our sample showed large cubical chromite inclusions when examined with the metallurgical microscope using plane reflected light. These appeared as single phase crystalline inclusions of a light gray color. Many of the same inclusions when examined with reflected polarized light under crossed nicols were birefringent and showed brilliant green polarization colors, while others were opaque. Rotation of the stage gives four extinctions of the color with one revolution of the specimen. We did not observe any red or brown polarization colors in any of the oxide phase.

Another alloy wire of 41 per cent chromium, 1.27 per cent silicon, and 0.08 per cent carbon was heated 10 hours at 2550 degrees Fahr. A section of this wire was examined before heating and showed very few silica or silicate inclusions and a few opaque chromite inclusions in the wire as manufactured. After heating, the wire showed a copious amount of globular glassy inclusions dispersed throughout the entire cross section, but appearing to be most highly dispersed under the outside surface. When examined with reflected polarized light crossed nicols, practically all of these glassy globules showed the optical cross and concentric rings identifying them as silica. Practically all of these were colorless, indicating a high degree of purity with little or no contamination from other metallic oxides. It would appear from these observations, that oxygen penetrated the sample combined with silicon and precipitated out very pure silica. We also observed some duplex inclusions similar to the type the author describes in Fig. 36 and 20, and which we believe were formed when the chromite already in the sample in the unheated wire was fused with the liquid silica. At the metal-oxide surface silicates were formed, and many fragments of the oxide skin enveloping the wire could be observed. These were bright in reflected polarized light with crossed nicols, and showed a distinct green color, very probably a contamination of iron and chromium oxides. The glassy oxide was isotropic and not birefringent as we had observed in the crystalline inclusions mentioned before.

Concerning the red colored oxide which the author observes in lower chromium steels, we were not able to observe this frequently, but we do find it present in a sample of special low carbon ferrochromium, containing 71.9 per cent chromium, 0.10 per cent silicon, and 0.02 per cent carbon. The polished inclusions when viewed in plane reflected light are the typical light gray chromite inclusions, being rectangular or cubical in shape. In reflected polar-

ized light with crossed nicols, we observed many of these crystals to be opaque and a few that were birefringent, and showed a red polarization color. In this particular sample we found no evidence of the green colored birefringent oxides. A few of the red birefringent oxides in this sample showed the interference bands, such as the author describes, and as first pointed out by Benedicks and Löfquist using dark field illumination.

Another alloy wire of 47 per cent chromium, 0.10 per cent silicon and 0.05 per cent carbon was heated 10 hours at 2550 degrees Fahr. This was examined at the burn out and at several other places along the heated wire. At the metal-oxide surface, the oxides are mostly opaque, but occasional green colored birefringent crystals were observed. In the metal dendritic shaped oxides were precipitated and these show a reddish color with crossed nicols.

The birefringent crystals with the polarization colors of green and red, as observed with reflected polarized light under crossed nicols, are probably the same type of crystals that the author describes as "colored by internal reflections" and observed by her with darkfield illumination. However, the reader should distinguish between (1) the isotropic, glassy, colored silicates, as obviously these are silicates contaminated by chromium and iron oxides, (2) the crystalline inclusions which show birefringence, and (3) the opaque crystalline inclusions which are chromite. Examination with the metallurgical microscope using plain illumination often fails to make a distinction between the crystalline inclusions, however, with the metallurgical polarizing microscope these inclusions may be examined for anisotropic character with reflected polarized light under crossed nicols, and in this manner, opaque chromite inclusions are distinguished from birefringent inclusions. The anisotropic crystals or those which show internal reflections are considered to be more complex oxides, probably Fe-Cr-Si-Al oxides, such as a spinel type of inclusion, and should be distinguhed from the isotropic chromite.

The statement by the author, that ferrous oxide appears to be precipitated only after the major portion of the silicon and chromium in the metal adjacent to the scale-steel interface has been oxidized, has been confirmed by the reader in several microscopic studies, however, we believe that some iron does oxidize and dissolve in the chromium oxide to form chromite inclusions. For instance, an alloy wire with 38 per cent chromium, 0.10 per cent silicon and 0.06 per cent carbon was scaled by heating electrically, and the scale that flaked off the wire was analyzed and found to contain 3 per cent FeO and 97 per cent chromium oxide.

We have not attempted to correlate the behavior or high temperature stability of these alloys with the occurrence of either type of colored birefringent oxide.

Oral Discussion

JOHN CHIPMAN:[3] Anyone who has worked on nonmetallic inclusions will appreciate the difficulties of technique which Miss Baeyertz has so beautifully overcome in preparing the excellent photomicrographs which she has shown us.

The order in which she has observed the oxidation of alloys to occur, sili-

[3]American Rolling Mill Co., Middletown, Ohio.

con, then chromium and then iron, is in agreement with what would be predicted from the known thermodynamic behavior of these metals. Some few years ago, the Geophysical Laboratory in Washington published a study of the system, chromic oxide-silica in which they showed that chromic oxide and silica were quite insoluble in each other and formed no compounds. I think Miss Baeyertz's work is in accord with this if we interpret the solution which she has observed in one or two cases as being a solution, not of chromic oxide in silica but perhaps of chromite in silica, or in a ferrosilicate. It will be interesting to know if she has observed any effects upon the formation of scale and its microscopic appearance which could be attributed to variations in melting practice of the alloy steels which were studied, particularly the effects that might be expected which could be tied up with the deoxidation practice in the manufacture of steel.

Author's Closure

First, I want to thank those who have taken the trouble to discuss this paper, particularly for the amount of additional evidence that has been given in these discussions.

In reply to Mr. Rickett's observations, I think that we really are talking about the same thing as regards the causes of the difference in rates of deoxidation, only we are looking at it from slightly different angles.

I would like also to point out that in these observations on oxidation, in many cases, especially in the precipitation of what we have called the red oxide high in chromium, oxidation resulted in the precipitation of a complete film of oxide around each grain of the metal, and only later, in the oxidation of the metal grain itself. This is quite in accord with Mr. Rickett's observations on penetration of sulphur with the formation of sulphides.

In reply to Dr. Schwartz, the observations are in a field beyond the scope of this paper, although very interesting.

In reply to Dr. Hoyt and Mr. Scheil, I am very much interested in their observations. There is only one thing with which I cannot quite agree, that is the question of calling the complex oxides which contain a green birefringent constituent chromite, because really chromite is isotropic and, as described by Dr. Chipman in one of his papers, corresponds quite well with what we have been calling the red oxides at lower temperatures in the low chromium alloys. It is a single-phase mineral and is isotropic in these alloys.

In reply to Dr. Chipman, we have not observed any correlation between furnace practice and the subsequent oxidation of stainless steels except insofar as residual deoxidants remain in the metal, such as residual silicon and aluminum. If these are high, then, of course, they affect the subsequent oxidation of the metal.

HIGH TEMPERATURE PROPERTIES OF NICKEL-COBALT-IRON BASE AGE-HARDENING ALLOYS—PART I

By Charles R. Austin

Abstract

Data on the nickel-cobalt-iron base alloys precipitation-hardened by addition of titanium and further modified by the addition of chromium have been reported previously by the author. Part I of the present investigation extends that work and deals with the mechanical properties, precipitation hardening at elevated temperatures, cold work hardenability and temperature softening properties.

The alloys studied have been considered in their correlation with the properties of the initial base alloy Konal (73 Ni 17 Co 10 FeTi) and with the modified chromium alloy K42B (46 Ni 25 Co 10 FeTi 19 Cr). Data on commercial 80-20 nickel-chromium and stainless 18-8 have been included for purposes of comparison.

At elevated temperatures alloys of high iron content are strong but exhibit brittleness. The maximum tensile strength at 600 degrees Cent. was obtained with 80 per cent cobalt.

It has been demonstrated that precipitation hardening may occur in the absence of nickel, cobalt or iron under certain conditions. Thus when cobalt is removed the iron content must be markedly increased. Raising both the iron and cobalt content appears to increase the precipitation hardening effect at 600 and at 750 degrees Cent. Titanium seems to be unique in imparting precipitation hardening to the ternary or modified ternary systems since silicon, zirconium and vanadium have no such effect.

The work hardenability of stainless 18-8 is outstanding but temperature softening occurs much more readily than with the K42B type of alloy. In this the behavior of both the quenched and pre-age hardened materials have been considered.

THE results of an investigation on certain high temperature properties of nickel-cobalt-iron base alloys were published in 1932.[1]

[1] C. R. Austin and G. P. Halliwell, "Some Developments in High Temperature Alloys in the Nickel-Cobalt-Iron System," *Transactions*, American Institute of Mining and Metallurgical Engineers, Institute of Metals Division, 1932, p. 78-96.

A paper presented before the Seventeenth Annual Convention of the Society held in Chicago, September 30 to October 4, 1935. The author, Charles R. Austin, is associate professor of metallurgy, Pennsylvania State College, State College, Pa. Manuscript received June 3, 1935.

This work dealt with the tensile properties, the age-hardening characteristics, and the resistance to deformation at elevated temperatures as revealed by the bend test. Particular attention was directed to two alloys. "Konal" containing 73 nickel, 17 cobalt and 10 ferrotitanium, was regarded as the base alloy since this was the one of early development, and K42B containing 46 per cent nickel, 25 per cent cobalt, 10 per cent ferrotitanium and 19 per cent chromium was considered the most interesting and promising alloy for high temperature service on account of its remarkable tensile properties at elevated temperatures. Data on the creep characteristics of "Konal" have also been recorded.[2]

The present investigation is a more extensive study of the properties of the alloys previously discussed, and provides an extended investigation on new or modified alloys, modification referring particularly to additions or substitutions of molybdenum, tungsten, vanadium and aluminum to alloy compositions approximating K42B.

In general the alloys considered are complex and hence from the practical point of view the alloy combinations are unlimited. Since economic limitations permit the study of relatively few alloys the conclusions drawn may be only tentative. From the academic viewpoint studies on alloy systems should proceed directly from a knowledge of the several binary systems but the important properties at elevated temperatures observed in complex alloy systems appear to warrant their immediate study.

In Part I attention is devoted to the mechanical properties, to the age-hardening or precipitation hardening characteristics, and to the work hardening and temperature softening properties of the alloys.

Part II will provide a study of their resistance to high temperature oxidation and to chemical corrosion. Information on the electrical resistivity and the metallography of the alloys will also be recorded.

For the purpose of affording a useful basis of comparison, test data on well known commercial alloys such as stainless 18-8 and 80-20 nickel-chromium alloys have been included. In considering the effects of modifications of composition within the basic alloys of the present paper it has been found useful to make reference to the two alloys previously emphasized, namely, "Konal" and K42B, since these alloys form a useful basis for comparison.

[2]C. L. Clark and A. E. White, "Properties of Non-Ferrous Alloys at Elevated Temperatures," American Society of Mechanical Engineers, 1930.

Mechanical, Age-Hardening, Work-Hardening and Temperature Softening Properties of the Alloys

The alloys were prepared in an induction furnace in 8-kilogram melts and chill cast in 2-inch square bars. The ingots were then usually homogenized at 1000 degrees Cent. (1830 degrees Fahr.), ground to remove surface imperfections and hot forged to 1 or ½-inch square. Before test the samples were quenched after annealing 1 hour at 950 degrees Cent. (1740 degrees Fahr.) and then subjected to a precipitation hardening treatment for 72 hours at 650 degrees Cent. (1200 degrees Fahr.).

Mechanical Properties of the Alloys

Many of the mechanical properties have been recorded in the author's previously cited paper. However, a few test data on alloys exhibiting low ductility were omitted but are now included in Table I for completeness and in order to permit a more precise evaluation of the effect of modifying the nickel-cobalt-iron ratios on the mechanical properties. This information is found in the 0-100 series, and illustrates the effect of increasing the iron content on various nickel-cobalt ratios of composition, above the 7.5 per cent introduced when 10 per cent ferrotitanium was added. The ferrotitanium contained approximately 75 per cent iron and 25 per cent titanium. Many of the alloys failed in forging or gave unsatisfactory tests on account of their apparent hard brittle nature. Where mechanical properties were evaluated it may be noted from the tabulated data that high yield and tensile values were obtained at 600 degrees Cent. (1110 degrees Fahr.) but ductility was low. It may also be noted that substantial substitution of nickel by cobalt (Alloys 63, 60, 65 and 75) renders the alloys extremely difficult to forge or too hard to test satisfactorily.

The second series (2700) provides more complete test data on similar type alloys. All but 2789 were prepared with 10 per cent ferrotitanium additions, and it is important to note that with only 0.45 per cent iron valuable high temperature properties have been obtained. Most of the alloys show at 600 degrees Cent. (1110 degrees Fahr.) a yield point of about 90,000 pounds per square inch, and the values for proportional limit (40,000-55,000 pounds per square inch) are considerably higher than for "Konal" although the ductility is low. At 600 degrees Cent. (1110 degrees Fahr.)

Table I
Chemical Composition and Physical Test Data on Several Alloys Examined

Test Pieces were Annealed at 950° Cent. and Quenched in Water
Then Aged at 650° Cent. for 72 Hours

Alloy No.	Composition Per Cent Ni	Co	Fe	Ti			Proportional Limit Lbs./Sq. In. Room Temp.	600° Cent.	Yield Point 0.2 Per Cent Room Temp.	600° Cent.	Tensile Strength Lbs./Sq. In. Room Temp.	600° Cent.	Elongation % in 2 In. Room Temp.	600° Cent.	Reduction in Area % Room Temp.	600° Cent.
53	42.25	40.07	14.46	2.29			60,000	48,700	109,500	98,600	169,500	114,500	20.0	4.2	38.7	8.6
56	13.14	40.24	44.07	2.18				13,200		63,000		110,000		1.0		1.5
59	33.73	12.39	51.00	2.22			Failed in forging. Unsuitable for test.									
60	5.03	20.00	75.00	....			Forged poorly. Unsuitable for test.									
63	13.50	11.92	71.42	2.61			Test samples showed cracks. Not tested.									
64	8.16	29.77	59.31	2.28			67,500	35,000	122,000	81,000	159,200	102,500	17.0	2.0	41.0	7.8
65	.....	38.90	58.8	2.50			Failed in forging.									
72	21.28	20.40	55.05	2.48			33,000	.....	.....	.....	103,000	.....	2.6	...	3.0	...
75	0.025	58.83	37.67	2.34			Material so hard that threads broke in machine.									
2789	35.40	61.69	0.45	2.08			.....	51,000	.....	92,250	.....	105,250	....	4.0	....	7.4
2790	31.76	51.08	13.31	2.82			60,000	49,500	101,000	93,500	160,250	113,000	25.5	5.5	36.3	10.4
2791	13.20	69.18	14.38	2.53			55,000	38,000	80,000	72,000	130,250	103,000	30.5	16.0	53.1	19.0
2792	61.04	12.81	22.39	2.52			80,000	56,500	101,500	91,000	166,000	97,000	25.5	1.7	36.9	6.3
2793	19.32	54.18	22.77	2.54			57,000	4,900	85,000	77,500	143,000	103,000	24.5	8.0	41.3	7.5
2794	42.63	13.88	40.76	2.41			44,000	40,000	110,500	88,000	152,500	99,000	20.0	5.0	39.7	5.5
2795	12.07	39.35	44.89	2.26			Material very brittle. One test run but no data.									
2796	30.66	10.00	55.84	2.32			26,500	.....	61,000	.....	185,000	.....	Broke in threads.			
2798	55.04	1.30	40.37	2.53			.....	51,500	.....	67,000	157,750	103,000	28.5	4.5	37.3	7.8
2910*	44	24	7.5	2.5	17 Cr	5 W	75,500	62,000	100,000	79,000	159,400	119,000	25.0	14.7	27.5	17.0
2911*	46	25	7.5	2.5		19 Mo	.....	72,500	.....	89,300	.....	118,500	....	5.7	....	8.7
2917*	60	25	10	...		5 W	20,200	11,700	36,500	26,500	87,050	54,500	41.0	19.0	54.9	21.0
2918*	50	20	10	...	15 Cr	5 W	36,000	25,600	54,200	42,500	104,000	76,000	....	11.5	....	13.4
2919*	72	18	7.5	...	2.5 Si		16,900	13,300	30,500	22,500	85,800	45,900	52.0	11.5	61.1	14.5
2920*	77	20	....	...	3.0 Si		.....	14,500	.....	21,300	.....	42,000	....	14.2	....	14.1
3123**	..	80	20	Ferrotitanium			.....	40,000	.....	76,500	.....	182,000	....	14.0	....	8.0
3124**	..	85	15	Ferrotitanium			.....	40,000	.....	59,500	.....	97,000	....	15.0	....	10.5
3125**	..	95	5	Ferrotitanium			.....	5,600	.....	18,000	.....	45,000	....	32.0	....	7.3
3123**							.....	32,500	.....	50,000	.....	87,500	....	37.0	....	40.0
3124**				Quenched but not aged.			.....	55,000	.....	56,000	.....	100,000	....	36.5	....	48.0
3125							.....	.....	.....	10,000	.....	45,500	....	49.0	....	75.5
Konal†	73.3	17.3	6.25	2.4			27,500	15,000	58,000	46,800	108,000	76,800	35.0	24.7	59.5	33.2
K 42†	46.1	24.86	7.02	2.19	18.74 Cr		70,000	57,500	104,000	86,000	167,750	127,100	29.0	21.5	37.0	21.7

*These test specimens were quenched in oil.
**Aged for 65 hours at 650 degrees Cent.
†Basic alloys from previously cited research. For purpose of reference.
The compositions given for 0-100 and 2700 series are from chemical analyses. Those for the 2900 and 3100 series are synthetic analyses.

"Konal" gave 15,000 pounds per square inch proportional limit, 47,000 pounds per square inch yield point, 77,000 pounds per square inch tensile strength and 25 per cent elongation. More than 40 per cent iron appears to render the alloys hard and brittle.

In the author's earlier paper frequent reference was made to Alloy K42B (46 Ni, 25 Co, 10 FeTi, 19 Cr) which exhibited a proportional limit of 57,000 pounds per square inch and 21 per cent elongation and reduction of area, after the quenching and aging treatment. These values were considered by Dr. Merica as remarkable for any metallic material.[3] The 2900 series Table I provides data on the effect of modifying with tungsten and molybdenum, two elements in the same group as chromium in the periodic table. The effects of substituting silicon for titanium and for ferrotitanium in "Konal" are also indicated. The addition of molybdenum to K42B or the complete substitution of chromium by molybdenum in this alloy materially raises the proportional limit at 600 degrees Cent. (1110 degrees Fahr.) but there is a corresponding reduction in ductility. Tungsten additions in the absence of titanium do not appear to merit attention.

It might be considered that silicon and particularly zirconium would confer on the nickel-cobalt-iron alloys high temperature properties similar to those observed when titanium additions are made, since all elements are found in the periodic group IV. A marked decrease in the values for the mechanical properties is noted when silicon substitutes titanium. Reference to substitution by zirconium will be made in the section on age-hardening.

Of considerable interest is the 3100 series where a study has been made of the effect of varying ferrotitanium additions to "pure" commercial cobalt containing 99.32 per cent cobalt and 0.42 per cent nickel. These alloys are all subject to hardening by the 650 degrees Cent. (1200 degrees Fahr.) aging treatment and alloy 3123 with 20 per cent ferrotitanium provides the highest tensile value for 600 degrees Cent. (182,000 pounds per square inch) of any alloy of the series tested. However, the proportional limit and yield point are relatively low.

Age-Hardening Characteristics

Undoubtedly one of the most important characteristics of these

[3]Paul D. Merica, "The Age-Hardening of Metals." Annual Lecture, American Institute of Mining and Metallurgical Engineers, Institute of Metals Division, 1932, p. 46.

Table II

Summary of Age-Hardening Characteristics of Various Alloy Modifications

Alloy No.	Vickers Hardness Number: Quenched 950° Cent.	Aged at 600° C. Max.	Aged at 600° C. 200 Hrs.	Aged at 750° C. Max.	Aged at 750° C. 200 Hrs.	Chemical Analysis: Ni	Co	Fe	Ti		
53	170	350	350 (370°)	234	235 (270°)	42.25	40.07	14.46	2.29		
56	390	750	520 (470°)	490	315 (290°)	13.14	40.24	44.07	2.18		
59	190	380	370	300	220	33.73	12.39	51.00	2.22		
63	350	450	355	400	290	13.50	11.92	71.42	2.61		
64	410	575	400	...	330	8.16	29.77	59.31	2.28		
67	145	290	280	220	205	Trace	75.71	21.46	2.19		
2789	150	325	310	175	165	35.40	61.69	0.45	2.08		
2790	140	325	310	245	175	31.76	51.08	13.31	2.82		
2791	130	275	260	150	150	13.20	69.18	14.38	2.53		
2792	150	300	300	260	230	61.04	12.81	22.39	2.52		
2793	150	300	300	160	160	19.32	54.18	22.77	2.54		
2794	150	330	330	270	220	42.63	13.88	40.76	2.41		
2795	390	620	450	405	360	12.07	39.35	44.89	2.26		
2796	175	405	400	285	220	30.66	10.00	55.84	2.32		
2797	240	280	250	250	240	0.43	38.96	60.05	1.76		
2798	145	320	310	235	220	55.04	1.30	40.37	2.53		
			50 Hrs.		50 Hrs.			Synthetic Analyses			
2866	110		115		102	70	20	10	.....		
2867	150		330		180	27	54	15	4		
2868	190		277		190	26	54	7½	2½	10 Cr	
2869	240		290		235	23	47	7½	2½	20 Cr	
2870	230		220		230	48	25	7	.....	20 Cr	
2871	136		160		140	75	20	.....	5		
2872	140		165		160	75	22	.....	3		
2873	170		375	340	260	48	12	30	10		
2874	150		170		170	75	20	.....	.....	5 Zr	
2875	150		170		165	75	22	.....	.....	3 Zr	
2876	150		175		150	73	17	7½	.....	2½ Zr	
2877	195		205		205	46	25	7½	.....	2½ Zr	19 Cr
			85 Hrs.		85 Hrs.						
2907	220		350	325	325	46	25	7½	2½	19 W	
2908	175		320		220	53	29	7½	2½	8 W	
2909	175		330		175	56	30	7½	2½	4 W	
2910	250		385	320	315	44	24	7.5	2.5	17 Cr	5 W
2911	285		385		340	46	25	7.5	2.5	19 Mo	
2912	200		300		210	53	29	7.5	2.5	8 Mo	
2913	200		310		230	56	30	7.5	2.5	4 Mo	
2914	150		150		150	30	58	10	.....	2 Va	
2915	150		160		155	30	50	10	.....	8 Cr	2 Va
2916	230		320		320	44	24	7.5	2.5	17 Cr	5 Mo
2917	150		150		160	60	25	10	.....	5 W	
2918	235		240		240	50	20	10	.....	15 Cr	5 W
2919	150		145		140	72	18	7.5	.....	2.5 Si	
2920	125		150		135	77	20	.....	.....	3 Si	
		Aged at 650° C. 200 Hrs.									
3123	140	380	275			.....	80	15	5		
3124	150	240	240			.....	85	11	4		
3125	130	160	155			.....	95	4	1		
K-11	115	130	125			90	.....	7.5	2.5		
		Aged at 600° C. 200 Hrs.			200 Hrs.						
Konal	140	260	260	...	...	73	17	7.5	2.5		
K42B	230	340	340	325	295	46	25	7.5	2.5	19 Cr	
K41B	230	350	350	330	260	50	30	7.5	2.5	10 Cr	

*Results of aging at temperature indicated for 2000 hours.

alloys is their property of age-hardening at elevated temperatures. In the early investigations it was determined that a period of aging of 72 hours at 650 degrees Cent. (1200 degrees Fahr.) usually pro-

duced about 80 per cent of the maximum hardenability of the alloy, so that these conditions were maintained prior to testing of samples in tension. While this procedure has probably not produced the maximum mechanical properties which could be obtained with all alloy combinations studied it was considered to form a satisfactory basis for comparison.

A general condensed tabulation of the chemical analyses, hardness as quenched from 950 degrees Cent. (1740 degrees Fahr), and hardness after aging at 600 and at 750 degrees Cent. (1110 and 1380 degrees Fahr.) is submitted in Table II. In the first series (0-100) it may be noted that the presence of nickel is not essential to marked age-hardening (67) and that the concomitant increase in the cobalt and iron content leads to very high aged hardness values even after the 750 degrees Cent. (1380 degrees Fahr.) treatment (alloys 56 and 64).

The 2700 series provides further data on similar alloys. Again, maximum hardness is shown with high iron and cobalt content (2795). This alloy has the greatest hardness in the quenched and in the aged condition which suggests that the iron-cobalt solid solutions or alloys per se are very strong at elevated temperatures. The iron-free alloy with high cobalt content (2789) exhibits good aging characteristics at 600 degrees Cent. (1110 degrees Fahr.) but the hardness falls markedly at 750 degrees Cent. (1380 degrees Fahr.).

The 2800 series consists of various modifications of "Konal" and K42B. Thus the omission of titanium from "Konal" (2866) or the substitution of zirconium (2874, 2875, and 2876) renders the alloy nonhardenable by precipitation aging. Similarly the omission of titanium (2870) or the substitution of zirconium (2877) in the chromium-bearing K42B eliminates the age-hardening feature. The iron-free "Konal" alloy (2872) has little power of age-hardening and the addition of extra titanium (2871) has little effect on the hardness of this nickel-cobalt alloy.[4] These results should be compared with the marked hardening obtained at 600 degrees Cent. (1110 degrees Fahr.) in alloy 2789 which is practically iron-free but is high in cobalt.

The effect of increasing the amount of ferrotitanium in "Konal" is recorded in the data for alloy 2873—super "Konal"—

[4]This statement must not be confused with the effect of increasing ferrotitanium or titanium in presence of iron.

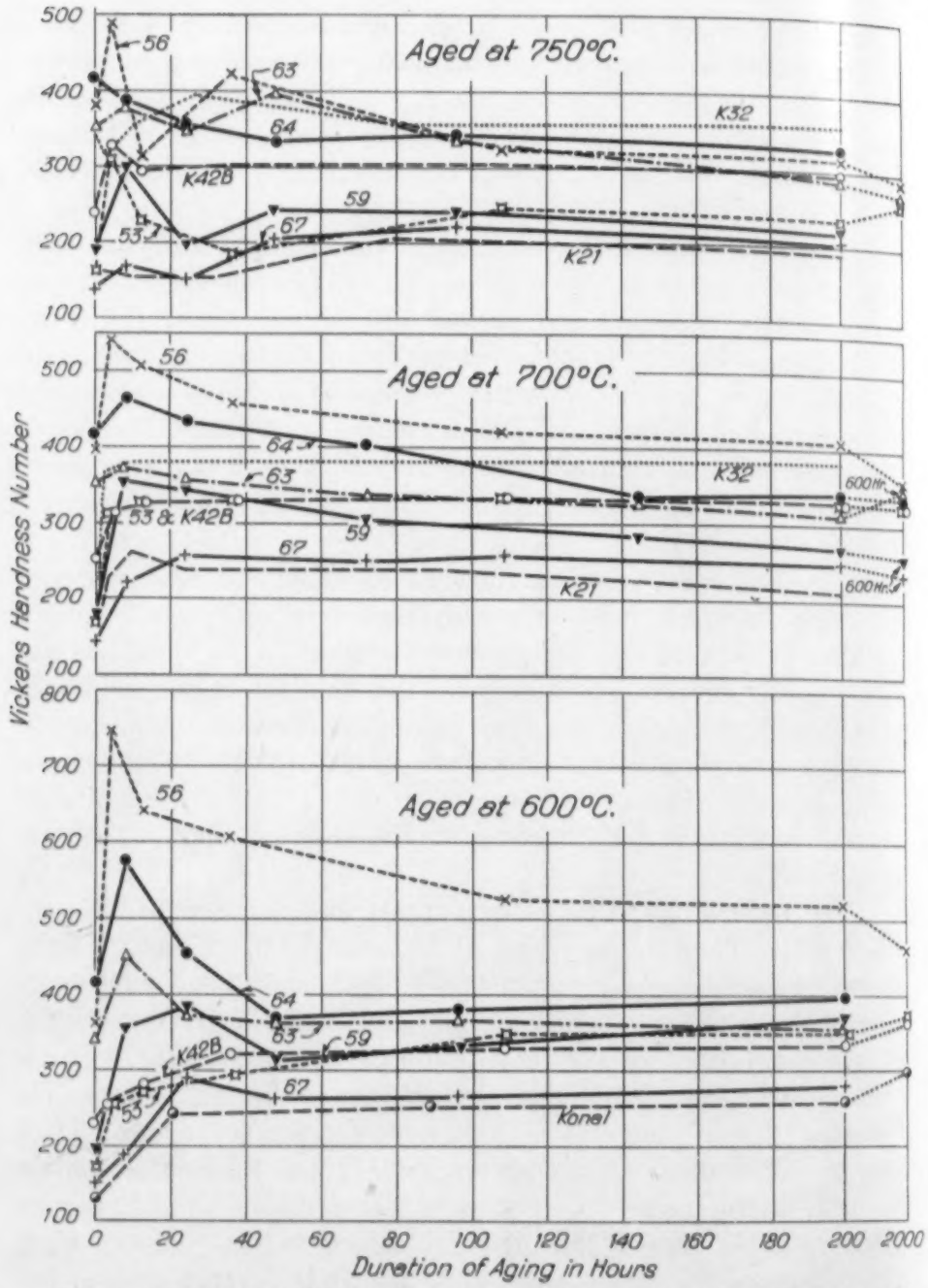

Fig. 1—Age-hardening Characteristics of Alloys in the 0-100 Series in Comparison with "Konal" and K42B. Alloy 67—Trace Ni, 75.7 Co, 21.5 F, 2.2 Ti. Other Analyses in Table I.

which reveals the maximum aged hardness in this series, at 600 and at 750 degrees Cent. (1110 and 1380 degrees Fahr.) although the hardness of the solid solution is relatively low. The influence of

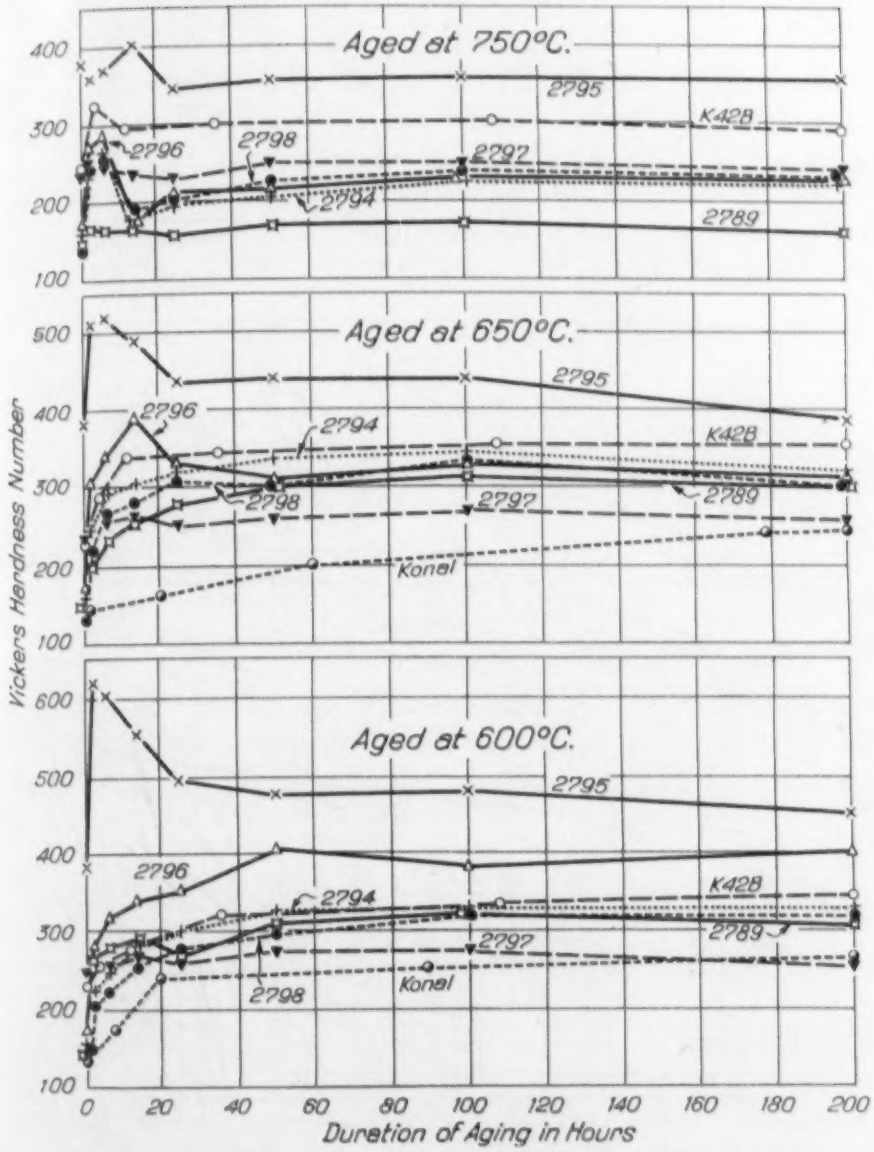

Fig. 2—Age-hardening Characteristics of Alloys in the 2700 Series in comparison with "Konal" and K42B. Chemical Analyses Recorded in Table II.

increased ferrotitanium may also be noted in alloy 2867 aged at 600 degrees Cent. (1110 degrees Fahr.). The profound hardening effect of increasing the titanium content in the presence of iron is at once evident when studying the curves in Fig. 1 used to indicate the age-hardening trend of K21 (58 Co, 32 Ni, 7.5 Fe, 2.5 Ti) and K32 (58 Co, 27 Ni, 10.5 Fe, 4.5 Ti) at 700 and 750 degrees Cent. (1290 and 1380 degrees Fahr.). Reversing the nickel-cobalt ratio in K42B results in little change on the quenched

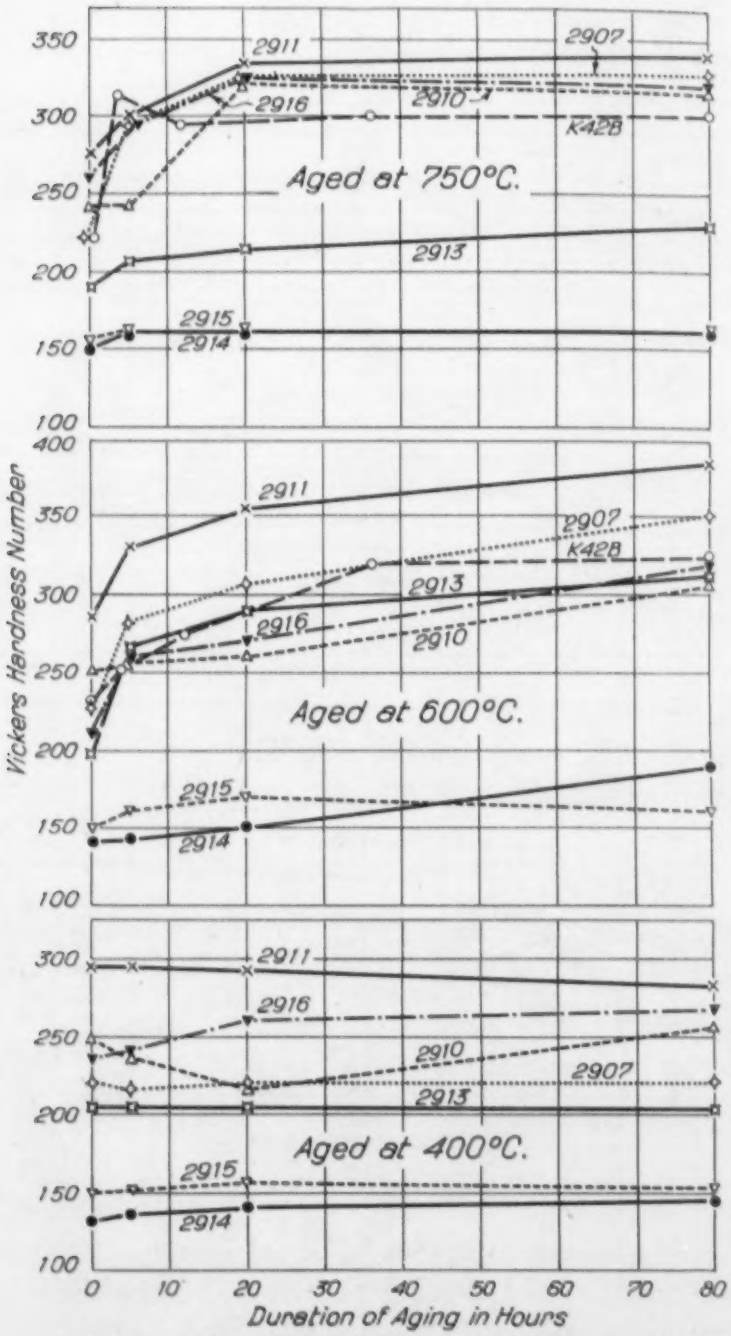

Fig. 3—Age-hardening Characteristics of Alloys in the 2900 Series in Comparison with K42B. Chemical Analyses Recorded in Table II.

hardness but it materially reduces the hardness of the aged alloy (2869). See Table II.

The 2900 series represents an analysis of the aging character-

istics of modifications of K42B. It demonstrates that the substitution of silicon for titanium completely eliminates the aging properties of the alloys (2919 and 2920). Decreasing the amount of tungsten substituted for 19 per cent chromium in K42B results in a decrease in the aged hardness of the alloys (2907-9), but the substitution of chromium by an equal amount of tungsten gives an appreciable increase in hardness (2907). More detailed information on this alloy is traced in Fig. 3. The substitution of molybde-

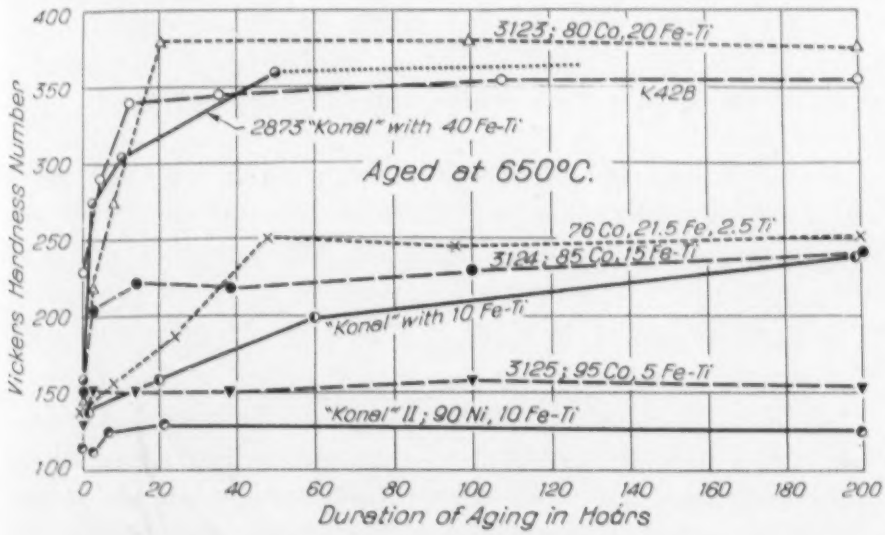

Fig. 4—Age-hardening Characteristics of High Cobalt and High Ferrotitanium Alloys Compared with Konal and K42B.

num for chromium in K42B results in a markedly harder alloy after aging at 600 and at 750 degrees Cent. (1110 and 1380 degrees Fahr.) (Alloy 2911, Fig. 3), and the hardness of the quenched alloy is much superior. Even with only 4 per cent molybdenum (2913) hardness values comparable with those of K42B are obtained after aging at 600 degrees Cent. (1110 degrees Fahr.). A marked falling off is noted after the 750 degrees Cent. (1380 degrees Fahr.) treatment (Fig. 3).

Alloys 2914 and 2915 illustrate the effect of replacing titanium by vanadium in a chromium-free and in a chromium-bearing alloy. Again the close relationship of vanadium to titanium in the periodic system might indicate a probable strong similarity of behavior. However, no age hardening is noted. Substitution of titanium by tungsten destroys the high temperature age-hardening feature (2917).

Fig. 3 also traces the effect of 5 per cent additions of tungsten (2910) and of molybdenum (2916) to K42B. After the 600 degrees Cent. (1110 degrees Fahr.) treatment the alloy additions soften the base alloy but at 750 degrees Cent. (1380 degrees Fahr.) the additions appear to be beneficial.

Figs. 1 and 2 provide information on the progress of age-hardening in the 0-100 and 2700 series respectively at 600, 650 and 750 degrees Cent. (1110, 1200 and 1380 degrees Fahr.). It may be noted that although the quenched and aged hardness of alloys 56 and 64 are superior to those for K42B the tensile properties are inferior (Table I). Marked secondary age hardening was found in several of these alloys, particularly at 750 degrees Cent. (1380 degrees Fahr.).

In Fig. 4 data are presented on high cobalt and high ferrotitanium alloys. Increasing additions of ferrotitanium to cobalt rapidly increase the amount of aging at 650 degrees Cent. (1200 degrees Fahr.). A similar marked increase is found in "Konal" when the ferrotitanium addition is raised to 40 per cent (Alloy 2873).

Work Hardenability

Although it is well recognized that metals and alloys harden to different degrees with cold work little attention appears to have been given to a quantitative study of the phenomenon. It is considered likely that the work-hardening characteristics of alloys will be regarded as an important property of the material in considering the application of metals for industrial purposes. This recognition has been particularly in evidence of late in the utilization of stainless 18-8 alloy in the hard rolled state, and a recent article on the effect of cold drawing gives quantitative data for carbon and low alloy steels. The increase in the yield point is particularly noteworthy.[5]

Many years ago Alkins[6] studied the effect of progressive cold work on properties of pure copper and found a discontinuity in tensile strength, hardness, etc., with increasing amounts of cold work. Apparently no satisfactory explanation of the phenomenon was forthcoming. More recently Rawdon and Mutchler[7] and

[5]J. D. Armour, "Cold Finished Bars," METAL PROGRESS, May 1935, p. 43-48.

[6]W. E. Alkins, "The Effect of Progressive Cold Work upon the Tensile Properties of Pure Copper," *Journal*, Institute of Metals, II, 1918, p. 33.

[7]H. S. Rawdon and W. H. Mutchler, "Effect of Severe Cold Working on Scratch and Brinell Hardness," *Transactions*, American Institute of Mining and Metallurgical Engineers, Vol. 70, 1924, p. 342.

Table III
List of Alloys Tested for Data Characteristic of Work-Hardenability in the Quenched and in the Quenched and Aged Condition

Alloy Number	Chemical Composition							Comments
	Nickel	Cobalt	Iron	Titanium	Other Elements			
2866	70	20	10	...	..			"Konal" without Titanium
2867	27	54	15	4	..			High Co:Ni ratio, and high Fe Ti
2868	26	54	7.5	2.5	10 Cr			Compare K41B with high Co:Ni ratio
2869	23	47	7.5	2.5	20 Cr			K42B with Ni:Co ratio reversed
2870	48	25	7	...	20 Cr			K42B without Titanium
2910	44	24	7.5	2.5	17 Cr	5 W		K42B with 5% W added
2916	44	24	7.5	2.5	17 Cr	5 Mo		K42B with 5% Mo added
2918	50	20	10	...	15 W	5 W		K42B type with 5% W and no Ti
2295	90	..	7.5	2.5	..			"Konal" without Cobalt
"Konal"	73	17	7.5	2.5	..			
3042	46	25	7.5	2.5	19 Cr			K42B
18-8	8	..	74	...	18 Cr			Stainless 18-8 Carbon 0.07%
Nichrome	..	..	86	...	20 Cr			Commercial "Nichrome IV"
Silchrome	..	..	86	...	9.5 Cr	4 Si	0.5 C	Commercial "Silchrome"
Iron	..	..	99.97	...	..			Pure Electrolytic Iron
Nickel	..	..	.....	...	..			Commercially Pure Nickel

Fogler and Quinn[8] have published data on the subject but found difficulty in reconciling their results although it was suggested that rate of deformation might be responsible for the appearance of a discontinuity by one investigation and the absence of such break by another, even with tests conducted on similar material.

In the present investigation selected alloys including well-known commercial materials were cold-rolled to predetermined reductions of thickness in the quenched and in the quenched and aged condition. A list of these alloys with comments and chemical compositions is given in Table III. The samples were prepared by cutting 12-inch lengths from ½-inch square forged bars. Two sets of samples of each alloy were then cold-rolled (in square grooved rolls) down to 0.355 inches across flats. Several intermediate anneals at 950 to 1000 degrees Cent. (1740 to 1830 degrees Fahr.) were used, the number of annealing operations depending on the work-hardening characteristics of the alloy.

The two sets of specimens were then thoroughly annealed at 950 degrees Cent. (1740 degrees Fahr.) and quenched in water, one series was aged at 650 degrees Cent. (1200 degrees Fahr.) for 72 hours. It was anticipated that this second treatment would have little effect on the work-hardening properties of the commercial comparison alloys such as nickel-chromium, and stainless 18-8 steel. The selection of 650 degrees Cent. (1200 degrees Fahr.) for aging

[8]M. F. Fogler and E. J. Quinn, "Scratch and Brinell Hardness of Severely Cold-Rolled Metals," *Transactions*, American Institute of Mining and Metallurgical Engineers, Vol. 71, 1925, p. 889.

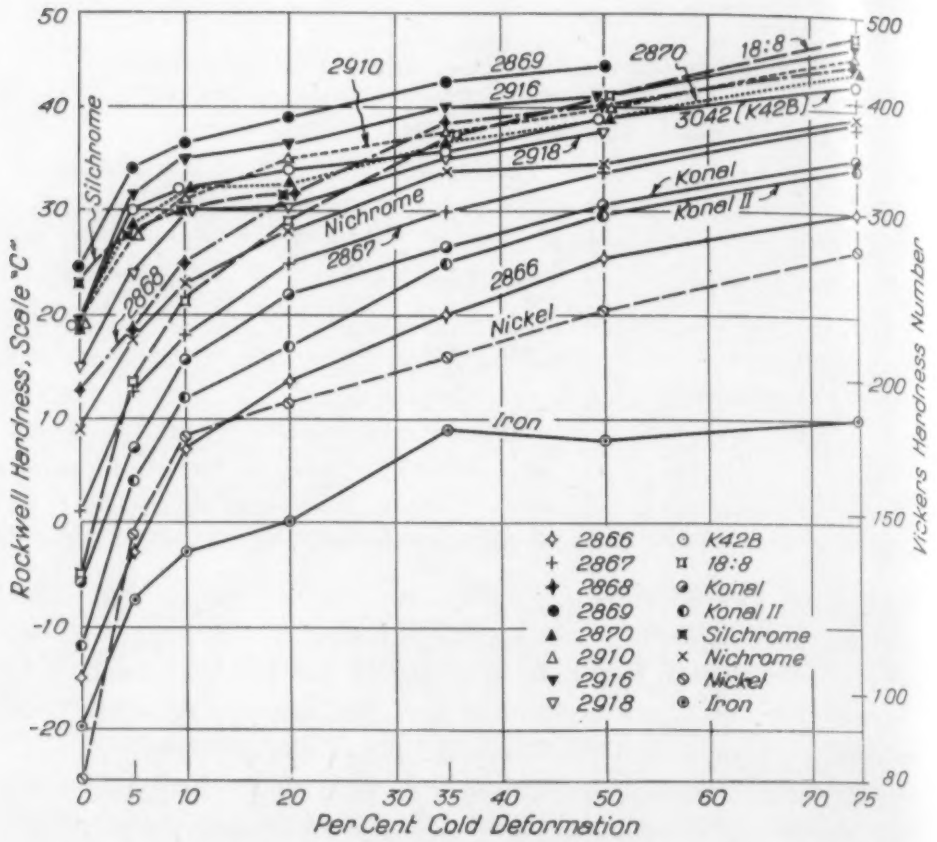

Fig. 5—Work-hardening Characteristics of Selected Alloys in the 2800 and 2900 Series Compared with Konal, K42B, Nichrome IV, Stainless 18-8, Silchrome and the Three Base Metals Ni, Co, and Fe. All Specimens were Oil-quenched from 950 Degrees Cent. (1740 Degrees Fahr.) Prior to Cold Rolling.

must not be regarded as the optimum temperature for all the alloys but rather as a mean temperature most suitable for the nickel-cobalt-iron base alloys.

Sections were cut from both series for hardness determination as heat treated. The bars were then cold-rolled between flat rolls until a reduction in thickness of 5 per cent had been obtained. Throughout these tests the number of passes naturally depended on the rate of work-hardening. Sections were again cut and rolling continued until specimens were obtained for 10, 20, 35, 50 and 75 per cent reduction in thickness. In a few instances the alloys could not be rolled down to the maximum reduction desired.

On account of the large amount of test data involved in this and subsequent work on temperature softening the hardness was measured by use of the Rockwell hardness machine. Although the values obtained on different alloys varied widely it was decided

Table IV

Vickers Hardness Data Showing Effect of 24 Hour Anneal on Selected Alloys Reduced 10 Per Cent and 50 Per Cent in Thickness by Cold Rolling

Alloy		K42B		2869		2916		2910		18-8		Ni Cr IV		2868		Konal		2867		2870	2918
		Quenched	Aged	Quenched	Aged	Quenched	Aged	Quenched	Aged	Quenched	Aged	Quenched	Aged	Quenched	Aged	Quenched	Aged	Quenched	Aged	Mean Values	Mean Values
Reduced 10%	Heat Treatment																				
	400	225	323	260	330	230	330	227	340	132	150	180	185	195	300	128	235	150	355	227	210
	500	315	408	355	385	340	420	305	420	243	245	248	257	263	380	208	315	222	413	315	303
	600	305	432	392	413	355	413	345	400	260	255	285	270	290	380	222	310	243	438	337	303
	650	315	425	385	455	370	425	355	450	257	245	288	257	305	395	270	263	257	460	340	310
	700	305	400	397	455	380	438	350	425	263	240	250	205	340	380	310	320	345	432	303	300
	750	395	432	400	420	438	438	413	432	255	245	267	205	350	365	365	310	408	420	315	300
	800	400	413	397	397	413	413	392	425	237	237	257	245	330	320	233	222	372	392	303	288
	850	360	365	350	350	385	380	350	385	230	227	185	240	225	270	175	185	305	323	218	280
	900	315	285	263	257	340	350	310	335	222	...	158	178	185	185	162	165	288	277	205	263
		245	215	245	257	255	257	220	210	220	208	178	178	178	188	122	123	255	285	205	205
		185	222	222	250	245	255	225	210	180	203	190	185	182	195	130	135	300	300	213	208

Temperature of Anneal °C.

Data on Effect of 24 Hour Anneal on Material Reduced 50 Per Cent by Cold Work

Alloy		K42B		2869		2916		2910		18-8		Ni Cr IV		2868		Konal		2867		2870	2918
		Quenched	Aged	Quenched	Aged	Quenched	Aged	Quenched	Aged	Quenched	Aged	Quenched	Aged	Quenched	Aged	Quenched	Aged	Quenched	Aged	Mean Values	Mean Values
Reduced 50%	Heat Treatment																				
	400	225	323	260	330	230	330	227	340	132	150	178	185	195	300	128	235	150	335	227	210
	500	380	475	438	475	400	475	392	455	400	395	337	330	395	413	300	355	335	445	385	375
	600	460	535	535	570	520	545	460	527	450	450	392	413	467	500	350	400	385	500	450	413
	650	475	565	590	635	545	563	490	527	438	450	395	408	563	527	373	380	432	565	475	425
	700	458	535	590	635	582	590	512	527	392	385	355	300	520	545	420	330	475	527	315	385
	750	420	500	395	408	545	553	490	520	257	240	240	245	380	385	263	337	400	460	275	275
	800	392	460	365	350	520	513	468	450	245	235	230	237	295	303	172	175	340	365	270	250
	850	345	340	310	337	475	458	400	365	225	225	225	225	230	245	168	165	320	290	263	255
	900	...	290	300	305	340	350	300	305	210	208	203	215	215	227	157	170	290	300	248	250
		240	245	263	263	295	...	240	245	185	208	205	180	208	205	135	137	203	...	237	240
		243	240	260	257	285	285	245	245	180	...	205	...	200	215	125	130	315	335	240	245

Temperature of Anneal °C.

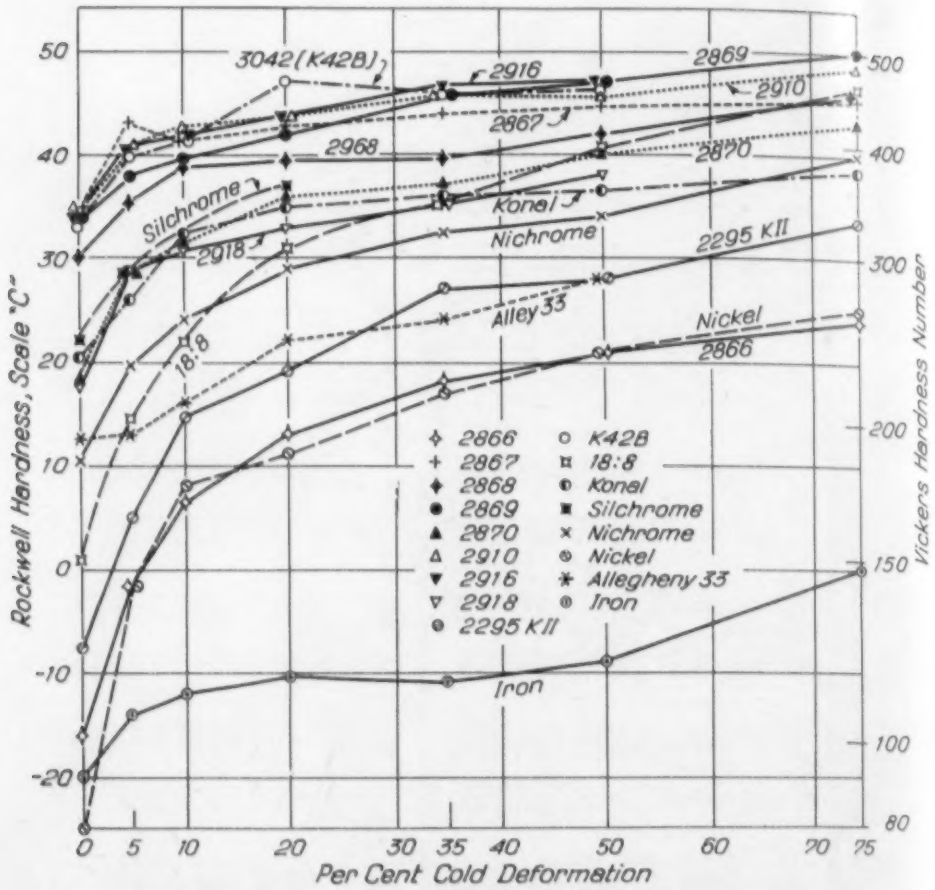

Fig. 6—Work-hardening Characteristics of Selected Alloys in the 2800 and 2900 Series Compared with Konal, K42B, Nichrome IV, Stainless 18-8, Silchrome and the Three Base Metals Ni, Co, and Fe. All Specimens were Oil-quenched from 950 Degrees Cent. (1740 Degrees Fahr.) and then Annealed (Aged) for 72 Hours at 650 Degrees Cent. (1200 Degrees Fahr.) Prior to Cold Rolling.

to observe all data with the diamond point ("C" scale) as the values thus obtained were considered to be more strictly comparable than would be the case by substituting the Rockwell "B" scale at lower hardness values. Careful correlation of some of the data with Vickers hardness tests has permitted the values to be expressed in the latter units (see Table IV). A more complete list of observed Rockwell "C" hardness values is recorded in Tables V to VIII inclusive.

The data illustrating the work-hardening characteristics of the quenched and aged alloys are plotted in Figs. 5 and 6 respectively. With the quenched alloys the effect of increasing the amount of cold work on the hardness is progressive although certain discontinuities are evident. It should be stated, however, that this section

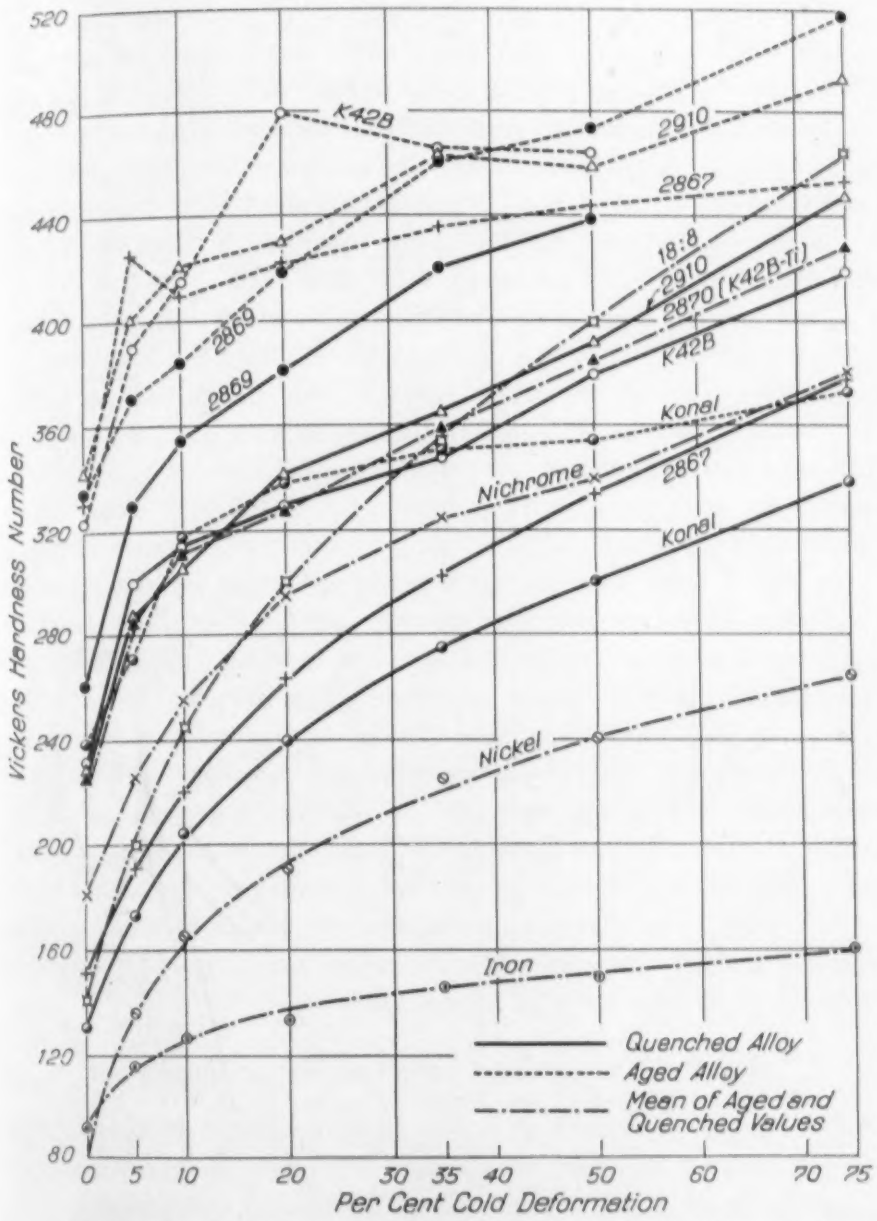

Fig. 7—Relation Between Per Cent Cold Deformation and Vickers Hardness of a Selected Number of Alloys as Quenched from 950 Degrees Cent. (1740 Degrees Fahr.) and as Aged at 650 Degrees Cent. (1200 Degrees Fahr.). Where no Marked Aging Occurred Mean Values for the Two Tests are Recorded on One Curve.

of the investigation was conducted for the purpose of relating the general work-hardening features of the alloys and not as an academic study of the exact relationship between cold deformation and hardness of any one particular material. Thus the rapid rate of hardening of stainless 18-8 is at once evident.

Considering first the quenched alloys (Fig. 5) the absence of titanium (2870) does not have much effect on the work-hardenability of K42B but a reversal of the nickel-cobalt ratio provides the alloy (2869) with the maximum quenched and worked hardness. Molybdenum addition (2916) also materially increases the hardening effect of deformation. Tungsten additions apparently do not lead to a similar increase (2910). The effect of cobalt as a hardener is also noted by comparison of "Konal" with alloy 2867.

Tests on the aged alloys provide data which are considerably more irregular (Fig. 6). K42B now hardens to a much greater extent than the titanium-free alloy (2870), and "Konal" and titanium-free "Konal" (2866) exhibit a considerably greater spread when aged. K42B type with a high ratio of cobalt to nickel content (2869) again provides the maximum worked hardness. Relatively small differences result from the addition of molybdenum or tungsten to K42B.

In Fig. 7 have been plotted data on the more interesting alloys in both the quenched and aged state. Mean values have been recorded for iron, nickel, nichrome, stainless steel and alloy 2870 since they naturally showed limited variation. The hardness is expressed in the form of Vickers hardness number as this scale is more open than Rockwell "C" in the higher hardness ranges. This diagram reveals more clearly the irregular or discontinuous nature of the hardening effect on the aged alloys, and demonstrates the much greater hardness which may be obtained by working the alloys in the aged condition. It is important to observe under what conditions this work hardness persists when the alloys are subject to annealing treatments at various elevated temperatures.

Temperature Softening Characteristics of the Alloys

The effects of annealing cold-worked metallic materials are imperfectly understood even when related to relatively pure metals. The softening of a cold-worked metal by raising the temperature is usually spoken of as recrystallization although crystal recovery can apparently lead to marked softening without the birth of new crystals. However, previous work on the subject is extensive and limited citation will be made.

It appears to be a commonly observed fact that when cold-worked metals are annealed at progressively increasing temperatures an increase in hardness is first noted which is followed by a progressive softening as the temperature is raised. This has been demon-

Table V

Work-Hardening and Temperature-Softening Characteristics of Alloys K42B, 2869, 2916 and 2910 in the Quenched and Aged Conditions. The Values Recorded Refer to Rockwell Hardness "C" Scale

Initial Heat Treatment Cold Deformation Per Cent Reduction of Thickness	Alloy 3042 (K42B) 46 Ni 25 Co 10 FeTi 19 Cr — Quenched from 950° C.						Quenched then Aged 72 Hours at 650° C.						Alloy 2869 23 Ni 47 Co 10 FeTi 20 Cr — Quenched from 950° C.						Quenched then Aged 72 Hours at 650° C.					
	5	10	20	35	50	75	5	10	20	35	50	75	5	10	20	35	50	75	5	10	20	35	50	75
As Heat Treated and Cold Rolled	30	32	34	36	39	42.5	40	41.5	47	46.5	46.5	....	34	36.5	39	42.5	44	....	38	39.5	42	46	47	50
400	29	31	29.5	38	46	....	40	43.5	45	....	51	....	37	40	44	48	51	....	42	42	46	50	53	56
500	31	32	39	42	47	....	40	43	42	....	52	....	39.5	39.5	47	51	54	....	44	45.5	47	53	56	59
600	32	31	42.5	44	45.5	....	43	41	42.5	....	51	....	37	40.5	45.5	51.5	54	....	41.5	45.5	47	53	56	57
650	37	40.5	43	44	42.5	....	43	43.5	43	....	49	....	39.5	41	46	44	40.5	....	41	42.5	46	46.5	41.5	45
700	39	41	41.5	42.5	40	....	37.5	42	42	....	46	....	37	40.5	43	32	37.5	....	37.5	40.5	41.5	36	36	41.5
750	35.5	37	39	38	35.5	....	34.5	37.5	39.5	....	35	....	34	36	28.5	31.5	31.5	....	35	36	29	34	34.5	34
800	31.5	32	34	27	....	....	33	28	30	....	29	....	33	25	27.5	29	30	....	32	24	30	32	31	29.5
850	11	15	18	20	21	....	14.5	17	17.5	....	22	....	19	22	24.5	25	25	....	21	22	25.5	27	25	25.5
900	15	11	19	20.5	21.5	....	17	18	20	....	21	....	16	18	25	22	24.5	....	21	23	27	25	24	24

Initial Heat Treatment Cold Deformation Per Cent Reduction of Thickness	Alloy 2916 44 Ni 20 Co 10 FeTi 17 Cr 5 Mo — Quenched from 950° C.						Quenched then Aged 72 Hours at 650° C.						Alloy 2910 44 Ni 24 Co 10 FeTi 17 Cr 5 W — Quenched from 950° C.						Quenched then Aged 72 Hours at 650° C.					
	5	10	20	35	50	75	5	10	20	35	50	75	5	10	20	35	50	75	5	10	20	35	50	75
As Heat Treated and Cold Rolled	31.5	35	36.5	40	41	45.5	41	42.5	43.5	46.5	47	....	28	31	35	37.5	40	45	41	42.5	43.5	46	45.5	48.5
400	31.5	36.5	39.5	45	50	53	41.5	42	46	50	51.5	....	31	35.5	37.5	44	46	51	41	45	48	50.5	53.5	
500	35	38	40	47	51.5	56	42.5	43	46.5	50	52.5	....	32.5	36.5	38	47	48	54	42.5	45	46.5	50	50.5	55.5
600	37.5	39	44	49.5	53.5	55.5	43	44	46.5	50.5	54	56	37	36	42.5	48	49.5	53	42	43	47	47.5	50.5	52
650	41	44	45	48.5	51.5	53.5	42	44	47	51	52	....	39.5	42	42.5	49	48	49	41	43.5	45	49.5	50	50.5
700	39.5	42	44	48	50	49.5	41	42	46.5	47.5	49.5	....	37.5	40	43	47.5	46.5	44	41.5	43	41.5	47	45	46
750	38	39.5	41	46	47	42	38.5	39	42	45	45.5	....	33.5	36	41	42	41	39	36	39.5	41	42	37.5	39.5
800	33.5	35	39	34.5	35	39.5	34.5	36	35	34.5	36	....	32.5	31.5	34.5	27	30	32.5	31.5	34.5	29.5	29	31	34.5
850	28.5	23	24.5	....	29.5	31	31.5	24	26	30	....	....	15.5	17.5	21	21	21	21	14.5	16	21	21	22	21.5
900	23	22	24	28	28	27.5	29.5	23.5	25.5	29	28	....	16	18.5	20	21	22	21	15	16	21	23	22	22.5

Quenched	Aged	Annealed 24 Hrs. at °C.
3042 2869		
18.5	33	
24.5	34	
2916 2910		
19.5	34	
19	33	

Table VI

Work-Hardening and Temperature-Softening Characteristics of Alloys 2868 and 2918

The Mean Values from the Quenched and from the Aged Samples are Recorded for Alloy 2918

The Values Recorded Refer to Rockwell Hardness "C" Scale

Initial Heat Treatment / Cold Deformation Per Cent Reduction of Thickness			Alloy 2868 26 Ni 54 Co 10 FeTi 10 Cr — Quenched from 950° C.						Alloy 2868 26 Ni 54 Co 10 FeTi 10 Cr — Quenched then Aged 72 Hours at 650° C.						Alloy 2918 50 Ni 20 Co 10 Fe 15 Cr 5 W — Mean of Values for Quenched and Aged Specimens					
Rockwell Hardness "C"			5	10	20	35	50	75	5	10	20	35	50	75	5	10	20	35	50	75
2868	13	2918 12-15	As Heat Treated and Cold Rolled																	
Quenched	30	17.5	400	19	29	36.5	44.5	46.5	51.5	37	39	42	47	49	53	28	30.5	34	39.5	42	....
Aged			500	27.5	31	36	45.5	52.5	53	35.5	40.5	42.5	49	50.5	55	29	31.5	36	40.5	43	....
Annealed 24 Hrs. at °C.			600	32	35	43	47.5	50	50.5	38	39	42	47	51.5	54	26	30	35	39	39.5	....
			650	33.5	36	43	42.5	39	41	36.5	37.5	41	40.5	39.5	37	27	30	34	27	26.5	....
			700	24.5	33.5	29	28	29.5	35	30.5	32.5	35	27	30.5	35	25	28.5	27.5	21	23	....
			750	20.5	18.5	17	21.5	19.5	20.5	22.5	26	19.5	20.5	22	22	25	27.5	18	20.5	23.5	....
			800	19.5	10.5	16	18.5	17	17.5	19.5	11	16	18	19	16	25	25	18.5	22	23	....
			850	8.5	9	14	....	15.5	12.5	7.5	11.5	11.5	13	15	11.5	23	15	17	18.5	21	....
			900	9.5	9.5	15	16	14	10	9.5	13	14.5	15	17	12	20	15.5	18	19	22	....

Table VII

Work-Hardening and Temperature-Softening Characteristics of Nichrome IV, Stainless 18-8, Pure Nickel and Iron and Alloys 2866 and 2870. The Mean of the Similar Values Obtained from the Quenched and from the Aged Materials are Recorded as Rockwell Hardness "C" Scale

Ni	IV	18-8	2870
	9	—5	19.5
	10.5	1	18

	Cold Deformed % Red. of Thickness H. T. and Cold Rolled	"Nichrome IV" Mean of Values for Quenched and Aged Specimens						Stainless 18-8 Mean of Values for Quenched and Aged Specimens						Alloy 2870 28 Ni 25 Co 7 Fe 20 Cr Mean of Values for Quenched and Aged Specimens					
		5	10	20	35	50	75	5	10	20	35	50	75	5	10	20	35	50	75
Quenched		19	23.5	29	33.5	34.5	39	14	22	30	36.5	41	47	28	32	34	36.5	39.5	44
Aged	Annealed 24 Hrs. at °C. 400	22.5	27	33.5	39	41	45	17.5	23.5	33.5	40	45	51.5	30	34.5	37.5	42.5	45	49.5
	500	23.5	26.5	33.5	39.5	40.5	46.5	20	23	34	40.5	44.5	48.5	30.5	35	38.5	43.5	46.5	40
	600	18	19	30.5	35.5	33	27.5	18	23	30	36.5	39.5	38	28	30.5	37	39.5	32	33.5
	650	20	20	19	18.5	21.5	23.5	17.5	22.5	29	28	22.5	26	27	32	22	24.5	26.5	28.5
	700	20	23	14	16.5	20	23	16	20.5	29	18.5	21	25	26.5	30.5	25.5	23.5	26	28.5
	750	20	16	13	16	18.5	20.5	14	19	27	16.5	18.5	21.5	25	17.5	19.5	22	25	26.5
	800	13.5	7.5	12.5	15	15.5	18.5	13.5	18	19	14.5	16	17	25	15	18	21	22.5	23
	850	12	9	11.5	14.5	12.5	....	10.5	16.5	8.5	10	13	11.5	14	15	17	19	20.5	20.5
	900	12.5	11	12.5	14	....	15.5	8	12.5	9	11	10	8	15	16.5	18.5	20.5	21	22

Ni	Fe	2866
—25	—20	—15
—25	—20	—16

	Cold Deformed % Red. of Thickness H. T. and Cold Rolled	Commercially Pure Nickel Mean of Values for Quenched and Aged Specimens						Pure Iron Mean of Values for Quenched and Aged Specimens					
		5	10	20	35	50	75	5	10	20	35	50	75
Quen.		— 3	6	11	17	21	25.5	—12	— 7.5	— 5	— 1	1	4
Aged	Annealed 24 Hrs. at °C. 400	— 4.5	4.5	12	18	20.5	26.5	—11	—11	— 8	— 5	— 2.5	2
	500	— 4.5	2	7	15	17	23.5	—17.5	—12	—14	....	—11.5	—17.5
	600	— 9	— 6.5	0	10	— 8	—20	—18	—16	—16	—16	—17	—20.5
	650	....	....	—24	—24	—20	—20	....	....	....	—20	—21	—21.5

Ni	Fe	2866
—25	—20	—15
—25	—20	—16

	Cold Deformation Per Cent Reduction of Thickness As Heat Treated and Cold Rolled	Alloy 2866 70 Ni 20 Co 10 Fe Mean of Values for Quenched and Aged Specimens					
		5	10	20	35	50	75
Quen.		— 2.5	7	13.5	19.5	23.5	27
Aged	Annealed 24 Hrs. at °C. 400	3	10	14.5	24	25.5	31
	500	1.5	5.5	12	19.5	23	28
	600	— 3	1	8	14	18	4.5
	650	— 6.5	— 2	6.5	—11	—14	— 8
	700	— 7.5	— 2	—15	—14	—13	—11
	750	— 8	—11	—15	—13	—14	—13

Table VIII
Work-Hardening and Temperature-Softening Characteristics of "Konal," Commercially Pure Cobalt and Alloys 2295 (Konal II) and 2867 in the Quenched and Aged Conditions

The Values Recorded Refer to Rockwell Hardness "C" Scale

"Konal" 73 Ni 17 Co 10 FeTi

Konal 2295	Quenched Aged	Initial Heat Treatment Cold Deformed % Red. of Thickness	Quenched from 950° C.						Quenched then Aged 72 Hours at 650° C.					
			5	10	20	35	50	75	5	10	20	35	50	75
—6 / 20.5	— 12 / — 7	H. T. and Cold Rolled	7	15.5	22	26.5	30	35	26	32	35	36	36.5	38.5
		Annealed 24 Hrs. at °C. 400	13	18	27	34	36	41	27	31.5	35.5	39.5	41	44
		500	17.5	26	31.5	32	38	42.5	28	25	26	39.5	39	45
		600	29	31.5	37	40	42.5	46.5	32.5	32.5	39	41	33.5	47
		650	26	27.5	29.5	25	25	30	29.5	31.5	31.5	33.5	34.5	33
		700	20	20	20	13.5	7	13	19.5	18	23	8.5	8	14
		750	6	8	3	4	6	10	6	11	3	8	5.5	9
		800	....	4.5	— 0.5	2.5	3	4	— 3	5	1	5	6.5	6
		850	— 7	— 8.5	— 5	— 2	— 4	— 5.5	— 7.5	— 8	— 4.5	— 3	— 3.5	0
		900	—10	— 5.5	— 3.5	— 5	— 7.5	—10	....	— 4	— 7.5	— 6	— 6	—12

Alloy 2295 (Konal II) 90 Ni 10 FeTi

Konal 2295	Quenched Aged	Initial Heat Treatment Cold Deformed % Red. of Thickness	Quenched from 950° C.						Quenched then Aged 72 Hours at 650° C.					
			5	10	20	35	50	75	5	10	20	35	50	75
—6 / 20.5	— 12 / — 7	H. T. and Cold Rolled	4	12	17	25	30	34.5	5	15	19	27	28	33.5
		Annealed 24 Hrs. at °C. 400	6.5	17	23	33	35.5	40	5	14.5	21.5	30	32	36
		500	6	14	24	25	30	37	15.5	20	26	29	29.5	34.5
		600	2	9.5	17.5	34	40	30	12	8.5	16	20	25.5	27
		650	0	7.5	15	14	10	1	17	8.5	15	9	1	— 2
		700	— 1	5	9.5	6	5	0	1.5	9	14	....	0	2
		750	— 2.5	4.5	6	1	1.5	....	0	3	— 6	— 5	— 4	1
		800	— 2	— 0.5	— 9	— 6	— 4	— 5	— 2.5	— 3	—10	— 7.5	— 6	— 7
		850	—12	— 9	—14	— 9	—13	—14	— 9	—12	—13	—11	—10	— 9
		900	....	....	....	....	....	....	....	....	....	....	....	....

Cobalt 11																							
2867 1 34.5																							
Quenched Aged	Initial Heat Treatment																						
	Cold Deformed % Red. of Thickness																						
	H. T. and Cold Rolled	13	18	25	30	34	39	43	42	42.5	44	44.5	45.5	24	23.5	31	35	....	....	20	20	25	35	....	....
Annealed 24 Hrs. at °C.	400	12	21.5	28.5	36	39.5	46	42	44	45.5	48	49	52.5	20	25	26	37	....	....	18.5	22	28	32.5	....	....
	500	23	24	29	39	43.5	50.5	41.5	46	46	47.5	52	55	16.5	18	24	30	....	....	19	26	27	32	....	....
	600	32.5	35.5	40	44.5	46.5	49.5	43	43.5	48.5	49.5	50.5	53	13.5	19	21	29	....	....	19	19	24	29	....	....
	650	38.5	41.5	42.5	42.5	41	42	41.5	42.5	46	46.5	46	41	12	15	19.5	28	....	....	13	14.5	19	26	....	....
	700	35	38	39	40	35	46.5	39	40	41	41	37.5	37	11	17	12	23	....	....	10	11	13	17	....	....
	750	30	31	34	35	32.5	....	31	33	38	34	29	32	10.5	14	21	20.5	....	....	12	15.5	18	19.5	....	....
	800	30.5	28.5	31	31	29	32	24	27	27	31	30	31.5	12.5	14.5	12	12.5	....	....	10	10	17	16	....	....
	850	25.5	23.5	24.5	33	30.5	29	30	28	27	29.5	....	31.5	....	....	....	....	....	....	....	....	....	....	....	....
	900	33.5	30	31	34	32	33	32.5	30	33	34	34	32.5	....	....	....	....	....	....	....	....	....	....	....	....

Table VIII (Continued)
Work-Hardening and Temperature-Softening Characteristics of "Konal," Commercially Pure Cobalt and Alloys 2295 (Konal II) and 2867 in the Quenched and Aged Conditions

		Alloy 2867 27 Ni 54 Co 3 Fe 16 FeTi												Commercially Pure Cobalt											
		Quenched from 950° C.						Quenched then Aged 72 Hours at 650° C.						Quenched from 950° C.						Quenched then Aged 72 Hours at 650° C.					
Initial Heat Treatment Cold Deformed % Red. of Thickness		5	10	20	35	50	75	5	10	20	35	50	75	5	10	20	35	50	75	5	10	20	35	50	75
H. T. and Cold Rolled		13	18	25	30	34	39	43	42	42.5	44	44.5	45.5	24	23.5	31	35	....	....	20	20	25	35	....	....
Annealed 24 Hrs. at °C.	400	12	21.5	28.5	36	39.5	46	42	44	45.5	48	49	52.5	20	25	26	37	....	....	18.5	22	28	32.5	....	....
	500	23	24	29	39	43.5	50.5	41.5	46	46	47.5	52	55	16.5	18	24	30	....	....	19	26	27	32	....	....
	600	32.5	35.5	40	44.5	46.5	49.5	43	43.5	48.5	49.5	50.5	53	13.5	19	21	29	....	....	19	19	24	29	....	....
	650	38.5	41.5	42.5	42.5	41	42	41.5	42.5	46	46.5	46	41	12	15	19.5	28	....	....	13	14.5	19	26	....	....
	700	35	38	39	40	35	46.5	39	40	41	41	37.5	37	11	17	12	23	....	....	10	11	13	17	....	....
	750	30	31	34	35	32.5	....	31	33	38	34	29	32	10.5	14	21	20.5	....	....	12	15.5	18	19.5	....	....
	800	30.5	28.5	31	31	29	32	24	27	27	31	30	31.5	12.5	14.5	12	12.5	....	....	10	10	17	16	....	....
	850	25.5	23.5	24.5	33	30.5	29	30	28	27	29.5	....	31.5	....	....	....	....	....	....	....	....	....	....	....	....
	900	33.5	30	31	34	32	33	32.5	30	33	34	34	32.5	....	....	....	....	....	....	....	....	....	....	....	....

strated in cold-rolled nickel,[9] in mild steel,[10] and in work on nickel-chromium alloys conducted by the author as part of an investigation on complex high temperature alloys.[11] In the case of nickel a maximum hardness (262 Brinell) was attained at 250 degrees Cent. (480 degrees Fahr.) and at 450 degrees Cent. (840 degrees Fahr.) the material was still harder (248 Brinell) than in the cold-rolled state (235 Brinell).

With cold-rolled steel an increase in hardness was shown on annealing at 500 degrees Cent. (930 degrees Fahr.). With the nickel-chromium alloys 20 per cent cold forged, the hardness increased from 255 to 285 Brinell for the 70-30 alloy when annealed 1 hour at 800 degrees Cent. (1470 degrees Fahr.).

The data for the present series have been condensed and presented in Tables V to VIII. Where marked aging characteristics were evident values indicating the behavior of the quenched and the aged series are recorded. Where little difference existed in the data for the two series a record of the mean of the two values was considered satisfactory.

The alloys investigated include those listed in Table III. The work-hardening properties in the quenched and aged condition have been graphically depicted in Figs. 5, 6, and 7. After completion of the hardness determinations for each of the successive increments in cold reduction, all the samples were annealed for 24 hours in a thermostatically controlled oil bath at 400 degrees Cent. (750 degrees Fahr.) and then air-cooled. Rockwell hardness numbers were then obtained on these samples (about 100) after cleaning on coarse metallographic polishing paper. They were then reannealed for 24 hours at 500 degrees Cent. (930 degrees Fahr.) in the oil bath and the hardness again recorded. This was repeated at 600 degrees Cent. (1110 degrees Fahr.).

For subsequent 24-hour anneals at 50 degrees Cent. (120 degrees Fahr.) increments up to 900 degrees Cent. (1650 degrees Fahr.) the specimens were packed in finely powdered fused alumina and heat treated in an electric furnace. Some of the specimens oxidized but this surface was removed by grinding. Air cooling was used after each anneal. The period of 24 hours was selected as

[9]W. B. Price and P. Davidson, *Transactions*, American Institute of Mining and Metallurgical Engineers, 1920, Vol. 64, p. 414.

[10]C. A. Edwards and K. Kuwada, "Influence of Cold Rolling and Annealing on the Hardness of Mild Steel," *Journal*, Iron and Steel Institute, 1927, II, p. 245.

[11]C. H. M. Jenkins, H. J. Tapell, C. R. Austin and W. P. Rees, "Some Alloys for Use at High Temperatures," *Journal*, Iron and Steel Institute, 1930, I, p. 237.

likely to produce the major part of any softening or hardening effect characteristic of the particular alloy and temperature involved.

Table V gives the quantitative effect of treatment for K42B, for that alloy with additions of molybdenum and of tungsten and for K42B with the ratio content of nickel to cobalt reversed. In each of these alloys the hardness due to maximum cold work (75 per cent) is not reduced to that of the less worked specimens until a temperature of about 700 degrees Cent. (1290 degrees Fahr.) is reached. The minimum general softening effect on heating to 750 degrees Cent. (1380 degrees Fahr.) is shown by the molybdenum alloy (2916), which also exhibits the maximum average hardness for various amounts of cold reduction after the softening anneals at 850 and 900 degrees Cent. (1560 and 1650 degrees Fahr.). The results for the tungsten-bearing alloy (2910) are similar to those of K42B. The high cobalt alloy (2869) is somewhat harder throughout the progress of the various heat treatments.

Alloy 2918 (titanium-free) is markedly inferior to any of the above alloys until the anneal is conducted at 850 to 900 degrees Cent. (1560 to 1650 degrees Fahr.) (Table VI). It is also interesting to compare the behavior of 2868 with 2869 (10 and 20 per cent chromium content respectively). It is at once evident that greater hardening is dependent on the increase in chromium content.

In Table VII are segregated the so-called non age-hardening metals. It is usual to associate a greater softness with increase in work-hardening at certain "recrystallization temperatures." This is apparent to only a limited extent in the data for nichrome and stainless steel. In both these alloys increased hardness on low temperature anneal may be noted followed by a marked decrease on annealing at 600 degrees Cent. (1110 degrees Fahr.). Hardening prior to softening is exhibited by all metals in this table with the exception of nickel and iron. It is important to note that iron which was extremely pure in the experimental work recorded shows complete absence of hardening on annealing within the range of temperature studied.

The remarkable increase in hardness attributed to high cobalt content and resulting from annealing cold-rolled material is illustrated by comparison of "Konal" with alloy 2867 (Table VIII). Undoubtedly much of the increased hardness at 700 degrees Cent. (1290 degrees Fahr.) may be due to higher ferrotitanium content but this is unlikely to persist at 850 to 900 degrees Cent. (1560 to 1650° F.).

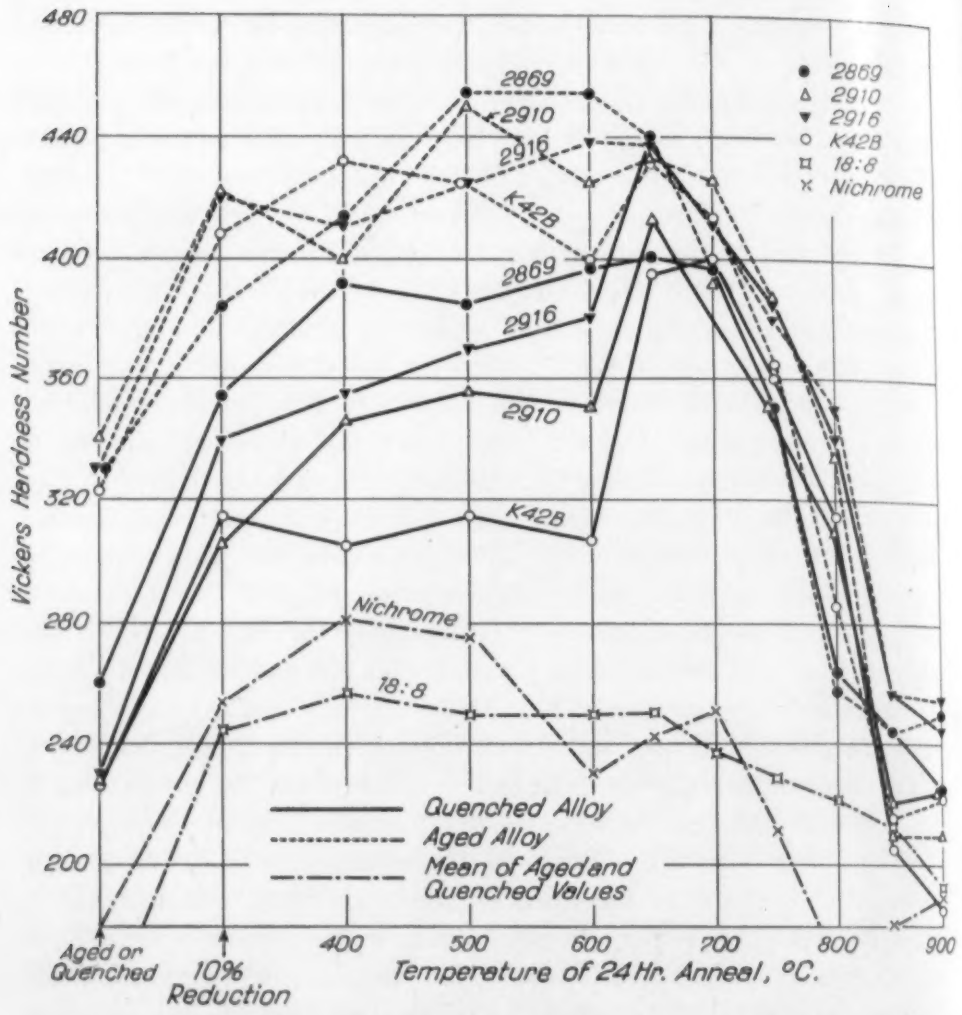

Fig. 8a—The Effect on Vickers Hardness of Annealing Cold-Rolled Quenched and Aged Alloys for 24 Hours at Temperatures from 450 to 950 Degrees Cent. (840-1740 Degrees Fahr.). Data for 10 Per Cent Reduction in Thickness is Plotted.

The data in this section of the investigation are too extensive to reproduce graphically but it was considered valuable to select some of the more important alloys and compare their behavior as revealed by hardness, with that of nichrome and stainless steel. For this purpose the experimental data from two widely different amounts of cold deformation were arbitrarily selected, 10 and 50 per cent reduction of thickness.

The alloys represented in Fig. 8a and 8b include K42B, K42B modified with 5 per cent addition of molybdenum (2916) and with 5 per cent addition of tungsten (2910). The result of modifying K42B by reversing the nickel-cobalt ratio is shown in alloy 2869. For

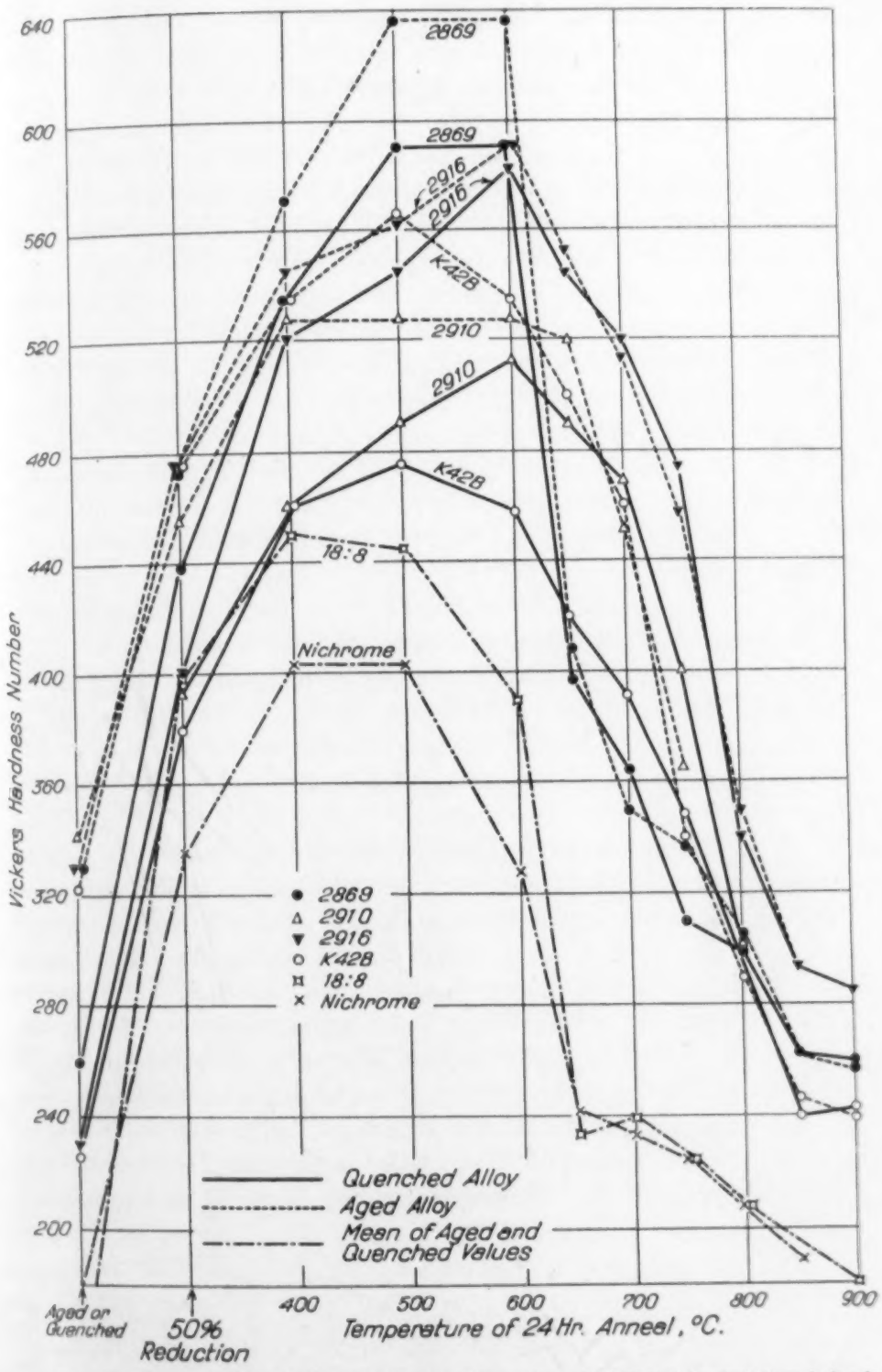

Fig. 8b—The Effect on Vickers Hardness of Annealing Cold-Rolled Quenched and Aged Alloys for 24 Hours at Temperatures from 450 to 950 Degrees Cent. (840-1740 Degrees Fahr.). Data for 50 Per Cent Reduction in Thickness is Plotted.

each of these materials there are four curves, two representing the effect of annealing treatment on the quenched and aged alloy reduced 10 per cent (Fig. 8a) and two representing similar treatments after 50 per cent reduction (Fig. 8b). For nichrome and stainless steel mean values for the quenched and aged alloys 10 per cent reduction and mean values for 50 per cent reduction have been used.

A careful study of the two diagrams readily brings out the variation in characteristics of the alloys and reveals the differences between the K42B type of alloy and the two well known commercial materials. It suffices to draw attention to the following general features.

1. There is markedly greater hardness in the pre-aged alloys when annealed up to about 600 degrees Cent. (1110 degrees Fahr.) whether cold-rolled 10 or 50 per cent reduction.

2. Above 650 degrees Cent. (1200 degrees Fahr.) the absolute magnitude and the changes in hardness for the quenched and aged alloys closely parallel each other for both per cent reductions considered.

3. The greater hardness induced in the more heavily cold-worked specimens persists up to about 750 degrees Cent. (1380 degrees Fahr.) and in some instances, although to a lesser extent, up to 800 degrees Cent. (1470 degrees Fahr.).

4. The much greater hardness developed by the K42B type alloy as compared with the two commercial alloys is strikingly evident.

5. Considering the sections of the curves which turn sharply down in the top half of the chart and which represent the temperature regions where softening of a 50 per cent cold-worked material occurs (Fig. 8b) it may be noted that nichrome and 18-8 exhibit this sharp fall at 500 to 600 degrees Cent. (930 to 1110 degrees Fahr.) while alloy 2916 exhibits a similar fall from 600 to 750 degrees Cent. (1110 to 1380 degrees Fahr.). Above 600 and 750 degrees Cent. respectively the rate of softening materially increases.

6. The hardest alloy of the series (2869) maintains its remarkably high hardness (590 and 635 Vickers) at 600 degrees Cent. (1110 degrees Fahr.). Thereafter the fall in hardness is extremely rapid.

General Considerations

In a study of the properties of complex alloys it is economically possible to study only a limited number of materials. Data on the

mechanical properties and age hardening characteristics of the nickel-cobalt-iron alloys containing 2.5 per cent titanium have been presented with such chemical analyses distribution as to provide a general survey of the ternary system. These data should be correlated with those previously published.

It has been shown that high iron content renders the alloys very hard and that high cobalt alloys with moderate amounts of nickel also exhibit high tensile and yield values at 600 degrees Cent. (1110 degrees Fahr.). Too much attention should not be given to difficulties resulting from forging because cracking and failure under the hammer are not necessarily intrinsic properties of the alloy but may depend on melting or casting conditions or on the introduction of a suitable "scavenging" agent prior to casting. Examples of this fact are readily cited in the development of the technique for casting malleable "pure nickel" and nickel-chromium alloys.

Furthermore a uniform heat treatment, quenched from 950 degrees Cent. (1740 degrees Fahr.) and aged 72 hours at 650 degrees Cent., has been employed for all the alloys subjected to mechanical tests. Additional work will unquestionably reveal heat treatments which would produce superior mechanical properties.

The investigation on the age-hardening characteristics demonstrates that precipitation hardening may be obtained under certain conditions by the addition of titanium when any one of the three elements nickel, cobalt, or iron is absent. Thus when cobalt is removed from "Konal" the iron content must be increased to obtain marked age-hardening. Raising both the iron and the cobalt content appears to markedly increase the precipitation hardening effect at 600 and at 750 degrees Cent.

In K42B type of alloy the substitution of molybdenum or tungsten for chromium does not materially modify the aging properties. Titanium appears to be unique in its property of imparting age-hardening to the ternary or modified ternary alloys. Silicon, zirconium and vanadium have no such effect within the temperature ranges studied. The profound effect of increasing the ferrotitanium in "Konal" from 10 to 40 per cent is noteworthy (compare "Konal" and 2873, Fig. 4).

The work-hardening and temperature softening properties of the alloys are considered to be important. The behavior on cold rolling as revealed by Rockwell hardness, is recorded in graphical form for the quenched and for the aged alloys. In general, the hardness in-

creases with the degree of cold deformation but discontinuities are apparent in both series. With the softest materials like nickel and iron the negative hardness values are naturally not so reliable but the data are included for purposes of comparison. The relative profound work-hardening property of stainless 18-8 steel is evident in both graphs, while the behavior of 80-20 nickel-chromium is strictly comparable to the general trend of the ternary alloys.

The last section of the paper on temperature softening is considered to outline the general high temperature properties of the materials. All hardness data, subsequent to the specified heat treatment, were obtained from measurements made at room temperature and it would be desirable to correlate with test data at elevated temperatures. However, it is usual to assume that such hardness tests are indicative of the high temperature properties. The data, presented in tabulated form, are grouped so that related alloys appear on any one chart and the characteristic features have been discussed.

The limited data for 10 and 50 per cent reduction of thickness for selected alloys, presented in the last figures, assist in evaluating the magnitude of the variations in behavior of the nickel-cobalt-iron base alloys as compared with those of the well-known commercial high temperature materials.

Acknowledgment

The author takes pleasure in acknowledging the general cooperation of the executives of the Westinghouse Electric and Manufacturing Company, and of P. H. Brace in particular. He is also indebted to his former colleague, J. R. Gier, for skilled experimental assistance, and to H. D. Nickol, senior student in metallurgy at the Pennsylvania State College, for help in various ways.

Publication of Part II

The second paper (Part II) on "Resistance to High Temperature Oxidation and to Chemical Corrosion with Electrical Resistivity and Metallographic Data on the Alloys" will appear in the September 1936 issue of Transactions along with the discussion of Part I.

uities are
ickel and
le but the
profound
t in both
ictly com-

ng is con-
of the ma-
treatment,
ure and it
tempera-
s tests are
esented in
n any one

thickness
evaluating
cobalt-iron
ommercial

al coopera-
anufactur-
o indebted
assistance,
nnsylvania

Tempera-
Resistivity
ne Septem-
of Part I.